INVESTIGATIONS OF

POLYSACCHARIDE CARBAMATE-COATED

CHIRAL STATIONARY PHASES

by

Sally Jane Grieb

A thesis submitted in partial fulfilment of the
requirements for the degree of Doctor of Philosophy
at the University of Warwick

Department of Chemistry,
University of Warwick.

September 1995

CONTENTS

ACKNOWLEDGEMENTS

I would like to sincerely thank the following persons and institutions

who have helped in the preparation of this thesis

Prof. Stephen Matlin, University of Warwick

for his guidance, supervision and continued encouragement

throughout my three years

*

Dr. Ana Belenguer, SmithKline Beecham Pharmaceuticals

for her unrivalled enthusiasm and willingness to help at every opportunity

*

Dr. Harald Ritchie and Mr. Paul Ross, Shandon HPLC

for their support and keen interest in my work

*

Mr. John Warrack, SmithKline Beecham Pharmaceuticals

for running the scanning electron microscopy samples

*

Dr. Alison Roger and Dr. Chris Samuel, University of Warwick

who kindly agreed to adopt me following the departure of Prof. Matlin

*

All my colleagues, family and friends

who have assisted and put up with me during my quest for this PhD

*

SERC and SmithKline Beecham Pharmaceuticals

for my research funding

*

Shandon HPLC

for kindly providing the Hypersil silica

DECLARATION

The observations and recommendations described in this thesis are those of the author, except where acknowledgement has been made to results and ideas previously published. The work was undertaken at the Department of Chemistry, University of Warwick, between October 1st, 1992 and August 31st, 1995 and has not previously been submitted for a degree at any institution.

SUMMARY

This thesis describes work carried out in order to increase knowledge concerning the influence of support structure and support surface chemistry on the enantioselectivity of cellulose tris(phenylcarbamate)-coated phases using high-performance liquid chromatography and flash chromatography.

In the past cellulose carbamates have been coated (25% w/w) onto large particle (7 to 10 μm), macroporous (4000Å) aminopropylated silica (APS) and packed into long (250 mm) HPLC columns. Therefore, the aim of the first part of this project was to use a small particle support, coated with a cellulose carbamate that could be packed into a short HPLC column in order to achieve rapid, efficient chiral separations.

Hypersil APS with a particle size of 2.5 μm and a mean pore diameter of 120Å was chosen as a potentially suitable support. As a result of using a small pore diameter support, the cellulose carbamate coating was not easily able to gain access to the pore volume and a 15% w/w cellulose carbamate loading was found to be optimum. As anticipated, 2.5 μm Hypersil APS coated with 15% w/w cellulose tris(3,5-dimethylphenylcarbamate) (CDMPC) was significantly more efficient than similarly coated 5 and 10 μm Hypersil APS phases and high eluent flow rates (≥ 1 ml/min) could be used without significant loss in efficiency. A 30 mm column packed with 15% w/w CDMPC-coated 2.5 μm Hypersil APS permitted the baseline separation of a range of chiral analytes in less than three minutes.

In the next phase of the work, the influence of the support surface chemistry on enantioselectivity was investigated. Hypersil supports which were both more polar (underivatised silica) and less polar (octadecylated silica) than APS, and Hypercarb, a very non-polar porous graphitic carbon (PGC) support, were chosen in order to span a wide polarity range.

Underivatised silica, due its small polar surface group, was able to accept a 20% w/w CDMPC loading and for many analytes this phase was found to be more enantioselective than a 15% w/w CDMPC-coated APS phase. In contrast, the large non-polar surface groups on octadecylated silica (ODS) appeared to significantly exclude CDMPC from the pore volume and a 15% w/w loading was found to be too high. However, because the octadecyl groups were able to shield acidic silanol sites to some extent, CDMPC-coated ODS showed potential for the separation of basic analytes. Hypercarb, which has a larger pore volume (250Å) than Hypersil supports and has virtually no surface functional groups, accepted a 25% w/w CDMPC loading. This phase showed superior enantioselectivity for basic and acidic chiral analytes over CDMPC-coated APS. However, since PGC interacts strongly with flat molecules, badly tailing peak shapes were observed for a few bi- and polyaromatic chiral analytes.

The high efficiency of the CDMPC-coated underivatised silica in HPLC columns led us to consider whether a modestly efficient, inexpensive flash chromatography silica coated with CDMPC could be used for preparative scale separations.

Initially, a standard flash chromatography column packed with 20% w/w CDMPC-coated Davisil irregular silica (40-63 μm, pore size 150Å) was used to investigate the separation of a range of chiral analytes. Resolutions were monitored by fraction collection with subsequent HPLC analysis. The method was found to be extremely easy, rapid and sample loadings of tens to hundreds of milligrams were achieved. Later two modifications were made; (i) in order to reduce the tedious collection of fractions, the flash column was modified to allow on-line UV detection and (ii) a 20% w/w CDMPC-coated Bondapak ODS flash column was prepared and was shown to dramatically improve the preparative resolution of basic analytes.

LIST OF ABBREVIATIONS

(in alphabetical order)

Abbreviation	Full Name
α	selectivity
Å	amstrong
ADCPC	amylose tris(3,5-dichlorophenylcarbamate)
ADMPC	amylose tris(3,5-dimethylphenylcarbamate)
ALP	alprenolol
APC	amylose tris(phenylcarbamate)
APS	aminopropylated silica
ATFE	1-(9-anthryl)-2,2,2-trifluoroethanol
BME	benzoin methyl ether
BMS	benzyl mesityl sulfoxide
BZ	benzoin
°C	degrees centigrade
ca.	approximately
CD	cyclodextrin
CDCPC	cellulose tris(3,5-dichlorophenylcarbamate)
CDMPC	cellulose tris(3,5-dimethylphenylcarbamate)
CE	capillary electrophoresis
cf.	compared with
C, H and N	carbon, hydrogen and nitrogen
cm^3/g	cubic centimetres per gram
CPC	cellulose tris(phenylcarbamate)
CSP	chiral stationary phase
CTA	cellulose triacetate
CTB	cellulose tribenzoate
CTMB	cellulose tris(4-methylbenzoate)
CTSP	cellulose tris(4-trimethylsilylphenylcarbamate)
DPhS	diphenyl bonded silica
et al	and co-workers
FLAV	flavanone
g	gram
GC	gas chromatography
GPC	gel permeation chromatography
HOMA	homatropine
HPLC	high-performance liquid chromatography
id.	internal diameter

IR	infra-red
k'	capacity factor
LC	liquid chromatography
µg, µl and µm	micrograms, microlitres and micrometres
m	metres
MA	mandelic acid
MCCT	microcrystalline cellulose triacetate
m^2/g	square metres per gram
mg	milligrams
ml/min	millilitres per minute
mm	millimetres
Mn	number average molecular weight
2-MPAA	2-methoxyphenylacetic acid
MPM	mobile phase modifier
m/s	metres per second
Mw	weight average molecular weight
N	plate number
nm	nanometres
NMR	nuclear magnetic resonance
N,N-DMA	N,N-dimethylacetamide
od.	outer diameter
ODS	octadecylated silica
ORP	orphenadrine
OXP	oxprenolol
1-PB	1-phenyl-2-butanol
4-PB	4-phenyl-2-butanol
2-PCCA	trans 2-phenylcyclopropane carboxylic acid
1-PE	1-phenylethanol
PGC	porous graphitic carbon
2-PPA	2-phenylpropionic acid
PROP	propranolol
psi.	pounds per square inch
PTrMA	poly(triphenylmethylmethacrylate)
2-PXBA	2-phenoxybutyric acid
2-PXPA	2-phenoxypropionic acid
Rs	resolution
SEC	size exclusion chromatography
SEM	scanning electron microscopy
SFC	supercritical fluid chromatography

SI	underivatised silica
SUP	suprofen
t_0	retention time for an unretained analyte
TB	Trogers base
THF	tetrahydrofuran
TLC	thin layer chromatography
TSO	trans stilbene oxide
UK	United Kingdom
USA	United States of America
UV detection	ultra-violet detection
v/v	volume for volume
% w/w	percentage weight for weight
L-ZGP	N-carbobenzoxyglycyl L-proline

CHAPTER 1

INTRODUCTION

A molecule is chiral if it has at least two isomers that are non superimposable mirror images of each other. Examples include, carbon surrounded by four different groups directed towards the vertices of a tetrahedron (eg glyceraldehyde), compounds with chiral axes (eg. allenes) compounds with chiral planes (eg. hexahelicene) or compounds which have restricted rotation around a single bond (eg. biphenyl derivatives). The two isomers are known as optical isomers or enantiomers and a 1:1 mixture of the two is called a racemic mixture or racemate. They have identical physical and chemical properties in their gaseous, liquid and solid states and when in solution in an achiral solvent. It is only when a chiral molecule is subjected to a chiral influence that chirality can be observed.

1.1 THE IMPORTANCE OF CHIRALITY

The existence of chiral molecules has been recognised for over a century.[1-3] However, it is only recently that the importance of chirality has been realised. In nature, biosynthesis and metabolism are extremely sensitive to chirality. For example, the majority of natural amino acids occur in the L form and interactions between biologically active compounds and receptor proteins almost always show high or complete enantiomer specificity. Therefore, it is not surprising that many chiral compounds display different pharmacodynamic, pharmacokinetic and toxicological effects with respect to their stereochemistry. This realisation has had a significant effect on the pharmaceutical, agrochemical and food and drink industries which produce or utilise chiral compounds.

The pharmaceutical industry was severely affected by the thalidomide tragedy in the 1960s. Racemic thalidomide (Figure 1-1), was given to pregnant women as a sedative and antinausea preparation. It was not until 1979 that it was recognised that the (S)-(-) enantiomer was teratogenic[4] and was responsible for the serious malformations in new born babies. Had the implications of the chirality been fully understood, this tragedy would have been avoided.

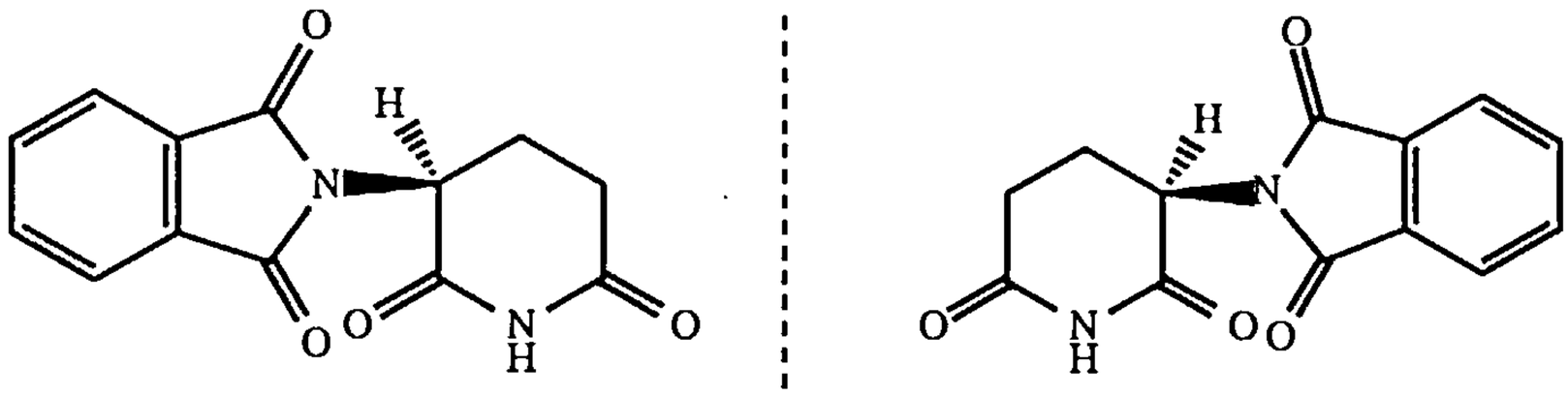

(S)-(-)-N-phthalylglutamic acid amide (tetratogenic form)

(R)-(-)-N-phthalylglutamic acid amide (non-tetratogenic form)

Figure 1-1 The enantiomers of thalidomide

Ariens[5,6] has continuously campaigned for both industry and academia to take the implications of chirality seriously and to stop the production of what he

calls "scientific nonsense". He maintains that it is rarely the case that one enantiomer is active whilst the other is completely dormant.

The pharmaceutical industry has had to change its view concerning the development of the active enantiomer instead of the racemate since regulatory authorities no longer allow new racemic drugs to be registered without an acceptable justification. In the agrochemical industry, although there is a much lower percentage of chiral compounds, the industry is pushing towards the preparation of single enantiomers in order to produce the most effective pesticide, economically and with minimum toxic effects. In the food and drink industry there are many examples of chiral compounds whose enantiomers either smell or taste differently; eg. the (R)-isomer of limonene has an orange odour, while the (S)-isomer has a lemon odour. Some single isomer natural products need to be monitored carefully since they can racemise with age and change the taste or the odour of the product.

The need for biological testing of the individual enantiomers has intensified the demand both for methods that can monitor optical purity and also for preparative systems that can provide small quantities of pure enantiomers for testing. Some of these techniques will be reviewed in the next section.

1.1.1 Methods used to Determine Optical Purity

Methods used to determine optical purity can be split into two groups: methods which involve separation and methods which do not. A brief introduction to some the more widely used techniques in both these groups will be given.

Methods not involving separation

Polarimetry makes use of the unique property of chiral compounds to rotate the plane of polarisation of plane-polarised light. Polarised light has only

one vibrational plane which is composed of two vectors that are right and left handedly circularly polarised. On passing polarised light through a solution containing a non racemic mix of enantiomers, the two vector components travel at different speeds and will rotate the plane of polarised light. The amount the plane is rotated is expressed by the angle of rotation and the direction by the appropriate sign which shows whether rotation is dextro (+) or levo (-). One of the main drawbacks of the technique is that, in order to make an accurate optical purity determination, data from the optically pure compound is required for comparison.

Nuclear Magnetic Resonance (NMR) can differentiate between chiral centres provided that they are in a diastereomeric environment. Birlingame and Pirkle[7] developed a range of chiral trifluoromethyl aryl carbinols as chiral solvating agents (CSA)s and these were shown to complex with a wide range of chiral compounds. The CSAs induce a difference in chemical shift between some signals for the two enantiomers which can then be integrated and the enantiomeric purity determined. One of the main advantages of using CSAs is that the CSA does not have to be optically pure as the optical purity will only affect the degree of splitting and not the integration. Optically active lanthanide shift reagents can also be used.[8] Paramagnetic complexes between lanthanide metals and β-diketones can complex with chiral analytes that have a group which has a lone pair of electrons, such as amines, alcohols or ketones. The result is a significant downfield or upfield shift for groups near to the complexing function.

<u>Methods involving separation</u>

Chromatography is certainly the most widely used separation technique. The different forms of chromatography take their definitions from the nature of the mobile and stationary phases and also from the physical shape of the chromatographic system. *High performance liquid chromatography* (HPLC), *gas chromatography* (GC) and *thin layer chromatography* (TLC) are well

established chromatographic techniques. *Supercritical fluid chromatography* (SFC) and *capillary electrophoresis* (CE) are relatively new chromatographic techniques which are beginning to gain much wider acceptance. All five techniques have been used to achieve chiral separations. However, it is outside the scope of this thesis to review them all.

For the purpose of relevance to this thesis, a review of HPLC and its use as a chiral discrimination technique will be given in the next section.

1.2 HIGH-PERFORMANCE LIQUID CHROMATOGRAPHY

1.2.1 The History of Liquid Chromatography

(details have been extracted from an account by Verzele and Dewaele[9])

Mikhail Semenovich Tswett, a Russian botanist, is the recognised inventor of liquid chromatography. Twsett published his first paper in Russian in 1903 on the separation of α and β carotene (red and yellow bands) using an inulin column eluted with ligroin. Later he translated this work into German and published experiments describing the use of a calcium carbonate column. He recognised that separation arose because the substrates had different affinities for the adsorbent and noted many of the important factors, including purity of packing materials, inertness of adsorbent and the importance of regular packing, that are now generally accepted as required for the preparation of a good column. However, very little attention was initially paid to his literature.

It wasn't until around the 1930s, when Kuhn and Lederer reproduced the separation of α and β carotene, that a much wider interest in chromatography was generated. Developments followed much more quickly and techniques such as TLC, partition chromatography, ion exchange chromatography, GC and size exclusion chromatography (SEC) were reported.

The development of equipment such as high pressure pumps and UV detectors, and chromatographic supports such as small particle spherical silica particles and polymer phases have made the HPLC technique that we know today.

1.2.2 The Basic HPLC System

The basic components of an HPLC system are shown in the form of a block diagram in Figure 1-2.

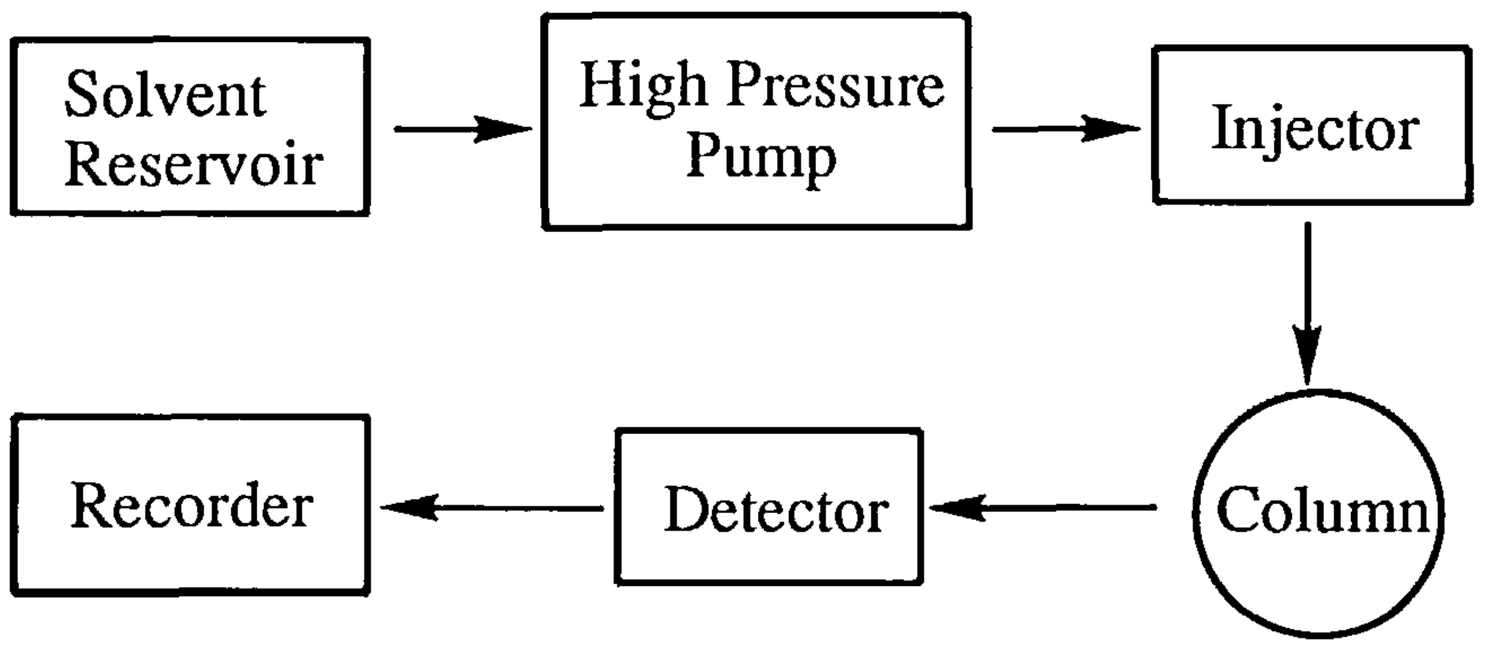

Figure 1-2 Block diagram of a basic HPLC system

The column, usually a stainless steel tube a few cm long and a few mm wide packed with the stationary phase, is the heart of the liquid chromatograph and the site where the separation takes place. Further information on the whole system can be obtained from relevant literature.[10,11]

The majority of stationary phases employed in HPLC are based on silica gel. Silica can be used as a stationary phase in its own right and also as a matrix for preparing the so-called bonded phases. Silica has some unique properties that makes it particularly useful in chromatography and these properties arise from the methods used to produce the silica.[12]

The silica used for chromatography is amorphous (ie. non crystalline) and is generally porous. The surface of the silica is hydroxylated with silanol groups. The silanols are responsible for the polar character of silica and can be used to graft organic moieties in order to change the polarity of the phase. Amorphous silica has a highly disordered structure with three possible types of surface silanols (Figure 1-3).

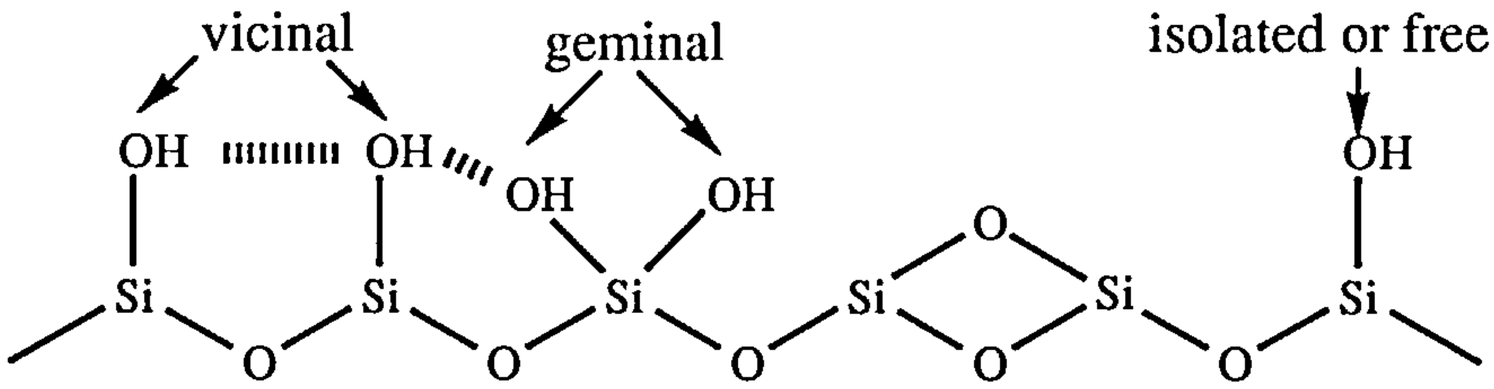

Figure 1-3 Three types of surface silanols

Vicinal or geminal silanol groups can hydrogen bond with themselves or each other as shown. The most acidic type is the isolated or free silanol group. Therefore, the higher the surface concentration of this type of silanol, the greater the hydrophilic character of the silica. This concentration can be varied by the mode of preparation and will differ for each make of silica. The method of preparation can also be tailored in order to produce porous silica with the required shape, particle size, pore size distribution, pore volume and surface area. Each manufacturer strives to produce high quality material with minimal batch to batch variation. The relevance of the above parameters will be discussed briefly.

Shape: Silica can be purchased as irregular or spherical particles, the latter being more expensive. Spherical particles produce a more homogeneous and dense column packing resulting in a column with higher efficiency and greater mechanical stability.

Particle Size and Distribution: Generally, the smaller the particle size and the narrower the distribution, the higher the efficiency. The most common size used for analytical HPLC is 5 μm. However, larger particles may be used for preparative work where back pressures are an issue or smaller particles may be used for capillary HPLC.

Pore Size, Pore Size Distribution and Pore Volume: A pore is a hole, cavity or channel communicating with the surface of the solid. The pore size defines the diameter of the pore opening, whereas the pore volume defines the volume inside the particle into which an analyte has access. The larger the pore volume the less mechanically stable the silica becomes. In chromatography, the rate of mass transfer of analyte molecules into and out of the stationary phase is controlled mainly by their diffusion within the pore volume of the particles. Therefore, the pore structure can greatly influence the efficiency of the packing. Due to irregularities in most porous silicas, the real shape is not known and models have to be used for an approximation. Two examples are given in Figure 1-4.

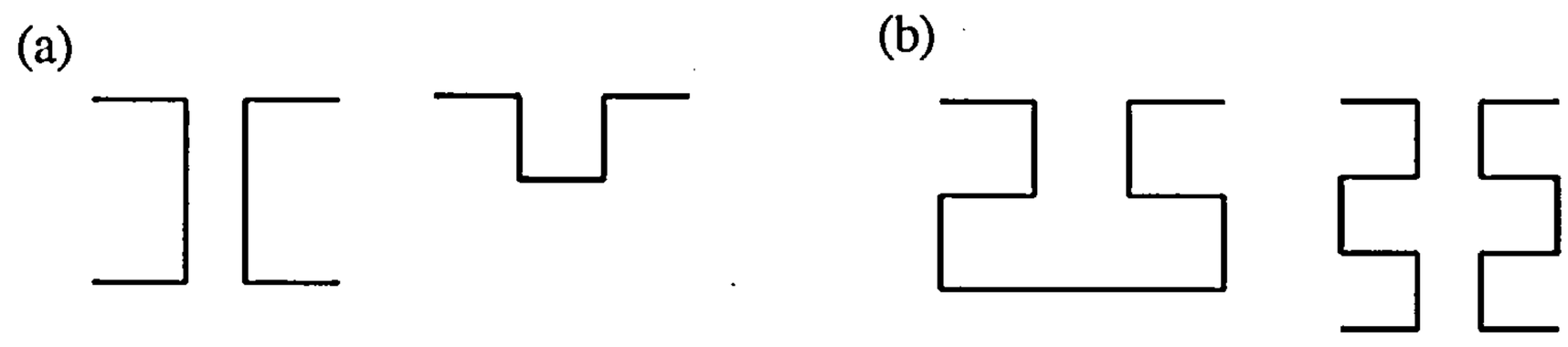

Figure 1-4 (a) Cylindrical pores. (b) Ink pot pores

Generally the wide pore diameter silicas (>1000Å) have large pore volumes and thus lower mechanical strength than narrow pore diameter silicas.

Surface Area: The specific surface area is the sum of all internal and external surfaces. Porous silicas with a high surface area have >99% of their surface area inside the particles.

The surface of the silica can be modified by bonding groups such as alkyl, phenyl, cyano or aminopropyl in order to change the polarity. Bonded phases are prepared from silica by reacting the surface hydroxyl groups with appropriate reagents to attach an organic chain to the silica. There are basically three types, brush type (or monomeric), bulk phases (cross-linked) or oligomeric phases. However, not all silanols will be derivatised. Therefore the acidity of the remaining silanols must be kept low to avoid strong interactions with basic analytes .

The stationary phase to some extent, determines the type of mobile phases that can be used in order to achieve the required resolution. If silica or a bonded phase which is strongly polar is used, then a dispersive type of solvent such as n-hexane or n-heptane is most appropriate. In this case the separation mode is termed normal phase. In order to elute the more strongly retained analytes, more polar solvents can be introduced progressively.

In contrast, polar mobile phases such as mixtures of water, methanol or acetonitrile are generally used with alkyl bonded silicas, which are relatively non-polar. The volume of organic solvent relative to water can then be used to change the elution strength of the mobile phase. If strong tailing occurs as a result of interactions with underivatised silanol groups, a buffer solution can be used to reduce ionisation. This type of chromatography is usually referred to as reversed phase chromatography.

The type of detection method used may also impose limitations on the choice of mobile phase. For example, if a UV detector is used then the mobile phase must be transparent to the UV light at the operating wavelength.

1.2.3 Equations used to Describe Separations in HPLC

The phenomenon of chromatography depends upon the differential distribution of analytes between the mobile phase and the stationary phase.

Ideally, the profile of a chromatographic band injected onto the column should have a Gaussian distribution resulting in a completely symmetrical peak. This is the case when the sorption isotherm is linear, that is, the phase distribution ratio is independent of concentration.

As the sample band moves along a column, it is broadened by a number of dispersion effects. The factors contributing to peak broadening can be split into 3 types: eddy diffusion, longitudinal diffusion (or axial) and mass transfer resistance.

Eddy diffusion occurs when some molecules are able to find a more direct path through the column than others. The use of small evenly sized particles reduces this effect. *Longitudinal diffusion* occurs as the sample molecules disperse in the mobile phase. It is therefore important to chose the correct mobile phase and velocity. *Mass transfer resistance* occurs if molecules are able to remain in stagnant pores within the stationary phase. Slowing down the mobile phase flow rate will reduce this effect.

The best known equation which describes the band spreading phenomenon in chromatography is the van Deemter equation (1).[13]

$$H = A + B/u + Cu \qquad (1)$$

where: H = height equivalent to a theoretical plate

A = eddy diffusion term

B = longitudinal diffusion term

C = mass transfer resistance term

u = mean linear solvent velocity

A graph relating plate height to flow velocity yields a curve from which the contributions of each term can be calculated and a diagnostic evaluation of the column can be performed.

The performance of the column, and the retention and separation of components can be described using a number of equations which require the measurement of the parameters shown on the chromatogram in Figure 1-5

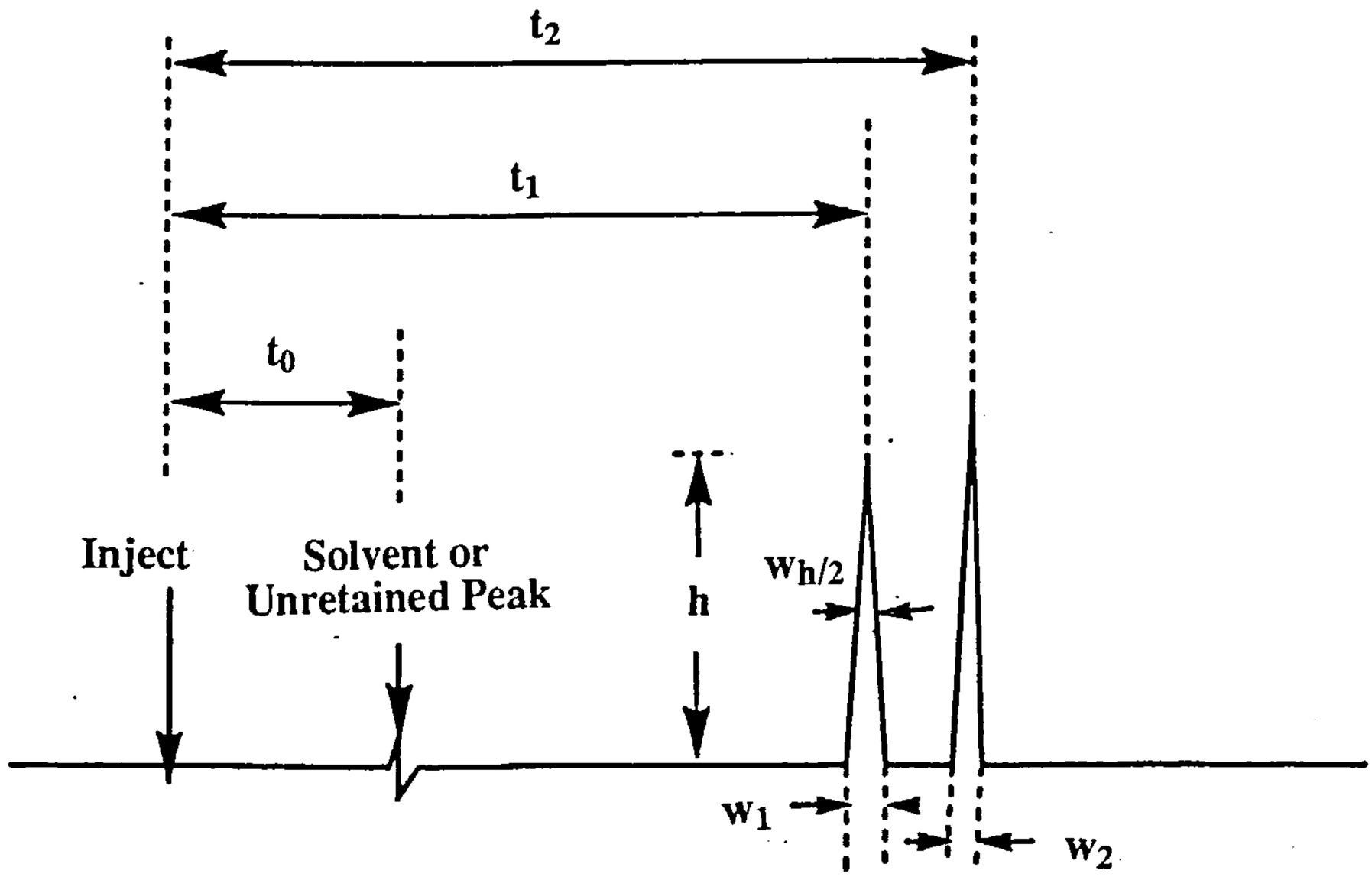

Figure 1-5 Characteristics of a chromatogram

A chromatographic column may be characterised by its *efficiency*, which is a measure of its ability to transport a compound with little peak broadening. Initially, the number of theoretical plates (N) in the column are calculated using equation 2.

$$N = 5.54(t_R/w_{h/2})^2 \qquad (2)$$

where N = number of theoretical plates

t_R = retention time for the peak

and $w_{h/2}$ = width at half peak height

Column efficiency is then expressed as height equivalent to one plate or plate height (H).

$$H = L/N \quad (3)$$

where L = length of column

The *retention* of a compound on a column can be expressed by its retention time (t_R), retention volume (V_R) or capacity factor k'

$$V_R = t_R F \quad (4)$$

where F = the flow rate

$$k' = (t_R - t_0)/t_0 \quad (5)$$

The *separation* of peaks is defined by the separation factor α. It is simply the ratio of the longer capacity factor to the shorter capacity (6). Thus to achieve separation, the value of α must be >1.

$$\alpha = k'_2/k'_1 \quad (6)$$

The value is constant under given analytical conditions. However, it does not provide a complete picture of the degree of separation achieved, since widely separated peaks may be extremely broad and thus be overlapped. Therefore, the term resolution (Rs) is used. Two equations defining *resolution* (7 and 8) are show below.

$$Rs = 2(t_2-t_1)/(w_1 + w_2) \quad (7)$$

where w_1 = peak width at base.

or

$$Rs = \frac{1}{4}\left(\frac{\alpha - 1}{\alpha}\right)\left(\frac{k'_{av}}{1 + k'_{av}}\right)\sqrt{N} \quad (8)$$

where k'_{av} = the mean capacity factor.

1.2.4 Chiral Separations using HPLC

Chiral separations using HPLC can be divided into two main groups, indirect and direct methods. In *indirect methods*, the chiral analyte is reacted with an optically pure reagent to form a pair of diastereomers. These diastereomers possess different physicochemical properties and hence can be separated by a variety of procedures such as fractional crystallisation, steam distillation or achiral chromatography. Following resolution, the enantiomers can be recovered by reversing the derivatisation process.

Indirect methods are still widely used in the process scale chemical industry since they do not require sophisticated equipment to carry out the separation. However, there are disadvantages, such as (i) the derivatising agent must have a high optical purity and therefore may be costly, (ii) the choice of derivatising agent is important since care must be taken when removing the reagent so as not to cause racemisation of the separated enantiomers and (iii) yield may be lost during removal of the derivatising agent.

Direct methods are chromatographic techniques in which an optically active moiety, termed a chiral selector, is used to achieve chiral recognition. The chiral selector may be present in the mobile phase or immobilised on the stationary phase and must interact preferentially with one of the enantiomers of the analyte.

Chiral mobile phase additives were first reported in 1979.[14.15] They have several advantages in that, (i) cheaper conventional columns can be used, (ii) chiral additives can be changed more easily than can chiral packing, (iii) a wide range of additives are available and (iv) selectivities can be different from those of chiral packings. Unfortunately, the disadvantages, such as the need to synthesise optically pure additives, the limited choice of detection system and the fact that preparative separations require further steps in order to remove the chiral derivatising agent have led to preference for chiral stationary phases (CSP)s. However, the use of this method should not be written off, since the

origins of a number of CSPs (eg cyclodextrins) stemmed from initial experimentation with mobile phase additives.

Before reviewing the types of CSPs in use, the mechanism of chiral recognition will be considered.

1.2.5 Theory of Chiral Recognition on CSPs

As a chiral compound passes over a CSP, the enantiomers may interact with the chiral selector to form transient diastereomeric complexes. In order for a separation to occur, the diastereomeric complexes must have a sufficient difference in free energy.

Calculations from investigations into the interactions between two chiral species led Pirkle and Pochapsky[16] to define chiral recognition in terms of a 'three point rule'. They stated that "chiral recognition requires a minimum of three simultaneous interactions between the CSP and at least one of the enantiomers, with at least one of these interactions being stereochemically dependent." A diagrammatic representation of this rule is shown in Figure 1-6.

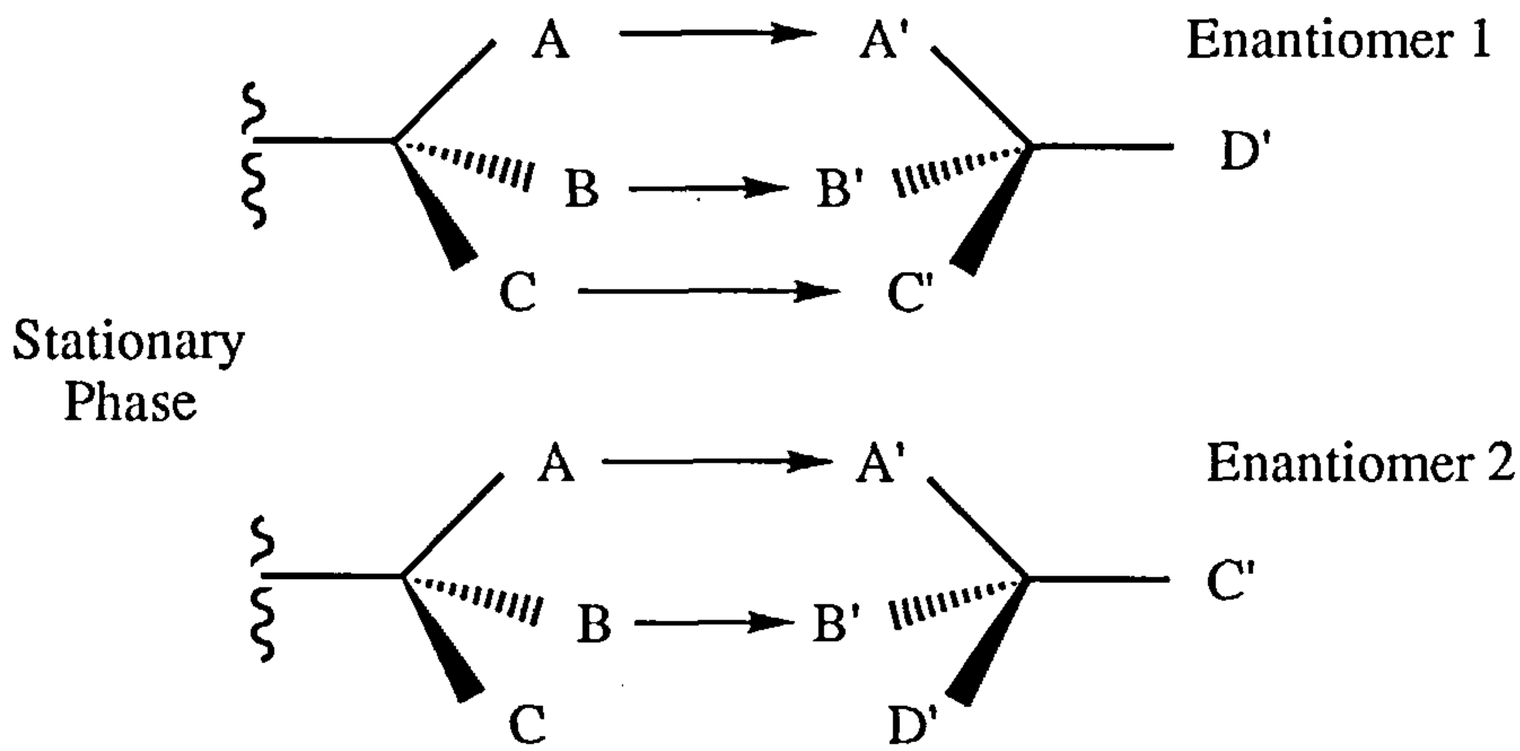

Figure 1-6 Diagrammatic representation of the 'three point rule'

The elution order of enantiomer 1 and 2 will depend on whether the C - C' interaction is attractive or steric. If C - C' is attractive, then enantiomer 1 will be retained on the column longer than enantiomer 2. If C - C' is repulsive or steric, then enantiomer 2 will be retained on the column longer than enantiomer 1. Ideally the interactions should all be different and may include, hydrogen bonding, π-π interaction, steric interaction or dipole-dipole stacking.

It must be born in mind however, that this representation is very simplistic and cannot fully explain the complex process of enantioseparation. Chiral recognition stems from a weighted time-average of the contributions of all possible complexes. This can entail different directions of approach, different conformers and different combinations of three (or more) simultaneous interactions.

1.2.6 Chiral Stationary Phases for HPLC

In the last decade the number of commercially available HPLC-CSPs for the resolution of enantiomers has increased rapidly, as indicated in recent books and reviews on the subject.[16-21] In an attempt to alleviate the problem of scanning through the many types, several workers have used various means to classify the CSPs into different groups.

Wainer[22] classified CSPs according to the mechanisms of formation of the analyte-CSP complexes involved. Taylor and Maher[21] noted that while the mechanism of operation of some phases remained unclear it would be simpler to use a classification based on both structural features and mechanisms of interaction. Vandenbosch *et al* [23] and more recently Francotte[24] classified the types of CSPs according to the principle of their design and/or the molecular size of the chiral selector molecules involved. They proposed that in general, two main groups can be distinguished: achiral matrices with small molecule chiral selectors and polymeric-type phases.

The following review is intended to give a brief introduction to some of the more well known and widely used CSPs. For a more thorough review, publications such as those noted above[16-21] should be consulted.

It has been suggested[25] that the widespread acceptance of HPLC-CSPs as extremely useful tools for the separation of enantiomers was prompted by the advent of the phases developed by Pirkle. These CSPs, made up of derivatised amino acids, such as 3,5-dintrobenzoylphenylglycine ionically or covalently bound to silica (Figure 1-7) showed good mechanical stability and were among the first readily available commercial chiral columns.

(a)

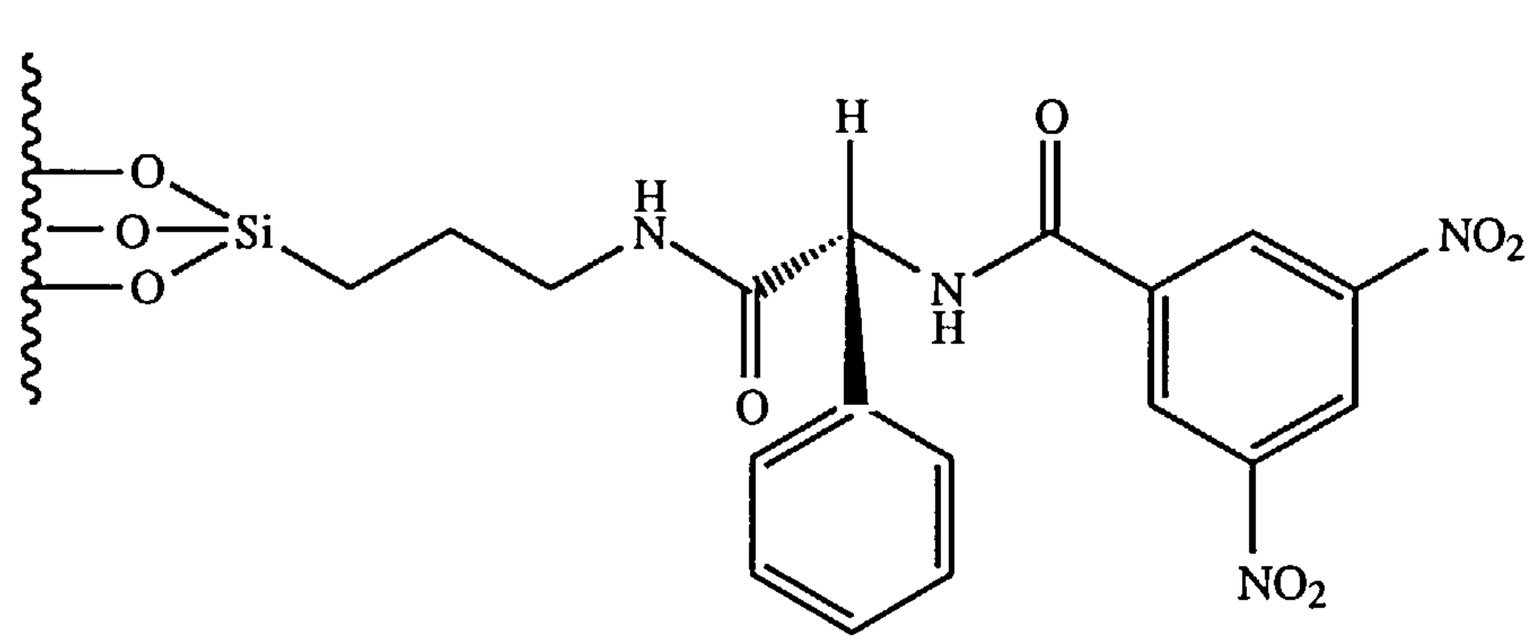

(b)

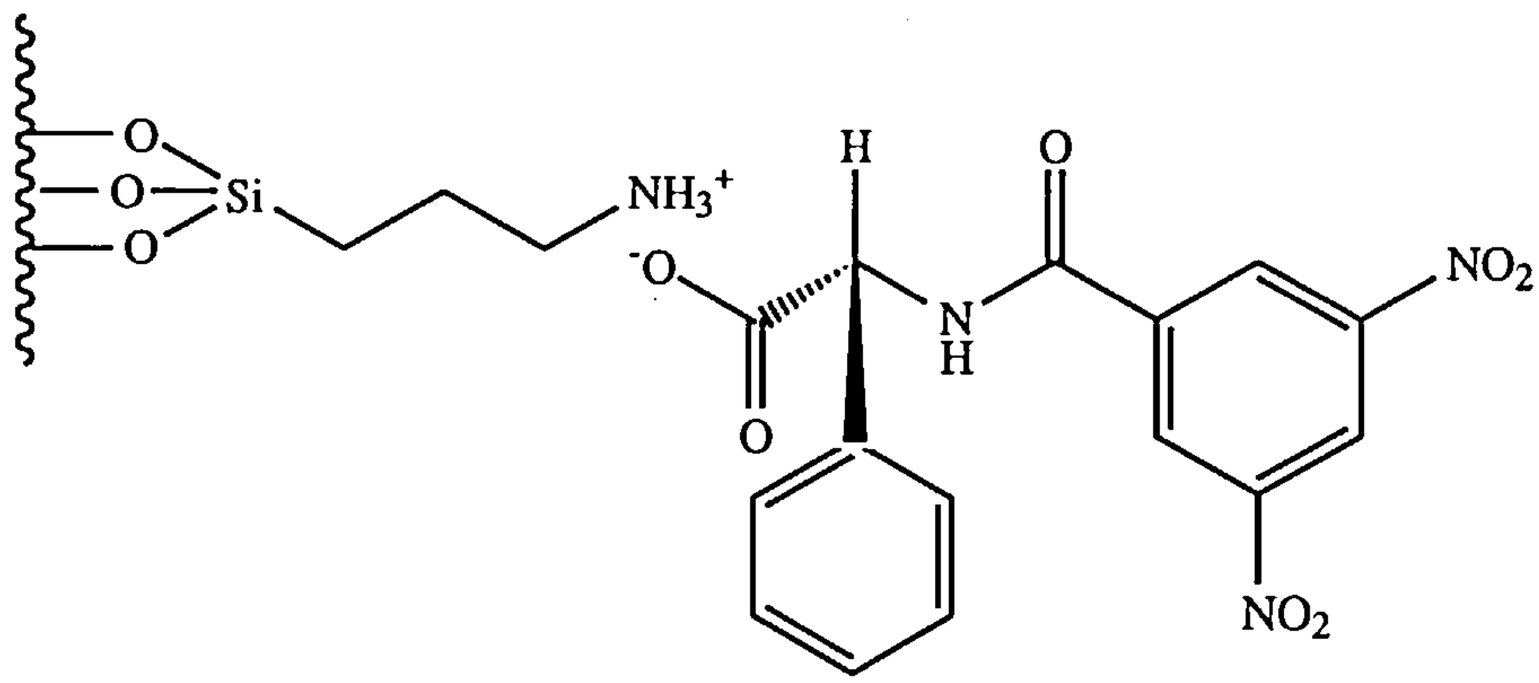

Figure 1-7 The Pirkle phase, (R) 3,5-dinitrophenylglycine (a) covalently and (b) ionically bonded to silica.

The idea for the Pirkle 'brush type' phases (so called because their organic groups are directed away from the silica matrix like the bristles of a brush) emerged from studies of chiral NMR shift reagents.[7] By using what

Pirkle termed the 'reciprocal' approach, he designed successive generations of CSPs.[27] Many of these phases were also commercialised and were shown to be useful for the separation of a wide variety of racemates.

The early Pirkle type phases are principally based on π-π charge transfer interactions (face-to-face and face-to-edge). Therefore if the chiral selector contains a π-acceptor group, the analyte must contain a complementary π-donor group and vice versa. However, in order to attain chiral recognition, other interactions such as hydrogen bonding, dipole-dipole and steric interactions must also take place, in accordance with the 'three point rule' (section 1.2.5). This requirement often necessitates derivatisation of the analyte to attain a separation.

More recently,[27] based on the constantly evolving understanding of molecular interactions, efforts in Pirkles group have concentrated not only on refining the existing phases but also designing new CSPs based on the desired separation of a target molecule. In a recent case, the design of a chiral selector which would contain the necessary chiral interactions to separate naproxen led to the discovery of a CSP now called the Whelk-O 1 phase. This phase contains a π-acid and π-base moiety and is reported[27] to be the most versatile Pirkle type phase developed to date.

Chiral discrimination on crown ether and cyclodextrin (CD) CSPs occurs predominantly via an inclusion mechanism and the phases are often termed chiral cavity packings.[21] The chiral discriminating ability of crown ethers was first realised when they were used as mobile phase additives for the separation of primary amines.[28] The protonated amine group (ammonium) is able to hydrogen bond to the ether group, while the hydrophobic moiety of the analyte enantiomers fit to a better or worse extent into the chiral cavity. Cram *et al* [29] noted this potential and covalently bonding them to a silica support (Figure 1-8). Later,[30] by changing the number of ethylene ether bridges in order to change the size of the cavity and adding different substituents onto the naphthyl groups of

the crown ethers they were able to optimise the selectivity for resolution of some racemates.

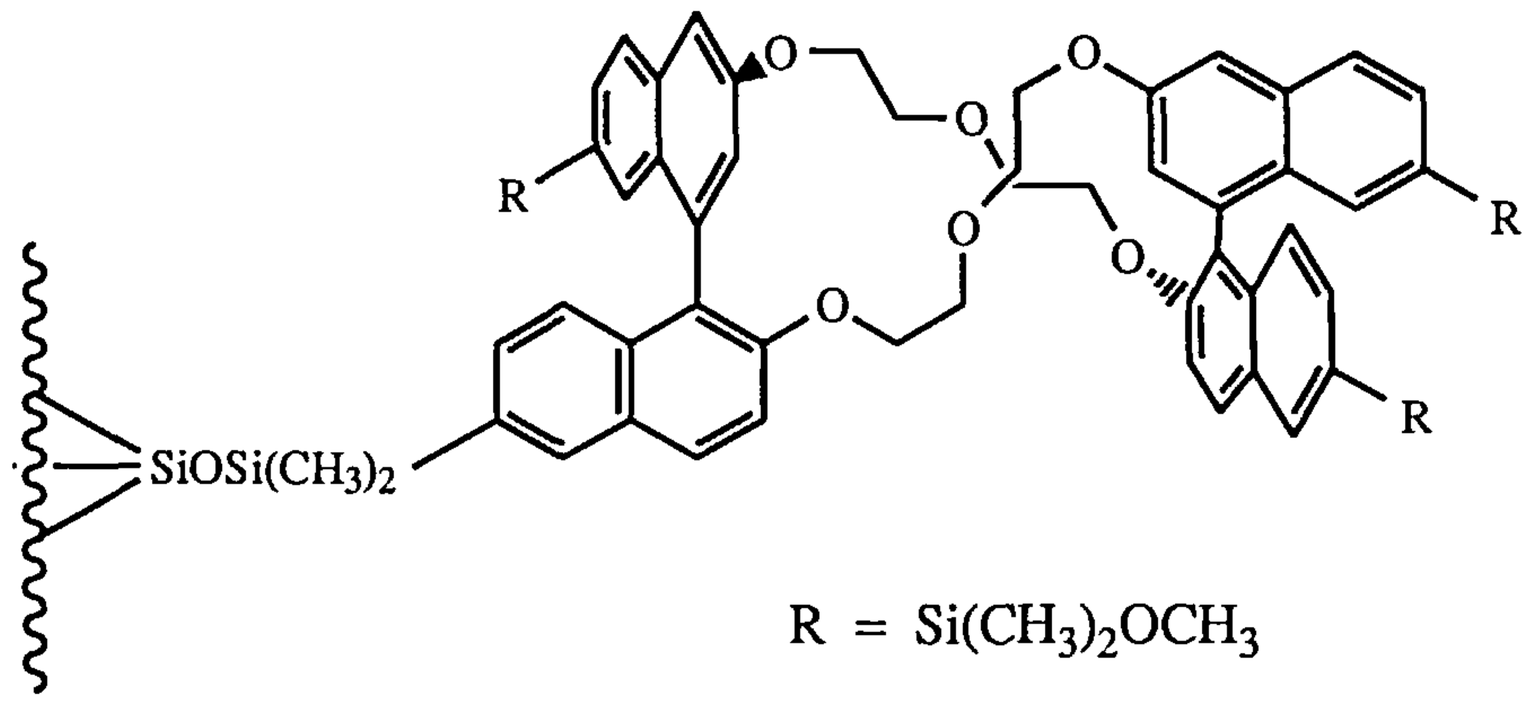

Figure 1-8 A Crown ether CSP

Much of the attention in the host-guest complexation field has now switched to CD and derivatives thereof. CDs are cyclic oligomers (6-8 units) of 1,4-linked α-D-glucose units which adopt a tapered cylindrical or toroidal shape. The size of the cavity depends on the number of glucose units, α-CD being the smallest (6 units) and γ-CD the largest (8 units). The numerous hydroxyl groups are located around the rims of the CD openings, so that the hydroxyl-free interior is relatively hydrophobic. The CD molecules are fixed via a spacer to a silica support, eg. Figure 1-9.

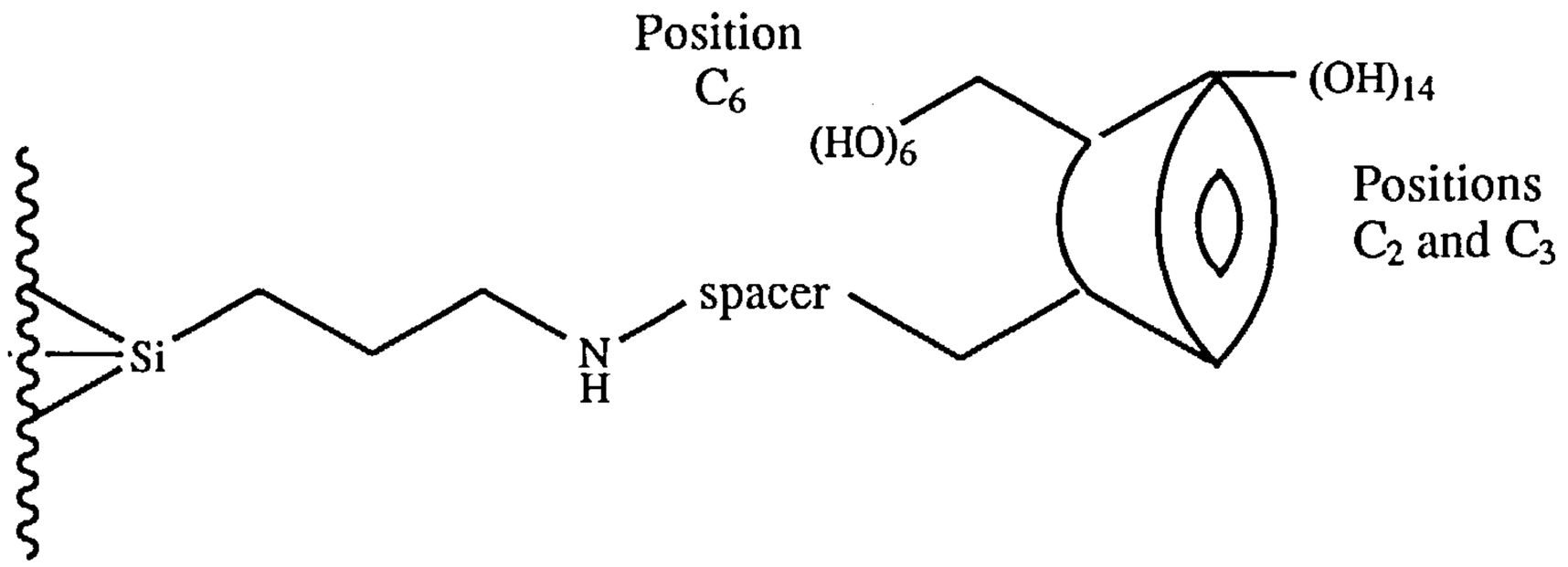

Figure 1-9 Schematic model of β-CD bound to silica.

Molecules possessing an aromatic group adjacent to the chiral centre as well as polar or H-bonding functionality have most chance of chiral discrimination on the CD phases. Molecular modelling[31] has indicated that the aromatic moiety is included through the larger opening of the CD cavity, while the polar groups interact with the hydroxyls that surround the opening. In order to attain a chiral separation, there must be a difference in the energetics of the inclusion complex, so that in many cases only one CD will produce a separation.

Most recently, derivatised CDs such as acetyl-β-CD[32], hydroxypropyl-β-CD[33] and 3,5-dimethylphenyl carbamoylated α-, β- and γ CDs[34] have been introduced. These CSPs can be used with both normal and reversed phase eluents and have greatly increased the number of separations possible on the CD phases. In the normal phase mode, derivatised CDs are thought not to act by an inclusion mechanism, but by a mechanism resembling that of a Pirkle phase.[20]

Another group of very useful CSPs are the polymeric type phases. These include polysaccharides and derivatives thereof, synthetic polymers and proteins. They may be in the form of the pure polymer, polymer coated onto a achiral support or a polymer grafted onto an achiral support. Analytes can form multimolecular interactions between the adjacent polymer chains. Therefore, these phases generally show high versatility. Interactions include both attractive interactions and inclusion mechanisms.

An important group of polymer CSPs are the derivatised polysaccharide phases. However, the merits of these phases will not be discussed here, since they are the subject of a much more thorough review in section 1.3.

Synthetic polymers were developed to rival the derivatised polysaccharide CSPs, although they have yet to enjoy the same widespread acceptance. Synthetic polymers can be prepared by polymerisation in the presence of a chiral catalyst, by using chiral monomers or by using a 'print molecule' to prepare tailor-made phases. The first of these methods was used by Okamoto *et al* [35] to prepare optically active poly(triphenylmethylmethacrylate)

(PTrMA), Figure 1-10. This isotactic polymer whose chirality arises from its helical structure found most use as a coating on a silanised silica support and was able to resolve various racemic compounds.[36]

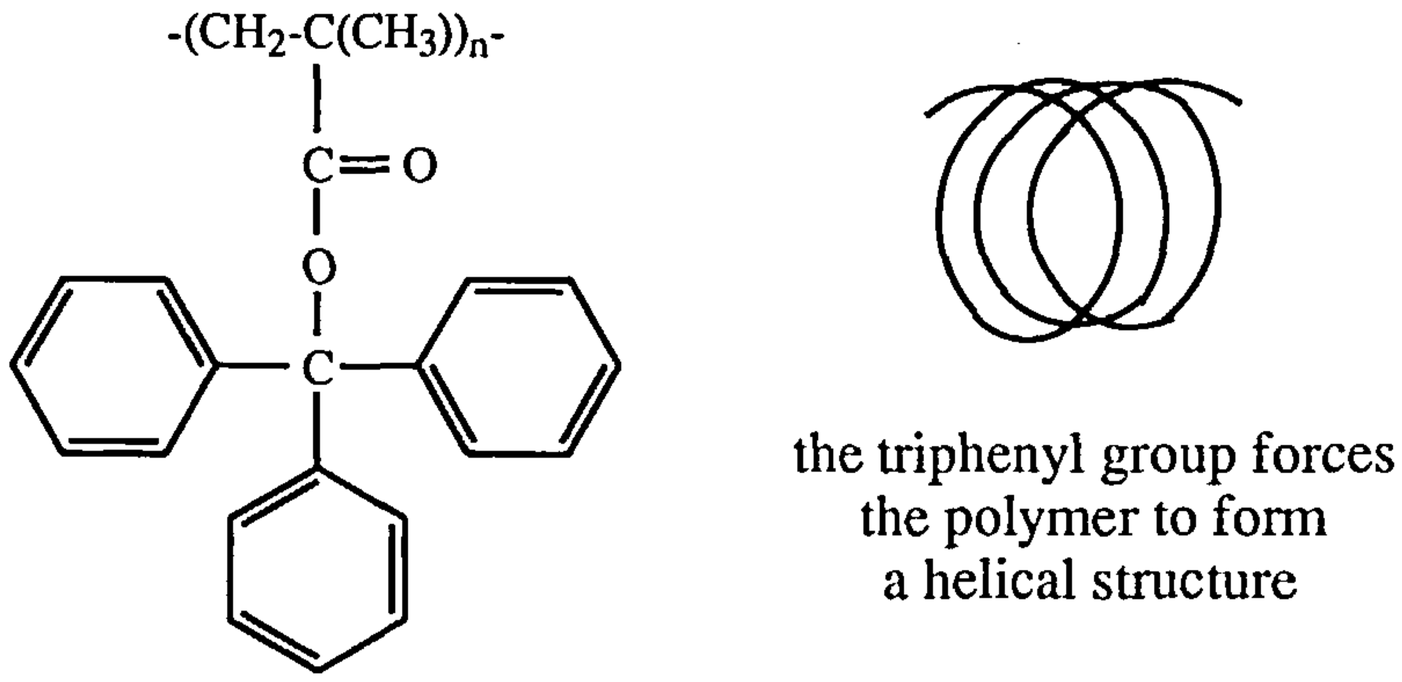

Figure 1-10 Structure of poly(triphenylmethylmethacrylate) (PTrMA)

Protein CSPs are one of the most versatile groups of phases to have emerged during the previous decade. The average protein contains several hundred chiral centres and secondary and tertiary organisation contribute to further levels of chirality. All protein-based phases operate under reversed phase chromatographic conditions with hydrophobic and electrostatic interactions predominating. Therefore, there are a large number of mobile phase variables, such as pH, type of organic modifier and buffer strength. In addition, the aqueous phase allows direct injection of biological samples.

Unfortunately, there are several drawbacks. All protein phases have very low sample loading capacities compared to other CSPs and can only be used in the analytical mode. This is a result of the large size of the protein molecules which lead to low coverage on the silica surface. The vast array of possible mobile phase compositions makes choosing a suitable one very difficult. In addition, the mobile phase composition is extremely sensitive, so that a change in pH of 0.1 can lead to a significant change in the stereoselectivity of the CSP. Finally, the stability of the protein phases is relatively low due to facile

disruption of the protein's structure by constituents in the mobile phase and injected samples.

Early examples of protein phases were based on either bovine serum albumin[37,38] or acid glycoprotein[39] covalently bound to silica. These early examples suffered from poor reproducibility. However, current commercial phases such as the α_1-acid glycoprotein and ovomucoid are much more reliable. The human plasma protein α_1-acid glycoprotein (AGP), is the most widely used protein phase. Developed by Hermansson[40], it has been shown to be extremely versatile and able to separate many racemates that were not separable on other types of CSP. The ovomucoid phase, developed from chicken egg white, is a relatively new phase which is becoming more widely used and in certain applications has been shown to exhibit higher efficiencies than the AGP phase.[41]

The most recent class of CSPs for the chromatographic separation of enantiomers are the covalently bound macrocyclic antibiotics.[42,43] Glycoproteins such as vancomycin, ristocetin and teicoplanin have been used. These interesting new phases appear to have many of the useful enantioselective properties of proteins and other polymeric chiral selectors without their inherent problems of instability and low capacity. They are also multimodal in that they can be switched between the reversed phase and normal phase without any detectable deterioration in performance. As with the protein phases, the mechanism of enantioseparation is not clear since several different mechanisms such as π-π complexation, hydrogen bonding, inclusion, dipole stacking, and steric interactions are all possible.

Even with the current understanding of the various CSPs, the decision as to which phase to select for a particular application is still a difficult one for the analyst. This is particularly true since many of the CSPs are expensive and a wrong decision would prove costly.

Roussel and Picas[44] have attempted to alleviate this problem by setting up a data base into which they have entered many chiral separations achieved in

recent years. The analyst is able to enter in the structure or part structure of the chiral analyte to be separated. The data base then searches for the most closely related structures and displays them along with the chromatographic conditions and separations achieved. The data base is now commercially available as ChirBase and the merits of the system have recently been reviewed.[45] Unfortunately, this data base is also extremely expensive and needs to be constantly updated.

In reality, the selection of the CSP is often made easier by the limited number of phases that the analyst has in hand.

1.3 POLYSACCHARIDES AS CSPs

1.3.1 History of the Development of Derivatised Polysaccharide Phases

Polysaccharides are high molecular weight sugar polymers containing in excess of ten monosaccharide units. Cellulose, the most abundant naturally occurring organic compound, consists of a linear polymer of D-(+)-glucose residues joined together by β-1,4 linkages. The β-glucose units have a chair conformation with the 2 -OH, 3 -OH and 6 -CH_2OH all in equatorial positions. The molecular weight can range from 250,000 to 1,000,000 (ie. 1500 to over 6000 units). It is optically active and possesses a highly ordered structure. X-ray analysis and electron microscopy have indicated that the chains lay side by side in bundles which are held together by hydrogen bonding between the numerous hydroxyl groups.[46]

The first chiral recognitions on native cellulose were observed towards the end of the 1940s. Amino acids such as tyrosine and glutamic acid were separated into two spots using paper chromatography.[47-49] An English scientist, Dalgleish[50] interpreted the observed separations using a "three point" attachment model. Although his observations were not unique they are often referred to

because they formed the basis for "Three Point Rule", later defined by Pirkle and Pochapsky[16] to interpret the structural requirements for asymmetric recognition (see section 1.2.5). However, although native cellulose has continued to be used as a chiral resolving agent with some degree of success,[51-53] for many analytes, slow mass transfer, slow diffusion and strong non-stereospecific interactions with the polar hydroxyl groups, led to poor chiral recognition.

In 1973, Hesse and Hagel[54] were the first to produce a completely acetylated microcrystalline cellulose, using a heterogeneous reaction, Figure 1-11. X-ray analysis confirmed that the supramolecular structure of the product was the same as that of the starting material and when packed into an HPLC column, the so-called microcrystalline cellulose triacetate (MCCT) was found to show good chiral recognition for several racemic compounds.[54,55]

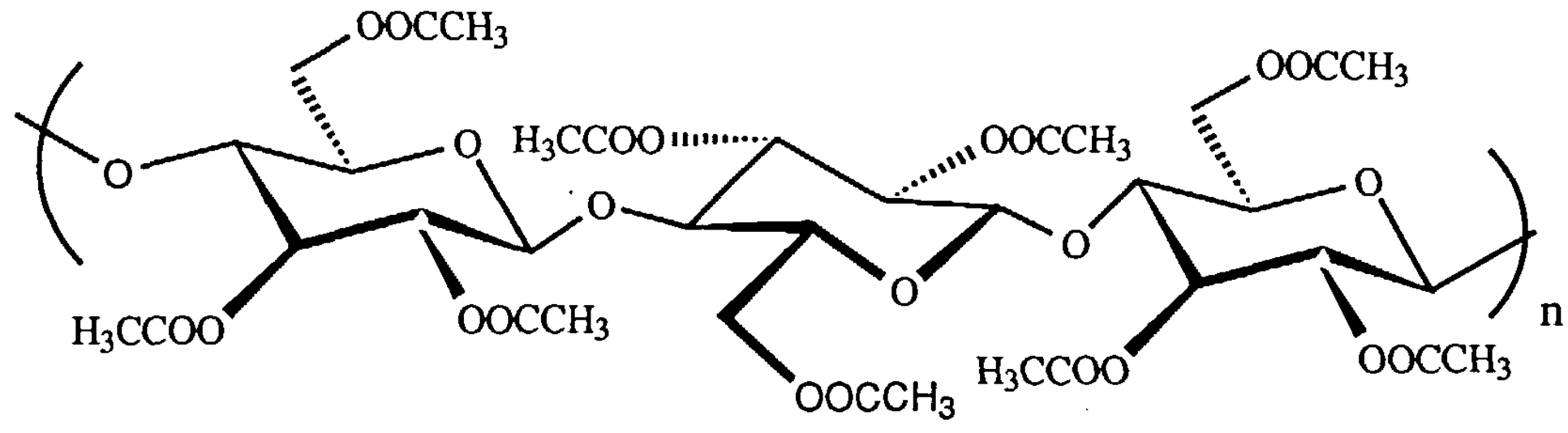

Figure 1-11 Structure of microcrystalline cellulose triacetate

One of the initial compounds studied by Hesse and Hagel[54,55] was Trogers base. Baseline resolution could be achieved on MCCT using ethanol as the mobile phase (Figure 1-12 (a)). However, when MCCT was dissolved and the reprecipitated material used as the CSP, the enantioselectivity for Trogers base was essentially lost and the elution order was reversed (Figure 1-12 (b)).

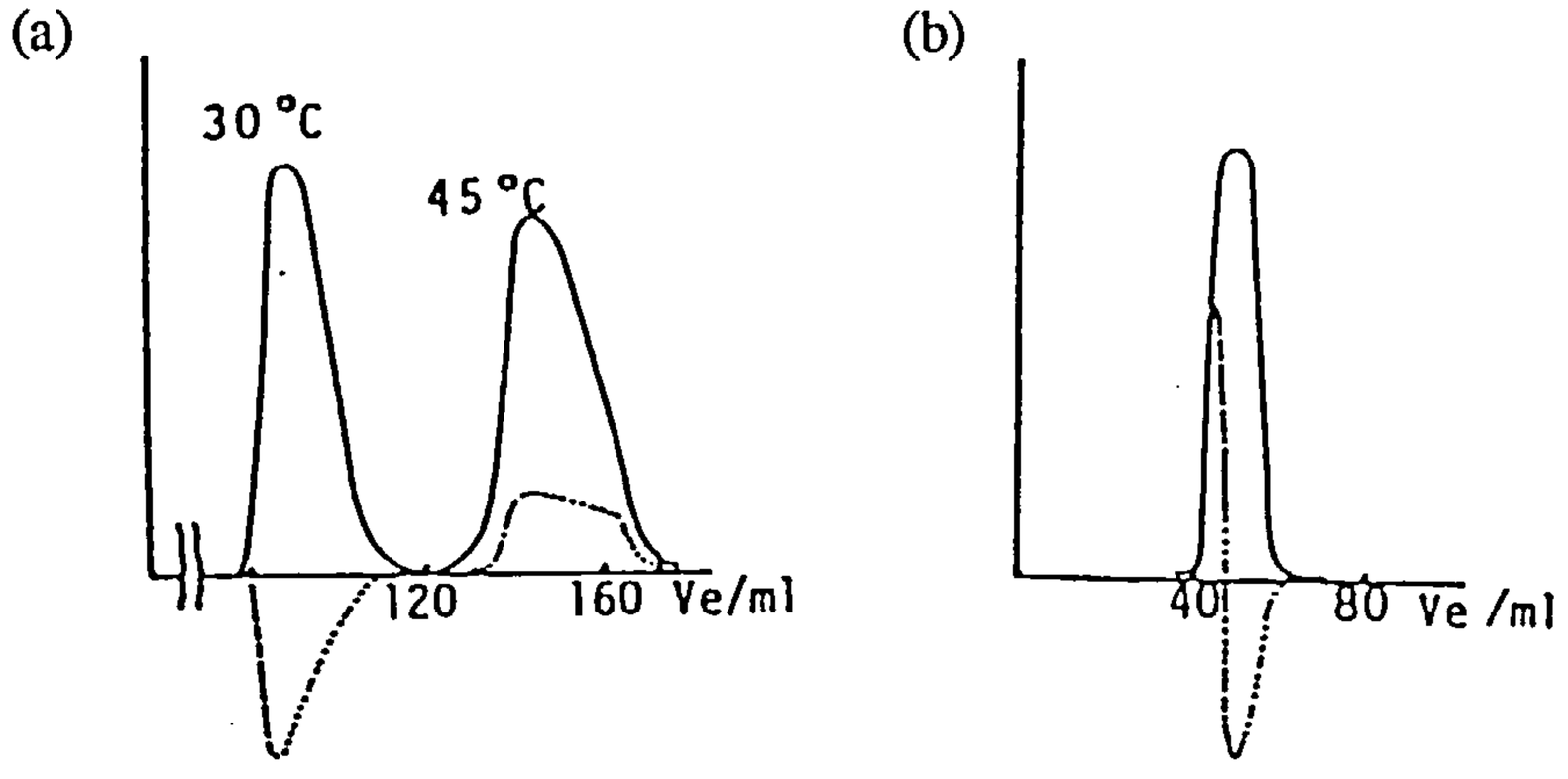

Figure 1-12 Chromatograms of Trogers base (for structure see appendix II, analyte K) (a) on MCCT (CTA-I) and (b) on CTA precipitated from acetone (CTA-II). Mobile phase: ethanol. Column length 160 mm. Solid lines, UV detection; dotted lines, optical rotation.

Hesse and Hagel[56] ascribed this observation to the fact that the original crystalline metastable polymorph of MCCT (also termed CTA-I) had become a more stable but less crystalline polymorph which they termed CTA-II. Therefore, since the crystallinity of the cellulose triacetate affected the enantioselectivity, they proposed that for Trogers base, interaction with the ester moiety was also accompanied by an inclusion mechanism.

In the following years many papers were published concerning the applications of MCCT.[57-62] However, MCCT had a few drawbacks including loss of enantioselectivity on dissolution, slow mass transfer which generally led to broad peaks and low mechanical stability.

In 1980, Okamoto *et al* [35] showed that the helical polymer (+)-PTrMA could be coated onto diphenyl bonded silica. The resulting phase showed higher chiral discrimination ability and mechanical strength than a phase made from the ground polymer. Shibata *et al* [63] have suggested that they were among the first to recognise the potential of similarly coating cellulose derivatives onto a solid support. However, at the time they still believed that crystallinity was an essential requirement. Therefore, they concentrated their efforts[63,64] on

investigating the relationship between the chiral discrimination ability and the crystalline structure of cellulose triacetate.

Their results showed that; (i) the discrimination ability of MCCT decreased with an increase in the degree of crystallinity and (ii) cellulose triacetate had chiral discrimination ability even if it was prepared under homogeneous conditions. By the time they realised this, Okamoto et al[65] had already reported on the enantioselectivity of cellulose triacetate coated onto macroporous (4000Å) aminopropylated silica (APS).

In general, the chiral recognition of the cellulose triacetate coated phase (CTA) was not superior to that of MCCT. However, the faster mass transfer led to narrower peaks and the much higher mechanical strength of this phase offered considerable advantages.

Almost immediately many more polysaccharide derivatives coated onto APS supports were reported by Okamoto *et al* [65-67] and Shibata *et al.*[63,68] Cellulose derivatives which exhibited good chiral recognition included benzoate, phenylcarbamate, nitrate, methylcarbamate, cinnamate and propionate. Phenylcarbamates of other polysaccharides such as amylose, xylan, curlan, chitosan, dextran and inulin were also synthesised and their enantioselectivity evaluated.[67] Okamoto *et al* [69,70] then showed that the chiral discrimination abilities could be enhanced by the introduction of substituents on the phenyl groups of the derivatives. Subsequently, the number of derivatised polysaccharide phases has increased considerably and many have been commercialised by Daicel (Table 1-1).

Table 1-1 Commercially available polysaccharide based chiral columns

Polysaccharide derivative	Trade Name
Microcrystalline cellulose triacetate	Chiralcel CA-1
Cellulose triacetate*	Chiralcel OA
Cellulose tribenzoate*	Chiralcel OB
Cellulose tris(phenylcarbamate)*	Chiralcel OC
Cellulose tris(3,5-dimethylphenylcarbamate)*	Chiralcel OD OD-H and OD-R
Cellulose tris(4-chlorophenylcarbamate)*	Chiralcel OF
Cellulose tris(4-methylphenylcarbamate)*	Chiralcel OG
Cellulose tris (4-methylbenzoate)*	Chiralcel OJ
Cellulose tricinnamate*	Chiralcel OK
Amylose tris(3,5-dimethylphenylcarbamate)*	Chiralpak AD
Amylose tris[(S)-1-phenylethylcarbamate]*	Chiralpak AS

* coated on bonded silica

Over the past eight years, the amount of literature emerging on the use of derivatised polysaccharides as chiral selectors has continued to rise at a rapid rate. The literature on polysaccharide derivatives will now be divided into sections so that a more detailed discussion can be carried out.

1.3.2 Cellulose Esters

MCCT has been known for over two decades now and has been used for the separations of a wide range of racemic compounds.[57-62] Compounds bearing an ionisable functional group such as carboxyl, hydroxyl or amino are generally poorly resolved on MCCT, but derivatisation of the analyte to the corresponding ester, carbamate or amide derivative often improves the

separation.[71] MCCT has a high loading capacity and the ease of preparation makes it an extremely useful material for preparative chromatographic purposes (see section 1.3.11).

The observed reversal of order for some analytes[54,64,65] on ground CTA-II and CTA coated onto APS compared to MCCT was particularly interesting since it demonstrated the importance of the highly ordered structure on resolving ability. During the preparation of CTA coated onto APS, Shibata *et al* [72] also noted that the enantioselectivity was influenced by the solvent used for the dissolution of the CTA. They found that a solvent of dichloromethane/phenol generally gave better selectivity than dichloromethane alone. They subsequently used solid state high resolution NMR and X-ray diffractograms to show that the former coating solvent yielded a higher order structure closer to that of MCCT than did the latter solvent.

Cellulose tribenzoate (CTB) and derivatives thereof also show high chiral recognition ability when adsorbed on macroporous silica gel.[63,64,70] The optical resolving abilities of the benzoate derivatives are dependent on the nature of the substituents on the phenyl group. Okamoto *et al* [70] investigated the influence of twelve substituted benzoates. In general they found that benzoates having a mild electron donating substituent such as a methyl group showed a higher chiral recognition than those having a mild electron withdrawing group such as chloro. They also found that CTB had very different chiral discriminating abilities to cellulose tris(4-methylbenzoate) (CTMB) eg. Trogers base gave an α of 6.05 on CTMB whereas on CTB there was no separation and 1-phenylethanol gave an α of 1.57 on CTB whereas on CTMB the α was only 1.17.

Wainer *et al* [73-75] have extensively investigated analyte interactions on CTB phases. They proposed that although the carbonyl group may be the most important adsorption site through dipole-dipole and hydrogen bonding interactions with the analyte, insertion of a portion of the analyte into a chiral cavity or ravine was also important (see section 1.3.8).

Recently, Francotte *et al* [76] reported the preparation of spherical beads of a pure polymeric form of benzoyl cellulose for HPLC. They pointed out that although the mechanical properties of the coated phases are advantageous, the cost of the bonded silica support is high and the low amount of chiral material compared to the silica support reduces the total loading capacity of the chiral phase. The benzoyl cellulose beads show good chromatographic properties (mechanical stability and efficiency) and in particular, potential for preparative applications (see section 1.3.11). A year later[77] they introduced ortho-, meta- and para-methylbenzoyl cellulose beads. These substituted benzoyl cellulose derivatives were found to be complementary, exhibiting different selectivities and often a reversal of elution order for the same analyte depending on the position of the methyl group. Therefore, a much broader range of analytes can be separated on these pure polymer phases.

1.3.3 Cellulose Phenylcarbamates

As observed for the CTB phases, the optical resolving ability of the cellulose tris(phenylcarbamate)-coated phases also depends on the nature of the substituents on the phenyl groups.[69] For a series of 4-substituted phenylcarbamates (Figure 1-13), those having mildly electron-donating substituents such as alkyl or mildly electron-withdrawing such as halogen, showed higher selectivity than the unsubstituted cellulose tris(phenylcarbamate) (CPC). It was proposed[69] that this was due to the changes in the polarity of the urethane group, which was thought to be the main adsorption site. However, the derivatives with methoxy or nitro groups (strongly electron donating and withdrawing respectively) showed low chiral recognition and this was thought to be due to analytes interacting with these very polar external groups and thus being prevented from approaching the main chiral discrimination site.

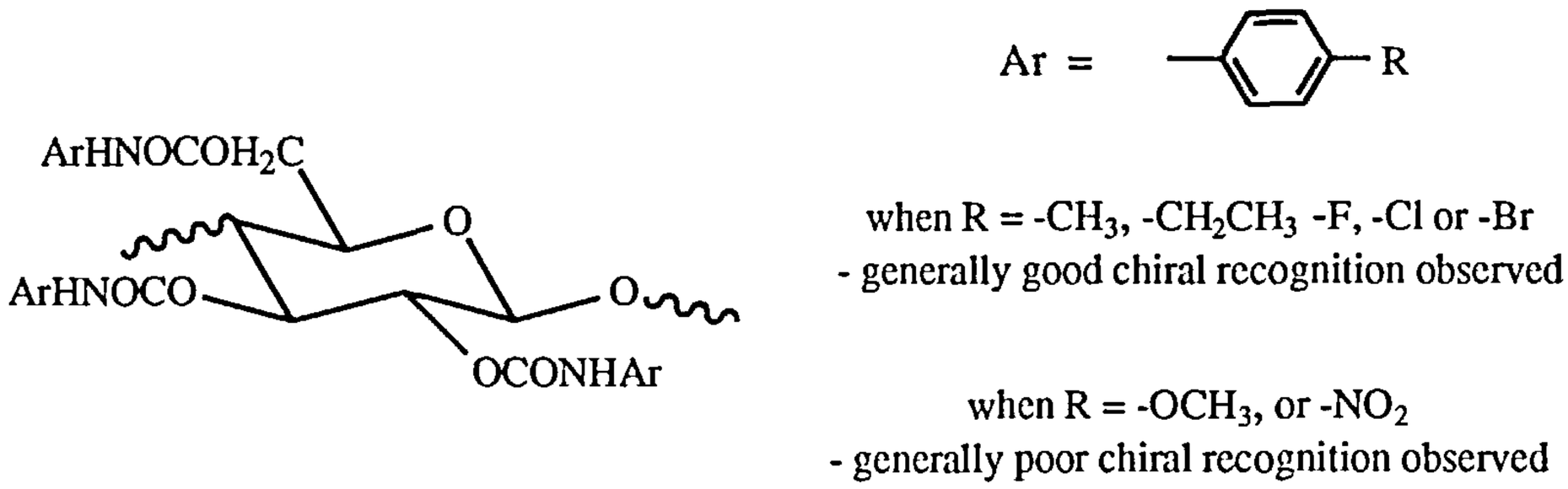

Figure 1-13 Series of para-substituted cellulose tris(phenylcarbamate)s investigated by Okamoto et al[69]

The position of the substituent on the phenyl group can also influence the chiral discriminating ability. Various mono substituted phenylcarbamates were examined.[69] The derivatives with substituents in the 3- or 4- position showed higher chiral recognition than derivatives with a substituents in the 2- position. In the case of the 3- and 4- substituents, liquid crystal phases formed when dissolved in the solvent used for coating and it was inferred from this that these derivatives may possess a regular high order structure on the silica surface. In contrast, liquid crystallinity was not observed for the 2- substituted derivative. It was proposed that substituents at the 2- or 6- positions, in addition to obscuring the chiral discrimination site, were preventing the phenylcarbamate from adopting a regular high order structure.

Several dimethylphenyl and dichlorophenyl derivatives were also prepared.[69] Not surprisingly, those with substituents in the 2- and 6- positions did not show good chiral recognition compared to those with substituents at the 3- and 4- or 3- and 5- positions. Both the 3,5-dimethylphenylcarbamate (Figure 1-14) and 3,5-dichlorophenylcarbamate of cellulose (CDMPC and CDCPC respectively) were found to demonstrate a particularly high chiral discrimination ability.[78] However, the CDCPC was found to be of less utility because of its high solubility in mobile phases containing >10% 2-propanol. As an indication of the success of CDMPC, during the resolution of 510 racemates on CDMPC it

was observed that 229 were completely resolved and 86 partially resolved, ie. approximately 62% in total.[79]

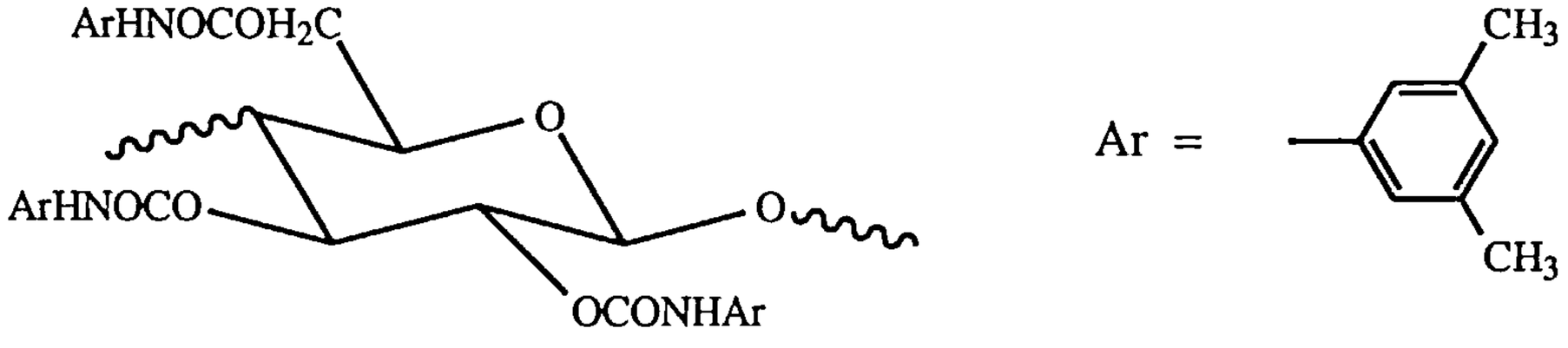

Figure 1-14 Structure of cellulose tris(3,5-dimethylphenylcarbamate).

Other derivatives, reported more recently are the 1-phenylethyl carbamate[80,81] and chloromethylphenylcarbamate.[82,83] In the case of the carbamate with a chiral side chain, the (R)-, (S)- and (R,S)-1-phenylethyl-carbamates were evaluated and the selectivity was found to be dependent on the nature of the chiral centre in the side chain. The chloromethylphenylcarbamates were prepared to investigate the effect on enantioselectivity of introducing both an electron withdrawing and electron donating group on the phenyl moiety. In contrast to the dichlorosubstituted derivatives, the 3-methyl-4-chlorophenyl and 3-chloro-4-methylphenylcarbamates were found to have good stability and high selectivity.

The cellulose phenylcarbamate derivatives have also been applied to techniques other than HPLC for the separation of racemates. Kaida and Okamoto[84] and more recently Whatley[85] demonstrated that the commercial cellulose phases can be used in an SFC mode. Juvancz *et al* [86] used a mixture of an achiral polymer and benzoyl cellulose to coat open tubular columns which were subsequently successfully used in an SFC mode. In a further novel use of the cellulose derivatives, Yashima *et al* [87] attempted to use a membrane coated with CDMPC to achieve stereoselective diffusion. Although none was observed, they demonstrated that the coated membrane could be used to adsorb the racemate and then by reducing the organic content of the solvent, one

enantiomer could be selectively desorbed, thus providing an enantiomerically enriched solution.

Overall, it has been shown that the cellulose tris(phenylcarbamate)s can be applied to a very wide range of analytes without the need for derivatisation. Okamoto has referenced many of the separations achieved on the commercial columns in a recent review article.[79]

1.3.4 Amylose Phenylcarbamates

Amylose has the same monomer unit as cellulose, but the D-glucose units are joined by an α-linkage, which causes amylose to form a helical structure.[79] Early interest concentrated mainly on the amylose tris (phenylcarbamate) and the tris(3,5-dimethyl- and 3,5-dichlorophenylcarbamate)s (APC, ADMPC and ADCPC respectively).[67,78] The highest chiral recognition for most analytes was found to be exhibited by ADMPC.

Although, as with the cellulose derivatives, it is proposed that the most important adsorbing site is the carbamate link, the optical resolving abilities of the amylose derivatives are different to those of the corresponding cellulose derivatives. For instance, propranolol and pindolol[88] are well resolved on CDMPC, but are not well resolved on ADMPC, whereas, verapamil and oxyphencyclimine and many of the 2-arylpropionic acids[89] can be resolved on ADMPC, but not on CDMPC. In addition, the (S)-methyl-benzylcarbamate derivative of amylose (Figure 1-15) has significantly better chiral discriminating ability compared to the corresponding cellulose derivative.[80] For example, β-lactams[81] and sulfoxides[90] were extremely well resolved on this phase.

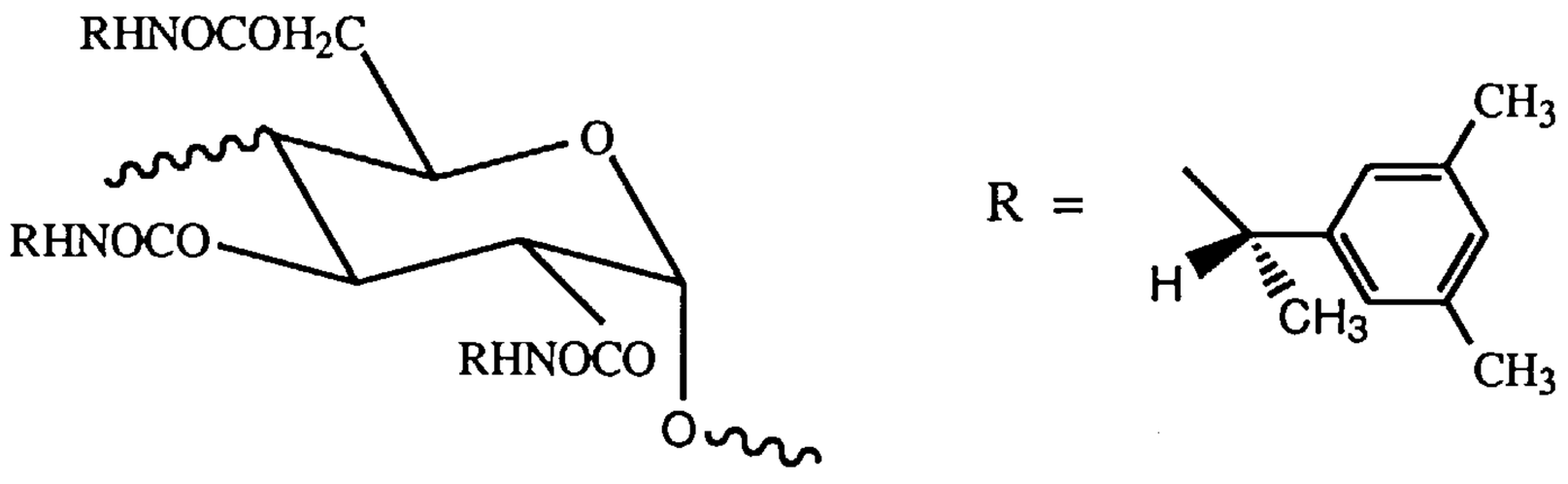

Figure 1-13 Structure of amylose tris[(S)-methylbenzylcarbamate]

In contrast to the cellulose tris(phenylcarbamate)s, there had been virtually no reported investigations into the effects that the type and position of substituents on the phenyl group of amylose derivatives had on enantioselectivity. However, recently Chankvetadze *et al* [93] prepared twelve dimethylphenyl-, dichlorophenyl-, and chloromethylphenylcarbamate derivatives of amylose. Interestingly, they found that the 5-chloro-2-methylphenylcarbamate exhibited the highest chiral recognition ability. This is in contrast to the cellulose derivatives in which an ortho substituent appears to upset the high order structure and lower the chiral recognition ability. Okamoto *et al* [81] have proposed that these contrasting observations are due to the different configuration of the glucose residues and high order structure.

Fortunately, as indicated by the examples above, the chiral discriminating ability of the phenylcarbamate derivatives of cellulose and amylose are often complementary and Okamoto and Kaida[79] have reported that in the optical resolution of 510 racemates by CDMPC and ADMPC, 400 (78%) of the racemates have been resolved on at least one of the two phases.

1.3.5 Other Polysaccharide Derivatives

Phenylcarbamates of other polysaccharides such as xylan, curdlan, chitosan, dextran and inulin were also synthesised in 1984.[67] However, in contrast to the derivatives of cellulose and amylose, there has been very little

information published about their performance as chiral phases. Of the few resolutions, that of nicaldipine,[92] a calcium ion antagonist, has been demonstrated on a xylan tris(3,5-dichlorophenyl carbamate)-coated phase and very recently, Cass *et al* [93] presented data demonstrating the resolution of various racemic compounds on a chitin diphenylcarbamate phase.

In 1993, Felix and Zhang[94,95] reported the use of amylopectin tris(phenylcarbamate) derivatives coated onto aminopropylated silica and demonstrated the resolution of several chiral analytes. They noted that, as with cellulose and amylose tris(phenylcarbamate)s, the resolution depended greatly on the type, position and number of substituents on the phenyl groups and that the amylopectin derivatives exhibited a different mechanism of separation to the cellulose and amylose derivatives.

1.3.6 Oligosaccharide Phenylcarbamates

In an attempt to obtain information about the influence of the high order structure of the polysaccharide derivatives, Aburatani *et al* [96] prepared 3,5-dimethylphenylcarbamates of linear oligomers of cellulose (cello-oligosaccharides) and amylose (maltooligosaccharides). In the case of the carbamates of the maltooligosaccharides (4 to 7 units), their chiral discrimination abilities were similar and not so different from the ability of ADMPC. However, the chiral recognition abilities of the carbamates of cellooligosaccharides (4 to 7 units), were lower than that of CDMPC. The lower chiral recognition of the cellooligosaccharide derivatives was attributed to the less ordered structure as indicated by circularly dichroism spectra.

Interestingly, Okamoto[97] recently reported that Daicel now use 6 to 8 unit maltooligosaccharide derivatives in their Chiralpak columns, the so-called amylose tris(phenylcarbamate)-coated columns.

1.3.7 Bonded Polysaccharide and Oligosaccharide Derivatives

One of the major drawbacks of the derivatised cellulose phases (coated or pure polymer) is that only a limited range of mobile phases such as hexane/alcohol or alcohol/water mixtures can be used. Solvents such as THF, dichloromethane and dioxan cannot be used because they swell or dissolve the polymer. In particular, it was the high solubility of the 3,5-dichloro derivative (CDCPC) in mobile phases with greater than 10% alcohol[78] that prompted Okamoto *et al* [98] to attempt to bond this derivative to APS using a diisocyanate. The bonded derivative was found to be stable over a range of solvents, but was found to exhibit lower chiral recognition than the coated version. Similar results were obtained for a bonded CDMPC derivative.

Despite continuous calls from industry for a chemically bonded phase which has wider solvent stability but has the chiral discrimination power of the current commercially available coated phases, it was not until very recently that literature has emerged on the subject again. Yashima *et al* [99] investigated the influence the amount of diisocyanate used for immobilisation and the hydroxy position used to regioselectively bond CDMPC and ADMPC to APS had on chiral recognition. Again, in many cases the coated phase had significantly higher chiral recognition ability than the bonded phases. However, they were able to demonstrate the separation of a few racemates which were unresolved or poorly resolved on the coated-type phases (Figure 1-16).

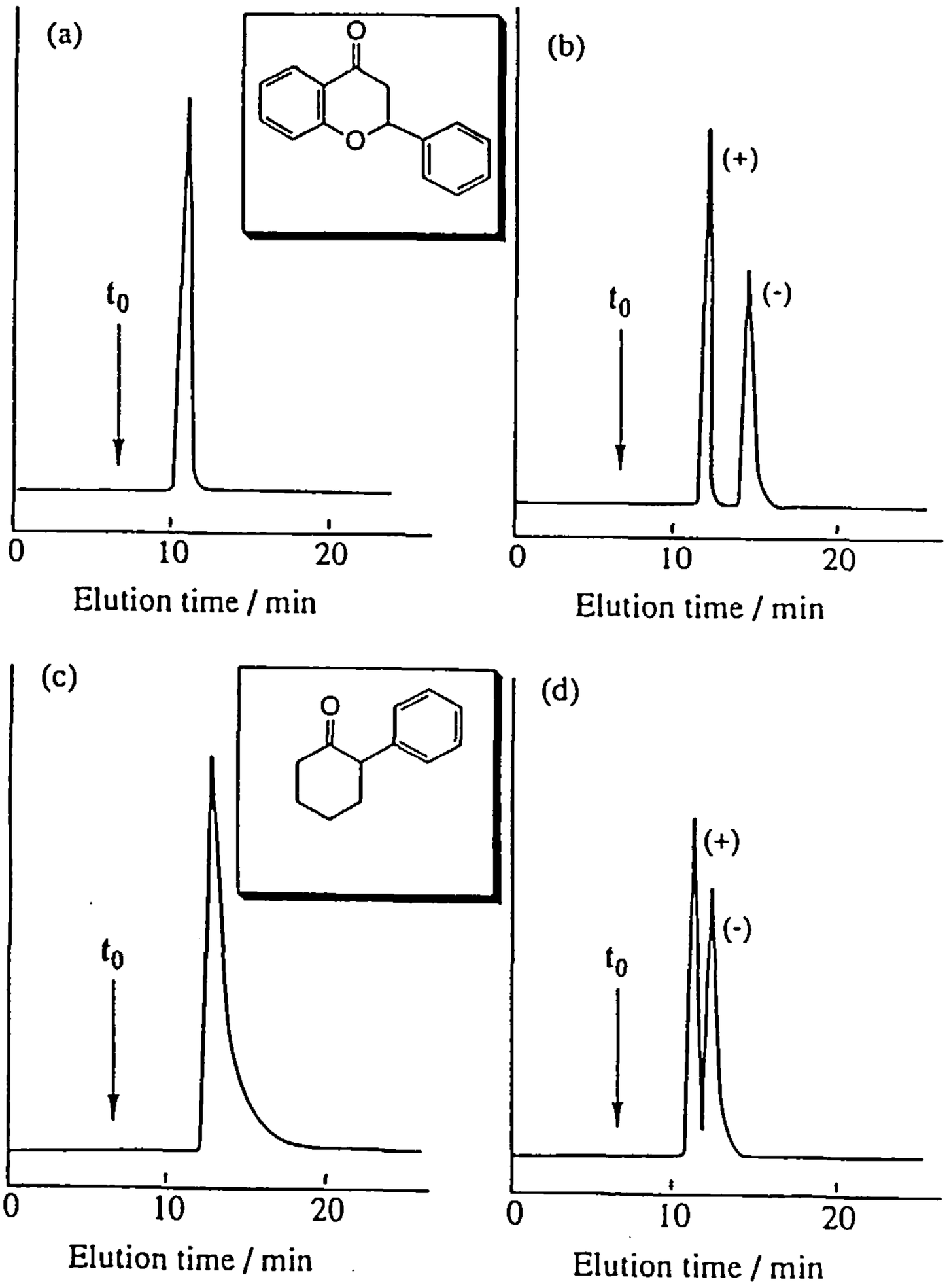

Figure 1-16 Separation of flavanone (a and b) and 2-phenylcyclohexanone (c and d) on a column packed with ADMPC bonded at the 6-postion to APS using mobile phases of hexane/2-propanol (90:10 v/v) (a and c) and hexane/chloroform (95:5 v/v) (b and d)

In addition, some interesting observations were made. It was found that for both CDMPC and ADMPC, a bonded phase prepared using a low amount (3 mol-%) of diisocyanate gave a higher chiral recognition ability than a phase prepared using a higher amount (10 mol-%) of diisocyanate. The enantioselectivity of the CDMPC immobilised phase was hardly affected by the position of the hydroxyl group used for immobilisation, whereas for ADMPC

immobilisation at the 6- position gave a higher chiral recognition than at the 2- or 3- positions. This latter result will be discussed in more detail in section 1.3.8.

In contrast, Oliveros *et al* [100] approached the issue of immobilisation from a different direction. They investigated the chiral recognition ability of a cellulose 3,5-dimethylphenylcarbamate and 10-undecenoate mixed derivative that was fixed to several different supports by adding a cross-linking agent. For the majority of supports, such as underivatised silica or graphite, the chiral phase was held on the surface by self-polymerisation, whereas for allyl silica, it was assumed that the undecenoate group cross-linked with the allyl group on the silica to form a bonded phase. Whilst the separations again were lower than on the CDMPC-coated phases, satisfactory separations were achieved for a variety of racemates and they found that a mobile phase of heptane/chloroform gave the best results. They have since investigated[101] the influence of support porosity and degree of fixation on the allyl silica bonded phase on enantioselectivity in an attempt to determine the optimum preparation conditions.

Very recently, Stalcup and Williams[102] reported on the preparation of 1-(1-naphthylethylcarbamate)s of maltooligosaccharides (mix of 2 to 8 units) bonded to a silica support. They noted several interesting observations about the extent of derivatisation and the degree of separation of 3,5-dinitrobenzoyl derivatives of racemic amines, amino acids and aminoalcohols. However, because of their choice of derivative and analyte, strong π-acid/π-base solute-CSP interactions were induced. Therefore, it was difficult to say whether the carbohydrate was playing a significant role in the chiral recognition process.

1.3.8 Chiral Discrimination Mechanism

The differences in enantioselectivity between the various polysaccharide derivatives have been discussed in the previous sections (1.3.2 to 1.3.7). Many

of the observations were explained by changes in the high order structure of the derivatised polysaccharide. In this section, some of the evidence discussed in the literature relating to the chiral interaction mechanism on the derivatised polysaccharide phases will be presented.

A chiral recognition mechanism for phenyl substituted analytes on MCCT was proposed by Hesse and Hagel,[54] Blaschke[103] and Francotte et al[104] This mechanism involves the penetration of a portion of the solute into cavities that are formed between the derivatised glucose units of the phase. It was proposed that the enantioselectivity was then due to differences in fit or inclusion of the enantiomers in the cavities of the phase. However, large molecules which would not be expected to intercalate between the chains were also separated, suggesting that adsorptive interactions were possible.

The reversal in enantiomeric elution order between MCCT and CTA-coated onto APS indicated a different mechanism for the two phases. Francotte and Junker-Buchheit[105] suggested that MCCT generally showed strong selective inclusion mechanisms characterised by slow sorption kinetics, whereas the coated CTA phase generally showed rapid but less selective adsorption-desorption processes.

Wainer *et al* [73-75] published several papers concerning the chiral discrimination of enantiomeric amides and aromatic alcohols on a cellulose tribenzoate column (Chiralcel OB). They probed the mechanism by investigating the effect on enantioselectivity when different alcoholic (molecular weight and steric bulk) mobile phases modifiers (MPMs) were used. They noted that MPMs compete for both chiral and achiral binding sites on the phase and may also bind to sites at or near the cavities, thus changing the steric environment. In addition they observed[106] a reversal of elution order for 2-phenoxypropanoic acid methyl ester as the steric bulk of the secondary alcohols changed, suggesting that two different chiral binding sites were in operation.

For the enantiomeric amides, Wainer *et al* [73,74] proposed that the chiral discrimination mechanism was due to; (i) the formation of diastereomeric analyte-CSP complexes through attractive interactions between the amide moiety of the analyte and the ester moiety of the CSP, (ii) the positioning of the analyte and the CSP within the complex and (iii) the steric fit of the aliphatic portion of the solute in the chiral cavity of the CSP. A similar mechanism was proposed by them[75] for the aromatic alcohols.

Okamoto *et al* [69] investigated the influence of substituted phenylcarbamates of cellulose on the enantioselectivity of several racemates. They showed by NMR that the electron withdrawing or donating effect of the substituent would affect the polarity of the urethane group. An electron withdrawing group, eg. chloro, increased the acidity of the N-H group (shifted downfield in NMR) and hence the retention time of analytes which interacted at this site were increased. An electron donating group, eg. methyl, increased the electron density of the C=O and hence the retention time of analytes which interacted at this site were increased.

Okamoto *et al* proposed[69] that interactions took the form of hydrogen bonding with N-H and C=O (Figure 1-17), dipole-dipole interactions with C=O or π-π interactions with the aryl group.

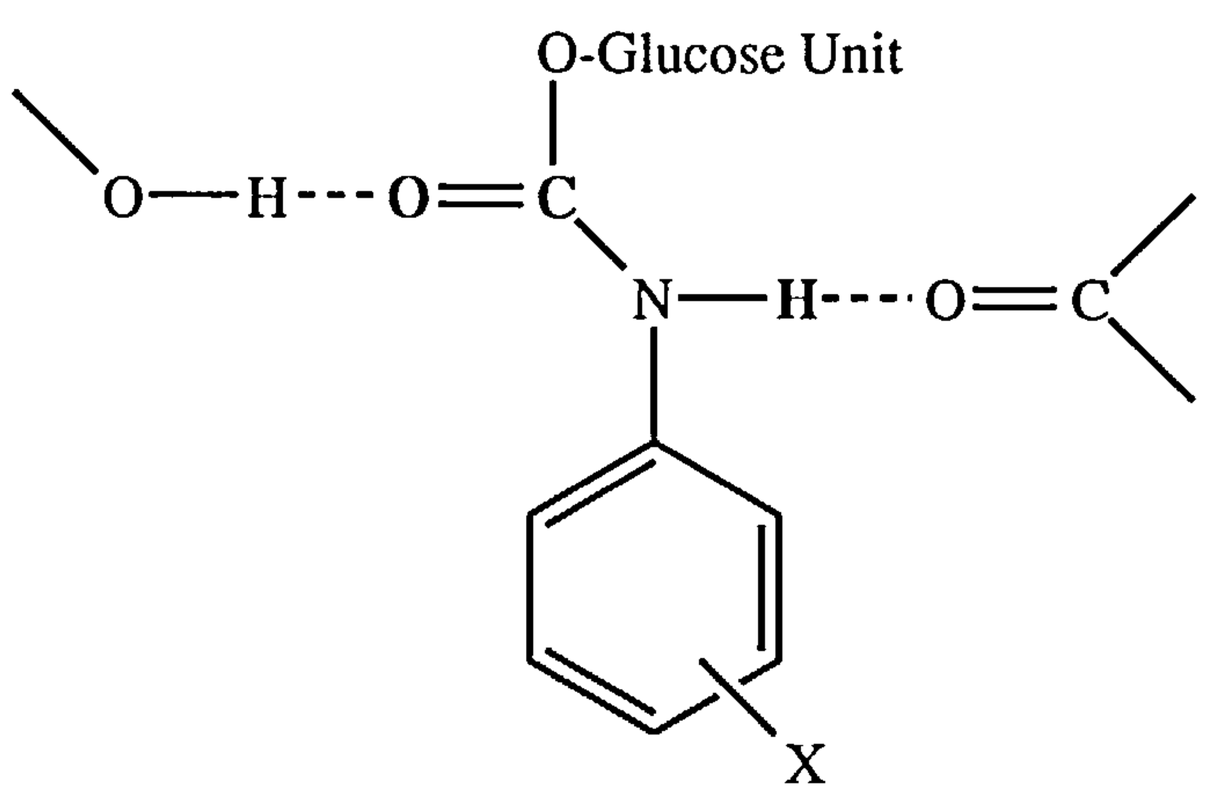

Figure 1-17 Illustration of hydrogen bonding interactions possible on phenyl carbamate derivatives.

Very recently, Chankvetadze *et al*,[73,91] whilst investigating the enantioselectivity of chloromethylphenylcarbamates of cellulose and amylose, looked more closely at the adsorption powers of the N-H group. Using infra-red (IR) to investigate the amount of 'free' and hydrogen bonded N-H, they proposed that the N-H groups of the carbamate moieties will contribute to the chiral recognition as local chiral adsorbing sites for the analyte and also by maintaining a high order structure via molecular bonding to other carbamate chains. Too little hydrogen bonding appeared to lead to a phase which was not stable eg. 3,5-dichlorophenylcarbamate[78] whilst too much hydrogen bonding appeared to lead to low enantioselectivity.

In 1986, from the H^1 NMR data concerning the shifts observed for the N-H resonance of CPC when pyridine was added to the solution, Okamoto *et al* [69] suggested that the three carbamate groups on each sugar unit possess different adsorbing powers. However, it was not until very recently when Yashima *et al* [99] investigated the regioselective bonding of the phenylcarbamates of cellulose and amylose, that it became possible to probe the adsorption differences between the 2-, 3 -and 6- positions. They found for CDMPC that the position of immobilisation on APS hardly affected the chiral recognition, whereas ADMPC regioselectively bonded at the 6- position generally possessed a higher optical resolving power than when immobilised by the 2- or 3- positions. This suggested that in the case of amylose, enantioselective discrimination occurs mainly on the carbamates at the 2- and 3-positions.

These results complemented the 3D structures of cellulose and amylose predicted by Vogt and Zugenmaier.[107] For cellulose, Vogt and Zugenmaier suggested a threefold (3/2) helix with the hydroxyl groups at the 2-, 3- positions of one glucose unit and the 6- position on a neighbouring unit located close together, thus allowing racemates to simultaneously interact with all three positions. However, for amylose, they suggested a left-handed fourfold (4/1)

helix in which the 2- and 3- positions of a glucose unit were remote from the 6-position of neighbouring units.

The predictions by Vogt and Zugenmaier[107] for the structure of cellulose were also used recently by Yashima *et al* [108] in order to perform computational studies in an attempt to gain greater understanding of the chiral discrimination mechanism of CPC. The structure of CPC was constructed based on the predictions by Vogt and Zugenmaier and the interaction energies between the enantiomers of trans stilbene oxide (TSO, for structure see appendix II, analyte A) and CPC were calculated. The calculations suggested that the most important adsorbing site for TSO on CPC was the N-H protons of the carbamate moieties at the 3- position of the glucose units and that the (S)-isomer of TSO interacts more closely than the (R)-isomer. The molecular modelling predictions agreed with the observed elution order for the chromatographic separation of TSO on CPC.

NMR spectroscopy has also been shown to be a useful technique for revealing the chiral recognition at a molecular level, especially for small molecule CSPs.[109,110] However, most of the polysaccharide derivatives with high chiral discriminating ability are only soluble in polar solvents such as THF, acetone and pyridine. In such solvents, enantioselectivity cannot be observed because of the strong interactions between the solvent and the CSP at the chiral binding sites.[69] However, recently Yashima *et al* [111] found that cellulose tris(4-trimethylsilylphenylcarbamate) (CTSP) was soluble in chloroform. They noted that in the H^1 NMR of TSO, the methine protons of the oxirane ring were enantiomerically discriminated to show a set of two peaks in the presence of CTSP in $CDCl_3$. Competition experiments between TSO and acetone for CTSP suggested that, as proposed by the molecular modelling, TSO appears to be adsorbed on the N-H proton.

Most recently, Oguni *et al* [112] examined the ^{13}C NMR spectrum of 1-phenylethanol (1-PE) in the presence of cellulose tris(4-methylbenzoate)

(CTMB) dissolved in $^{13}CHCl_3$ and attempted to determine the position at which 1-PE is chirally recognised. However, they noted that their solution data may not reflect the real interactions in an HPLC packed column using hexane/2-propanol as the mobile phase.

The multiple interaction possibilities provided by the polysaccharide derivatives make prediction of the separation very difficult. However, it should be remembered that it is these multiple interaction sites that provide these phases with their broad applicability and hence the reason why they are so extensively used. The complex nature of these interactions will probably mean that the resolution mechanisms on the polysaccharide derivatives will remain obscure for some time to come. However, with the advent of ever more sophisticated molecular modelling programs and the new physical techniques developed for probing structures, it may be hoped that there will be increased attention given to tackling this challenging problem.

1.3.9 Choice of Derivatised Polysaccharide Phase

The structural factors and functional group selectivity requirements for resolution of chiral analytes have been intensively investigated. Ichida *et al* [64] were among the first to suggest structural features and solvents which generally led to successful resolutions on cellulose triacetate, tribenzoate, tris (phenylcarbamate), tribenzylether and tricinnamate columns. Later, Aboul-Enien and Islam[113] published a more thorough review discussing the structural factors affecting the chiral recognition and separation on cellulose based phases. They presented a simple guide to aid the choice of the appropriate derivatised cellulose phase for the required application.

Perhaps not surprisingly, Daicel[114] have a different approach to the selection of the most appropriate column. They noted that of the many hundreds of chiral separations carried out on the derivatised polysaccharide phases, several

columns in particular have greater versatility than the others. Therefore, Daicel reccommend the purchase and screening of four columns: Chiralcel OD, Chiracel OJ, Chiralpak AD and Chiralpak AS (see Table 1-1) since they claim that 70 to 80% of the samples they receive for analysis can be separated on one or more of these columns.

1.3.10 Operational Conditions

Separations on MCCT[57-62] have generally been carried out using a mobile phase of ethanol/water, since this combination appears to provide a suitable amount of swelling of the MCCT structure.

In contrast, the majority of separations on the derivatised polysaccharide-coated phases have been generated using normal phase conditions. For neutral analytes, a mobile phase of hexane/2-propanol is often cited. However, the addition to the mobile phase of a silanol suppressor such as diethylamine (0.1% v/v) for basic analytes,[115] or an ionisation suppressor such as trifluoroacetic acid (0.5% v/v) for acidic analytes,[116] has been recommended to reduce peak tailing. It is also possible to use other organic mobile modifiers such as methanol, ethanol and higher straight chain and branched alcohols and these can have a dramatic effect on the separation of the racemate.[73,75,117]

Ichida *et al* [118] demonstrated that it was also possible to use reversed phase conditions. They found that perchlorate buffer/acetonitrile eluents could be used with a CDMPC-coated phase for the resolution of a few drugs such as verapamil and propranolol and that the resolution was greatly influenced by the pH and buffer of the eluting system. Later Ishikawa and Shibata[119] conducted a more thorough investigation. They noted that a simple mixture of water and acetonitrile was suitable for neutral racemates, for basic racemates it was necessary to add an anionic ion-pair reagent such as perchlorate and for acidic

racemates, the addtion of a strong acid such as perchloric acid gave the best results. See Figure 1-18.

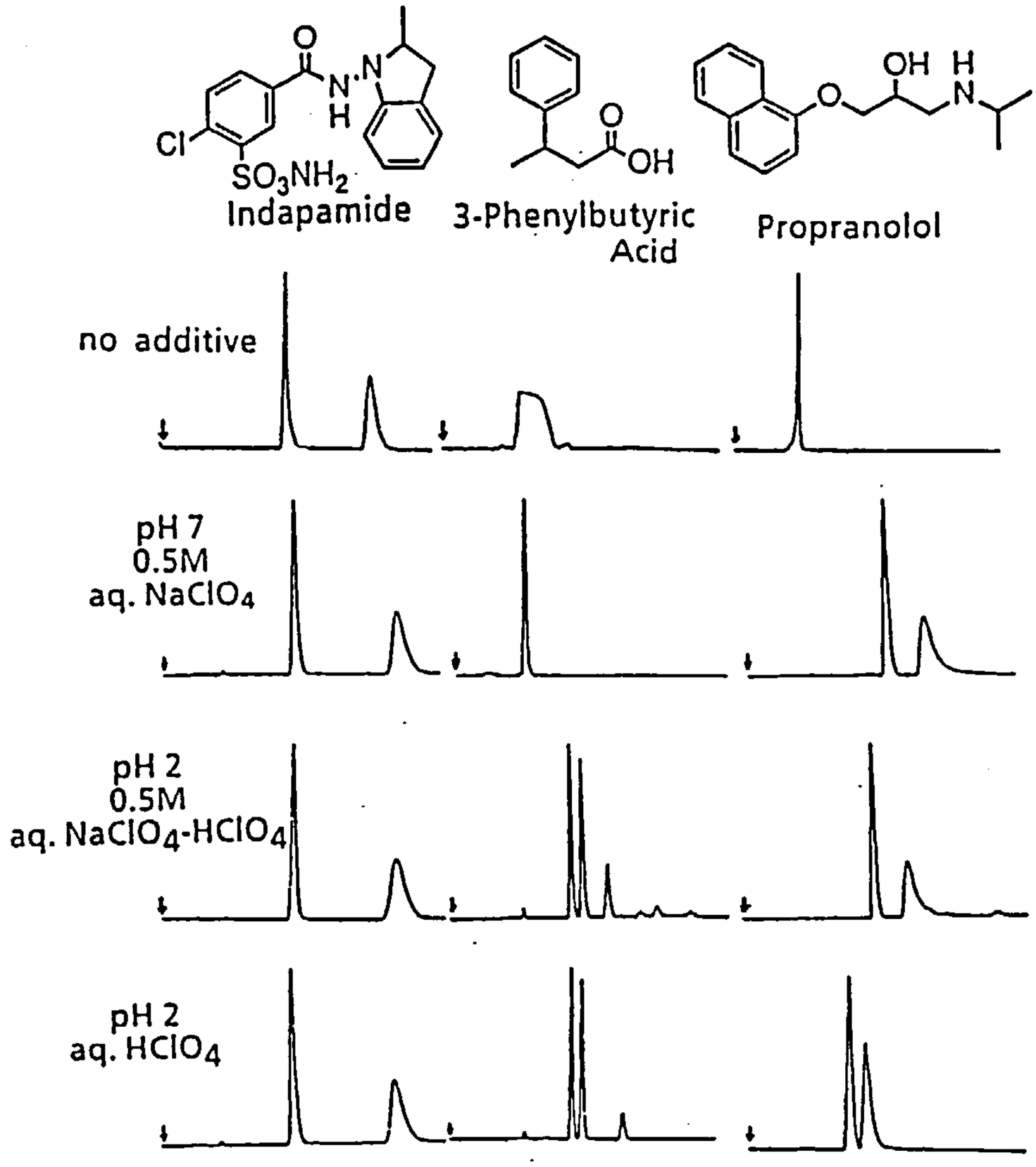

Figure 1-18 Separation of neutral (indapamide), acidic (3-phenylbutyric acid) and basic (propranolol) on a Chiralcel OD-R using four kinds of mobile phase. No additive = acetonitrile/water (60:40 v/v). Other mobile phases contain 60:40 v/v acetonitrile/aq phase quoted at side of chromatogram. Flow rate: 0.5 ml/min.

The number of reported separations using reversed phase conditions is still very small compared to those reported on normal phase. Successes such as the reversed phase separation of verapamil and trimepramine,[118-120] which could not be separated under normal phase conditions, are exceptions. However, the reversed phase system does provide an alternative mechanism for the

separation and has proved to be most useful with analytes that have limited solubility in hexane mixtures and in the direct analysis of biological samples.

Temperature can also be used to control the elution of racemates on the derivatised polysaccharide phases. However, the effect of temperature on the resolution depends very much on the racemate under examination.[121,122] Dingenen[117] illustrated the effects of temperature on the retention and separation of several isomers of nebivolol, an aminoalcohol with 4 chiral centres, on a Chiralpak AD column (ADMPC). For this example, the optimum temperature was found to be 45°C. He also noted that the optimisation of temperature can be particularly useful when conducting preparative separations on a large scale or if separation can only be obtained at long retention times.

1.3.11 Preparative Separations

By far the most widely used chiral preparative sorbent is MCCT,[105] its main advantages being its easy and cheap preparation, high versatility and high loading capacity. These advantages largely compensate for the drawbacks which include (i) the relatively slow kinetics of the adsorption-desorption process, resulting in peak broadening and thus reduced resolution and (ii) the dissolution or strong swelling of the phse in numerous solvents such as chloroform, THF and acetone. The influence of factors such as flow rate, temperature, eluent compositon and loading capacity on the enantioselectivity of MCCT have been investigated by workers such as Rimbock *et al* [123], Rizzi[124] and Isaksson *et al*.[125] Recently Francotte and Junker-Buchheit[105] presented a review in which many of the separations that have been achieved on MCCT were reported.

In contrast to MCCT, the number of preparative separations reported on the coated polysaccharide derivatives is very small.[24] It has been proposed[24] that the reason for their slow acceptance is due to the high cost of the columns and lower sample loading capacity compared to MCCT. However, the number

of applications is beginning to increase, perhaps helped by papers such as that by Miller *et al* [126] in which they describe the systematic development of a preparative chiral separation, from chosing the most suitable derivatised polysaccharide coated phase through to automation of the optimised method.

The new benzoyl and methylbenzoyl cellulose beads developed by Francotte and Wolf[76,77] may become more widely used for preparative separations in the near future. The versatility, low preparation costs (since they do not contain silica) and high loading capacity make these phases ideal sorbents for preparative applications. Unfortunately, due to patent issues, they are not yet commercially available.

1.3.12 Summary

The recent description of the derivatised polysaccharide phases as 'Beauty and the Beast' by Bopp *et al* [114] is very apt. 'Beauty' was used to emphasize the fact that these phases are close to universal in their applications and have been highly successful in separating a wide variety of chiral compounds. On the other hand, the mechanism for separation is not fully understood, hence the 'Beast'. However, we expect, in the near future, to see further work in search of a highly selective derivatised polysaccharide phase which overcomes the problem of solvent incompatability observed for the coated phases and also intense work to continue to gain greater understanding of the chiral recognition mechanism.

1.4 PREPARATION AND EVALUATION OF CELLULOSE TRIS(PHENYLCARBAMATE)-COATED PHASES

1.4.1 Reaction of Cellulose with Isocyanates

Cellulose tris(phenylcarbamate) derivatives can be easily prepared in good yields by the reaction of cellulose with an excess of phenyl isocyanate in the presence of an organic base such as pyridine (Figure 1-19).[127]

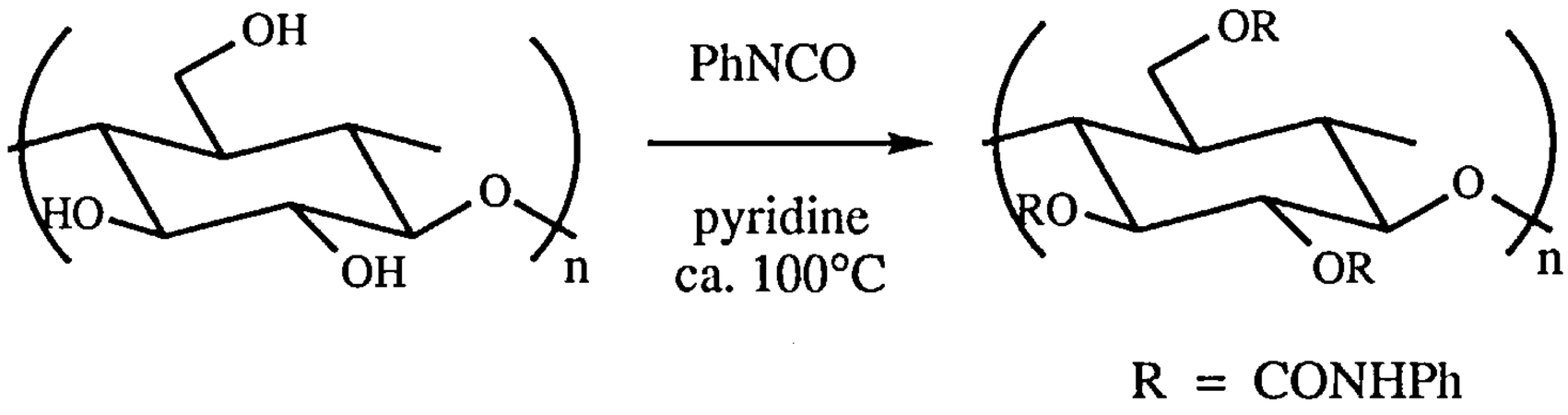

Figure 1-19 the reaction of cellulose with phenyl isocyanate.

The extent of derivatisation depends on the nature of the cellulose material, the concentration of the isocyanate, the temperature and the reaction time employed. A proposed reaction mechanism is shown in Figure 1-20.

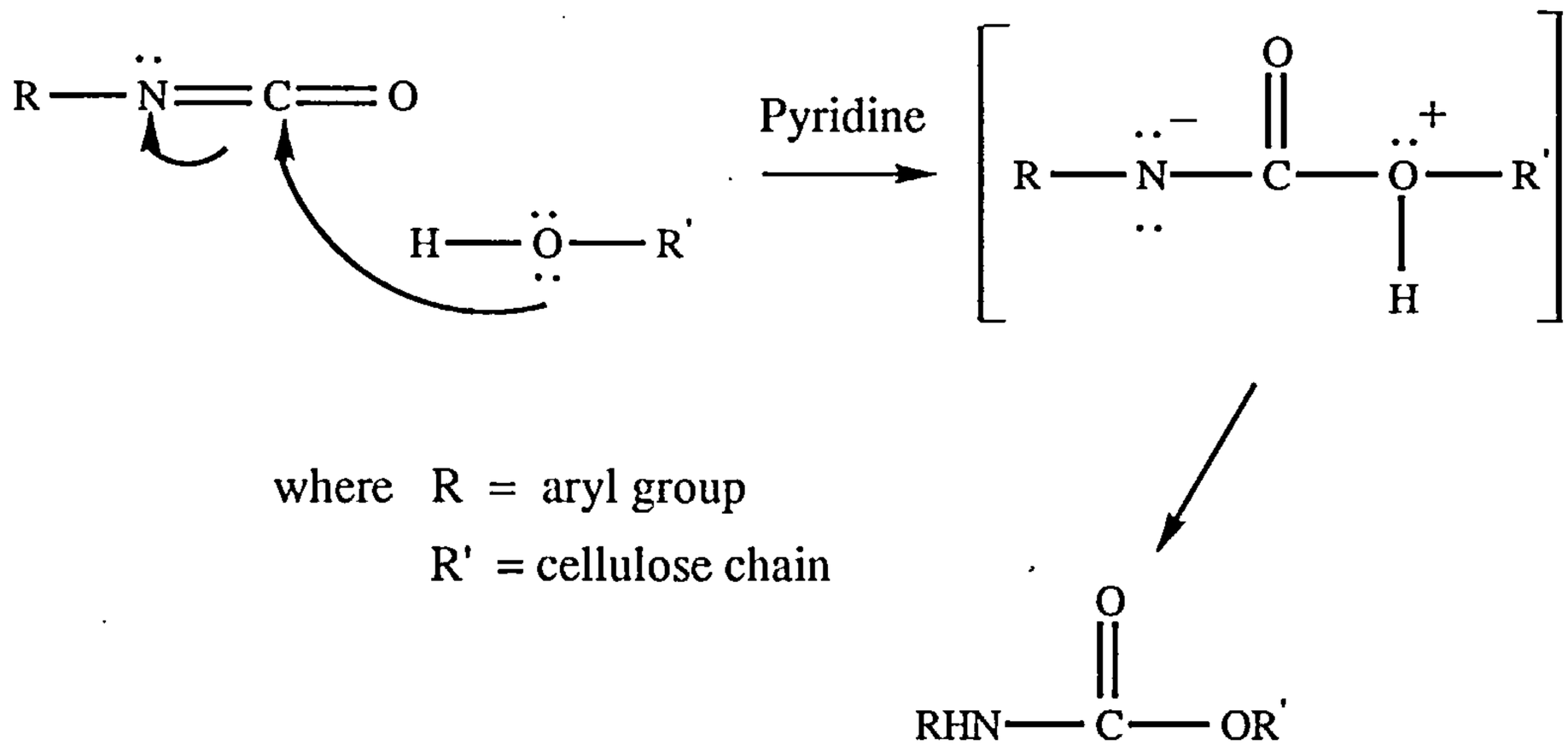

Figure 1-20 Mechanism for reaction of cellulose with an isocyanate

The mechanism involves nucleophilic attack by the cellulose hydroxyl groups on the carbonyl carbon of the isocyanate to form an intermediate which may be assisted by the presence of a Lewis base catalyst such as pyridine.

The reaction should be carried out in anhydrous conditions, since the isocyanate can react with water to form a symmetrical urea (Figure 1-21) which would be a nuiscance to remove later.

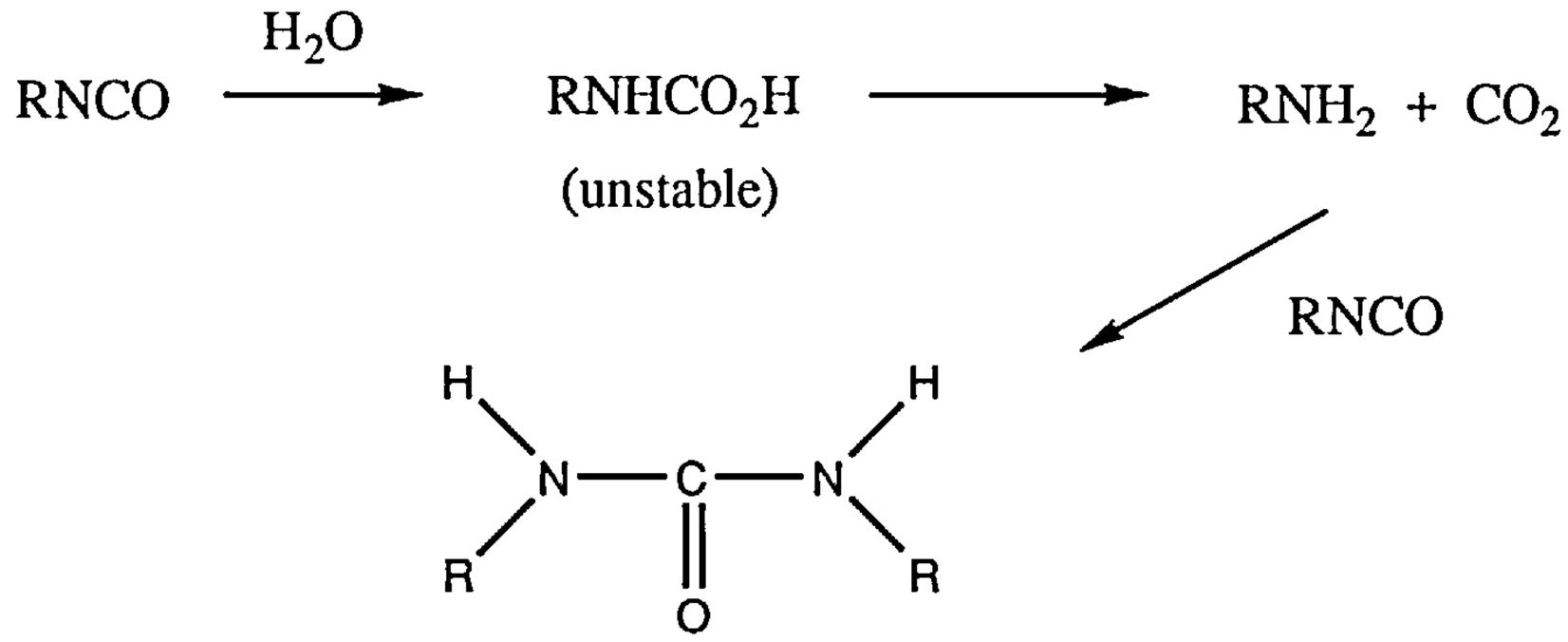

Figure 1-21 Reaction of an isocyanate with water to yield a symmetrical urea.

1.4.2 Methods for the Preparation of Cellulose tris(phenylcarbamate)-coated Phases

In 1984, Okamoto *et al* [129] filed a patent on the preparation and use of polysaccharide derivatives as CSPs. In it they detail for example, the type and molecular weight of polysaccharide, the type of isocyanate and the solvents that can be used to produce the derivatised polysaccharide phases. However, the examples given are all for the preparation of cellulose triacetate. In a later publication, Okamoto *et al* [69] reported on the conditions for the preparation of the cellulose tris(phenylcarbamate) phases:

The cellulose carbamates were prepared by the reaction of microcrystalline cellulose (Avicel, Merck) with an excess of corresponding

isocyanate in pyridine as ca. 100°C and isolated at the methanol insoluble fraction. Yields of 60-100% were claimed.

The coated phases were prepared by adding a solution (5 ml) of the cellulose tris(phenylcarbamate) derivative (0.75g dissoved in 10 ml THF) to macroporous silica gel (LiChrospher SI 4000) which had been treated with 3-aminopropyltriethoxysilane. The wetted silica was dried under vacuum and the coating procedure repeated with the remaining carbamate solution. The packing material was then packed into a stainless-steel HPLC column (250 x 4.6 mm) at 300kg/cm^2 using a slurry method.

The published method did not present many of the important details such as the dryness or volume of reagents, the time taken to complete the reaction of cellulose with the isocyanate, the method used to ensure complete removal of the THF or the solvents used to slurry pack the HPLC column. However, based on the original method of Okamoto *et al*,[69] Crawford[130] recently carried out his own investigation into the preparation of cellulose tris(phenylcarbamate)-coated phases. He presented a much more detailed preparation for polysaccharide phenylcarbamates, which he showed to work consistently well:

The cellulose (either Avicel, Merck or Sigmacel, Sigma) was dried over phosphorus pentoxide in a vacuum desiccator for 24 hours. It was transferred to very dry apparatus and refluxed for 24h in pyridine which had been previously dried over KOH. It was anticipated that the reflux would 'wet' the surface of the polysaccharide and thus allow the reagents to penetrate more easily. After cooling, 3.5 equivalents of the isocyanate were added and the mixture refluxed with stirring for a further 72h. After cooling the solution was poured into a large quantity of methanol. The white solid was filtered off, washed well with methanol and dried at 60°C to constant weight. Yields of >80% were achieved.

To prepare the coated phase, APS (eg Nucleosil APS 500 - 4000Å) was refluxed in tetrahydrofuran (ca. 2.5 g in 10 ml) for 30 minutes in order to wet the surface and remove any air pockets before adding the dissolved polysaccharide

carbamate. The polysaccharide carbamate was dissolved in THF (20 ml) and added in one batch. A special round bottom flask which had 4 baffles (indents in the glass) was used so that during evaporation the carbamate-silica suspension was constantly turned over. It was anticipated that this would give a more even coating of carbamate on the support. Crawford also noticed that after evaporation the coated particles tended to aggregate, especially if the pore size was small (<500Å). A powder suitable for packing was produced when the material was gently pushed through a fine mesh sieve (38 μm).

Finally, the coated material was slurried in hexane/2-propanol 1:1 v/v and was high pressure slurry packed at 4500 psi using hexane/2-propanol 4:1 v/v into a stainless steel HPLC column.

1.4.3 Evaluation of Cellulose tris(phenylcarbamate)-coated Phases

Both Okamoto *et al* [69] and Crawford[130] used IR and elemental analysis to confirm the success of the reaction. In IR, the presence of an intense peak at approximately 1720 cm^{-1} due to the carbonyl stretch of the urethane link and the absence of a broad peak at 3600cm^{-1} due to free hydroxyl were indicative of a successful reaction. In addition, IR can also be used to detect the presence of the symmetrical urea (carbonyl stretch at 1635 cm^{-1}).

Okamoto *et al* [69] used NMR to confirm the extent of derivatisation. However, this technique can be more troublesome than elemental analysis since care must be taken to reduce errors that could result from the presence of solvent or catalyst trapped in the polysaccharide matrix and from the presence of other impurities such as the symmetrical urea. Therefore, Crawford[130] generally used elemental analysis to determine more precisely the degree of derivatisation.

Neither Okamoto or Crawford used methods to evaluate the compositon or physical structure of the final, coated derivatised polysaccharide phase.

1.4.4 Methods used in this Thesis for the Preparation of Cellulose tris(phenylcarbamate)-coated Phases

Where appropriate, the materials and methods described by Crawford[131] for the preparation of columns containing cellulose carbamate-coated phases were used. Similar evaluation of the cellulose derivatives was carried out. However, it was also deemed useful to determine the particle size distribution of the coated sample prior to packing and compare it to the uncoated silica.

CHAPTER 2

INFLUENCE OF SUPPORT STRUCTURE ON ENANTIOSELECTIVITY

One of the main priorities, when carrying out chiral separations for applications such as the analysis of pharmaceuticals, is achieving baseline separation in the shortest possible time. In addition to this, a low solvent consumption is also desirable. In all early work by Okamoto *et al* [67,69,129] they used large particle (7 to 10 μm) aminopropylated silica (APS) as the support media for the polysaccharide carbamate coatings. In order to gain significant plate numbers, a typical column length was 250 mm. Therefore we decided to investigate the use of much smaller particle (≤5 μm) supports that could be packed into shorter columns (≤ 150 mm) in order to achieve rapid chiral separations.

2.1 SILICA SUPPORTS USED IN THE PAST

Okamoto *et al* [67,69,129] have consistently cited the use of macroporous (4000Å) APS with a polysaccharide carbamate loading of 20 to 25% w/w. However, they have neither justified the need for such a macroporous particle nor rationale for the coating amount.

Very few manufacturers supply silica with such a large pore diameter and the material is more expensive and less mechanically stable than the widely used smaller pored silicas. Crawford recently concluded[130] that for several polysaccharide carbamate phases, there appeared to be no advantage in using larger pore sizes (≥1000Å) and a 500Å APS was found to give the highest separations for the chiral analytes tested. Felix and Zhang[94] also found that the use of macroporous bonded silica did not seem necessary when they investigated the enantioselectivity of amylopectin phenylcarbamate-coated phases and they chose APS with a pore diameter of 300Å as optimum.

The only publication in which Okamoto details a loading study was during his very early work with (+)-PTrMA-coated macroporous silanised silica,[36] which pre-dated the coating of cellulose derivatives onto this type of support. In this publication, he proposed that at low loadings of (+)-PTrMA (<10% w/w), the polymer molecules may be randomly arranged, whereas at high loadings (>15% w/w), the polymer chains probably associate in an ordered structure in which new chiral adsorption centres were produced between the polymer chains. These results led him to chose a 20 to 25% w/w loading of the (+)-PTrMA polymer as optimum.

2.2 THE USE OF A SMALL PARTICLE SUPPORT TO ACHIEVE RAPID, HIGHLY EFFICIENT CHIRAL SEPARATIONS[131]

For our investigation into the use of small particle phases, we decided to use APS with a small pore diameter. Small pore supports are readily available

from several manufacturers and have high mechanical strength. We chose APS from the Hypersil range, manufactured by Shandon HPLC as a potentially suitable support. Hypersil has a mean pore diameter of 120Å, a surface area of approximately 180 m^2/g and a pore volume of 0.65 cm^3/g. The APS is ordinarily available with a narrow particle size distribution and mean particle diameters of 3, 5 and 10 μm. However, for the purpose of the study, Shandon additionally prepared a batch of APS with a mean particle diameter of approximately 2.5 μm.

The two most common polysaccharides used for the preparation of the polysaccharide carbamate-coated phases are cellulose and amylose. We decided to use cellulose phenylcarbamates for the study since, (i) cellulose is significantly cheaper than amylose and (ii) cellulose phenylcarbamates in general were found to be more soluble in solvents such as THF than their amylose counterparts, facilitating coating.

2.2.1 Determination of Optimum Cellulose Carbamate Loading for 120Å, Hypersil APS

Crawford[130] had already investigated the influence of percentage cellulose tris(phenylcarbamate) (CPC) loading on enantioselectivity using a 120Å, 5 μm Hypersil APS support. He noted that at a 20% w/w CPC loading, the phase appeared "sticky" with particles tending to aggregate and he could not pack the column. However, from his limited data, Crawford was not able to determine whether a lower CPC loading would have been more suitable for the small pore support. Therefore, it was decided to re-examine the influence the CPC loading has on enantioselectivity for the 120Å, 5 μm Hypersil APS support. In order to complement the study by Crawford, we also chose CPC as the chiral selector.

As expected, the photograph of the uncoated APS showed a range of particle sizes close to 5 μm, with some of the particles not being spherical and some apparently broken. However, the appearance of the 15% w/w CPC-coated phase was substantially altered, compared to the uncoated support. The CPC coating appears to build up in clumps on the surface of the support and there are a lot of small, irregularly shaped particles which may be pieces of CPC that have clumped together separately or have broken away from the APS surface, possible during sieving. In addition, it is impossible to determine whether a film of CPC is completely covering the APS particles.

All four phases were high pressure slurry packed into columns (150 x 4.6 mm; columns **1** to **4**). The columns filled with the 5 to 15% w/w CPC-coated phases appeared to pack very well, with high solvent flow rates observed during packing. However, during the packing of the column containing the 20% w/w CPC-coated phase, the solvent flow decreased very rapidly and was very slow for the majority of packing time. Subsequently, it was not surprisingly to find that the columns packed with the 5 to 15% w/w CPC-coated phases had low back pressures (≤ 300 psi. at 0.5 ml/min) when tested by HPLC, whereas the column packed with the 20% w/w CPC-coated phase had a much higher back pressure (ca. 1200 psi. at 0.5 ml/min)

Each column was tested using two chiral analytes: trans stilbene oxide (TSO, **A**) and 1-(9-anthryl)-2,2,2-trifluoroethanol (ATFE, **B**). Plots showing the effect on capacity factors (k'), separation (α) and enantiomeric resolution (Rs) for the two analytes as the percentage w/w CPC loading is increased are shown in Figure 2-2.

5 μm Hypersil APS phases which carried increasing amounts (5, 10, 15 and 20% w/w) of CPC (**CPC-1**) coating were prepared. The 5 to 15% w/w CPC-coated phases sieved easily (**5μ-1** to **5μ-3**) and the particle size distributions were found to be gaussian in shape centred around a mean particle size similar to the uncoated APS. However, the 20% w/w CPC-coated phase (**5μ-4**) was more difficult to sieve since the coating had bound the particles together. The particle size distribution revealed the presence of a high percentage of fines (< 2.5 μm).

At this time, we were fortunate to have the possibility of producing some scanning electron microscopy (SEM) photographs. The SEM photographs of an uncoated and 15% w/w CPC-coated 5 μm Hypersil APS are shown in Figure 2-1.

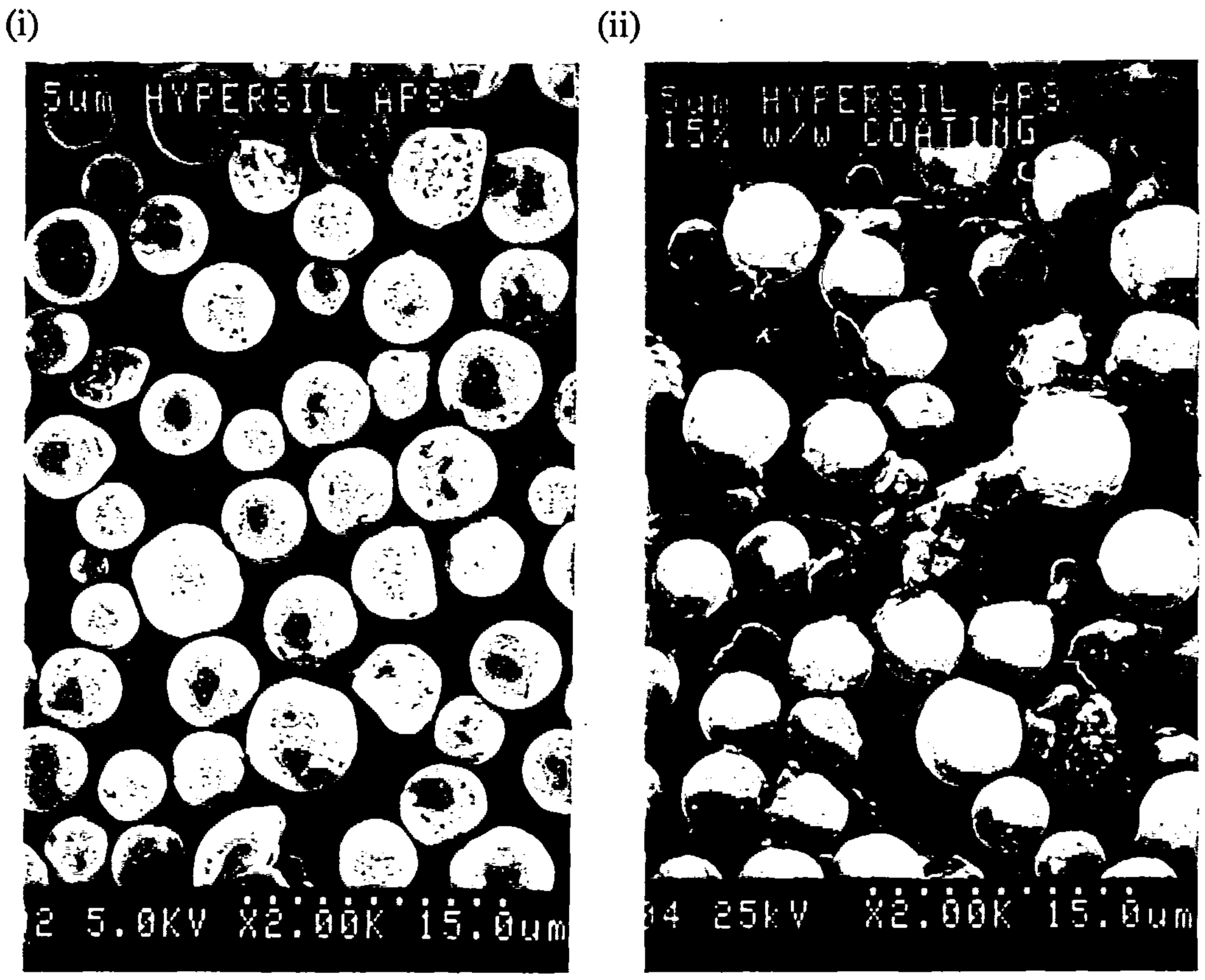

Figure 2-1 SEM photographs of (i) uncoated and (ii) 15% w/w CPC-coated 5 μm Hypersil APS (**5μ-3**).

(i)

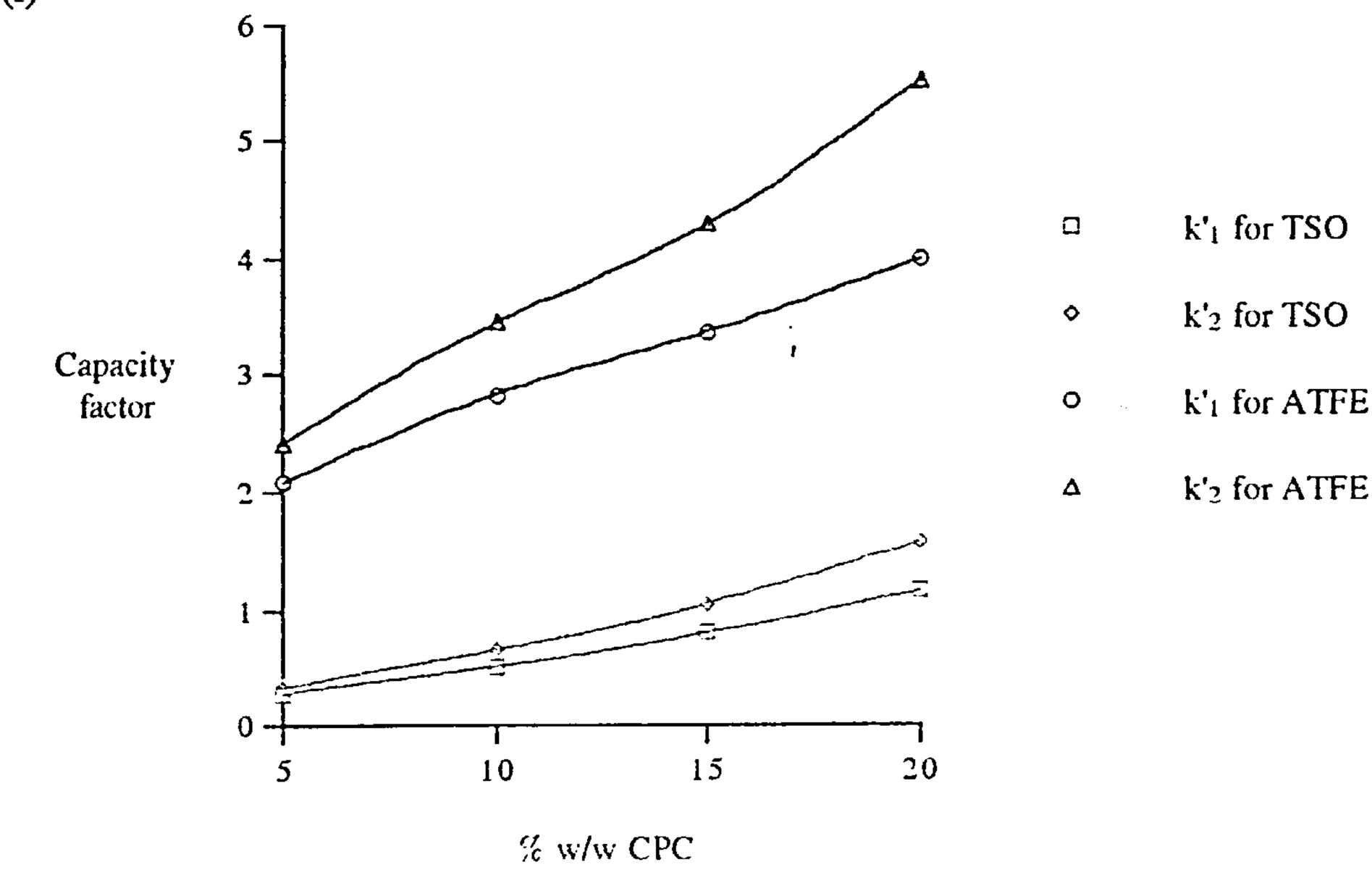

(ii)

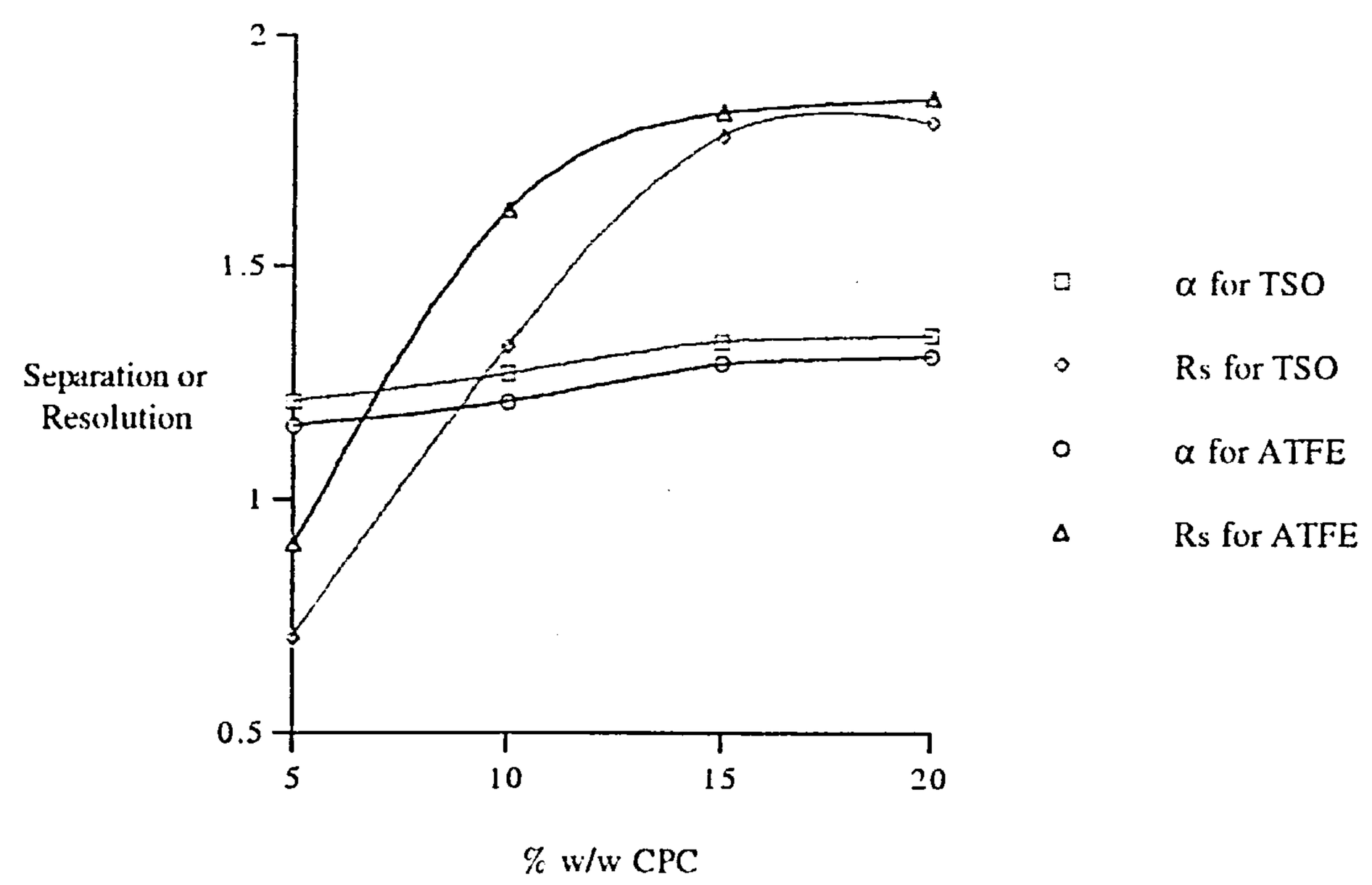

Figure 2-2 (i) capacity factor (k') and (ii) separation (α) and resolution (Rs) versus phase loading of CPC on 5 μm Hypersil APS for TSO and ATFE. Mobile phase: hexane/ 2-propanol (90:10 v/v). Flow rate: 0.5 ml/min.

Both k' values increased with increasing CPC loading, demonstrating that there are more interaction sites available (non-stereospecific and/or stereospecific) due to the heavier CPC loading. The α values for both analytes also increased gradually with increasing CPC loading confirming that some of the extra interaction sites are stereoselective.

In contrast, the Rs values increases steadily up to a loading of 15% w/w CPC and appeared to reach a plateau. The extra band broadening observed for the 20% w/w loading may be due to the 'stickiness' and large amount of fines observed in the particle size distribution and SEM photograph.

For both analytes, the 20% w/w CPC-coated phase had a marginally better Rs values than the 15% w/w CPC-coated phase. However, the peak shapes for both analytes on the former column were fronting slightly. Very low concentrations (10 µg/ml) of the analytes were injected, therefore, the fronting was thought not to be due to column overloading effects. It is proposed that because of the large amount of fines in the 20% w/w CPC-coated phase, the fronting is due to a poorly packed chromatographic bed which contains small cracks or voids that would allow some of the sample injected to elute more quickly than the main band.

These results led us to propose a 15% w/w cellulose carbamate loading as optimum for a 120Å, Hypersil APS support. This loading amount is significantly lower than the loading amount (20 to 25% w/w) reported by Okamoto *et al* [67,69,129] for the macroporous supports. Initially this may seem surprising, since the Hypersil APS has a considerably larger surface area. However, what appears to be more important is that the Hypersil particle has a much narrower pore diameter and a smaller pore volume than the macroporous supports. The surface area and pore volume data generated by the manufacturers for Hypersil and Nucleosil silicas are shown in Table 2-1

Table 2-1 List of surface area and pore volume measurements for silicas with different pore diameters.

Silica	Pore Diameter (Å)	Surface Area (m^2/g)	Pore Volume (cm^3/g)
5 μm Hypersil	120	180	0.65
7 μm Nucleosil	1000	25	0.75
7 μm Nucleosil	4000	10	0.75

It must be remembered that all these figures were generated before the bonding process was carried out. Aminopropylation of the silica surface will affect the pore structure, since the attachment of a monolayer will decrease the mean pore diameter by the thickness of the layer. Correspondingly, the specific surface area and specific pore volume will also decrease.

Crawford[130] used equations defined by Unger to determine the reduction in surface area and pore volume caused by the aminopropyl layer. He estimated the thickness of an extended aminopropyl layer to be 6.63Å and then calculated reductions for the 120, 1000 and 4000Å APS supports. The calculations are shown in Table 2-2.

Table 2-2 Reduction in silica surface area and pore volume following bonding of an aminopropyl group.

Silica	New Pore Diameter (Å)	New Surface Area (m^2/g)	New Pore Volume (cm^3/g)
Hypersil	107	160.2 (11.0%)	0.51 (20.9%)
Nucleosil	987	24.7 (1.3%)	0.73 (2.6%)
Nucleosil	3987	9.7 (0.3%)	0.74 (0.7%)

In parenthesis are the percentage decrease in surface area or pore volume calculated from Unger's formula

The surface area and pore volume for the macroporous Nucleosil particles are not significantly altered following aminopropylation. However, in the case of the microporous Hypersil particles, both the surface area and pore volume are considerably reduced by the introduction of an aminopropyl group.

Therefore in contrast to the macroporous particles, it is proposed that the narrower pore opening and reduced pore volume for the 120Å, Hypersil APS are likely to result in the pores becoming more rapidly filled during coating with the cellulose carbamates and thus a lower loading will be required.

2.2.2 Choice of Cellulose Carbamate and Coating Solvent

One of the most versatile cellulose carbamate is the cellulose tris(3,5-dimethylphenylcarbamate) (CDMPC).[69,78] Therefore it was decided to use this derivative in further studies in preference to CPC. To test the methodology, a preliminary, small batch (0.5 g) of 15% w/w CDMPC (**CDMPC-1**) coated 120Å, 2.5 µm Hypersil APS (**2.5µ-1**) was prepared using the same coating method (THF as coating solvent) used for the preparation of the CPC-coated phases in the previous section. Following evaporation, the material was found to be extremely hard and almost impossible to push through the sieve. A particle size distribution of the sieved material showed an extremely broad particle size distribution with many aggregated particles compared to the uncoated APS.

Subsequently, it was not surprising to find that in a similar manner to the 20% w/w CPC-coated phase described in the previous section, the solvent flow rate slowed dramatically during packing. The column had a high back pressure (1600 psi. at 0.5 ml/min) and fronting chromatographic peaks, analogous to those seen on the column packed with the afore mentioned CPC-coated phase.

Okamoto had cited[69] the use of 100% N, N-dimethylacetamide (N,N-DMA) for the dissolution of polysaccharide carbamates that do not dissolve well in THF. Although no dissolution problems had been observed for CDMPC in

THF, we decided to investigate the use of this solvent. However, N,N-DMA is significantly less volatile than THF. Therefore, N,N-DMA was added to THF, in a ratio of 9:1 v/v THF:N,N-DMA, for the dissolution of the CDMPC. Following evaporation of a 15% w/w CDMPC loading, the phase (**2.5μ-2**) sieved very easily and gave a much narrower particle size distribution with significantly fewer fines. The reason for this improvement in phase handling and particle size distribution is not known. After drying in a vacuum oven at 60°C for an extra 2 hours to ensure that all the N,N-DMA had been removed, the 15% w/w CDMPC-coated 2.5 μm APS was packed into an HPLC column (100 x 4.6 mm; column **5**).

It has been reported[63,72] that the coating solvent can affect enantioselectivity for derivatised polysaccaride-coated phases (see section 1.3). Therefore, it was of interest to examine whether the performance of the CDMPC-coated phase would be affected by the use of N,N-DMA in the coating solvent. The separation of TSO is shown in Figure 2-3.

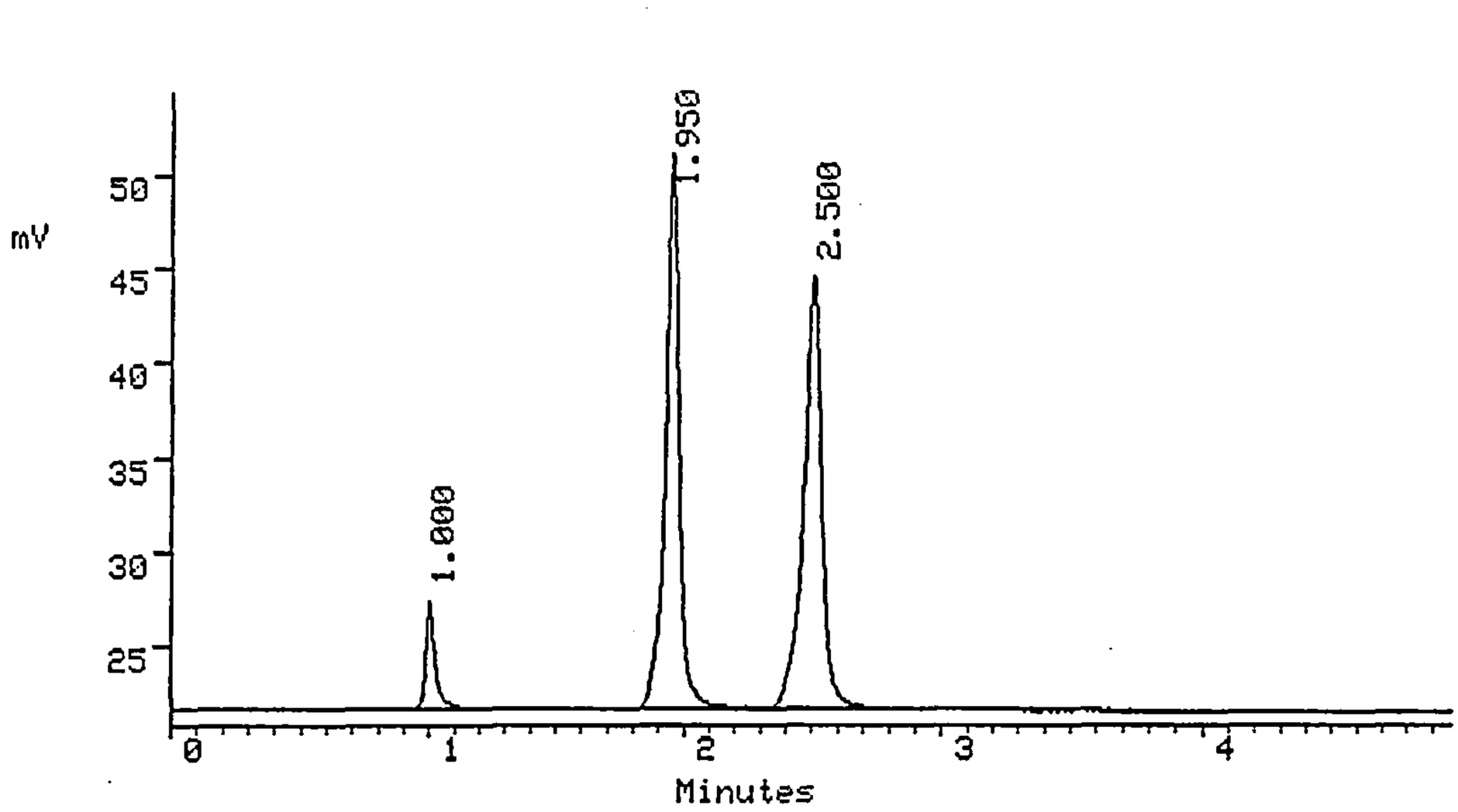

Figure 2-3 Separation of TSO on column (100 x 4.6 mm) packed with 15% w/w CDMPC-coated 2.5 μm Hypersil APS. Mobile phase: hexane/2-propanol (90:10 v/v). Flow rate: 0.5 ml/min.

A very good separation of TSO was observed suggesting that the CDMPC-coated phase had high chiral discriminating ability. To check this, the result was compared with the separation of TSO reported by Okamoto et al[69] using a column (250 x 4.6 mm) packed with 20% w/w CDMPC-coated 4000Å, 10 μm APS. A slightly lower α value was observed on our column compared to the column used by Okamoto et al (1.58 cf. 1.68). However, we observed a much higher Rs (5.19 cf. 3.22) confirming the high efficiency of our column.

2.2.3 Stability of 15% w/w CDMPC-coated 2.5 μm Hypersil APS

The majority of the chiral separations carried out by Okamoto *et al* [67,69] were achieved using a flow rate of 0.5 ml/min and a mobile phase containing ≤ 20% v/v alcoholic modifier (eg 2-propanol or ethanol) in hexane. It was conjectured that, in our work, the use of the smaller-pored Hypersil APS supports, with possibly more of the coated phase located externally, might result in a poorer mechanical stability and greater tendency for loss of phase due to column bleed. Therefore, in order to test the stability of the 15% w/w CDMPC-coated 2.5μm APS phase we sequentially tested the performance of the column at ambient temperature during 170 hours of constant use. A flow rate of 1 ml/min (back pressure 800 psi) was maintained using hexane/2-propanol (80:20 v/v) as mobile phase (total volume 10 litres). The mobile phase was then changed to hexane/2-propanol (90:10 v/v), the flow rate was increased to 3 ml/min (back pressure 3000 psi.) and a further 10 litres of mobile phase was passed. For the combined treatments, there was no deterioration in column performance, as judged by the lack of change in k', N or Rs for a test mixture.

2.2.4 Influence of Particle Size and Flow Rate on Column Efficiency

In order to be able to effectively demonstrate the advantages of using a 2.5 μm CDMPC-coated APS phase, we decided to prepare similarly coated 5 and 10 μm Hypersil APS phases. Therefore, larger quantities (7 g each) of 15% w/w CDMPC (**CDMPC-1**) coated 2.5, 5 and 10 μm Hypersil APS phases (**2.5μ-3, 5μ-5** and **10μ-1**) were prepared so that several columns could be packed. For each coated phase, the particle size distributions were gaussian in shape with means similar to those of the uncoated APS supports. Each batch was slurry packed into 3 different column lengths (30, 100 and 150 mm; 4.6 mm id.; columns **6** to **14**).

All columns packed satisfactorily except the 2.5 μm, 150 mm column. During packing of this column, the solvent flow rate decreased rapidly and in subsequent testing, the column displayed an extremely high back pressure(1500 psi.) and gave badly fronting peak shapes. This suggested that the 150 mm column length was too long to allow efficient packing of the small coated particles.

In order to compare the efficiency of the three different particle sizes and to determine the optimum flow rate for each size, a van Deemter curve was plotted (Figure 2-4). This type of plot relates column plate height (H) to the flow rate, for columns of the same internal diameter (id.) (see section 1.2.3). The results were generated by measuring the efficiency of (-)-TSO (first eluting enantiomer) on the three 100 x 4.6 mm columns.

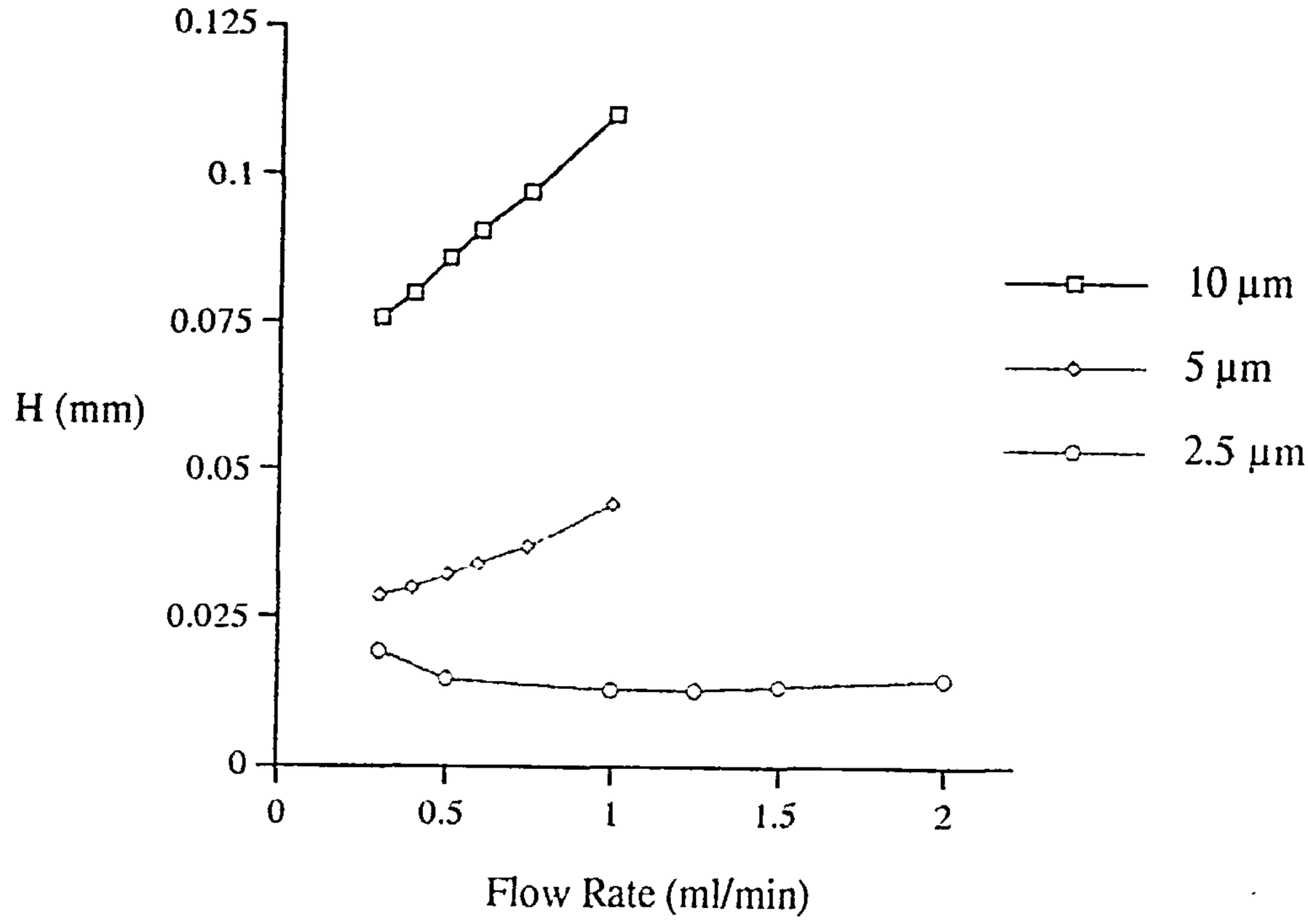

Figure 2-4 Plate height (H) versus flow rate for columns packed with 15% w/w CDMPC-coated 2.5, 5 and 10 µm Hypersil APS. Sample: (-)-TSO. Mobile phase: hexane/2-propanol (90:10 v/v).

As expected, the plate height decreases (ie. column efficiency increases) as the particle size decreases from 10 to 5 to 2.5 µm. The steepest curve is seen for the 10 µm phase demonstrating the importance of running at low flow rates (< 0.5 ml/min) when using large particles. The curve for the 5 µm phase is less steep, but maximum efficiencies are still obtained at low flow rates (< 0.5 ml/min). The flattest curve is seen for the 2.5 µm phase and maximum efficiencies are achieved at higher flow rates (ca. 1 ml/min). It is also evident that, for the 2.5 µm phase, flow rates greater than 1 ml/min can be used with very little loss in efficiency.

Therefore, in the following studies, 0.4 ml/min was adopted for the 10 and 5 µm phases and 1 ml/min for the 2.5 µm phase.

2.2.5 Comparison of CDMPC-coated 10 μm APS, 150 mm column with CDMPC-coated 2.5 μm APS, 30 mm column

The chromatographic parameters for 6 chiral analytes: TSO; ATFE; 1-phenylethanol (1-PE, C); flavanone (FLAV, H); homatropine (HOMA, L) and oxprenolol (OXP, P) are shown in Table 2-3.

Table 2-3 Chromatographic parameters for 6 chiral analytes on 15% w/w CDMPC-coated 10 μm APS, 150 mm column (10μm, 150 mm) and 15% w/w CDMPC-coated 2.5 μm APS, 30 mm column (2.5 μm, 30 mm).

Analyte	Column	k'_1	k'_2	α	Rs	Run Time (mins)
TSO	10 μm, 150 mm	1.0	1.51	1.51	2.78	10
	2.5 μm, 30 mm	0.86	1.29	1.50	2.24	0.9
ATFE	10 μm, 150 mm	4.54	8.65	1.91	4.19	40
	2.5 μm, 30 mm	3.40	6.72	1.98	4.90	3
1-PE	10 μm, 150 mm	5.79	6.76	1.13	1.48	30
	2.5 μm, 30 mm	4.46	5.24	1.17	1.52	2.3
FLAV	10 μm, 150 mm	1.93	2.53	1.31	2.0	14
	2.5 μm, 30 mm	1.67	2.13	1.28	1.73	1.3
HOMA	10 μm, 150 mm	2.05	2.76	1.35	2.36	15
	2.5 μm, 30 mm	1.58	2.07	1.31	1.83	1.1
OXP	10 μm, 150 mm	2.03	5.94	2.94	3.88	30
	2.5 μm, 30 mm	1.79	4.61	2.75	4.81	2.1

Mobile phases: hexane/2-propanol: TSO, ATFE and FLAV: 90:10 v/v; 1-PE: 98:2 v/v; HOMA and OXP: 80:20 v/v + 0.1% diethylamine. Flow rates: 10 μm column: 0.4 ml/min; 2.5 μm column: 1 ml/min.

Similar k', α and Rs values were seen on both columns for all compounds tested. However, as expected, the separation times on the 2.5 µm, 30 mm column are substantially lower; eg. the separation for ATFE was completed in approximately 3 minutes on the 2.5 µm, 30 mm column, whereas approximately 40 minutes was required for the same separation on the 10 µm, 150 mm column (Figure 2-5).

(i)

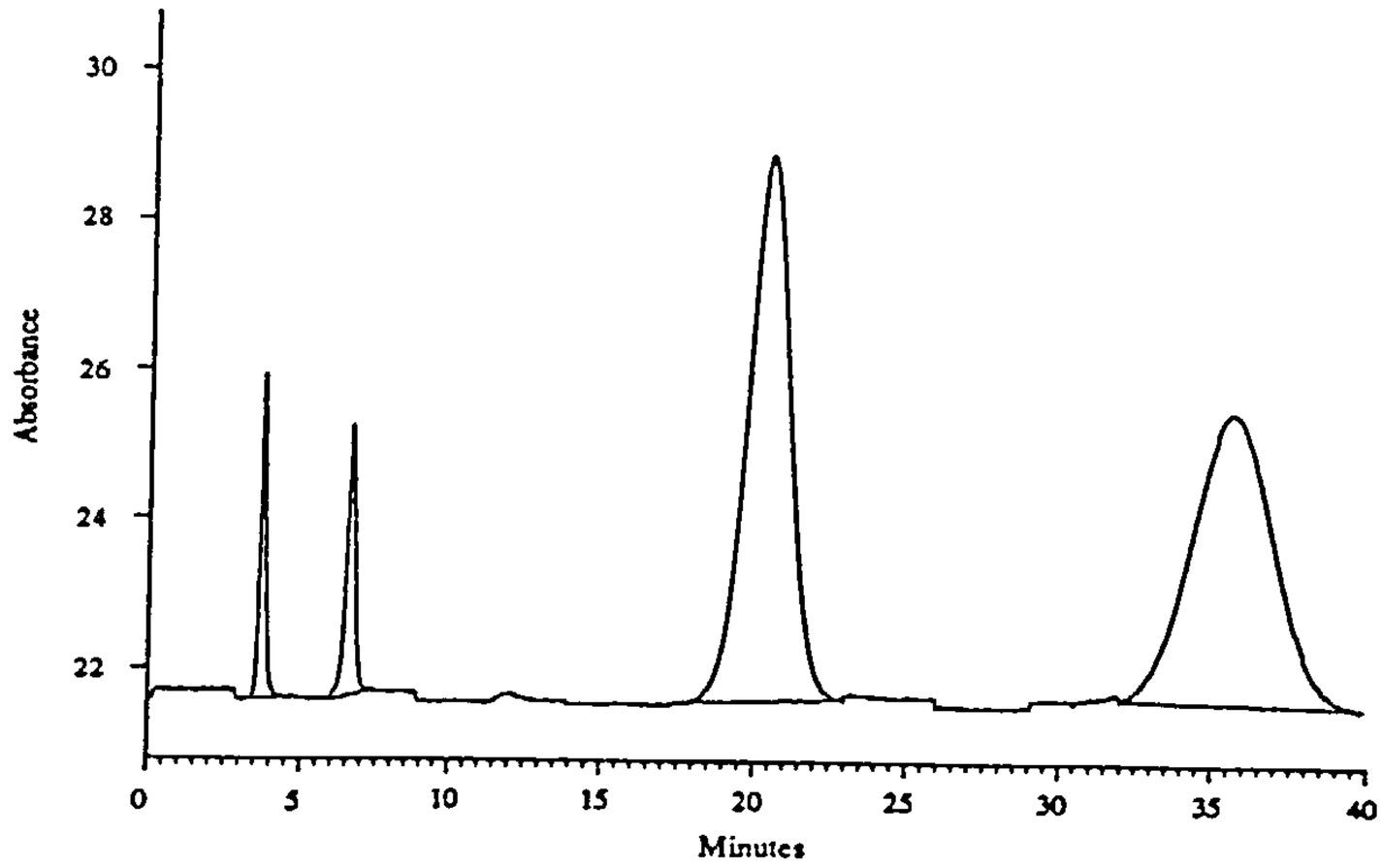

(ii)

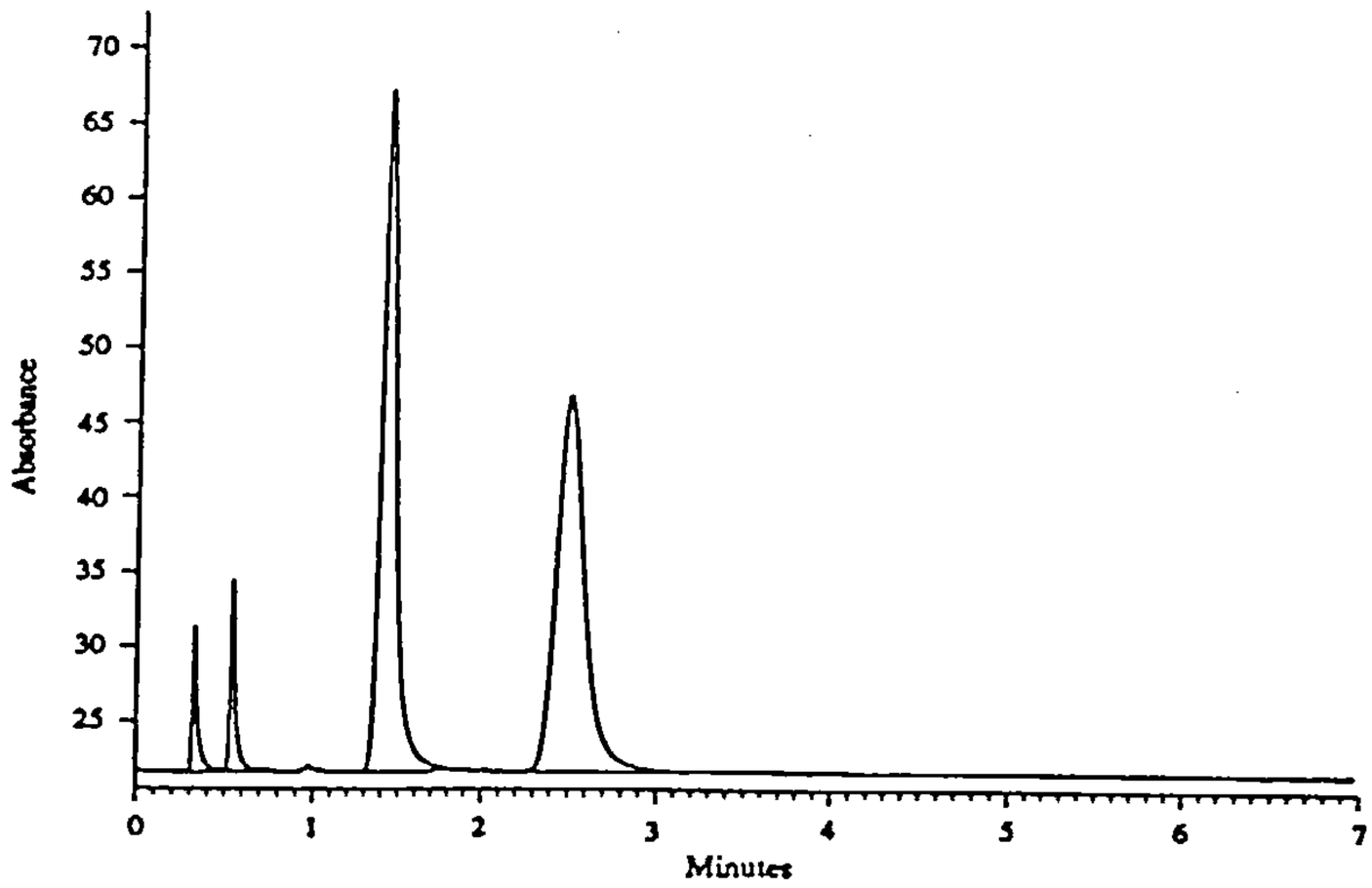

Figure 2-5 Separation of ATFE on (i) column (30 mm) packed with 15% w/w CDMPC-coated 2.5 µm Hypersil APS and (ii) column (150 mm) packed with 15% w/w CDMPC-coated 10 µm Hypersil APS. Mobile phase: hexane/2-propanol (90:10 v/v). Flow rate: 0.5 ml/min.

2.2.6 Comparison of CDMPC-coated 5 μm APS, 100 mm column with CDMPC-coated 2.5 μm APS, 100 mm column

The chromatographic parameters for TSO, ATFE, 1-PE, FLAV, HOMA and OXP are shown in Table 2-4.

Table 2-4 Chromatographic parameters for 6 chiral analytes on 15% w/w CDMPC-coated 5 μm APS, 100 mm column (5μm, 100 mm) and 15% w/w CDMPC-coated 2.5 μm APS, 100 mm column (2.5 μm, 100 mm).

Analyte	Column	k'_1	k'_2	α	Rs	Run Time (mins)
TSO	5 μm, 100 mm	1.08	1.70	1.57	3.71	6.8
	2.5 μm, 100 mm	0.96	1.51	1.57	5.19	2.8
ATFE	5 μm, 100 mm	4.75	9.35	1.97	5.69	28
	2.5 μm, 100 mm	3.68	7.49	2.04	8.86	8.8
1-PE	5 μm, 100 mm	5.95	6.77	1.14	1.55	20
	2.5 μm, 100 mm	4.49	5.16	1.15	2.17	6.4
FLAV	5 μm, 100 mm	2.12	2.72	1.29	2.41	10
	2.5 μm, 100 mm	1.84	2.37	1.29	3.36	3.6
HOMA	5 μm, 100 mm	2.17	2.92	1.35	2.63	10
	2.5 μm, 100 mm	1.74	2.36	1.36	3.72	3.5
OXP	5 μm, 100 mm	2.22	6.10	2.75	5.25	20
	2.5 μm, 100 mm	1.88	4.93	2.62	8.34	7.0

Mobile phases: hexane/2-propanol: TSO, ATFE, FLAV: 90:10 v/v; 1-PE: 98:2 v/v; HOMA and OXP: 80:20 v/v + 0.1% diethylamine. Flow rates: 5 μm column: 0.4 ml/min; 2.5 μm column: 1 ml/min.

Compared to the results given in Table 2-3, both 100 mm columns show enhanced Rs values for all compounds. As expected, the 2.5 μm phase is significantly more efficient than the 5 μm phase and because the flow rate is higher (1 ml/min cf. 0.4 ml/min), the separation times are much shorter.

2.2.7 High Efficiency Separations, Short Analysis Times

An added advantage of the 2.5 μm, 100 mm column is that, provided back pressure remains within acceptable limits, the flow rate can be increased above 1 ml/min without significant loss in efficiency, allowing separations with improved resolution within a similar run time to the 30 mm column (Figure 2-6).

(i)

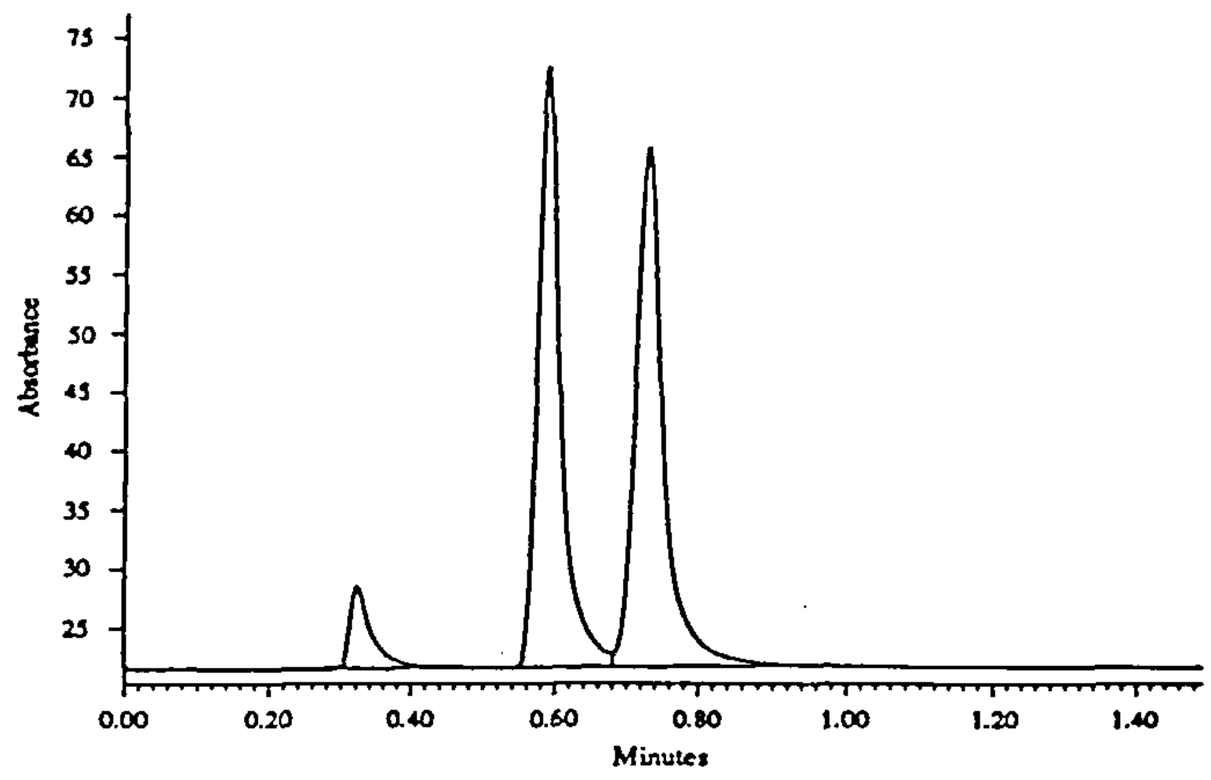

(ii)

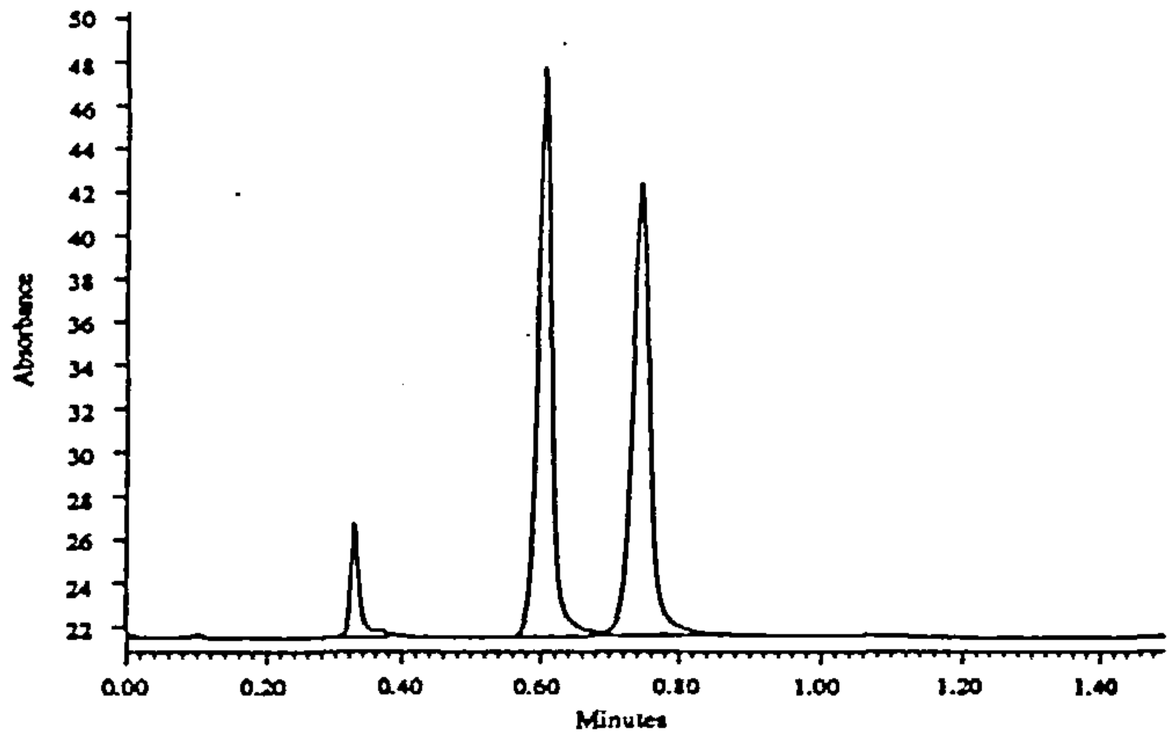

Figure 2-6 Separation of TSO on columns packed with 15% w/w CDMPC-coated 2.5 μm Hypersil APS (i) 30 mm column, flow rate: 1 ml/min, back pressure: 400 psi. and (ii) 100 mm column, flow rate: 3 ml/min, back pressure: 3000 psi. Mobile phase: hexane/2-propanol (90:10 v/v).

2.2.8 Summary and Conclusions

The results clearly demonstrate the advantages of using small particle CDMPC-coated APS phases compared to those used by Okamoto et al.[67,69,130] Much shorter retention times were achieved by using shorter column lengths and higher flow rates.

Another potential use for these small particle coated phases, which was not explored, is in capillary LC. Some workers such as Wannman *et al* [132], have already investigated the use of packed fused silica columns for chiral separations. Their methods utilised either β-CD in the mobile phase, BSA adsorbed on silica or a covalently bound L-dinitrobenzoyl phenylglycine phase. Among the advantages cited for using such a system were the significant reduction in solvent consumption and the possibility, owing to the use of very long columns, of separating enantiomers with very low separations. However, in this publication, they only achieved similar enantiomeric separations on their capillary columns to those reported on conventional (4.6 mm id.) HPLC columns under the same conditions. Part of the reason for this may have been due to problems in packing an efficient column bed using larger than ideal 3 - 5 µm particles.

Packing difficulties may not be the only reason why there has not been a large scale acceptance of capillary LC. New equipment has to be purchase since, (i) very low flow rates can not be achieved by conventional HPLC pumps; (ii) small injection volumes must be used and (iii) very sensitive detection methods that keep band broadening to a minimum are required. In addition, the concentration sensitivity is poorer owing to smaller injection volumes.

However, with the continued development of very small particle phases, more sensitive equipment and with the cost and environmental pressures on users to reduce solvent consumption, chiral capillary chromatography may become more widespread in the near future.

2.3 INVESTIGATION INTO THE SAMPLE LOADING CAPACITY OF CDMPC-COATED HYPERSIL APS WITH DIFFERENT PORE DIAMETERS

One question posed in relation to the use of small particle coated phases was whether, in view of the larger surface area of the support, CDMPC-coated 120Å, Hypersil APS would have a larger sample loading capacity, thus making it more effective for preparative separations.

2.3.1 Definition of Overload Conditions

Preparative chromatography has the objective of separating and collecting sufficient quantities of compounds for subsequent use. Therefore, in order to maximise the mass throughput per chromatographic pass, separations are usually carried out using high sample loads. However, chromatography works best with the smallest sample loadings. When the sample load is gradually increased, the column efficiency decreases very rapidly, the peaks become asymmetric and their retention times usually becomes shorter.

To be able to determine whether a column has a greater sample loading capacity, it is necessary to be able to define the point at which the separation is considered to be overloaded. This is a question that has been subject to much debate.

Snyder[133] defined overload conditions as having been reached when the capacity factor had decreased by 10% with respect to the constant capacity factors associated with very low solute amounts. In addition, he noted that this decrease was accompanied by a 10% increase in plate height which actually turned out to be a coincidence, although some workers have also used this as a definition of column overload conditions. However, as pointed out by Verzele and Dewaele[9] the setting of an arbitrary value such as a 10% change in capacity factor to define overload conditions is inappropriate for preparative

chromatography, since even at this level of deterioration in performance, the chromatography is still often useful.

Verzele and Dewaele[9] defined preparative overload as having been reached when the desired separation is no longer achieved, ie. injection of a larger sample results in a reduction of the amount of separated material that can be collected because of the excessive peak overlap. Therefore, they proposed the existence of two kinds of overload conditions (i) chromatographic capacity or overload, as defined by Snyder[133] and (ii) preparative capacity or overload as defined above. In the following study, both definitions were used to investigate the sample loading capacity of CDMPC-coated 5 μm Hypersil APS with different pore diameters.

2.3.2 Determination of Optimum Cellulose Carbamate Loading for 90 and 500Å, Hypersil APS

Hypersil APS is ordinarily available with a mean pore diameter of 120Å. However, for the purpose of this study, Shandon additionally provided 5 μm Hypersil APS particles with mean pore diameters of 90 and 500Å. The surface area and pore volume measurements for the underivatised 90, 120 and 500Å supports are shown in Table 2-5. However as highlighted previously (Table 2-2) the bonding of an aminopropyl monolayer can significantly reduce the surface area and pore volume available for the cellulose carbamate coating. Therefore, the reduction in surface area and pore volume estimated for the three different pore diameter Hypersil supports is also shown in Table 2-5. Values were calculated using the method described previously (section 2.2.1).

In view of the significant differences in surface area and pore volume between the three supports, it was deemed necessary to investigate the optimum CDMPC loading for the 90 and 500Å pore diameters.

Table 2-5 Surface area and pore volume measurements for 90, 120 and 500Å Hypersil silicas and % change following bonding of an aminopropyl group

Pore Diameter (Å)	Surface Area (m^2/g)	Pore Volume (cm^3/g)	% Change in Surface Area	% Change in Pore Volume
90	318	0.75	14.7	27.3
120	180	0.65	11.1	20.9
500	45	0.55	2.7	6.2

The most suitable CDMPC loading for the 120Å, Hypersil APS support has already been shown to be 15% w/w (section 2.2.1). For the 90 and 500Å Hypersil APS supports, different amounts of CDMPC (**CDMPC-2**) were coated onto small batches (0.5 g) of the APS in order to determine the most suitable CDMPC loading. Drawing on past experiences with phases that did not pack well (eg. **5µ-4** and **2.5µ-1**), the most suitable loading was judged by the relative ease of sieving and the shape of the particle size distribution.

90Å support

A 15% w/w CDMPC loading on this support (**5µ-6**) was difficult to sieve and the particle size distribution was very broad, indicating some aggregation. The ease of sieving and particle size distribution of a 12.5% w/w CDMPC loading (**5µ-7**) was satisfactory.

500Å support

This support readily accepted the 15% w/w CDMPC loading (**5µ-8**) and a gaussian shaped particle size distribution with a mean of 5.13 µm was obtained. Therefore the loading was increased to 20% w/w CDMPC. This material (**5µ-9**) was difficult to sieve and the particle size distribution had a high percentage of fines. At 17.5% w/w CDMPC, the coated material (**5µ-10**) was relatively easy to sieve and again gave a gaussian shaped particle size distribution.

Using these observations, a 12.5% w/w CDMPC loading was chosen for the 90Å support; a 15% w/w loading for the 120Å support and a 17.5% w/w loading for the 500Å support.

2.3.3 Comparison of CDMPC-coated 90, 120 and 500Å, Hypersil APS

Larger batches (3 g) of the 90, 120 and 500Å Hypersil APS supports were coated with their respective CDMPC (**CDMPC-2**) loadings (**5µ-11** to **5µ-13**) and were high pressure slurry packed into stainless steel HPLC columns (150 x 4.6 mm; columns **15** to **17**). The enantioselectivity of each column was tested with TSO, 1-PE and FLAV. Bar graphs illustrating the separation and resolution of these compounds on the three phases are shown in Figure 2-7.

In general, the α and Rs values for the three analytes on the 120 and 500Å phases were similar. However, α and Rs on the 90Å phase were noticeably lower than those on the 120 and 500Å phases.

The poor enantioselectivity seen for the 12.5% w/w CDMPC-coated 90Å, APS was disappointing. Evidently, the reduced pore volume resulting from bonding an aminopropyl group onto the 90Å support lowers the capacity of this material to hold the CDMPC coating. The lower loading of the latter inevitably results in reduced α (compared with section 2.2.1 and Figure 2-2). Similarly, the dependancy of Rs on $[(\alpha - 1)/\alpha]$ means that Rs is also lower for this phase. A further effect on Rs may operate, since poor mass transfer of analyte molecules into the restricted pores may have caused additional peak broadening.

In practical terms, the lower α and Rs values obtained on the 90Å phase make it unsuitable for maximising preparative loading capacity. Therefore, only the 120 and 500Å phases were used for the investigation into the sample loading capacity.

(i)

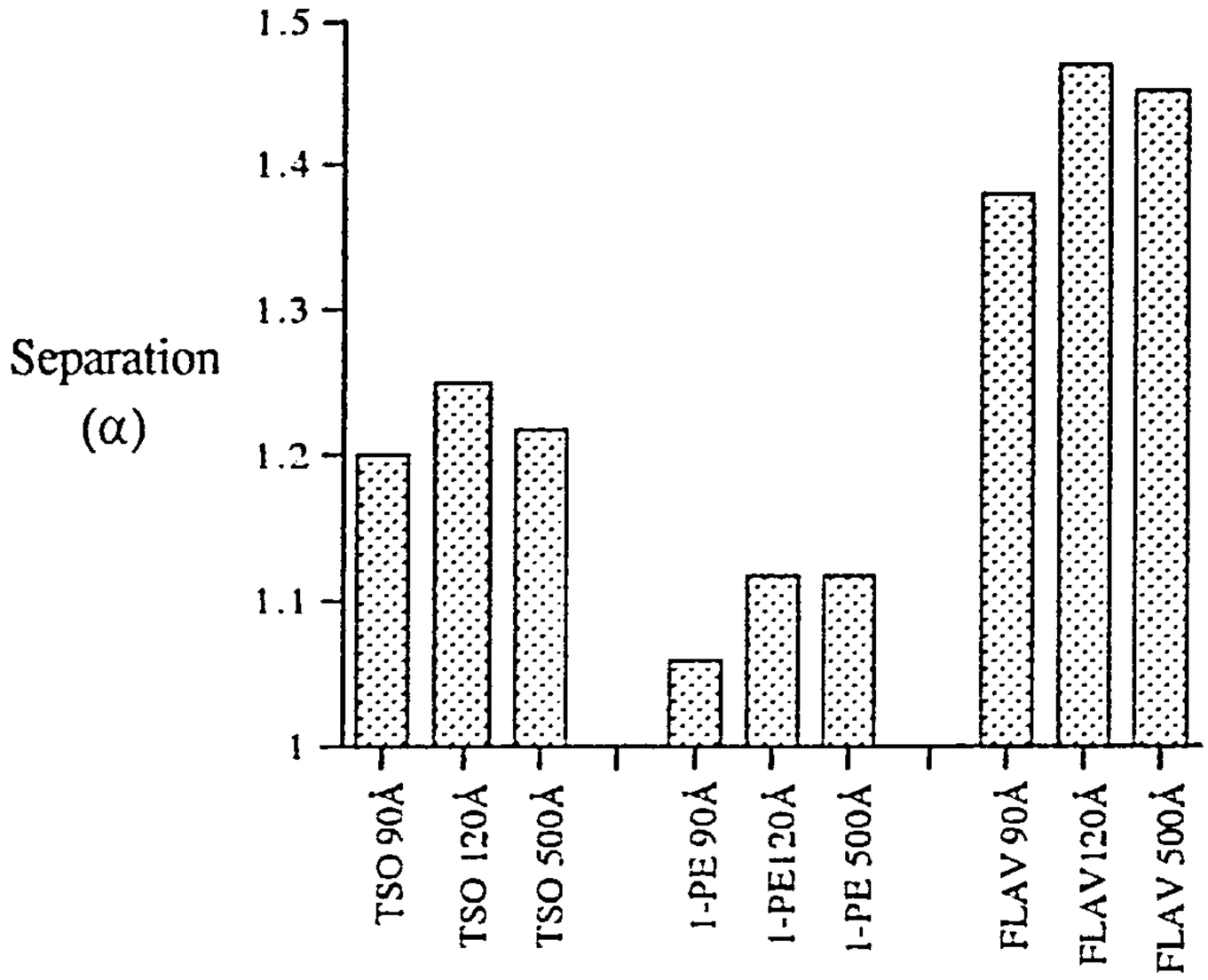

(ii)

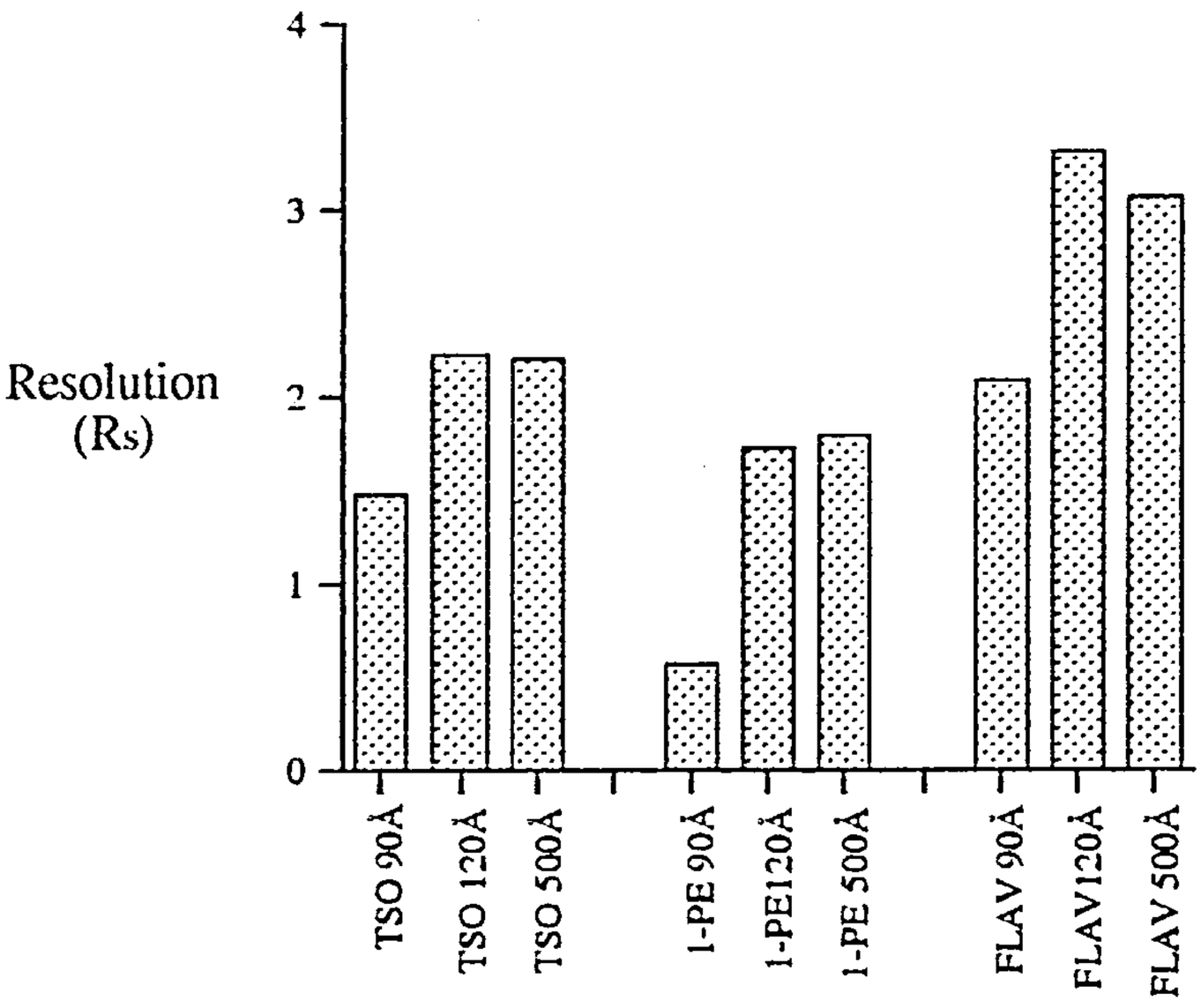

Figure 2-7 (i) separation (α) and (ii) resolution (Rs) for TSO, 1-PE and FLAV on columns (150 x 4.6 mm) packed with CDMPC-coated 5 µm Hypersil APS: 12.5% w/w for 90Å, 15% w/w for 120Å and 17.5% w/w for 500Å. Mobile phase: TSO and FLAV: hexane/2-propanol (90:10 v/v) and 1-PE: hexane/2-propanol (98:2 v/v). Flow rate: 0.5 ml/min.

2.3.4 Determination of Suitable Preparative Injection Volume

The volume of the injected solution can greatly influence the efficiency of the column in preparative chromatography.[134,135] For small sample amounts, small, more concentrated injection should be made in order to minimise band broadening. However, as the sample size increases, small very concentrated samples would cause localised column overloading and therefore larger, less concentrated sample injections should be made. Consequently, it was deemed necessary to first find a suitable injection volume for our sample loading study.

In order to determine this, a 1 mg sample amount of 1-PE, which was large enough to cause slightly asymmetric peaks, was loaded onto the 120 and 500Å phases in 10, 20, 50 and 100 µl injection volumes (10, 20, 50 and 100 µl fixed loop respectively). The plate number of the first eluting enantiomer was measured and was plotted against the injection volume. The results are shown in Figure 2-8.

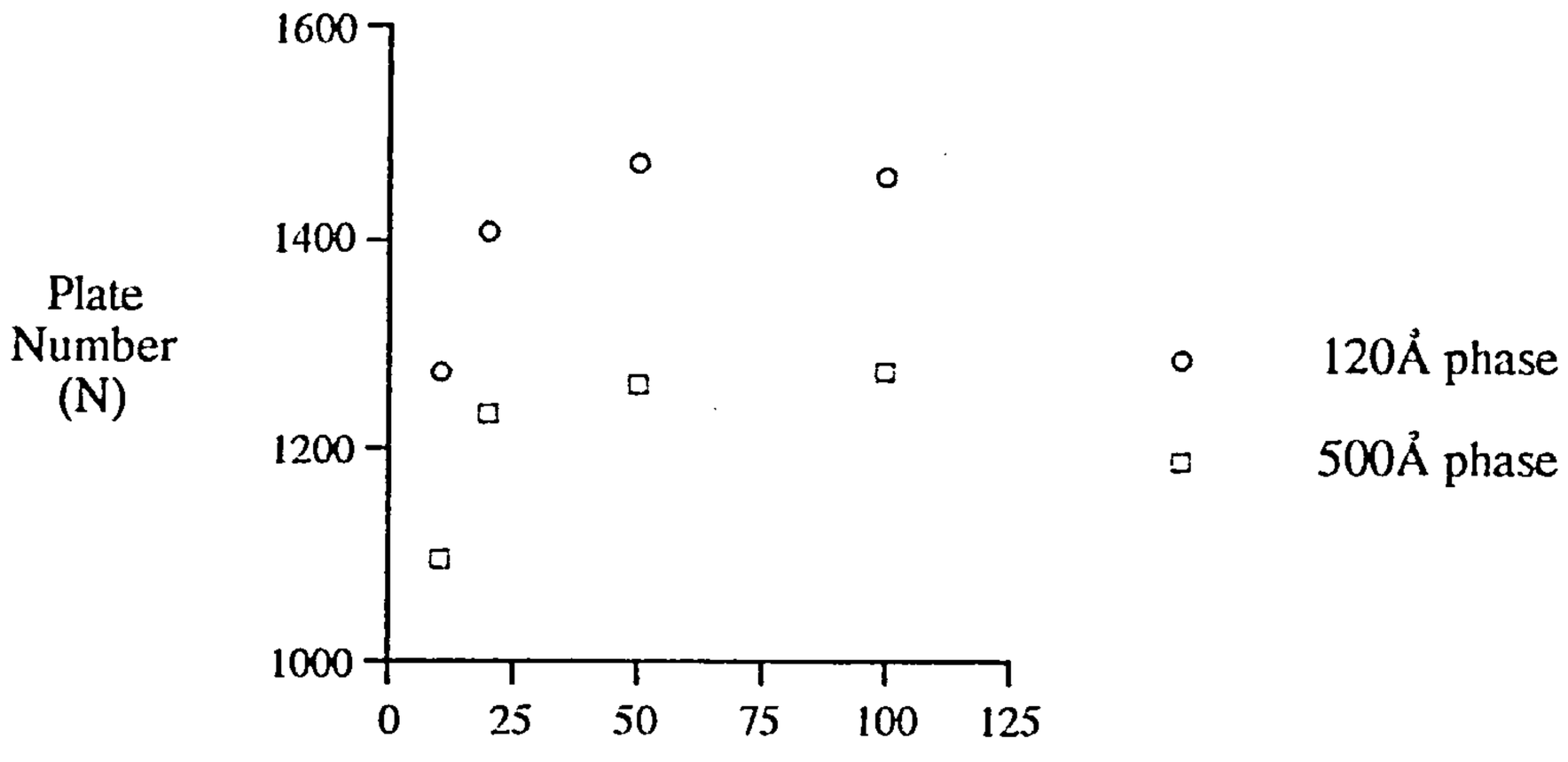

Figure 2-8 Plate number versus injection volume for the first eluting enantiomer of 1-PE (1 mg) on columns (150 x 4.6 mm) packed with CDMPC-coated 5 µm Hypersil APS: 15% w/w for 120Å and 17.5% w/w for 500Å. Mobile phase: hexane/2-propanol (98:2 v/v). Flow rate: 0.5 ml/min. Fixed injection loop.

As predicted by the literature, the results demonstrated that for a large sample amount, highest efficiencies were achieved using large sample injections. The 50 and 100 µl sample volumes gave the highest efficiencies for the 1 mg 1-PE sample loading. The higher, 100 µl injection volume was chosen for the subsequent studies, since many analytes have low solubility in the relatively non-polar solvents which have to be used with the cellulose carbamate-coated phases.

2.3.5 Sample Loading Capacities for CDMPC-coated 120 and 500Å Hypersil APS

TSO, 1-PE and benzoin methyl ether (BME, G) were chosen for the study, since these compounds all had relatively high solubilities in the mobile phase. They were investigated over the range 2-5000 µg for TSO and 10-2000 µg for 1-PE and BME.

Chromatographic capacity or overload

Initially Snyders definition[133] of chromatographic overload was used to compare the three analytes on the 120 and 500Å phases. The % change in the second capacity factor (k'_2) with increasing sample load was plotted, since it is the overlap by the second eluting enantiomer that significantly reduces the amounts of enantiomerically pure compound that can be collected. The results are shown in Figure 2-9.

(i)

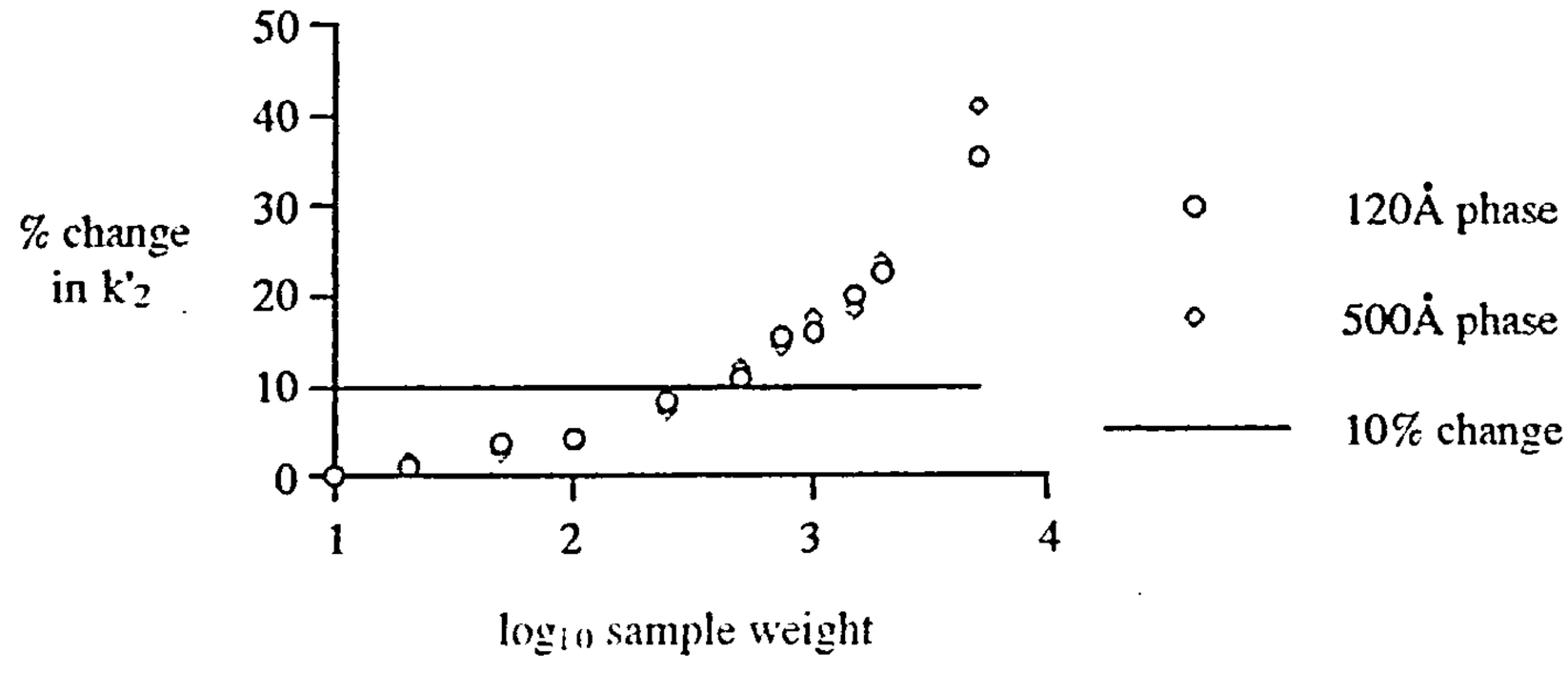

(ii)

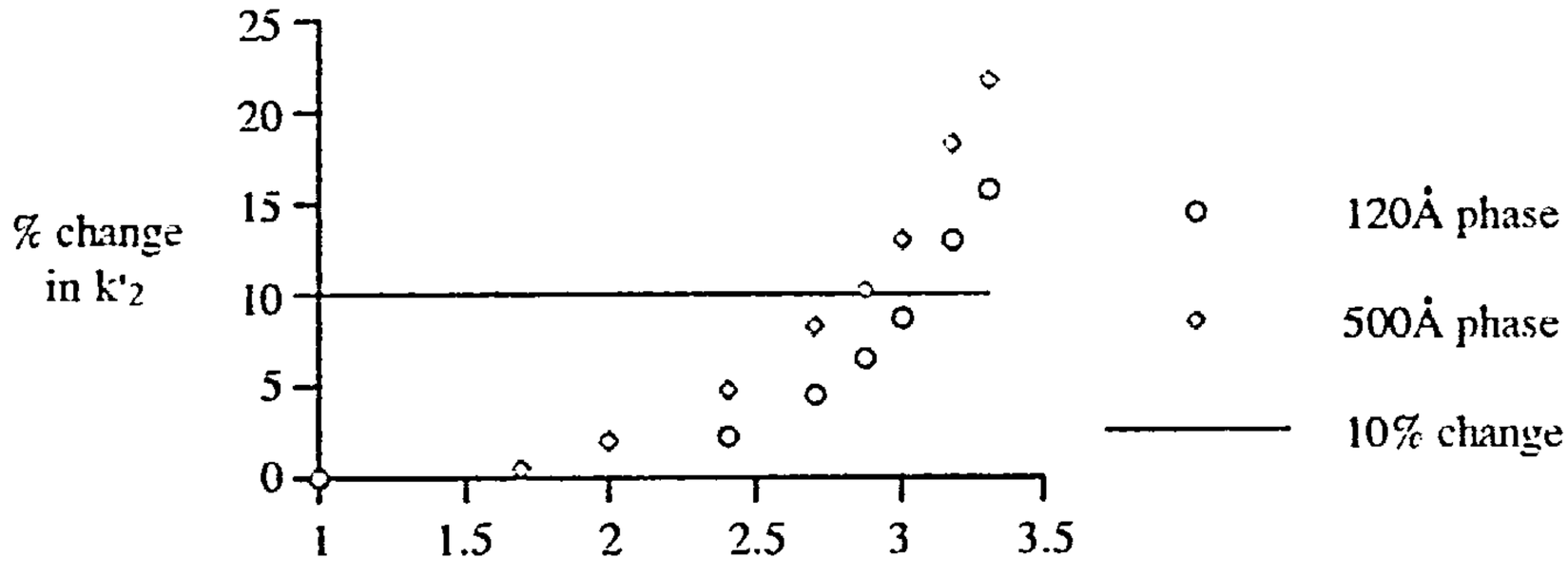

(iii)

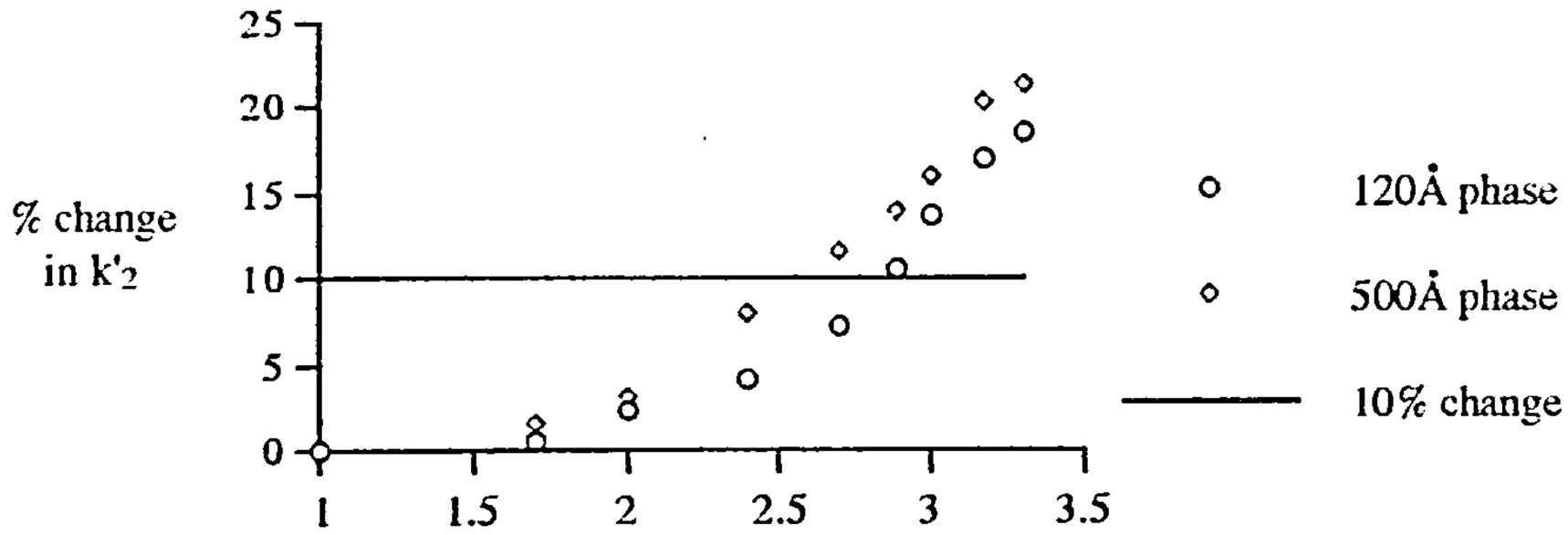

Figure 2-9 Percentage change in k'_2 versus $\log_{10}$ sample weight for (i) TSO, (ii) 1-PE and (iii) BME on columns (150 x 4.6 mm) packed with CDMPC-coated 5 µm Hypersil APS: 15% w/w for 120Å and 17.5% w/w for 500Å. Mobile phase: hexane/2-propanol TSO and BME: 90:10 v/v and 1-PE: 98:2 v/v. Flow rate: 0.5 ml/min.

The sample weight at which there is a 10 % change in second capacity factor for 1-PE and BME was slightly more favourable on 120Å phase compared to the 500Å phase (ca. 1100 and 700 μg cf. 750 and 400 μg) suggesting that for these two compounds the 120Å phase had a higher chromatographic capacity. However, for TSO there was virtually no difference between the two phases.

These results suggest that there are more interaction sites on the 15% CDMPC-coated 120Å, APS for 1-PE and BME compared to the 17.5% CDMPC-coated 500Å, APS. Whereas for TSO there are a similar number of interaction site on both phases.

Preparative capacity or overload

In order to try to determine the preparative overload for the 120 and 500Å phases, a plot of separation and resolution for the three test compounds against $\log_{10}$ sample amount was constructed. The results are shown in Figure 2-10.

For 1-PE and BME, the α value is identical for both the 120Å and 500Å phases and hardly changes over the sample weight range. However, for TSO the 120Å phase has a slightly higher α value and there is a very slow decrease in α value as the sample size is increased.

As expected, Rs reduces rapidly with increasing sample weight for all three analytes. For 1-PE and BME, the initial value of Rs at low concentrations and the reduction of Rs over the sample range is identical for both phases. Therefore, it is proposed that the sample load at which the chromatography would become no longer useful for preparative purposes would be approximately the same. However, for TSO, the slightly higher Rs on the 120Å phase at low concentrations was maintained over the sample range. Therefore for TSO, it is predicted that a slightly higher sample load could be achieved before the chromatography is deemed unsuitable.

(i)

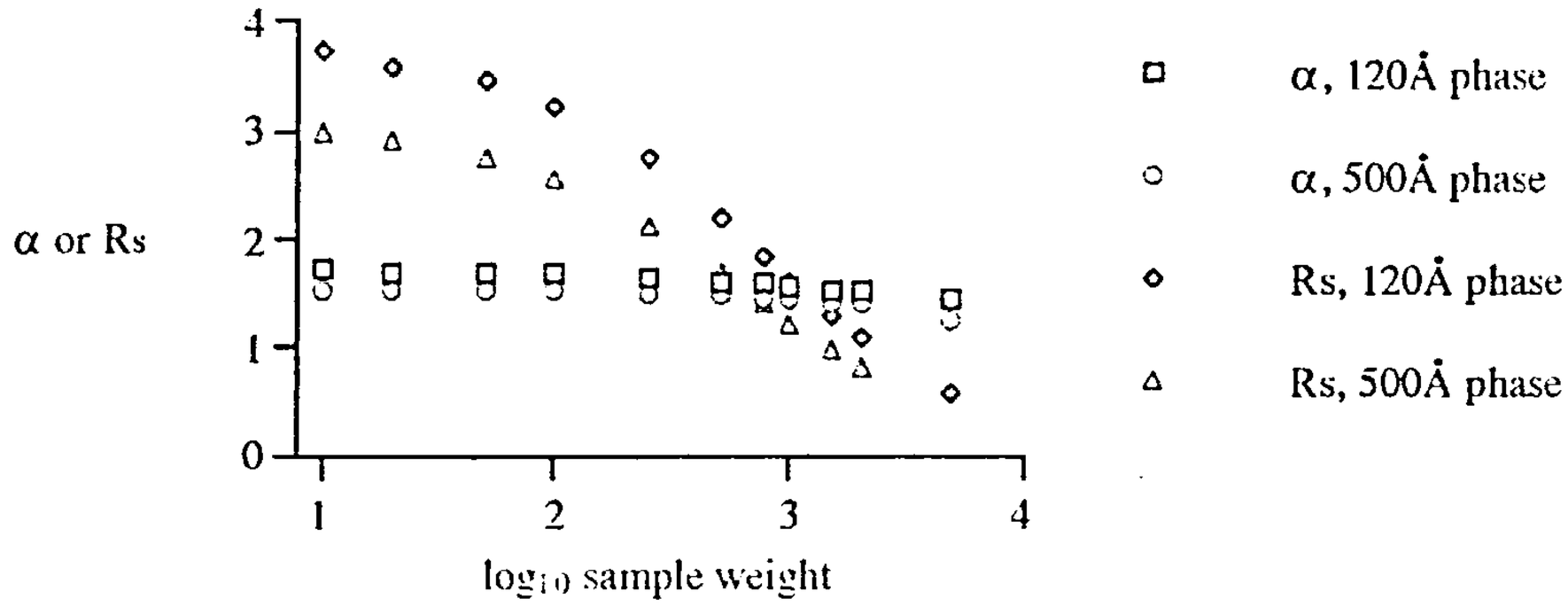

(ii)

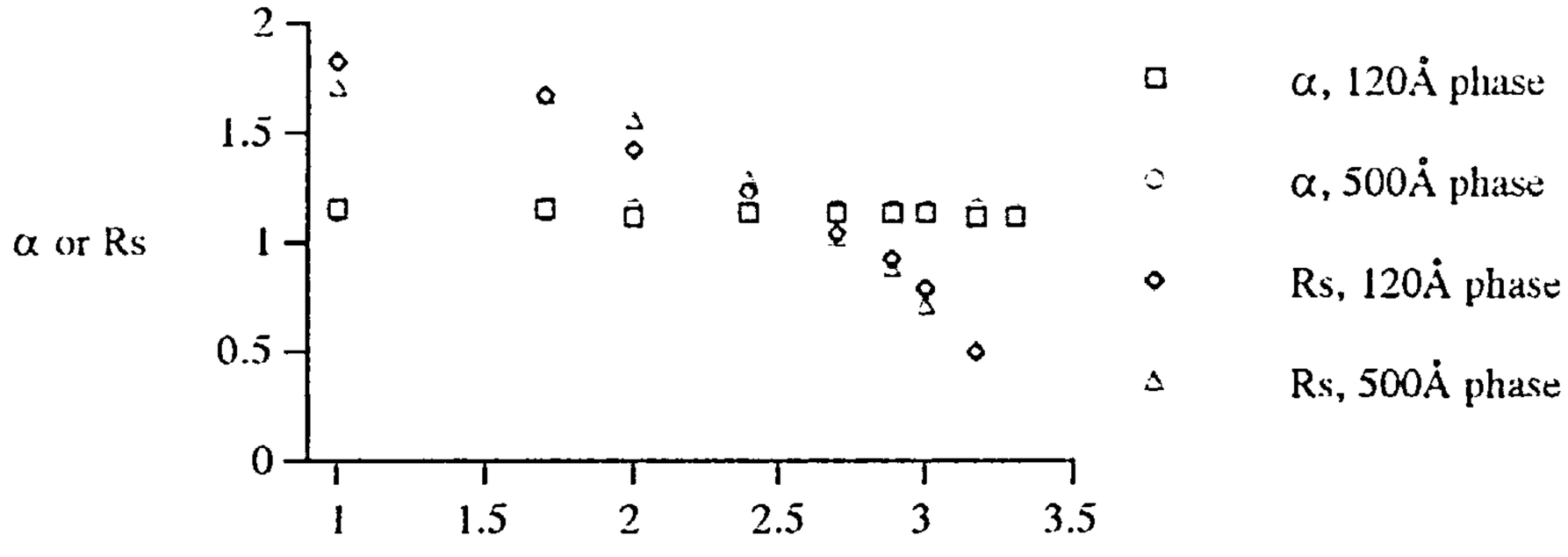

(iii)

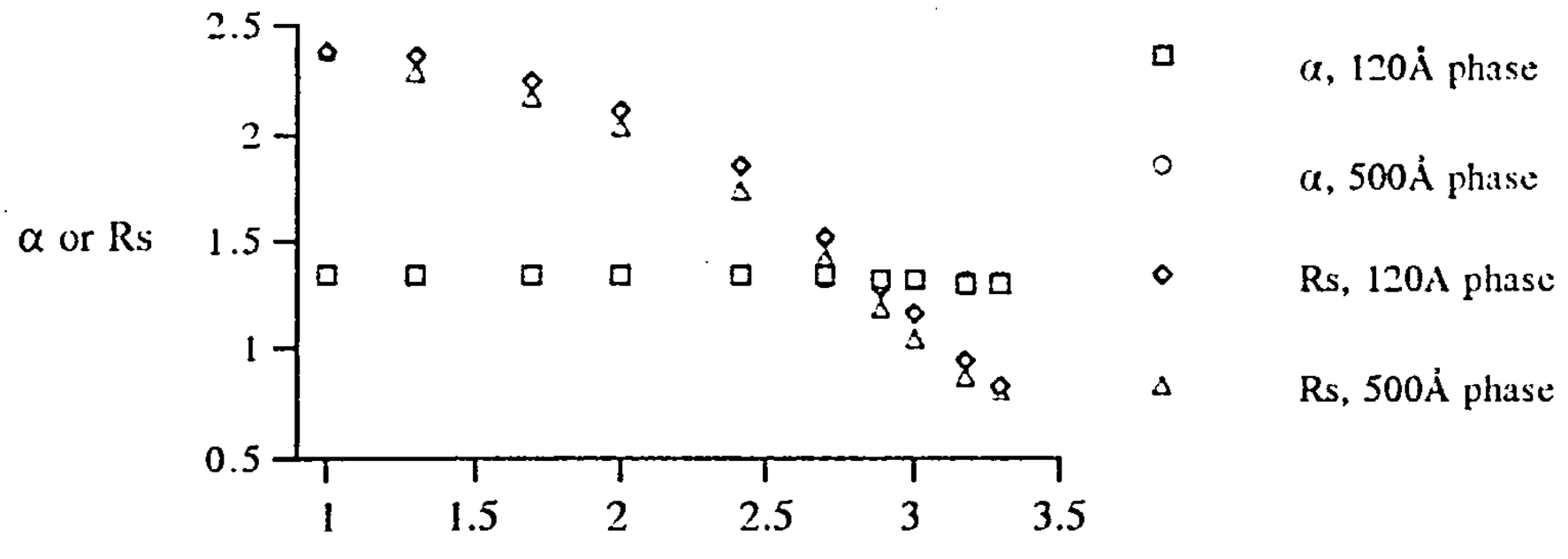

Figure 2-10 Separation and resolution for (i) TSO, (ii) 1-PE and (iii) BME on columns (150 x 4.6 mm) packed with CDMPC-coated 5 μm Hypersil APS: 15% w/w for 120Å and 17.5% w/w for 500Å. Mobile phase: hexane/2-propanol, TSO and BME: 90:10 v/v and 1-PE: 98:2 v/v. Flow rate: 0.5 ml/min.

2.3.6 Summary and Conclusions

The results indicate that the 15% w/w CDMPC-coated 120Å, Hypersil APS does not provide additional sample loading capacity over CDMPC-coated APS supports which have larger pore diameters (eg 500Å).

However, the fact that the 120Å support with a 15% w/w CDMPC loading had a similar sample loading capacity to the 500Å support with a higher CDMPC loading for the analytes tested is noteworthy. Therefore, there appears to be no disadvantage in using a smaller pored support, provided that its pore diameter is not less than 120Å. On the contrary, since less CDMPC is needed, use of the 120Å support would be financially advantageous if the phase needed to be scaled up to preparative (25 mm or more) diameter columns.

It was interesting to find that although the second eluting enantiomer of 1-PE and BME had higher chromatographic capacity on the 120Å phase (Figure 2-9), the α and Rs values were virtually identical to the 500Å phase (Figure 2-10). Whereas for TSO, the second enantiomer had similar chromatographic capacity on both the 120 and 500Å phases, α and Rs values were slightly higher on the 120Å phase. These results appear to indicate that TSO has a different chiral interaction mechanism to 1-PE and BME.

CHAPTER 3

INFLUENCE OF SUPPORT SURFACE CHEMISTRY ON ENANTIOSELECTIVITY

APS is widely accepted as a suitable support for the polysaccharide carbamate-coated phases. However, to our knowledge, there have been no reported studies justifying why this particular bonded silica phase should be used. Our aim was not only to understand the influence these APS groups might have on the stability and enantioselectivity of polysaccharide carbamate-coated phases, but also to investigate whether other types of support may give better chromatographic results. We decided to investigate the use of both more polar, underivatised silica (SI) and less polar, octadecylated silica (ODS) and also a relatively new very non-polar HPLC stationary phase, porous graphitic carbon (PGC), as potentially suitable supports for CDMPC.

3.1 SUPPORT SURFACE CHEMISTRIES USED IN THE PAST

As highlighted in Chapter 1 (section 1.3.1), it was the work by Okamoto *et al* [35] with (+)-PTrMA-coated macroporous aryl bonded silica that prompted Okamoto *et al* [67] and Shibata *et al* [63] to coat CTA on a bonded silica support. (+)-PTrMA had initially been coated onto diphenyl bonded macroporous (1000Å) silica (DPhS).[35] However, a few years later, Okamoto *et al* [36] presented limited results on the use of (+)-PTrMA coated APS and ODS supports and compared the results to a similarly coated DPhS support. For five test racemates they found that the capacity factors and separation were affected by the type of support used. In general, for the few test analytes, APS did give the better separations. However, they did not comment on the merits of the three phases and only noted that the differences in separation values might be due to the different morphology of the (+)-PTrMA coating on the DPhS, APS or ODS supports.

In the first publication[67] describing the enantioselectivity of a CTA-coated phase, APS was used as the support medium. Okamoto *et al* [129] have suggested that the APS group can; (i) decrease non-stereoselective interactions by shielding the acidic silanol groups and (ii) increase the stability of the coating by providing sites for hydrogen bond formation with the polysaccharide carbamate.

Felix and Zhang,[94] assuming that hydrogen bond formation would occur between the aminopropyl group and their amylopectin tris(phenylcarbamate) coating, attempted to increase the stability of the phase by using di- or triaminopropyl bonded silica as the support medium. However, they found that there was a decrease in chiral resolution as the number of amino groups increases and for all test racemates, the resolution was higher with the monoamino-bonded silica. They made no comment about the stability of the chiral coating.

To my knowledge, the only workers who have reported results using a support other than APS for a polysaccharide derivative were Krause and Galensa.[136] They coated CTA onto LiChrosorb diol (7 μm, 1000Å; Merck) for the separation of a series of polyhydroxylated flavanones. They found that their CTA phase gave comparable results to a commercially available CTA phase (support chemistry unknown).

3.2 THE USE OF SI, APS AND ODS AS SUPPORTS FOR CELLULOSE CARBAMATES[137]

Following on from the success of our small particle, Hypersil APS study, we decided to use commercially available small particle (3 μm) Hypersil silicas for this study. In order to span the polarity range, in addition to APS we chose SI and end-capped ODS spherical silicas as potentially suitable supports for CDMPC.

As shown in Chapter 2 (section 2.2.1) a loading of 15% w/w CDMPC was found to be optimum for the 120Å, Hypersil APS support. Therefore, the Hypersil SI, APS and ODS supports (2.5 g) were also coated with 15% w/w CDMPC (**CDMPC-3**; **3μ-1** to **3μ-3**). All three coated-phases had a gaussian shaped particle size distribution and a mean particle size similar to the uncoated silica and were high pressure slurry packed into stainless steel columns (100 x 4.6 mm; columns **18** to **20**). The separation of TSO on the three columns are shown in Figure 3-1.

Good peak shapes were obtained for TSO on all phases.

(i)

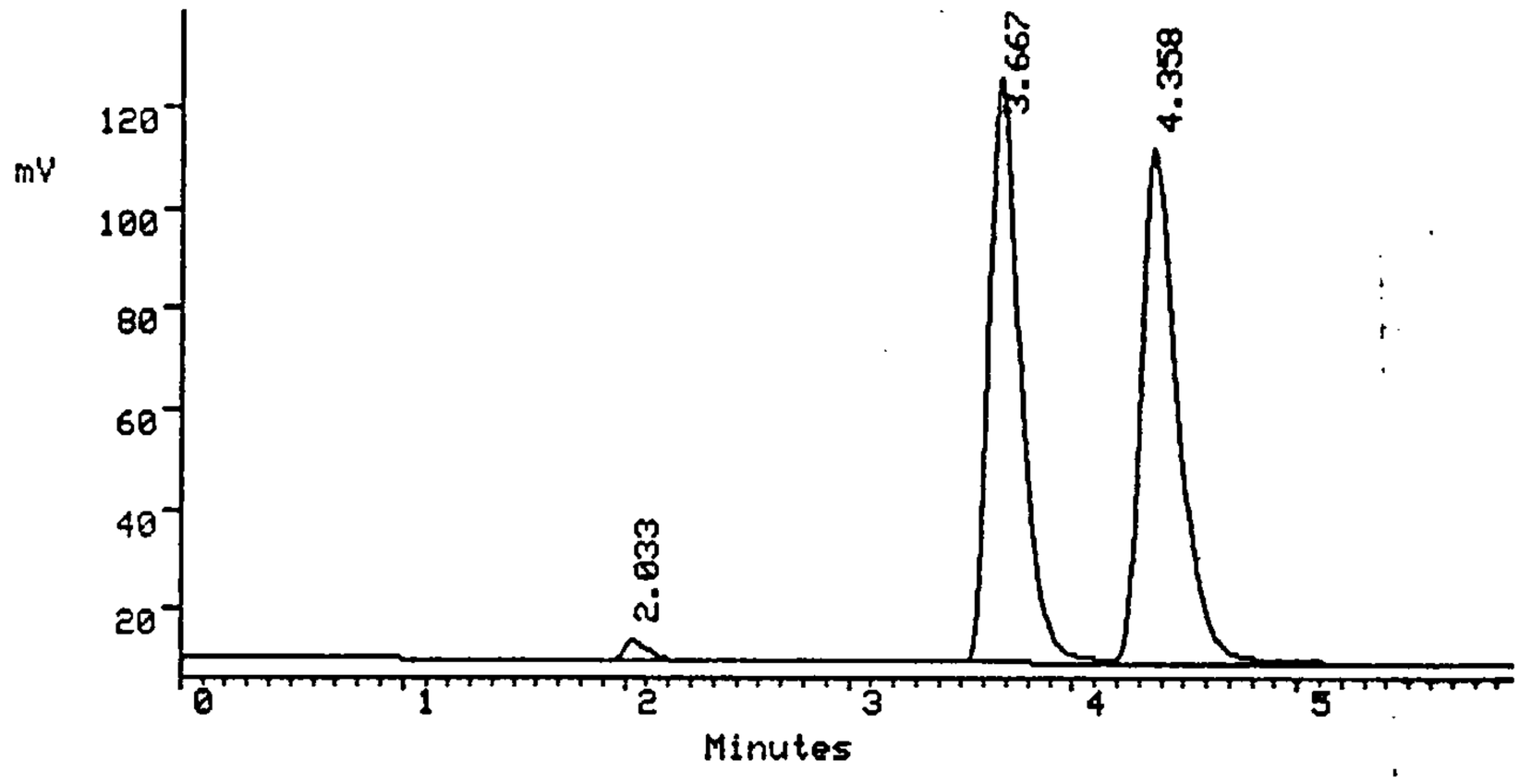

(ii)

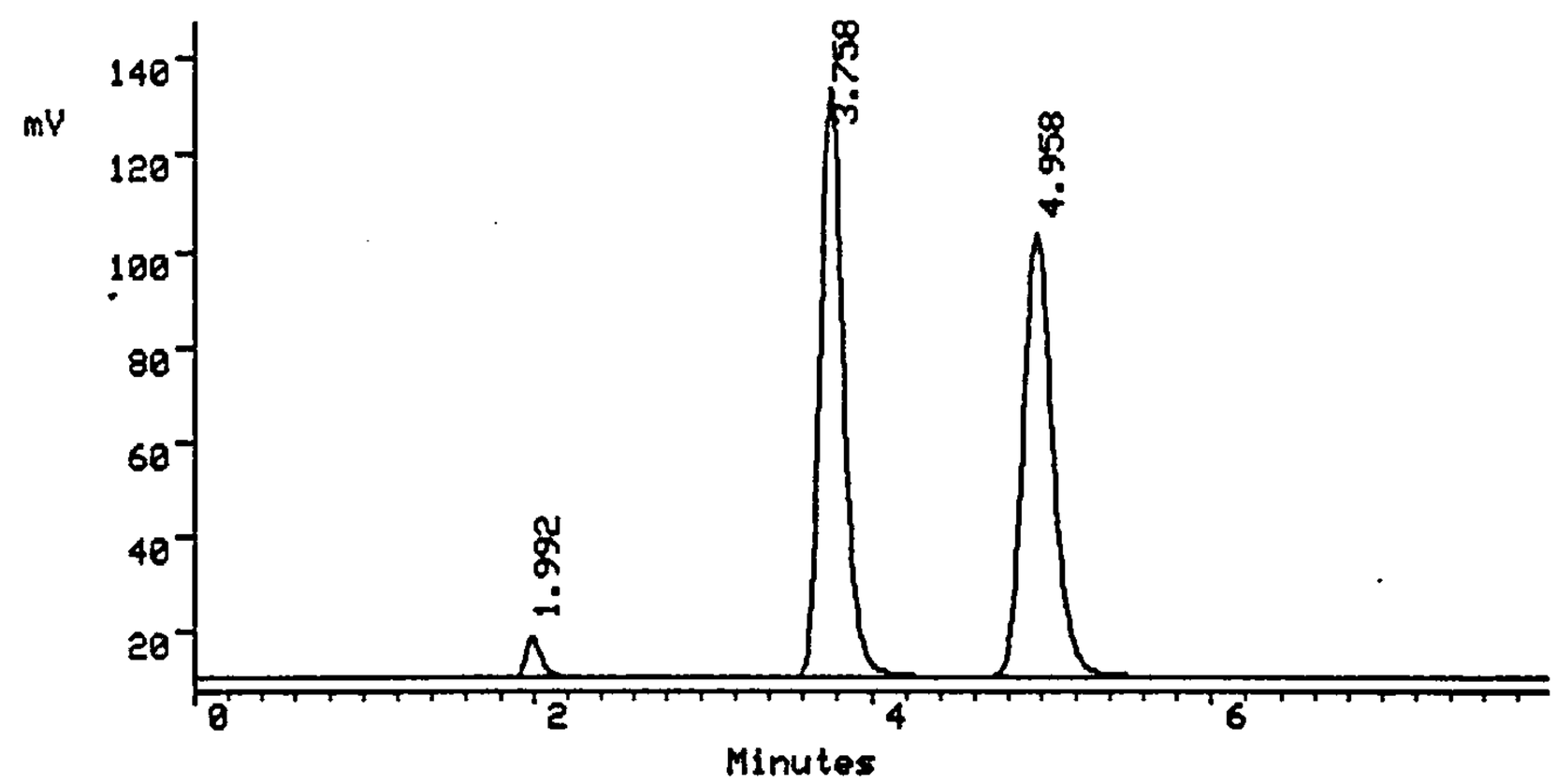

(iii)

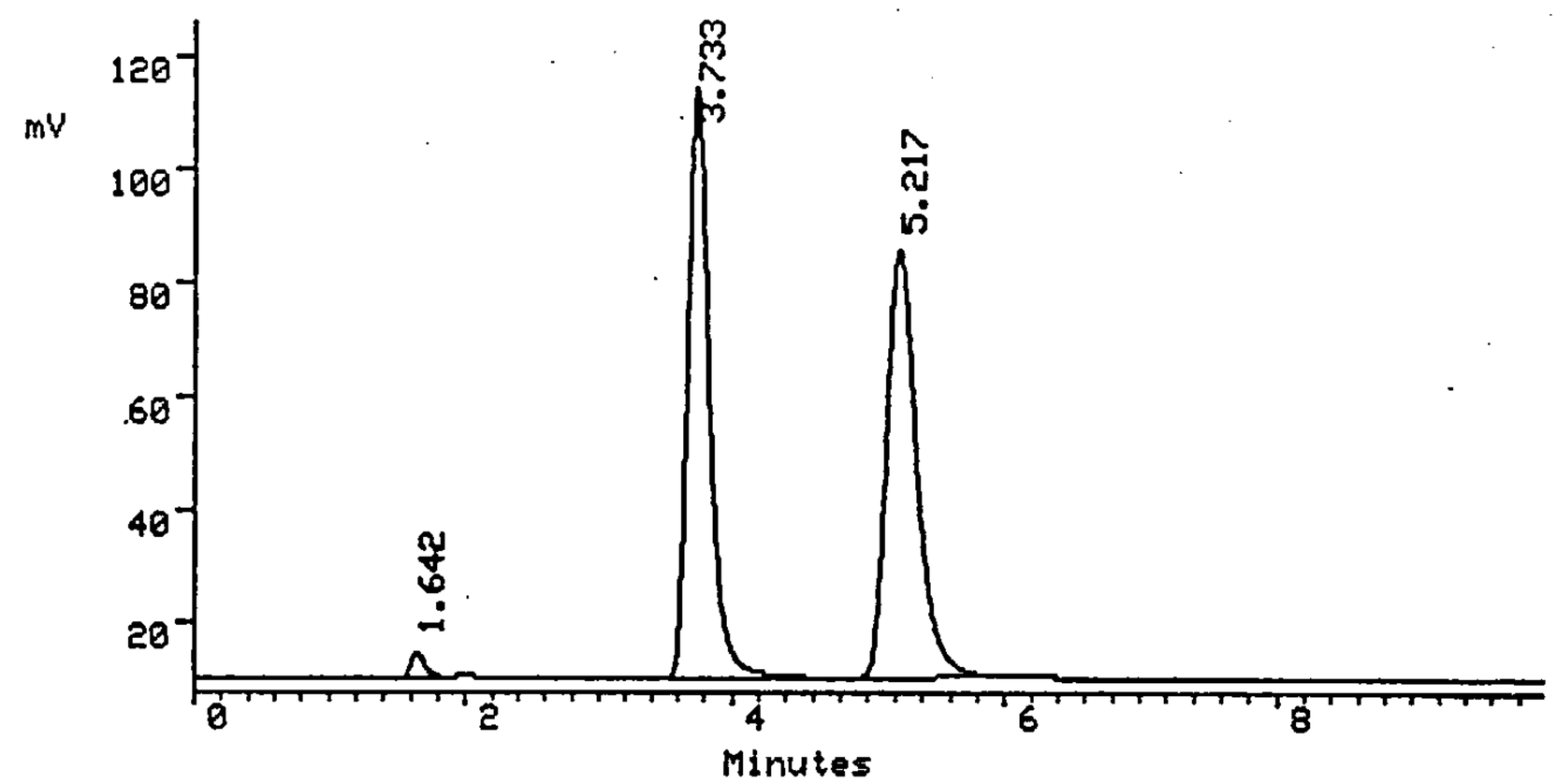

Figure 3-1 Separation of TSO on columns (100 x 4.6 mm) packed with 15% w/w CDMPC-coated 3 μm Hypersil (i) SI; (ii) APS and (iii) ODS. Mobile phase: hexane/2-propanol (90:10 v/v). Flow rate: 0.5 ml/min.

3.2.1 Stability of 15% w/w CDMPC-coated SI, APS and ODS Phases

In a similar study to that carried out in Chapter 2 (section 2.2.3), the stability of each 15% w/w CDMPC-coated phase was examined for 170 hours under a flow rate of 1 ml/min (total volume ca. 10 litres) at ambient temperature using hexane/2-propanol (80:20 v/v) as the mobile phase. There was no deterioration in column performance for any of the supports, as judged by the lack of change in k', N or R_S for a test mixture.

This result does not prove that intermolecular hydrogen bonding cannot take place between the cellulose carbamate and moieties on the surface of the silica such as amino or silanol groups. However, it is noteworthy that the end capped-ODS phase is stable to the test conditions. This support would be expected to have minimal exposed silanol groups with which hydrogen bonds could be formed. Therefore, this result suggests that surface hydrogen bonding may not be necessary to ensure the stability of the polysaccharide carbamate coating. Inter- and intra- strand hydrogen bonding would appear to be sufficient for ensuring the stability of the CDMPC coating.

3.2.2 Enantioselectivity of 15% w/w CDMPC-coated SI, APS and ODS Phases

The influence of support surface chemistry on column performance was investigated by examining the enantiomeric resolution of 16 chiral analytes: 6 neutral [ATFE; 1-PE; benzoin (BZ, **F**); BME; FLAV and benzyl mesityl sulfoxide (BMS, **J**)]; 5 basic [Trogers base (TB, **K**); HOMA; orphenadrine (ORP, **M**); alprenolol (ALP, **N**) and OXP] and 5 acidic [mandelic acid (MA, **S**); 2-methoxyphenylacetic acid (2-MPAA, **T**); 2-phenoxypropionic acid (2-PXPA, **U**) 2-phenyl-1-cyclopropane carboxylic acid (2-PCCA, **W**) and suprofen (SUP, **X**)]. The results can be seen in Tables 3-1 to 3-3.

Table 3-1 Chromatographic parameters for neutral chiral analytes on CDMPC-coated SI, APS and ODS 3 µm Hypersil supports

Analyte		APS 15% w/w	ODS 15% w/w	SI	
				15% w/w	20% w/w*
ATFE	k'_1	3.25	3.49	2.22	3.96
	k'_2	7.30	9.09	4.91	9.14
	α	2.25	2.61	2.21	2.31
	Rs	6.89	6.00	7.63	6.56
1-PE	k'_1	5.04	5.21	4.81	5.80
	k'_2	5.85	6.16	5.25	6.85
	α	1.16	1.19	1.09	1.18
	Rs	1.89	1.65	1.03	1.99
BZ	k'_1	3.50	4.35	3.17	3.75
	k'_2	4.67	5.97	3.99	5.24
	α	1.33	1.37	1.26	1.40
	Rs	3.04	2.97	2.40	3.27
BME	k'_1	1.49	1.74	1.31	1.59
	k'_2	1.96	2.52	1.68	2.24
	α	1.32	1.44	1.28	1.41
	Rs	2.47	2.91	2.06	2.86
FLAV	k'_1	1.78	2.49	1.62	2.12
	k'_2	2.30	3.15	1.96	2.78
	α	1.29	1.26	1.21	1.31
	Rs	2.46	2.14	1.80	2.53
BMS	k'_1	3.50	3.93	3.25	3.76
	k'_2	6.65	8.36	5.55	8.17
	α	1.90	2.13	1.71	2.17
	Rs	5.56	4.77	4.96	6.04

* The reason for the preparation of this phase will be explained in section 3.2.4.
Mobile phases: hexane/2-propanol: ATFE, BZ, BME, FLAV and BMS: 90:10 v/v and 1-PE: 98:2 v/v. Flow rate: 0.5 ml/min.

Table 3-2 Chromatographic parameters for basic chiral analytes on CDMPC-coated SI, APS and ODS 3 µm Hypersil supports

Analyte		APS 15% w/w	ODS 15% w/w	SI 15% w/w	SI 20% w/w*
TB	k'_1	1.39	1.62	1.59	2.01
	k'_2	1.75	2.27	2.10	2.46
	α	1.25	1.40	1.32	1.22
	Rs	1.71	2.21	2.24	1.49
HOMA	k'_1	1.52	1.37	1.27	1.41
	k'_2	2.10	2.21	1.84	2.17
	α	1.38	1.62	1.45	1.54
	Rs	2.65	3.04	2.49	3.20
ORP	k'_1	0.90	0.63	2.16	2.00
	k'_2	1.23	1.05	2.49	2.44
	α	1.37	1.67	1.15	1.22
	Rs	2.02	2.18	1.07	1.40
ALP	k'_1	1.11	0.41	4.23	3.52
	k'_2	1.70	0.88	4.54	4.27
	α	1.53	2.14	1.07	1.21
	Rs	2.48	2.42	P.R.	1.21
OXP	k'_1	2.26	1.11	6.56	5.27
	k'_2	5.43	3.61	8.54	9.38
	α	2.40	3.26	1.30	1.78
	Rs	5.48	5.40	1.50	3.69

* The reason for the preparation of this phase will be explained in section 3.2.4. P.R. = partial resolution (<0.5). Mobile phases: all mobile phases contain 0.1% diethylamine; TB and ORP: hexane/2-propanol (90:10 v/v); HOMA, ALP and OXP: hexane/2-propanol (80:20 v/v). Flow rate: 0.5 ml/min

Table 3-3 Chromatographic parameters for acidic chiral analytes on CDMPC-coated SI, APS and ODS Hypersil 3 µm supports

Analyte		APS 15% w/w	ODS 15% w/w	SI	
				15% w/w	20% w/w*
MA	k'_1	8.93	5.67	5.46	6.94
	k'_2	9.52	6.94	6.09	7.85
	α	1.06	1.11	1.12	1.13
	Rs	0.72	0.73	1.08	1.29
2-MPAA	k'_1	4.82	3.26	3.66	5.09
	k'_2	5.33	3.74	4.05	5.82
	α	1.11	1.15	1.11	1.14
	Rs	1.32	1.17	1.19	1.67
2-PXPA	k'_1	3.14	2.48	2.67	3.17
	k'_2	4.52	4.51	4.12	4.99
	α	1.44	1.82	1.54	1.57
	Rs	3.89	4.42	4.10	4.34
2-PCCA	k'_1	5.48	4.78	4.67	6.45
	k'_2	6.25	5.13	5.35	7.49
	α	1.14	1.07	1.14	1.16
	Rs	1.78	P.R.	1.73	1.93
SUP	k'_1	11.78	12.34	11.64	12.60
	k'_2	12.83	14.22	12.83	13.91
	α	1.09	1.15	1.11	1.10
	Rs	1.07	1.23	1.56	1.14

* The reason for the preparation of this phase will be explained in section 3.2.4.
P.R. = partial resolution (<0.5). Mobile phase: hexane/ethanol/trifluoroacetic acid (96:4:0.5 v/v/v). Flow rate: 0.5 ml/min

Neutral Analytes (Table 3-1)

For all neutral analytes examined, k' values are highest on the ODS phase and lowest on the SI phase. This result may seem surprising, since the test analytes are all relatively polar in nature and would not be expected to interact strongly with the non-polar ODS surface. However, the α values also show the same trend, thus there must be more CDMPC interaction sites on the ODS phase than there are on the SI phase. An explanation for this, along with a possible reason for the lower than expected Rs values observed on the ODS phase, will be given in section 3.2.3.

Basic Analytes (Table 3-2)

A marked difference in chromatographic behaviour can be seen between analytes with a sterically hindered basic group (TB and HOMA) and those in which the basic group is more accessible (ORP, ALP and OXP).

The analytes which have the more accessible basic group have high k' values on the SI phase and low k' values on the ODS phase. This is consistent with previously reported studies[115,138] suggesting that there are strong interactions between accessible basic amino groups in the analytes and any exposed acidic silanol groups. In the case of the SI phase, interactions with the support surface are so strong that the chromatography is extremely poor. The analytes in which the basic group is more sterically hindered are not able to interact as strongly with the surface groups and the k' values for the three phases are more similar.

For all the basic analytes, the α values are highest on the ODS phase and, in general, lowest on the SI phase. This is consistent with the earlier suggestion that there are more CDMPC interaction sites on the ODS phase.

Acidic Analytes (Table 3-3)

In general, k' values are largest when APS is the support. This is the counterpart of the effect seen with the basic compounds on the SI phase, ie. the acidic moiety appears to be interacting with exposed APS groups. For the majority of analytes, α values are slightly higher on the ODS phase, but in general are lower than have been described in the literature.[116] Reasons for this are as yet unclear. SUP shows a somewhat different pattern of behaviour to the other acidic analytes, possibly as a result of its polyfunctional nature.

3.2.3 Interpretation of Results from Section 3.2.2

In order to explain the chromatographic trends seen for the three coated phases, the effects of introducing a bonded group onto the surface of a small pored phase need to be considered. As explained in Chapter 2 (section 2.2.1), a bonded group will not only change the chemical nature of the surface (examples of non-stereospecific interactions between the analyte and the surface group have already been discussed) but will also affect the pore structure (Figure 3-2).

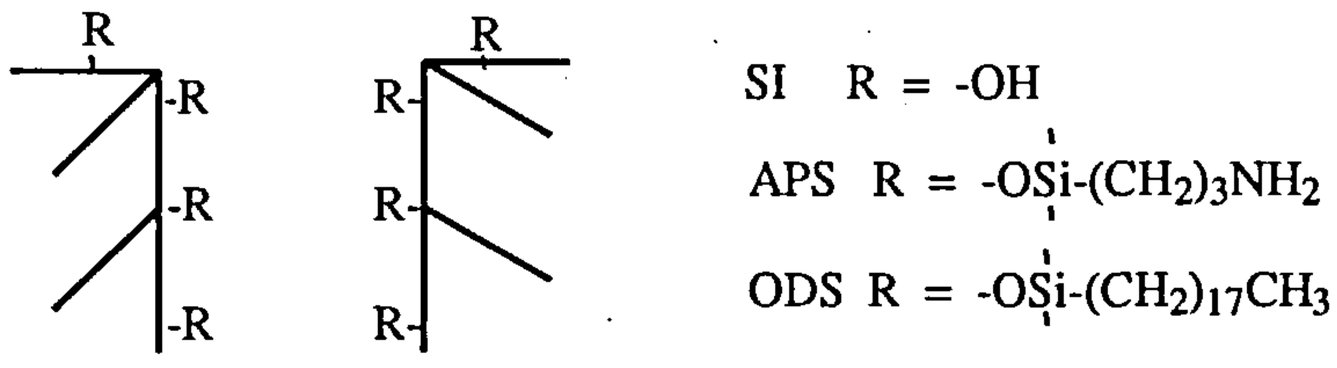

Figure 3-2 Diagrammatical view of a pore

An aminopropyl or octadecyl group will reduce the pore diameter and thus the pore volume, compared with the underivatised silica, thus leading to an increase in the amount of CDMPC which is prevented from entering the pores (see Table 2-2 for the predicted reduction in surface area and pore volume for APS). A calculation of the reduction in pore volume caused by bonding an octadecyl group has not been made since the magnitude of this effect would very much depend on the spatial arrangement and conformation of this large bonded

group. These would be very difficult to predict and would be highly dependant on the local environment.

In addition to the changes in pore volume, the polar SI and APS supports may have an attractive or stabilising effect on the relatively polar CDMPC coating, via hydrogen bonding or dipole interactions (as discussed earlier). However, the more lipophilic ODS may have a repelling or destabilising effect which will further deter the CDMPC from entering the pores, but does not compromise the stability of the phase.

The idea that the pores are more filled or blocked in the case of the ODS phase and least filled or more open in the case of the coated SI phase was confirmed by using a mercury intrusion method (carried out by Shandon HPLC) to measure pore volume and pore diameter of the coated phases. The results are shown in Table 3-4. In addition, a reduction in the retention time of a non-retained analyte (1,3,5-tri-*tert*-butyl benzene) was observed as the support was change from SI to APS to ODS (see Figure 3-1). The column dead volume changes are also shown in Table 3-4.

Table 3-4 Mercury intrusion measurements and column dead volume for CDMPC-coated phases

Phases	Pore Volume (cm^3/g)	Pore Diameter (Å)	Column Dead Volume (ml)
Uncoated SI	0.590	120	-
15% w/w CDMPC on SI	0.329	110.2	1.015
15% w/w CDMPC on APS	0.312	104	0.985
15% w/w CDMPC on ODS	0.163	98.8	0.819
20% w/w CDMPC on SI*	0.320	107.5	0.994

* The reason for the preparation of this phase will be explained in section 3.2.4.

The results clearly demonstrate the reduction in pore volume caused by the CDMPC coating. The ODS phase has a significantly lower pore volume compared to the other three coated phases. The column dead volume appeared to correlate well with the pore volume. Therefore, a graph was plotted to investigate this (Figure 3-3).

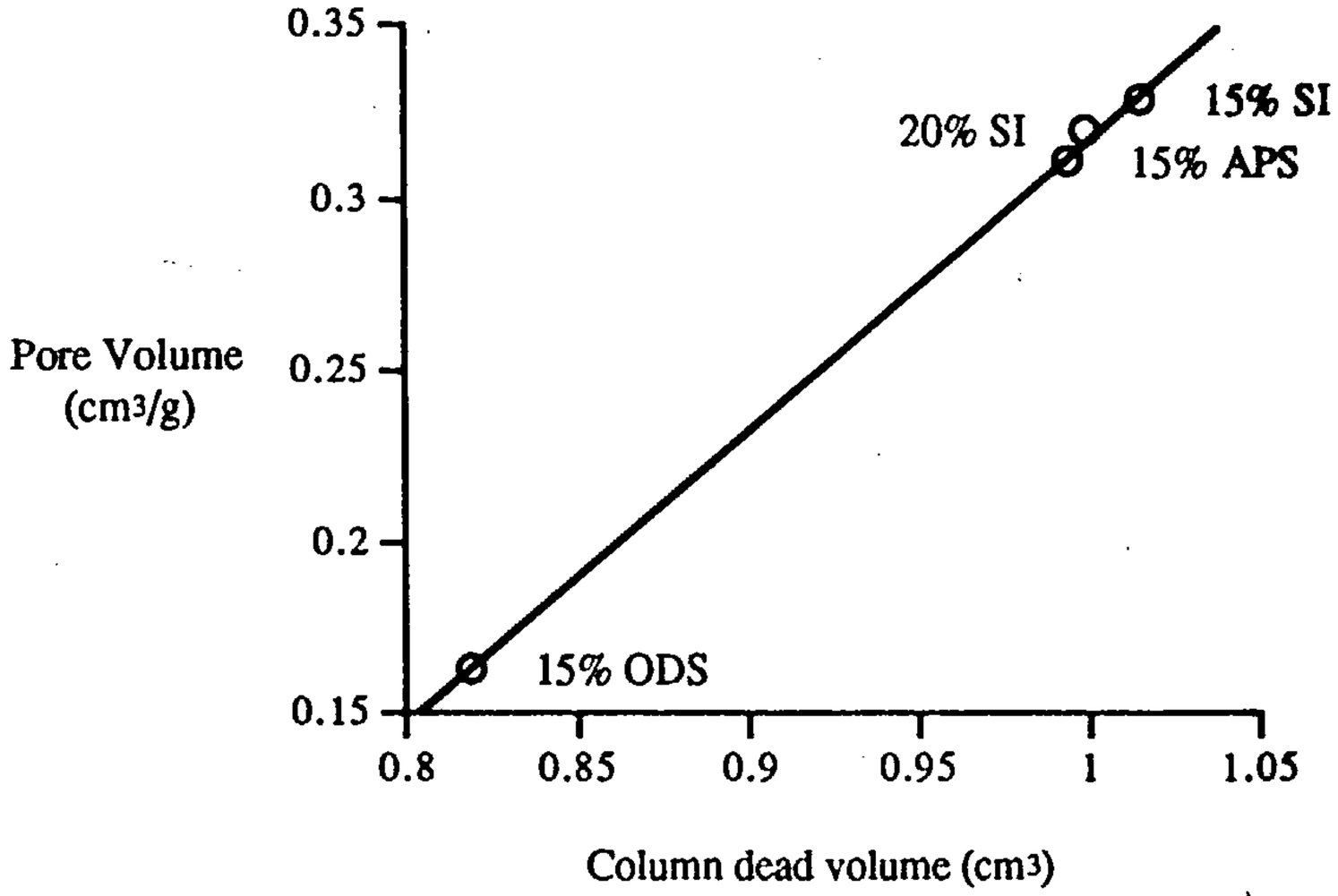

Figure 3-3 Pore volume versus column dead volume for CDMPC-coated phases.

From the limited data, the measured pore volume does correlate very well with the column dead volume. Ideally there should have been data points between the 15% ODS and APS points. However, it appears to be possible to gauge the pore volume for CDMPC-coated phases by measuring the dead volume of the packed column.

The slightly lower than expected Rs values for the ODS phase may have been caused by the depth of the CDMPC coating. As noted above it appears that much of the CDMPC has been excluded from the narrow non-polar ODS pores thus producing a thick CDMPC coating around the particles. It is this thick coating that may be causing very slow mass transfer, which would in turn cause

the enantiomer peaks to broaden. However, in contrast to the apparently overloaded 20% w/w CPC-coated phase described in Chapter 2 (section 2.2.1), the 15% w/w CDMPC-coated ODS did not have a large percentage of fine particles and the gaussian shaped chromatographic peaks suggested that the chromatographic bed was packed well.

Taking account of the chromatographic results (Tables 3-1 to 3-3), the support pore model (Figure 3-2) and the observations from the loading experiments, the following phase descriptions are proposed:

<u>15% w/w CDMPC-coated SI</u>

Owing to its polar nature and relatively large pore volume, the SI support is able to accommodate the polar CDMPC coating more easily than the other two supports. Therefore, it has the least amount of CDMPC coating around the outside of the particles, which reduces the number of chiral interaction sites, leading to the lowest α values. The strong interactions seen with some basic analytes indicate that there are regions where the coverage of accessible silica surface by CDMPC is low.

<u>15% w/w CDMPC-coated APS</u>

The APS support appears to have slightly more CDMPC coating on the outside of the particles, demonstrated by higher k' and α values for neutral analytes compared to the SI phase. High Rs is observed for many of the analytes and loading experiments (section 2.2) have confirmed that a 15% w/w CDMPC loading is close to optimum for this support. Higher than average interactions with some acidic analytes suggest that, as with the SI phase, there are regions where the density of the CDMPC coating is low.

15% w/w CDMPC-coated ODS

The ODS support, due to its large non-polar bonded group, does not so readily accommodate CDMPC into its pore volume. Therefore it has the largest amount of CDMPC on the outside of the particles, which provides the largest number of chiral interaction sites, as demonstrated by the high α values observed for the majority of analytes. However, in contrast to the APS phase, the amount of CDMPC on the outside of the ODS particles appears to have exceeded the optimum. Whilst the column has still packed satisfactorily, the poor mass transfer is affecting the efficiency of the phase and hence the resolution.

3.2.4 Improved Enantioselectivity of 20% w/w CDMPC-coated SI

It was of particular interest that, contrary to popular belief, the 15% w/w CDMPC-coated SI phase showed good chromatography for many test analytes. It was noted that (i) SI appears to most readily accept the CDMPC loading, due to its polar nature and larger pore volume and (ii) in previous studies, wider pore[67,69] APS was able to accept loadings of 20 to 25% w/w. Consequently, the behaviour of a 20% w/w CDMPC (**CDMPC-3**) loading on 120Å, 3 µm Hypersil SI was investigated.

The SI support readily accepted this higher loading (**3µ-4**) and the chromatographic results (column **21**) are shown in Tables 3-1 to 3-3. The 20% w/w coated SI phase was significantly more efficient than the 15% w/w coated SI phase for the majority of analytes tested. The separation of BME on the 15 and 20% w/w CDMPC-coated SI phases are shown in Figure 3-4.

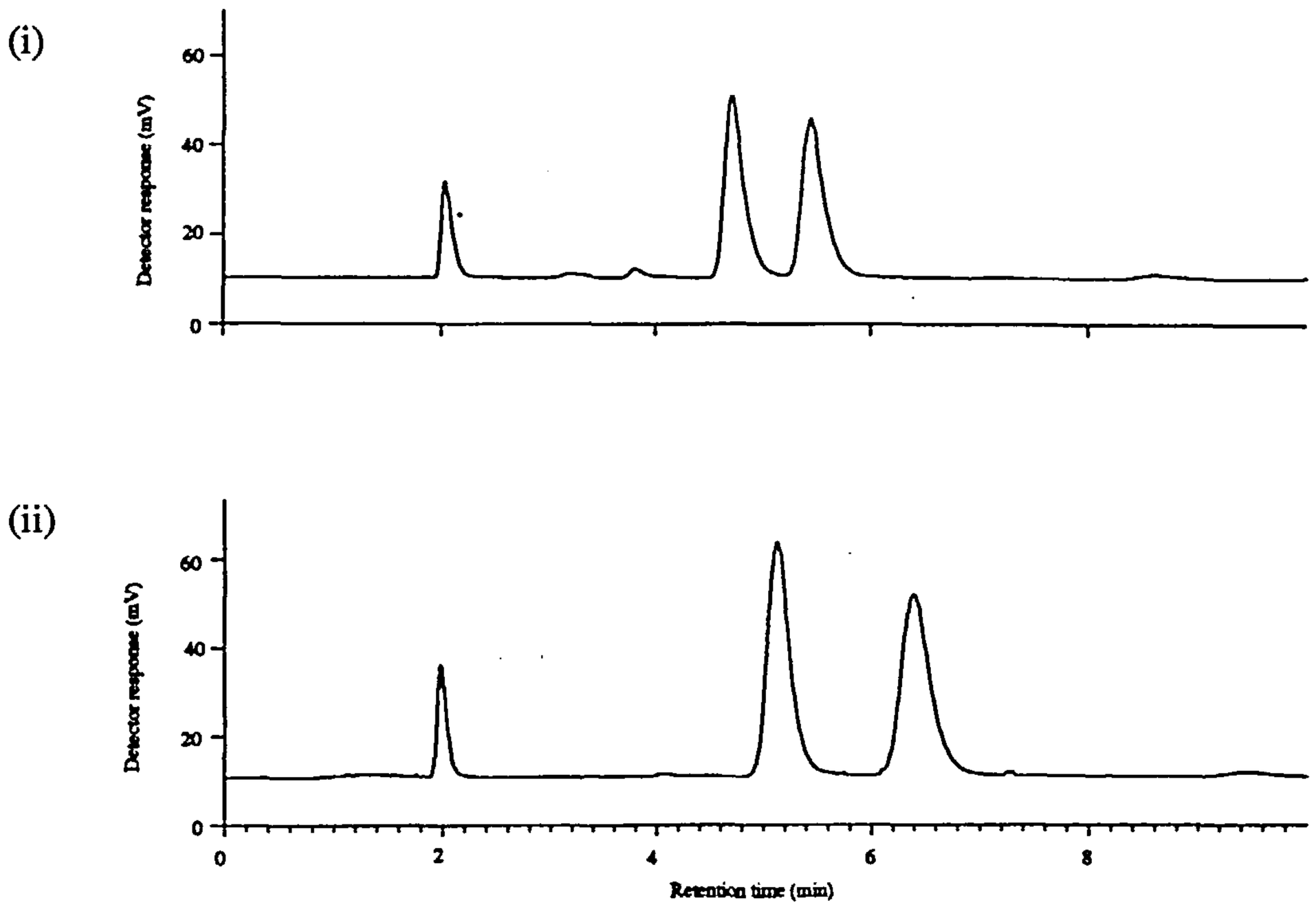

Figure 3-4 Separation of BME on column (100 x 4.6 mm) packed with CDMPC-coated 3 µm Hypersil SI: (i) 15% w/w, (ii) 20% w/w. Mobile phase: hexane/2-propanol (90:10 v/v). Flow rate 0.5 ml/min

For many analytes, the 20% w/w coated SI phase also gave superior performance to either the ODS or APS 15% w/w coated phases. Of remaining concern were the poor results seen with some basic analytes, due to interactions with exposed surface silanol groups. Compared to the 15% w/w coated SI phase, an improvement was seen in the k' and α values on the 20% w/w coated SI phase, indicating that interactions with Si-OH groups had been reduced by the heavier loading. However, although the peaks were still tailing slightly, a significant improvement was made by increasing the amount of diethylamine, a silanol suppressor, in the mobile phase from 0.1 to 1.0% v/v. For example, for OXP on the 20% w/w coated SI phase, the k'_1 value decreased from 5.27 to 2.86 and the α and Rs values increased from 1.78 to 2.48 and 3.60 to 5.30 respectively.

The column continued to remain stable with this mobile phase composition for the duration of the study and showed no deterioration in performance after return to standard test conditions.

3.2.5 Summary and Conclusions

We have shown that it is possible to produce stable CDMPC-coated phases using both a polar SI and a non-polar ODS supports.

It was particularly exciting to find that, contrary to popular belief, SI could be used as the support media. The optimum CDMPC loading for the SI support was higher than for the APS support (20% w/w rather than 15% w/w). It was proposed that this was due to the SI support having a wider pore diameter and larger pore volume. The 20% w/w CDMPC-coated SI phase was found to give both superior separation and resolutions compared to the 15% coated APS phase for many of the test analytes.

The optimum CDMPC loading for the ODS support may have been exceeded at 15% w/w, since, the Rs values were slightly lower than might have been expected for the observed α values. However, α values were significantly better on this phase compared to the 15% w/w coated APS phase for many analytes. In particular, the coated ODS phase appeared to be most effective for the resolution of basic analytes with non-hindered amino groups such as the β-blockers, ALP and OXP. This is because the ODS groups, along with the trimethylsilane end-capping, most effectively reduce any interactions between the acidic silanol groups and the amine moiety.

3.3 THE USE OF POROUS GRAPHITIC CARBON AS A SUPPORT FOR CELLULOSE CARBAMATES[139]

The results obtained in section 3.2 demonstrated that both polar SI and non-polar ODS small pore supports can be used and, for particular applications, may offer significant advantages over APS supports. However as reported, all three supports were found to have some limitations and/or to give poor results for specific analytes. Therefore, in a search to find other, potentially better, polysaccharide carbamate supports, we have expanded our investigations to the use of PGC (commercially called Hypercarb; Shandon HPLC).

3.3.1 Introduction to PGC

PGC is an extremely hydrophobic phase composed of sub-units which contain flat layers of hexagonally arranged carbon atoms (Figure 3-5). These units are closely packed to form spherical particles with high mechanical stability.[140] Within the sheet, the carbon atom valence is fully satisfied by σ and π C-C bonding. Therefore, in contrast to silica-based supports, there are virtually no surface functional groups. PGC also has a completely different retention mechanism and selectivity to silica-based supports. Whilst the latter rely mostly on dipole-dipole and hydrogen bond interactions, molecules are held on the surface of PGC primarily by dispersive interaction forces.

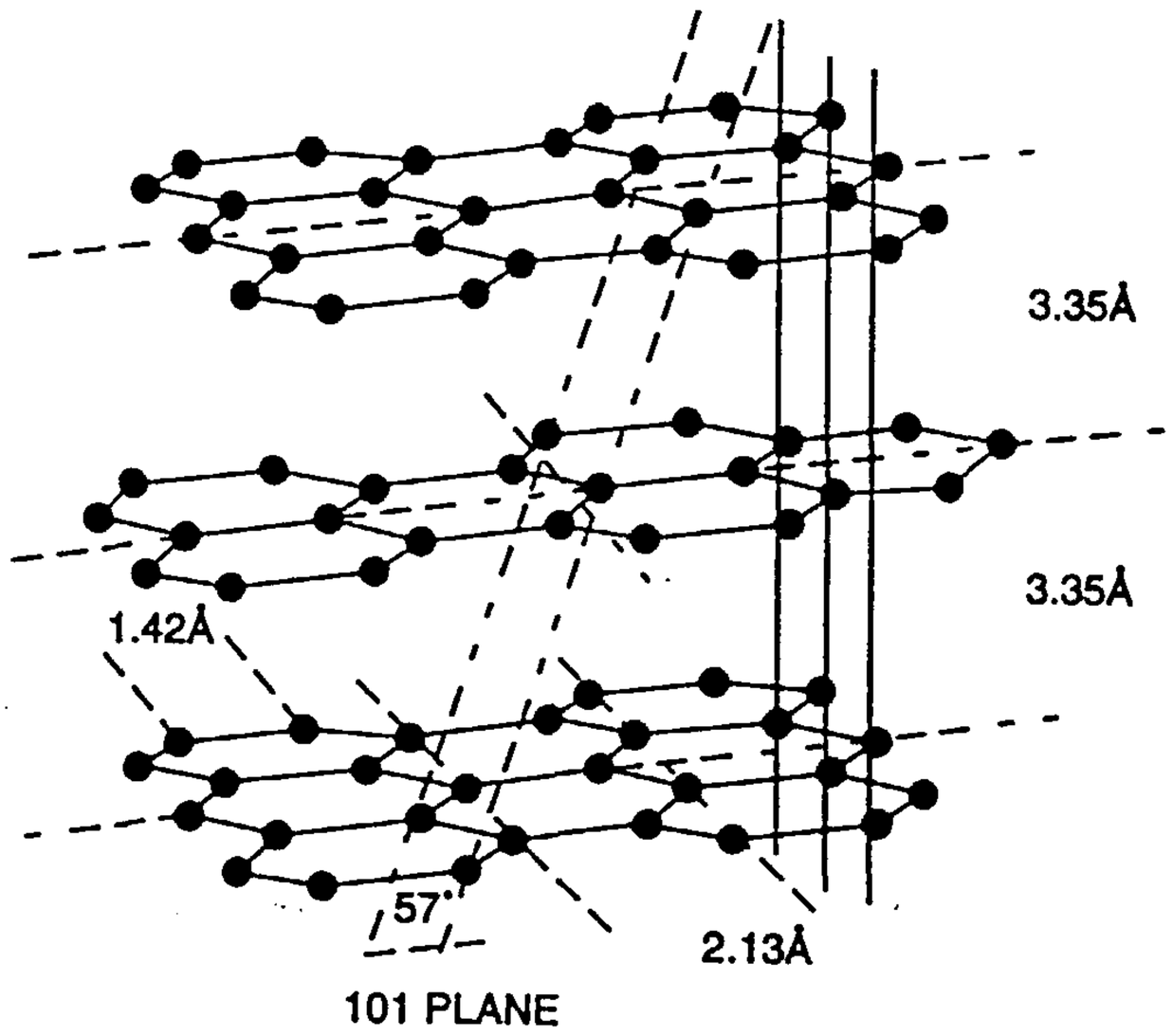

Figure 3-5 Structure of porous graphitic carbon (PGC)

Chiral separations have been carried out on PGC columns by using chiral mobile phase additives[141-143] such as N-carbobenzoxy glycyl L-proline (L-ZGP) and β-cyclodextrin. More recently, Wilkins *et al* [144] adsorbed a chiral anthrylamine derivative onto the surface of a pre-packed PGC column and was able to demonstrate the enantioseparation of several chiral analytes. However, to our knowledge, PGC has not yet been evaluated as a support for cellulose carbamate coatings.

3.3.2 Rationale for CDMPC Loading on PGC

As demonstrated in Chapter 2 (section 2.2.1), a single phase loading of 15% w/w cellulose carbamate was optimum for 120Å, Hypersil APS. However, as indicated in the literature[67,69] and concluded in section 3.2, supports which have larger pore diameters can more easily accommodate the cellulose carbamates, thus the chiral phase loading needs to be increased.

PGC has a mean pore diameter of 250Å. Therefore, in a preliminary attempt to produce an efficient phase, a 25% w/w CDMPC (**CDMPC-1**) loading on 7 μm PGC was prepared by building up 5 layers of 5% w/w CDMPC. It was anticipated that repeated layering of the CDMPC might (i) provide a more homogeneous CDMPC surface, thus minimising the chance of exposed PGC surfaces and (ii) reduce the possibility of distortion of the CDMPC 3D structure on the outer surface due to attraction of the flat phenyl groups to the PGC surface.

The PGC particles readily accepted the 25% w/w loading and the coated material was high pressure slurry packed (at Shandon HPLC, UK) into a stainless steel HPLC column (100 x 4.6 mm; column **22**). The separation of three chiral analytes; 1-phenyl-2-butanol (1-PB, **D**), TB and 2-PXPA are shown in Figure 3-6.

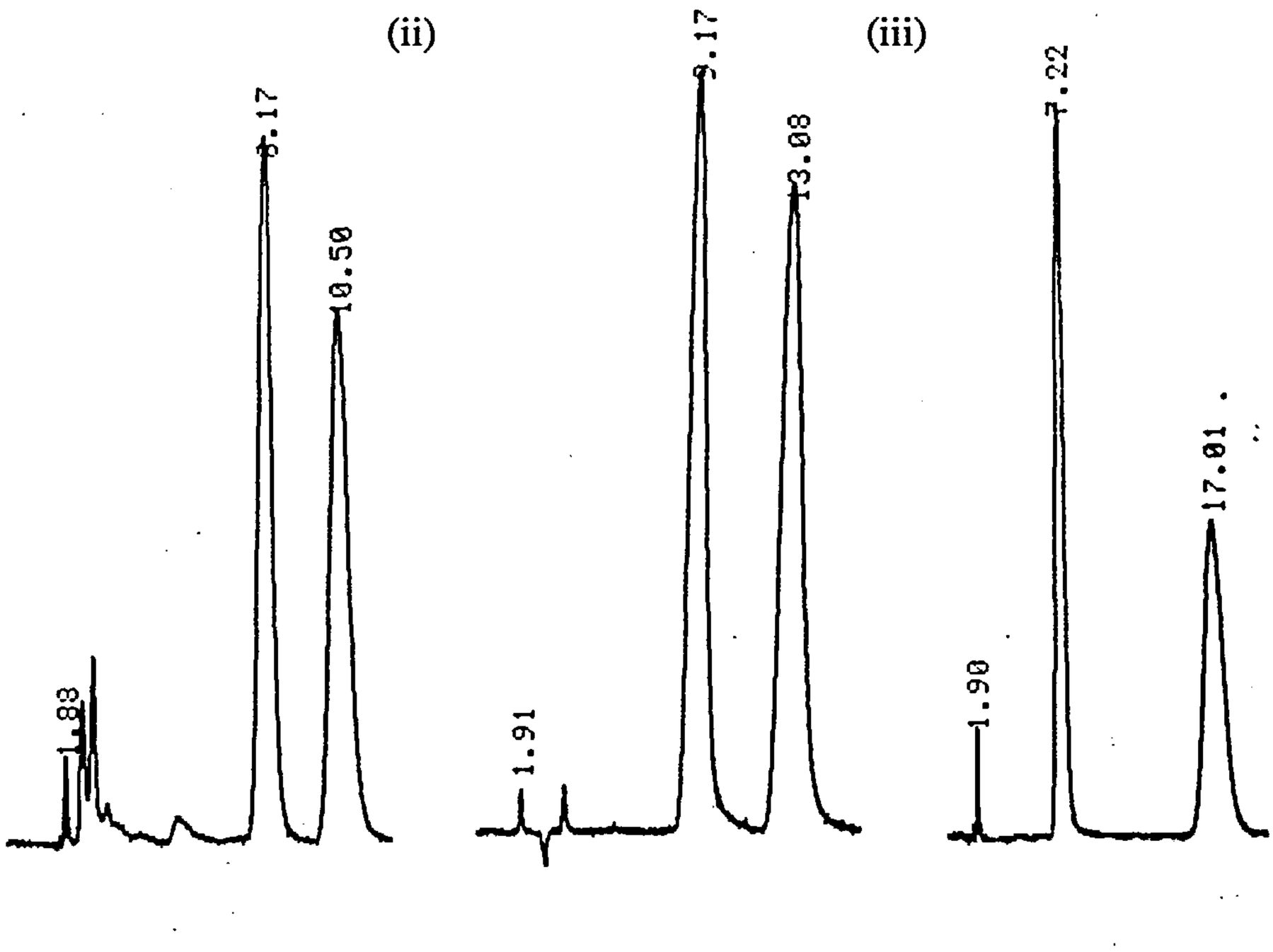

Figure 3-6 Separation of (i) 1-PB; (ii) TB and (iii) 2-PXPA on column (100 x 4.6 mm) packed with 25% w/w CDMPC-coated 7 μm Hypercarb. Mobile phase conditions listed at the foot of Tables 3-4 to 3-6. Flow rate: 0.5 ml/min.

3.3.3 Enantioselectivity of 25% w/w CDMPC-coated PGC

Since, excellent resolutions were observed for all three analytes, the separation of 15 chiral analytes: 6 neutral [1-PE, 1-PB, 4-phenyl-2-butanol (4-PB, **E**), BZ, BME and BMS]; 5 basic (TB, HOMA, ORP, ALP and OXP) and 5 acidic [2-phenylpropionic acid (1-PPA, **R**), MA, 2-MPAA, 2-PXPA and SUP] were examined on this phase. In order to be able to gauge the performance of the CDMPC-coated PGC phase in terms of previously examined CDMPC-coated APS phases, the results are shown alongside results from a column (100 x 4.6 mm) packed with 15% w/w CDMPC-coated 5 µm Hypersil APS (column **16**). See Tables 3-5 to 3-7.

Neutral analytes (Table 3-5)

All neutral analytes examined had higher k' values on the PGC phase compared to the APS phase, demonstrating that there were more interaction sites on the former phase than there were on the latter. For three of the analytes, this was also accompanied by an increase in α and Rs values. However, for the other three, similar or lower α and Rs values were observed.

Basic analytes (Table 3-6)

The majority of basic analytes would not elute from the PGC phase without the use of an additive in the mobile phase. On addition of diethylamine (0.1% v/v) the majority of basic analytes exhibited similar or slightly lower k'_1 values on the PGC phase compared to the APS phase. This result was in contrast to the results obtained for neutral analytes. However, the α and Rs values for the majority of these analytes were significantly higher on the PGC phase.

Table 3-5 Chromatographic parameters for neutral chiral analytes on CDMPC-coated 7 µm Hypercarb and 5 µm Hypersil APS phases.

Analyte		Hypercarb 25% w/w CDMPC	Hypersil APS 15% w/w CDMPC
1-PE	k'_1	2.97	2.62
	k'_2	5.11	3.78
	α	1.72	1.44
	Rs	4.18	3.14
1-PB	k'_1	1.97	1.62
	k'_2	2.78	2.05
	α	1.41	1.27
	Rs	2.40	1.63
4-PB	k'_1	4.34	3.19
	k'_2	8.72	5.59
	α	2.01	1.75
	Rs	4.78	4.34
BZ	k'_1	7.80	5.89
	k'_2	10.67	8.19
	α	1.37	1.39
	Rs	2.87	2.93
BME	k'_1	2.81	2.11
	k'_2	3.89	3.00
	α	1.38	1.42
	Rs	2.45	2.48
BMS	k'_1	12.51	7.51
	k'_2	20.08	15.35
	α	1.61	2.04
	Rs	3.16	4.60

Mobile phases: 1-PE, 1-PB and 4-PB: hexane/n-butanol (95:5 v/v); BZ, BME and BMS: hexane/2-propanol (90:10 v/v). Flow rate: 0.5 ml/min.

Table 3-6 Chromatographic parameters for basic chiral analytes on CDMPC-coated 7 µm Hypercarb and 5 µm Hypersil APS phases.

Analyte		Hypercarb 25% w/w CDMPC	Hypersil APS 15% w/w CDMPC
TB	k'_1	3.67	2.46
	k'_2	5.00	3.89
	α	1.36	1.58
	Rs	2.04	3.08
HOMA	k'_1	2.24	2.41
	k'_2	3.83	3.35
	α	1.71	1.39
	Rs	3.20	2.37
ORP	k'_1	1.05	0.92
	k'_2	1.95	1.39
	α	1.86	1.51
	Rs	2.68	1.54
ALP	k'_1	0.89	1.19
	k'_2	2.35	2.03
	α	2.64	1.71
	Rs	3.04	2.05
OXP	k'_1	2.29	2.46
	k'_2	9.99	7.41
	α	4.36	3.01
	Rs	5.68	4.62

Mobile phases: all mobile phases contained 0.1% diethylamine. TB: hexane/ ethanol (98:2 v/v); HOMA: hexane/2-propanol/methanol (85:15:5 v/v/v); ORP: hexane/2-propanol (90:10 v/v); ALP and OXP: hexane/2-propanol (80:20 v/v). Flow rate: 0.5 ml/min.

Table 3-7 Chromatographic parameters for acidic chiral analytes on CDMPC-coated 7 µm Hypercarb and 5 µm Hypersil APS phases.

Analyte		Hypercarb 25% w/w CDMPC	Hypersil APS 15% w/w CDMPC
2-PPA	k'_1	7.00	6.36
	k'_2	8.20	7.11
	α	1.17	1.12
	Rs	1.24	0.86
MA	k'_1	8.67	10.15
	k'_2	10.47	11.50
	α	1.21	1.13
	Rs	1.63	1.19
2-MPAA	k'_1	4.73	4.81
	k'_2	6.00	5.76
	α	1.27	1.20
	Rs	1.60	1.16
2-PXPA	k'_1	3.07	2.24
	k'_2	8.27	4.59
	α	2.69	2.05
	Rs	6.61	4.53
SUP	k'_1	17.45	8.86
	k'_2	18.12	9.74
	α	1.04	1.10
	Rs	P.R.	0.82

P.R. = partial resolution (<0.5). Mobile phases: all mobile phases contained 0.5% trifluoroacetic acid; 2-PPA: hexane/2-propanol (98:2 v/v); MA and SUP: hexane/ethanol (95:5 v/v); 2-MPAA and 2-PXPA: hexane/2-propanol (95:5 v/v). Flow rate: 0.5 ml/min.

Acidic analytes (Table 3-7)

In contrast to the APS phase, the chromatography of acidic analytes on the PGC phase was satisfactory without the use of an ionisation suppressor in the mobile phase. However, the addition of trifluoroacetic acid (0.5 % v/v) to the mobile phase improved separation and reduced peak tailing. For the majority of acidic analytes, the α and Rs values on the PGC phase were significantly superior to those on the APS phase, although there was no clear trend in the k' values. SUP was the exception showing a long retention time and badly tailing peak shapes.

3.3.4 Interpretation of Results from Section 3.3.3

The chromatographic results (Tables 3-5 to 3-7) have confirmed that, despite the attempt to completely coat the surface by using a 25% w/w CDMPC loading and a five -fold layering technique, the PGC support is still able to influence the chromatography of some of the test racemates. These influences can be divided into two groups:

(i) analytes whose chromatography can be improved by the addition of mobile phase additives (eg. basic analytes).

(ii) analytes whose lower than expected resolution or poor chromatography could not be improved by using mobile phase additives (eg SUP).

(i) Addition of mobile phase additives to improve chromatography

It was interesting to find that when a base co-solvent had not been added, basic analytes showed significantly stronger interactions when PGC was the support compared to APS. It has been well documented[115,138], that even at high polysaccharide carbamate loadings, basic analytes can interact with unreacted silanol groups on the surface of APS supports, leading to increased retention

times and reduced efficiency. However, PGC is reported[145] to have virtually no functional groups on the surface.

Studies on PGC over the past five years have highlighted several unusual retention phenomena that cannot be explained on the basis of dispersive interaction forces. The study by Bassler[146] on the retention behaviour of 24 substituted aromatic compounds under non-polar solvent conditions concluded that along with dispersive interactions, electronic interactions with the delocalised band of electrons on PGC were possible. Lim *et al* [147,148] also reported that the conduction band of electrons on PGC may be responsible for the strong retention of inorganic and organic cations and anions in aqueous mobile phases.

In contrast, Karlsson *et al* [141] suggested that strong adsorption sites with limited capacities may be responsible for the retention of aminoalcohols in normal phase solvents when concentrations of a chiral ion pairing reagent (L-ZGP) were low. However, more recently Josefsson *et al* [149] again suggested that it was interactions between the delocalised band of electrons on PGC and the unshared pair of electrons on a primary amine that was responsible for the long retention times. In the latter two cases, diethylamine was added to the mobile phase to competitively displace the analyte from the surface thus improving the chromatography.

Our results are consistent with those reported by Karlsson *et al* [141] and Josefsson *et al* [149] in that when diethylamine was added to the mobile phase, the chromatography of the basic analytes improved dramatically. However, from these initial results it is not possible to say whether either of the proposed retention mechanisms may be responsible.

(ii) Analytes whose resolution cannot be improved by the addition of mobile phase additives

It was noticeable that SUP (Table 3-7) showed strong retention and extremely poor α values on the PGC phase. Similarly, ATFE and FLAV two neutral analytes (not included in the tables) that separate efficiently on CDMPC-coated APS also showed greatly increased retention times and virtually no separation when PGC was the support. In addition BZ and BME and BMS were notable for not showing increased separation as observed for the other neutral analytes.

The reason for these results is not clear although some observations can be made. ATFE might be expected to interact strongly with the PGC surface via dispersive forces because of the flat aromatic anthryl portion. However, pre-flushing the column with phenanthrene to try to mask any exposed PGC surfaces did not lead to a reduction of retention time. The other analytes are notable for having bi-aromatic functionalities.

If it is not the PGC support that is influencing the separation of these analytes, then it could be the CDMPC coating. As discussed in Chapter 1 (section 1.3.8), it has been proposed that the mechanism of separation on polysaccharide carbamate-coated phases primarily involves interaction with the urethane linkage via hydrogen bonding or dipole interactions. However, the conformation of the CDMPC also plays an important part in the discrimination process. It is conceivable that PGC may interact with flat portions of CDMPC, such as the 3,5-dimethylphenyl group, resulting in changes to the highly ordered structure and thus the size or shape of chiral cavities compared with those when APS is the support medium. Unfortunately, there are too few examples in this initial study to make any firm conclusions.

3.3.5 Summary and Conclusions

PGC has proved to be a suitable support for CDMPC and the 25% w/w CDMPC-coated phase gave excellent separations and resolutions for many of the test analytes. In particular CDMPC-coated PGC appears to be very effective for the separation of basic and acidic analytes. The main reason for this is probably due to the fact that PGC has very few surface functional groups. Strong interactions with basic analytes were observed, but these were readily saturated by the addition of a small amount (0.1% v/v) of diethylamine in the mobile phase.

Unfortunately a few analytes were retained very strongly on the CDMPC-coated PGC phase and the interactions could not be suppressed by the addition of mobile phase additives. The reason for the strange behaviour of these analytes is not fully understood. It is proposed that perhaps the conformation of the CDMPC had been altered due to attraction of the dimethylphenyl groups to the surface of the PGC. However, there were too few examples to make any firm conclusions.

It is not known if the 25% w/w CDMPC loading is optimum for the PGC support or whether the five-fold coating technique provides a more homogeneous coating. This, and the strange behaviour of some analytes, will require further investigation.

CHAPTER 4

INVESTIGATIONS INTO THE CONTENTS OF A CHIRALCEL OC COLUMN AND COMPARISON OF THE ENANTIOSELECTIVITY OF SIGMACEL AND AVICEL PHENYLCARBAMATES COATED ON 120Å, HYPERSIL APS

Daicel provide very few details about the materials they use in their commercial columns. Therefore, we decided to investigate the contents of a used Chiralcel OC column, including the nature of the silica, such as particle size, pore volume and surface chemistry and the nature of the carbamate coating such as the molecular weight range of the cellulose used. The latter investigation led us to compare the enantioselectivity of Sigmacel and Avicel cellulose carbamates coated on 120Å, Hypersil APS.

4.1 ANALYSIS OF CHIRALCEL OC COLUMN

As noted in Chapter 2 (section 2.1), Okamoto *et al* [67,69] consistently cited the use of large particle (10 μm) macroporous (1000 - 4000Å) APS with a polysaccharide carbamate loading of 20 to 25% w/w. The only details Daicel[150] provide about the commercial Chiralcel and Chiralpak type columns are the nature of the carbamate coating and the particle size of the silica. Neither the amount of chiral coating or the nature of the underlying silica is published.

A Chiralcel OC which had become completely blocked was donated to us for examination. Chiralcel OC columns contain CPC coated onto a 10 μm silica-based support. The column had been damaged beyond repair by flushing dichloromethane through the column. This would have partially dissolved the CPC coating and would explain why the column was blocked.

The column was unpacked by removing the top end fitting and pumping mobile phase through the column from the bottom. There was a very large void at the top of the column. The column was split into 5 portions as shown in Figure 4-1.

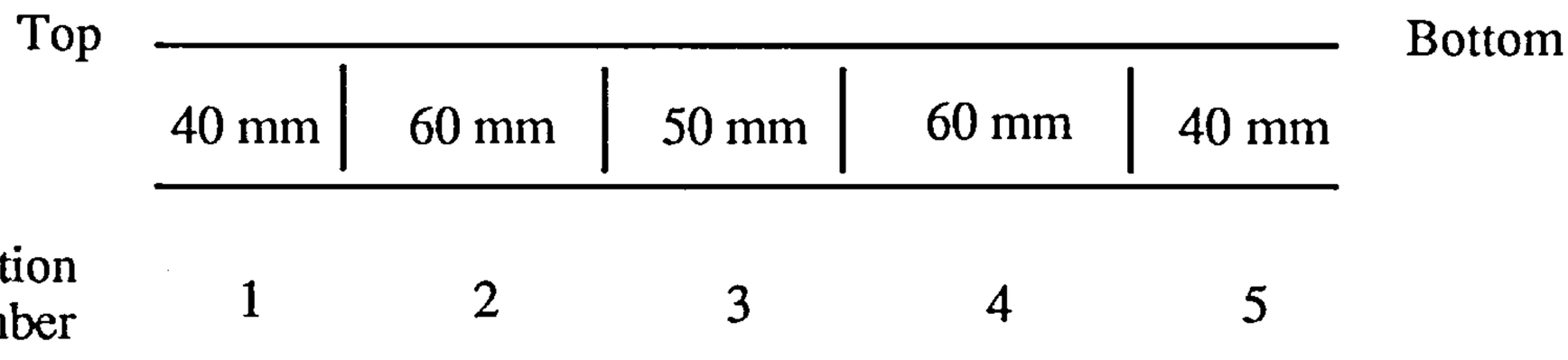

Figure 4-1 Dissection of the Chiralcel OC column.

The material from the middle portions of the column (fractions 2 and 3) were discoloured (slightly yellow) and, when dry, these two portions of the column were hard with particles bound strongly together. The particle size distribution of each fraction was measured. The results are shown in Table 4-1.

Table 4-1 Particle size distributions for fractions 1 to 5 taken from a Chiralcel OC column.

Fraction	Mean particle size (μm)	% particles < 5 μm	% particles > 16 μm
1	8.42	13.1	5.0
2	8.54	13.8	11.8
3	9.39	15.3	11.5
4	9.34	16.1	7.5
5	9.00	20.3	1.9

The mean particle size ranged between 8.42 and 9.39 μm. The amount of fine particles increased towards the bottom of the column (fractions 4 and 5) suggesting that some fracturing of the phase had occurred before the column was ruined.

Duplicate C, H and N measurement were also made for each fraction. Good agreement was obtained for fractions 1, 4, and 5, but not for fractions 2 and 3. This was thought to be due to the difficulty in obtaining a homogeneous sample from these two fractions due to aggregation and possibly contamination of the phase. The results are shown in Table 4-2.

There was less CPC coating on the silica at the top of the column (fractions 1 and 2) than there was on the silica further down the column (fractions 4 and 5). These results appear to further confirm that a solvent which was able to partially dissolve the CPC coating had been flushed through the column.

Table 4-2 C, H and N analyses for fractions 1 to 5 taken from a Chiralcel OC column.

Fraction		%C	%H	%N
1	1	10.38	0.83	1.12
	2	10.32	0.79	1.08
2	1	12.23	0.97	1.36
	2	11.01	0.82	1.07
3	1	14.37	1.17	1.67
	2	13.20	0.99	1.35
4	1	14.52	1.11	1.60
	2	14.71	1.13	1.62
5	1	13.50	1.04	1.48
	2	13.48	1.02	1.47

The CPC coating was removed from fractions 1, 4 and 5 by refluxing overnight in THF. The THF solution was decanted and was reduced in volume before pouring into methanol to precipitate the CPC. The silica was then washed several more times with THF so that all traces of the CPC coating were removed.

4.1.1 Analysis of the Silica

A decoated silica sample from fraction 4 was sent for pore volume measurement by mercury intrusion (Shandon HPLC). The mean pore diameter was found to be 535Å and the pore volume, 0.602 cm^3/g. This mean pore diameter is significantly lower than the pore diameter reported by Okamoto *et al* [67,69] (4000Å) and appears to confirm the observation by Crawford[130] and Felix *et al* [94], that is not necessary to use a silica with such a large pore diameter.

Samples of silica from fractions 1 and 5 were sent for duplicate C, H and N analyses. For comparison, the mean results are shown in Table 4-3, alongside mean C, H and N analyses for Hypersil APS (120Å) and Nucleosil APS (1000 and 4000Å).

Table 4-3 C, H and N analyses for decoated silica taken from a Chiralcel OC column and typical APS supports

Silica	%C	%H	%N
Fraction 1	1.49	0.13	-0.1
Fraction 5	1.58	0.14	-0.01
Hypersil APS (120Å)	1.95	0.62	0.50
Nucleosil APS (1000Å)	0.57	0.16	0.22
Nucleosil APS (4000Å)	0.26	0.17	0.07

The results were very surprising. The %C value was higher than expected and there was zero %N reading for the silica taken from the Chiralcel OC column. If there had been CPC coating left on the silica, this would have given a small %N reading. Therefore, the results suggest that Daicel may be using some kind of alkyl or aryl bonded silica. On closer inspection, the %C:%H ratios observed are consistent with those expected for phenyl groups (expect 1.49:0.12; actual 1.58:0.13) indicating that a phenyl bonded silica may have been used.

4.1.2 Analysis of the CPC coating

The CPC collected from fraction 4 was sent for duplicate C, H and N analyses. The mean results are shown in Table 4-4 along with the theoretical value and results obtain for two CPC samples prepared from Sigmacel cellulose.

Table 4-4 C, H and N analyses for CPC taken from Chiralcel OC and two CPC samples prepared in house

CPC	%C	%H	%N
Theoretical	62.42	4.85	8.09
Fraction 4	60.14	4.69	7.79
CPC-1	61.17	4.77	7.84
CPC-2	61.30	4.82	7.94

The low percentage of C, H and N values initially appear to suggest that the CPC taken from the Chiralcel OC column had a lower degree of derivatisation compared to samples prepared in house. However, it is possible that the values are lower than expected because, (i) a small amount of the silica may still be present in the sample, or (ii) a small amount of hydrolysis of the carbamate groups may have occurred during the lifetime of the column.

The CPC coating from fraction 4 was also subjected to gel permeation chromatography (GPC). The GPC trace and results are shown in Figure 4-2.

The most surprising feature of these results was the very low polydispersity value. Polydispersity is calculated by Mn/Mw and is a measurement of the molecular weight distribution. The lower the number, the narrower the molecular weight distribution. Therefore, the molecular weight distribution for CPC in the Chiralcel OC column is very narrow. Okamoto *et al* [71] have quoted values of $M_n = 1.08 \times 10^5$ (203 units) and a polydispersity of 4.46 for CPC prepared from Avicel cellulose. Since there is no known synthetic procedure for preparing cellulose with such a narrow molecular weight range, it appears that Daicel are preparatively isolating this molecular weight fraction.

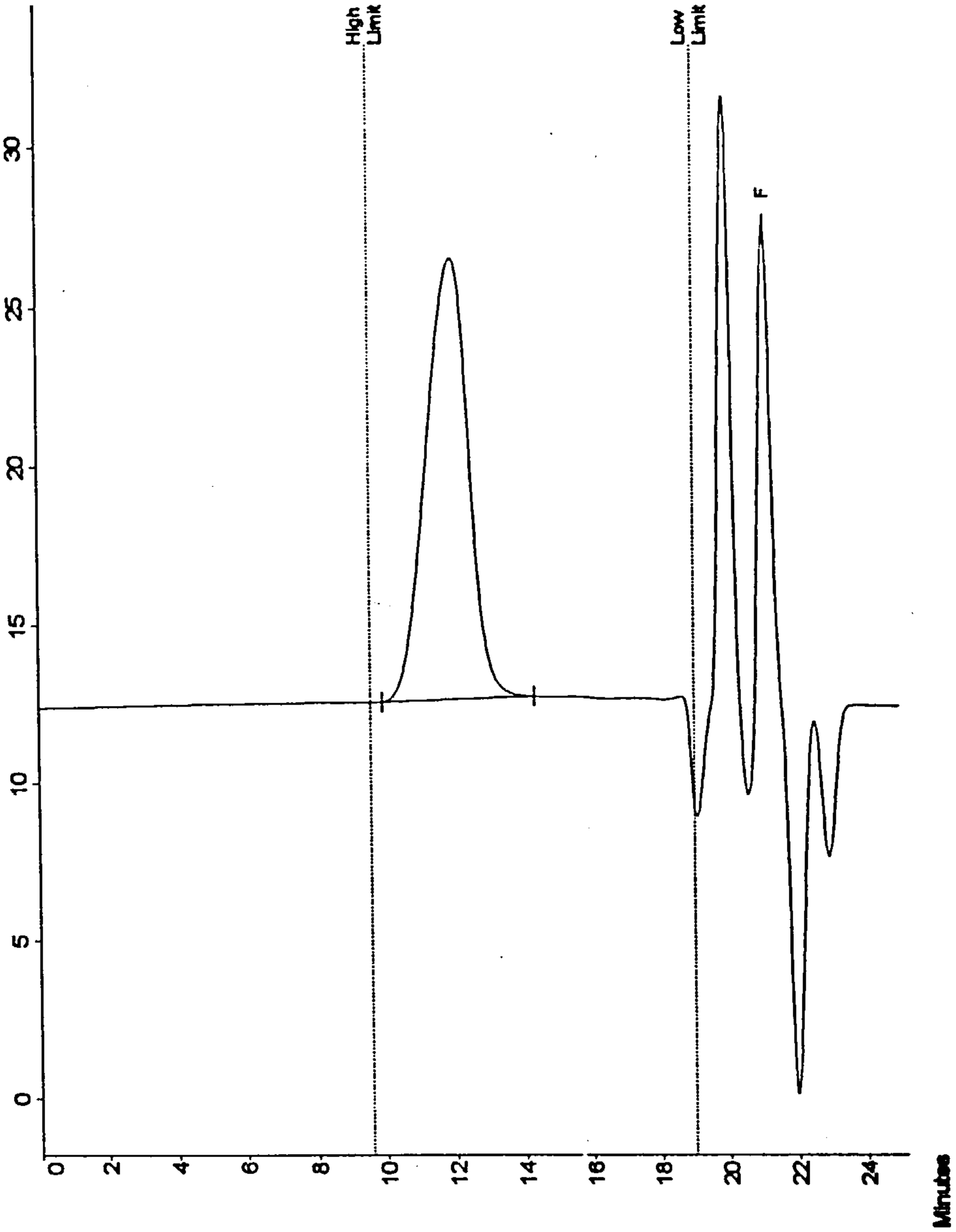

M_n	Nº Units	M_w	Polydispersity
87528	165	115874	1.324

Figure 4-2 GPC analysis of CPC coating taken from a Chiralcel OC column. M_n is the number average molecular weight and M_w is the weight average molecular weight.

For comparison, the GPC analyses of phenylcarbamates prepared from Avicel and Sigmacel celluloses were investigated. The results are shown in Table 4-5.

Table 4-5 GPC analyses of CPC coating taken from a Chiralcel OC column and phenylcarbamates prepared from Avicel and Sigmacel celluloses.

Cellulose carbamate	M_n	Mean N° Units	Polydispersity
CPC ex Chiralcel OC	87528	165	1.32
CPC-1 ex Sigmacel	100653	190	5.68
CDMPC-1 ex Sigmacel	100932	164	5.46
CDMPC-5 ex Avicel	51045	83	4.18

The results clearly show the difference in polydispersity between the CPC sample extracted from the Chiralcel OC column and CPC and CDMPC samples prepared from the commercially available celluloses. The reason for using this narrow molecular weight fraction is not known. It is possible that it is used in order to reduce the variability between columns.

4.1.3 Summary of findings from Sections 4.1.1 and 4.1.2

The findings of this investigation into the contents of the Chiralcel OC column are extremely interesting. It is clear that the commercial packing differs in several respects from the original materials reported by Okamoto *et al.*[67,69] The Chiralcel OC column appears to contain a 9 µm phenyl bonded silica with a pore size of approximately 500Å, coated with CPC which has a narrow molecular weight range centred around 87528 (165 units). Investigations into the contents of other types of Chiralcel columns need to be carried to determine whether these characteristics are typical for the range of Daicel commercial columns.

4.2 GEL PERMEATION CHROMATOGRAPHY OF SIGMACEL AND AVICEL PHENYLCARBAMATES

Apart from the broad molecular weight distribution noted for the phenylcarbamates of Sigmacel and Avicel compared to CPC taken from the Chiralcel OC column, it was interesting to find that Mn for the Avicel and Sigmacel derivatives were significantly different. The GPC analyses are shown in Figure 4-3.

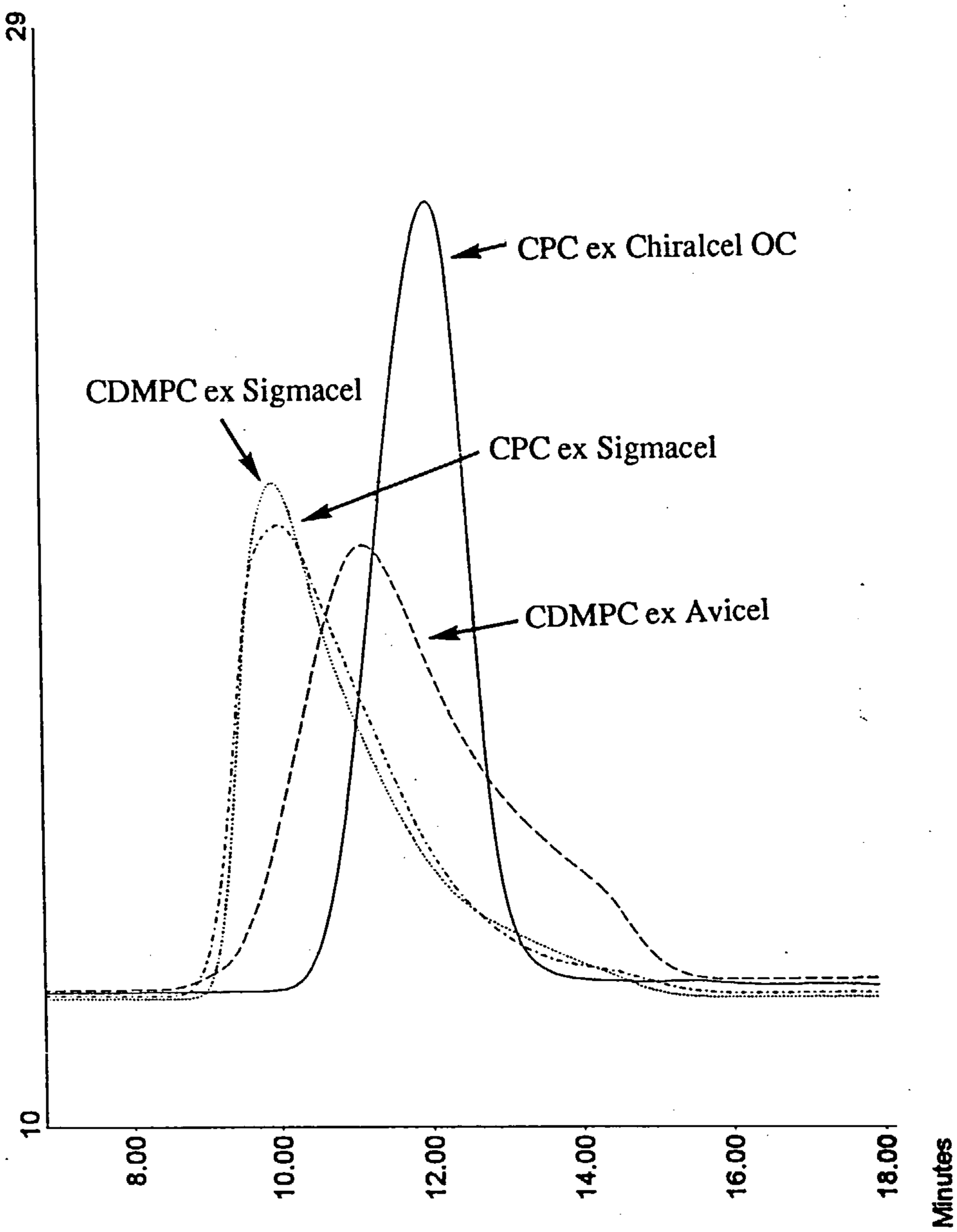

Figure 4-3 GPC analyses of CPC taken from a Chiralcel OC column and cellulose carbamates prepared from Avicel and Sigmacel celluloses.

It must be remembered that the detection method is refractive index, and therefore longer chains will give higher responses. However, it can be clearly seen that the molecular weight distribution ranges for the Sigmacel and Avicel derivatives are very different. The average chain length for the Avicel derivative was approximately half the average chain length of the Sigmacel derivatives (Table 4-5).

The Mn for our Avicel derivative is not consistent with the value reported by Okamoto *et al* [69] They noted that the GPC analysis of CPC prepared from Avicel cellulose showed a peak at $M_n = 1.08 \times 10^5$. Therefore the average number of cellulose units (203) was even higher than the number of units found for our Sigmacel derivatives. The reason for this is not known. It may be that the manufacturer supplying the cellulose to Merck had changed (Okamoto *et al* paper written in 1986) or that a different GPC calibration method was used. The calibration method was not stated in the paper.[69]

4.3 COMPARISON OF SIGMACEL AND AVICEL PHENYL-CARBAMATE-COATED PHASES

Shibata *et al* [63] claim that the average molecular weight and molecular weight distribution of a cellulose derivative can affect the chiral recognition of the coated phase. They reported that it was sometimes observed that a substrate which did not resolve well on a low molecular weight cellulose derivative (< 100 units), did resolve well on a higher molecular weight cellulose derivative and vice versa. Some substrates were found to be insensitive to cellulose molecular weight changes.

The observations noted above were not substantiated by data and to date, there have been no other publications discussing the effect of average molecular weight and molecular weight distribution of polysaccharide derivatives on enantioselectivity.

4.3.1 Enantioselectivity of Sigmacel and Avicel DMPC-coated 120Å, Hypersil APS

We have already shown in Chapters 2 and 3, that phenylcarbamate derivatives prepared from Sigmacel cellulose give enantioselective chiral phases when coated onto small pore silica supports. In the light of the observations in section 4.2 and the comments by Shibata *et al*,[63] a comparison of the enantioselectivity of Avicel and Sigmacel tris(3,5-dimethylphenylcarbamate) (Avicel DMPC and Sigmacel DMPC respectively) coated 120Å, 5µm Hypersil APS phases was carried out.

Since the average chain length of the Avicel derivative was significantly shorter than that for the Sigmacel derivatives (Table 4.5), we envisaged that the Avicel DMPC chains might be able to gain increased access to the pores. Therefore, we prepared 15%, 20% and 25% w/w Avicel DMPC (**CDMPC-4**) coated 120Å, 5 µm Hypersil APS (**5µ-14** to **5µ-16**). All three loadings were accepted by the APS support and the particle size distributions were found to be gaussian in shape with a mean particle size similar to the uncoated APS. The phases were then packed into HPLC columns (150 x 4.6 mm; columns **23** to **25**). The chromatographic parameters for five chiral analytes (2 neutral: BME and FLAV; 2 basic: ORP and ALP; and 1 acidic: 2-PXPA) on the three Avicel DMPC phases and for comparison, on a previously prepared (section 2.3.3) 15% w/w Sigmacel DMPC-coated 120Å, 5µm Hypersil APS phase (column **16**) are shown in Table 4-6.

Table 4-6 Chromatographic parameters for 5 chiral analytes on columns (150 x 4.6 mm) packed with 15%, 20% and 25% w/w Avicel DMPC-coated 5 µm Hypersil APS and 15% Sigmacel DMPC-coated 5 µm Hypersil APS

Analyte		Avicel DMPC			Sigmacel DMPC
		15% w/w	20% w/w	25% w/w	15% w/w
	k'_1	1.24	1.61	2.40	1.53
BME	α	1.46	1.52	1.48	1.33
	Rs	2.44	4.41	2.95	2.60
	k'_1	1.67	2.30	3.39	1.84
FLAV	α	1.35	1.38	1.34	1.30
	Rs	2.16	3.97	2.90	2.57
	k'_1	0.97	0.94	1.43	1.14
ORP	α	1.43	1.70	1.64	1.33
	Rs	1.80	3.47	2.67	1.81
	k'_1	1.66	1.09	1.85	2.43
ALP	α	1.63	2.06	2.28	1.41
	Rs	1.90	3.93	3.37	1.62
	k'_1	1.05	1.40	1.88	1.14
2-PXPA	α	2.07	2.20	2.21	1.84
	Rs	4.05	6.00	5.28	4.44

Mobile phases: BME and FLAV: hexane/2-propanol (90:10 v/v); ORP and ALP: hexane/2-propanol (90:10 and 80:20 v/v respectively + 0.1% diethylamine) and 2-PXPA: hexane/2-propanol (90:10 v/v + 0.5% trifluoroacetic acid). Flow rate: 0.5 ml/min.

Comparison of 15%, 20% and 25% w/w Avicel DMPC-coated Phases

The k' values for the two neutral analytes and the acidic analyte increase as the loading is increased. This is consistent with results obtained in Chapter 2 (section 2.2.1). For the two basic analytes, k'_1 values decrease as the Avicel DMPC loading is increased from 15% to 20% w/w. We propose that this phenomenon is due to the higher 20% w/w loading being able to more effectively block strong non-stereospecific interactions between the basic moiety on the analytes and acidic silanol groups on the surface of the support. However, k'_1 values for both basic analytes increase when the loading is increased from 20% to 25% w/w. This may be due to the fact that the silanol groups are already well shielded and the thicker CDMPC coating thus provides more sites for interaction.

For the two neutral analytes and the acidic analyte, α values are fairly similar for all three Avicel DMPC coating levels. However, for the two basic analytes, the poor shielding of the silanol groups provided by the 15% w/w loading is reflected by a low α.

In all cases the Rs values are higher on the 20% w/w coated phase than on the 15% or 25% w/w coated phases. The lower Rs values on the 15% w/w coated phase might be expected since α values are lower, but lower Rs values on the 25% w/w coated phase may be due to slow mass transfer and band broadening caused by the heavier loading or by a poorly packed column bed. An observation similar to this was made in Chapter 3 (see section 3.2.3) when considering the results obtained from the 15% w/w CDMPC (prepared from Sigmacel) coated Hypersil ODS phase.

In summary, a 20% w/w Avicel DMPC loading appears to be optimum for the 120Å, Hypersil APS support.

Comparison of Avicel DMPC and Sigmacel DMPC-coated Phases

The k'_1 values for the two neutral analytes and the acidic analyte on the 15% w/w Sigmacel DMPC phase were intermediate between the k'_1 values observed on the 15% and 20% w/w Avicel DMPC phases. However, for the basic analytes and in particular ALP, the k'_1 values were higher than expected on the Sigmacel DMPC phase, suggesting that it was not able to shield the acidic silanol groups as effectively as the Avicel DMPC phase.

All α values on the Sigmacel DMPC phase were lower than on the three Avicel DMPC phases. The Rs values for the two neutral analytes and the acidic analyte on the Sigmacel DMPC phase were intermediate between the 15% and 25% w/w Avicel DMPC phases. The two basic analytes had similar or lower Rs values on the Sigmacel DMPC phase compared to the 15% w/w Avicel DMPC phase.

Comparison of Dead Volume Measurements for Columns packed with Avicel DMPC and Sigmacel DMPC-coated phases

It was noted in Chapter 3 (section 3.2.3) that there appeared to be a good correlation between column dead volume measurements and the pore volume (as measured by a mercury intrusion method) of the packing material. Therefore in order to compare the pore volume of the 15% w/w Sigmacel DMPC-coated phase with the 15%, 20% and 25% w/w Avicel DMPC-coated phases, the dead volume for each column (150 x 4.6 mm) packed with these phases were determined. The results are shown in Table 4-7.

Table 4-7 Dead volume determinations for phases packed into columns, 150 x 4.6 mm.

Phase	Column Dead Volume (ml)
15% w/w Avicel DMPC	1.573
20% w/w Avicel DMPC	1.498
25% w/w Avicel DMPC	1.374
15% w/w Sigmacel DMPC	1.546

As expected, the column dead volume decreased as the Avicel DMPC loading increased demonstrating that the 25% w/w loading had filled the APS pore volume more than the 15% w/w loading. The dead volume for the column packed with 15% w/w Sigmacel DMPC-coated phase was intermediate between the columns packed with 15% and 20% w/w Avicel DMPC-coated phases. This suggests that the amount of pore volume filled and hence the amount of coating located around the outside of the APS particle for the 15% w/w Sigmacel DMPC loading is higher than on the 15% w/w Sigmacel DMPC loading, but lower than on the 20% w/w Avicel DMPC loading.

The latter proposal compliments the observation that k' values for neutral and acidic analytes on the 15% w/w Sigmacel DMPC-coated phase are higher than on the 15% w/w Avicel DMPC-coated phase, but lower than on the 20% w/w Avicel DMPC-coated phase (see discussions in section 3.2.3). However, it does not explain why basic analytes are retained more strongly on the 15% w/w Sigmacel DMPC-coated phase compared to the 15% w/w Avicel DMPC-coated phase. A possible explanation for this may be that the Sigmacel DMPC coating, with has longer polymer chains is less compact than the Avicel DMPC coating and thus allows analytes to penetrate the coating and interact with the support surface.

4.3.2 Summary and Conclusions

The optimum loading for the Avicel DMPC on 120Å, Hypersil APS was 20% w/w, compared to the optimum of 15% w/w for Sigmacel DMPC. This result confirms the prediction that the shorter chains of the Avicel DMPC are able to gain access to the support pores more easily than can the longer Sigmacel DMPC chains.

The 20% w/w Avicel DMPC-coated phase was significantly more enantioselective than the 15% w/w Sigmacel DMPC-coated phase for all test analytes. All Avicel DMPC loadings masked undesired non-stereoselective interactions between basic moieties on the analyte and acidic silanol sites on the support surface more effectively than the 15% w/w Sigmacel DMPC loading.

Column dead volume determinations indicated that, as the Avicel DMPC phase loading was increased, the amount of APS pore volume occupied by the phase increased. The pore volume occupied by the 15% w/w Sigmacel DMPC coating was intermediate between the 15% and 20% w/w Avicel DMPC coatings.

Avicel appears to be a much better cellulose to use for the preparation of cellulose carbamates that are to be coated onto small pore silicas. Most of the changes in enantioselectivity and efficiency observed during this study can be explained by considering the relative ease with which the derivatised Avicel and Sigmacel chains can enter the narrow APS pores. It would be very difficult to compare these observations (using relatively few test analytes) with those of Shibata *et al* [63] noted earlier, since they used macroporous (1000 or 4000Å) APS to support the cellulose derivatives and thus all chain lengths would have had greater opportunity to enter the pores.

CHAPTER 5

THE DEVELOPMENT OF FLASH CHIRAL CHROMATOGRAPHY

Despite the great versatility and efficiency of the cellulose and amylose tris(phenylcarbamate)-coated phases, there are still very few preparative-scale applications reported. Amongst the possible reasons for this are the high cost of the columns and associated preparative equipment. It has already been shown in Chapter 3, that SI can be used as a support medium for CDMPC. In most cases, chiral analytes had high separation and resolution on a 20% w/w CDMPC-coated 120Å, Hypersil SI phase. Therefore, in an attempt to find an inexpensive, easy to use preparative method, we decided to investigate the use of CDMPC-coated flash chromatography silica for preparative-scale applications in a flash chromatography mode.

5.1 BACKGROUND ON FLASH CHROMATOGRAPHY

Flash chromatography was first described in 1978 by Still *et al.*[151] Defined as a simple adsorption technique for the routine purification of organic compounds, it has gained great acclaim amongst synthetic chemists and is now extensively used.

The apparatus described by Still *et al* [151] consisted of a glass column, fitted with a tap at the bottom and a quickfit joint at the top. A flow controller valve which was connected to an air line was used to drive the eluent. The column bed height was typically 5-6 inches (which was usually dry packed) and it was reported that silica with a particle size range of 40-63 μm gave higher efficiency than silica with a particle size ranges of 25-40 μm or 63-200 μm. The diameter of the column was chosen to accommodate the amount of sample to be separated and it was noted that, to maintain efficiency, the flow rate should kept high (2.0 ± 0.1 inch/min).

The main advantages of the technique were the minimal equipment and running costs, the speed (run times were normally 10-15 minutes) and the sample loading capacity of the technique (amounts of 0.01 to 10 g were claimed).

In 1985, Pirkle *et al* [152] described the first preparative separation of enantiomers by flash chromatography. The method was developed to demonstrate how enantiomers which had high enantioselectivity ($\alpha > 2$) on a covalently bound 3,5-dinitrobenzoylphenylglycine type silica HPLC column could be separated easily on a modestly efficient flash column of the same type. They used the standard procedure for flash chiral chromatography described by Still *et al* [151] as far as apparatus, packing, flow rate and sample application were concerned.

Pirkle *et al* [152] reported that a 200 mg sample of a racemic benzodiazepinone was completely resolved into its enantiomers on a flash column (150 x 40 mm) packed with a covalently bound 3,5-dinitrobenzoylphenylglycine silica phase (300g, equivalent to 0.67 mg benzodiazepinone per gram of CSP). The success of this separation was ascribed to the high separation factor of the

analyte ($\alpha > 2$). However, it was noted that for racemates with smaller separation factors ($\alpha < 2$), flash chromatography would be of reduced utility unless only relatively small amounts were required.

Despite the simplicity and economy of the technique, as far as we are aware there has been no further literature reporting the use of this chiral flash chromatographic technique. The reason for this is not clear.

The preparation of the cellulose carbamate-coated phases are particularly facile and numerous preparations of these phases carried out in our laboratories, have shown the coating procedure to be reproducible. Therefore, it was anticipated that, if separations at least as good as those reported by Pirkle *et al* [153] could be achieved, flash chiral chromatography with cellulose carbamate-coated phases would be very attractive for widespread application.

5.2 CHOICE OF FLASH SILICA

The silica that is supplied commercially for flash chromatography purposes is an inexpensive, large particle, irregular silica. In order to achieve the high loading capacities required in preparative chromatography, it is most commonly purchased with a pore size of 60Å. Depending on the source, this provides in many cases a surface area which is greater than 500 m^2/g. However, as demonstrated in Chapter 2 (section 2.3.2 & 2.3.3) small particle supports (eg. <100Å) can only accept a modest amount of CDMPC, thus reducing the enantioselectivity of the coated phase. Therefore, an irregular flash grade silica with a pore size 120Å or greater was sought.

Davisil SI (Aldrich) which has a pore size of 150Å and a surface area of 300 m^2/g was identified as a potentially suitable support. Several particle size ranges were available. However, based on the findings of Still *et al*,[151] the 40-63 µm size range was selected.

5.2.1 Determination of Optimum CDMPC Loading for 150Å, Davisil Irregular Silica

In response to the findings in Chapter 4 (section 4.3) we decided to use CDMPC prepared from Avicel cellulose as coating for the flash silica support. In section 4.3, a 20% w/w Avicel DMPC was identified as optimum loading for the 120Å, Hypersil APS support. However, since it was not known how the irregular nature and the slightly larger pore size of the Davisil SI would affect the CDMPC coating, a check on the loading capacity of the flash silica was conducted.

A 20% w/w CDMPC (**CDMPC-4**) loading was applied to a small amount (0.5 g) of the Davisil SI (**40/63μ-1**). Following evaporation, the coated material was removed from the flask, and the material sieved (250 μm mesh) relatively easily. The particle size distribution was found to gaussian in shape with a mean particle size distribution similar to the uncoated Davisil SI.

A higher CDMPC loading was attempted (25% w/w), but following evaporation, the coated material was extremely hard and was difficult to remove from the flask. Since it would have been almost impossible to sieve, the sample was discarded. Therefore a 20% w/w CDMPC loading was chosen as optimum for the 150Å, Davisil SI support.

5.3 FLASH CHIRAL CHROMATOGRAPHY WITH CDMPC-COATED DAVISIL SI[153]

A standard glass flash chromatography column (id., ca. 24 mm), fitted with a tap at the bottom and a quickfit joint at the top of the column body was chosen for the investigation. It was observed that 40 g of the Davisil SI support would give a column length of approximately 250 mm. Therefore, a large batch (ca. 45 g) of 20% w/w CDMPC (**CDMPC-5**) coated Davisil SI was prepared **(40/63μ-2)**.

The glass chromatography column was prepared for use by inserting a plug of glass wool in the neck above the tap, followed by a fine layer of sand. The coated flash material (40g) was slurried in hexane/2-propanol (80:20 v/v) which been previously sonicated (5 minutes) to remove any dissolved air. The slurry was poured into the glass column and packed immediately using an air pressure of 30 psi. This was accompanied by gentle tapping with a piece of thick rubber tubing to ensure a well packed column bed. The column bed (height 250 ±10 mm) was topped with a further layer of sand to facilitate easier sample loading with minimal bed disturbance. The column set-up is shown in Figure 5-1.

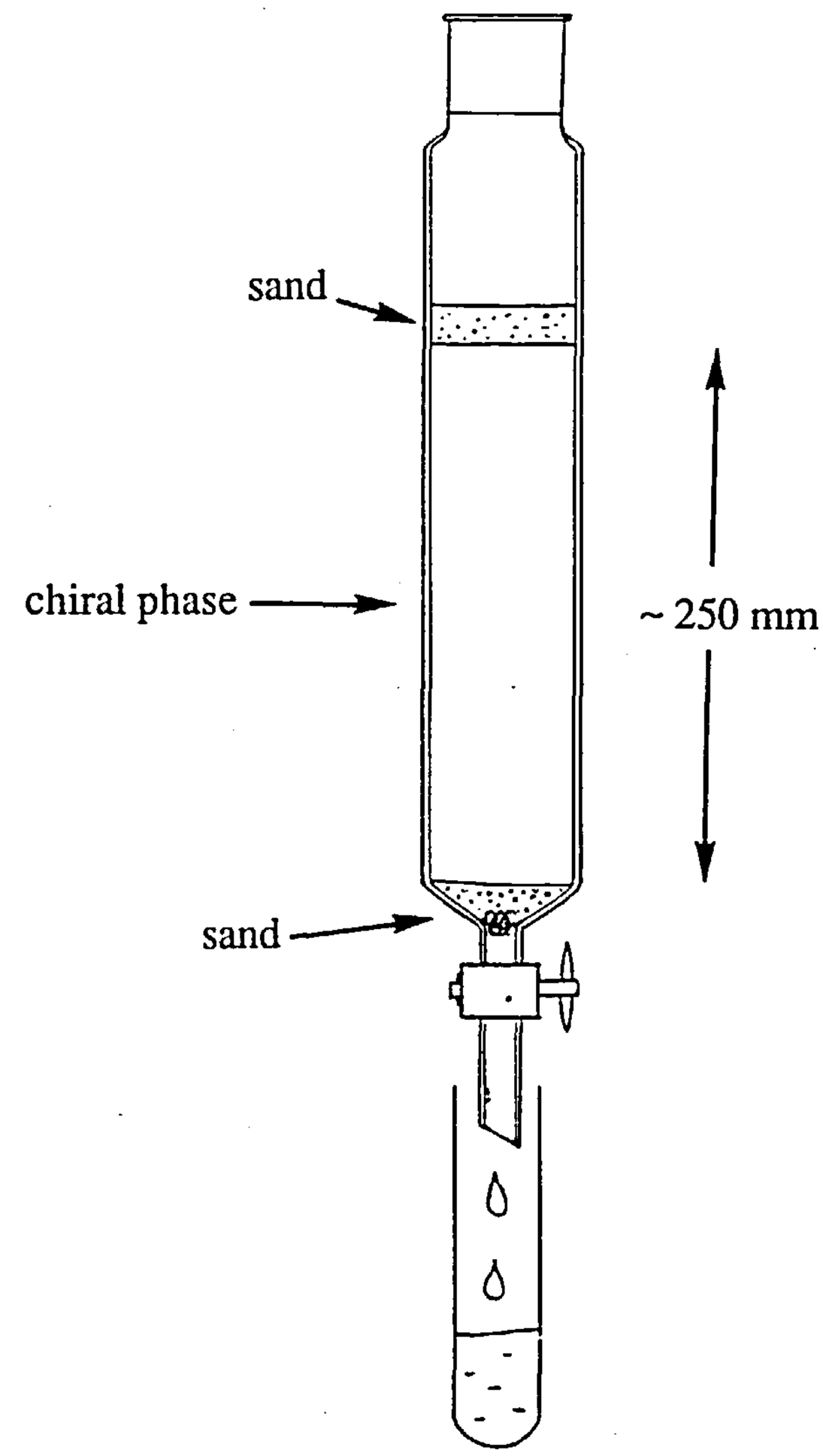

Figure 5-1 Flash chromatography equipment.

An HPLC column packed with CDMPC-coated SI was required for the analysis of the fractions collected from the flash column. Therefore, an HPLC column (150 x 46 mm) packed with 15% w/w CDMPC (**CDMPC-4**) coated 5 μm Hypersil SI (**5μ-17**; column **26**) was specially prepared for the purpose. It was anticipated that this column would not only be useful for measuring the success of the flash separation, but also could be used to evaluate the performance (efficiency) of the flash column.

5.3.1 First Preparative Separation using Flash Chiral Chromatography

BME was identified as a suitable test analyte, since (i) it is inexpensive, (ii) it has a reasonable solubility in hexane/2-propanol (90:10 v/v) mobile phases (> 20 mg/ml) and (iii) it has a relatively short analysis time (< 10 minutes) on column **26** (hexane/2-propanol 90:10 v/v; 0.5 ml/min). The chromatographic parameters for BME on column **26** using a mobile phase of hexane/2-propanol (90: 10 v/v) and a flow rate of 0.5 ml/min were: $k'_1 = 0.55$, $k'_2 = 0.99$, $\alpha = 1.43$ and $R_S = 2.89$.

For the flash column separation, a 20 mg loading of BME (0.5 mg per gram of CSP) was chosen as a sensible initial sample amount. The same mobile phase as used for the HPLC separation was selected and since it was suspected that these phases would have slow mass transfer, a gravity driven flow rate was chosen.

BME (20 mg) and a small amount of 1,3,5-tri-*tert*-butylbenzene an unretained analyte (t_0 marker) were dissolved in a minimum amount of mobile phase (0.65 ml). The solution was pipetted onto the top of the column and was allowed to run into the column bed by washing with a small amount (1 ml) of mobile phase. A reservoir flask (250 ml) was placed on top of the column and was filled with mobile phase (approximately 150 ml). The tap was opened and

gravity flow (ca. 4 ml/min) was allowed to operate. The amount of eluent in the reservoir was continually topped up.

Since neither the dead volume of the column nor the volume required for the BME enantiomers to elute were known in advance, the fractions were collected at 1 minute intervals for the first 10 minutes and then at 30 second intervals for the remaining time (60 minutes). Each fraction was analysed using column **26**. The peak areas of the components (t_0 marker, or BME enantiomer 1 or 2) were manually plotted against volume of elution solvent . The separation of BME on the flash column is depicted in Figure 5-2.

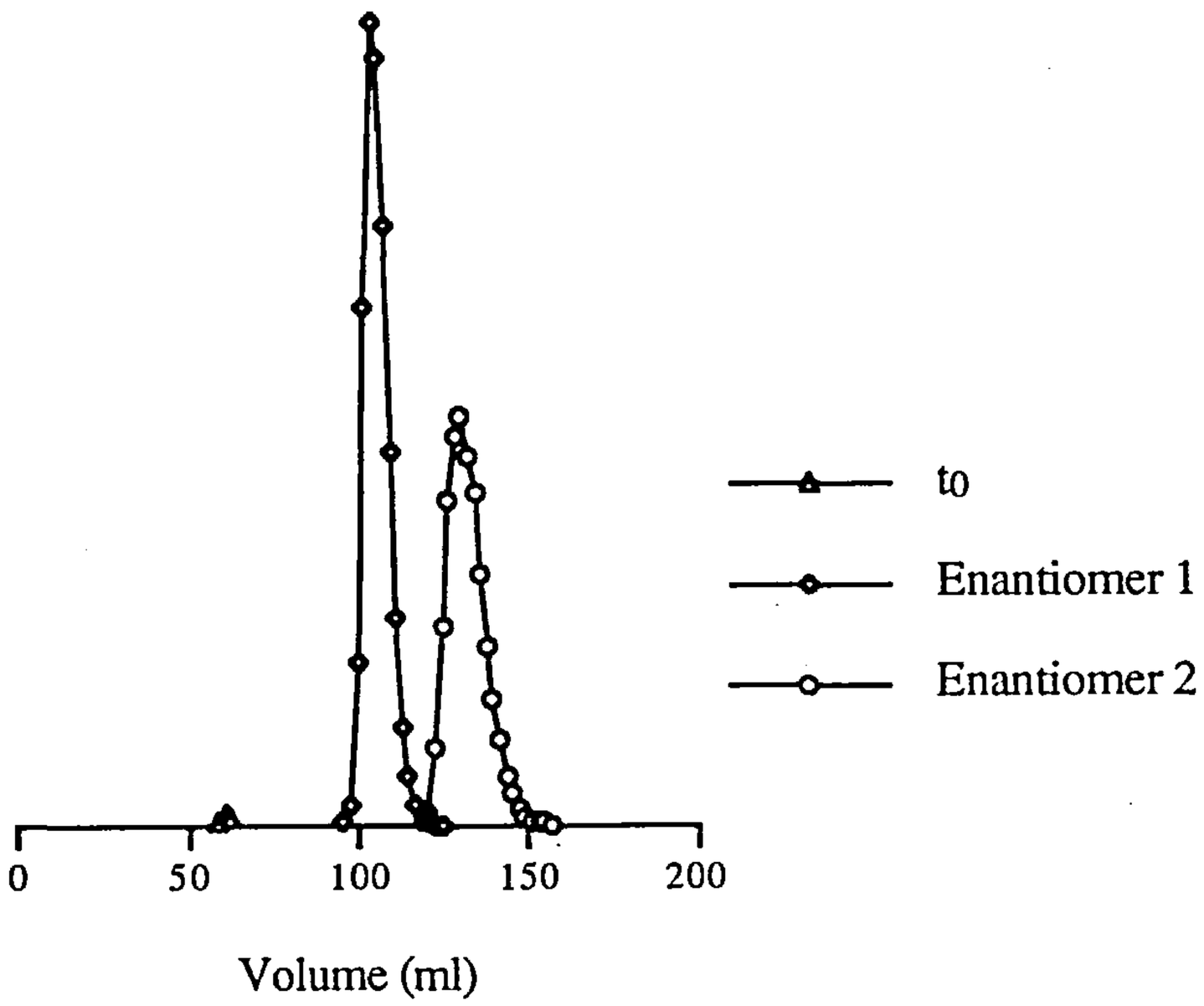

Figure 5-2 Separation of BME (20 mg) on flash column (24 mm id.) packed with 20% w/w CDMPC-coated 40-63 μm Davisil SI (40 g). Eluent: hexane/2-propanol (90:10 v/v). Gravity driven flow rate (ca. 4 ml/min).

It was extremely encouraging to observe the excellent peak shapes and the almost baseline separation of BME achieved on the CDMPC-coated flash silica

phase. For the 20 mg sample load, the enantiomer peaks were only overlapping slightly, yielding a potential recovery of almost 100% for enantiomer 1 and 97% for enantiomer 2.

Having determined that the flash column had potential for preparative scale separations, it appeared prudent to investigate the influence of the flow rate on the efficiency to see whether faster separations could be carried out without significant loss in resolution. The linear velocity for column **26** at 0.5 ml/min (1.25×10^{-3} m/s) was approximately 5 times greater than the linear velocity of the flash column under gravity flow (4 ml/min; 2.48×10^{-4} m/s).

5.3.2 Influence of Flow Rate on Column Efficiency

A series of experiments were carried out with flow rates over the range 4 - 12 ml/min. A 20 mg loading of BME (mobile phase and loading conditions as described previously) was made and the column efficiency (plate height) for the first eluting enantiomer was calculated at each flow rate. The results are shown in Figure 5-3.

It was perhaps not unexpected to find that, as indicated in the literature,[9] the curve for the large particle flash column was very steep, ie. an increase in the flow rate results in a significant loss of efficiency. However, as a compromise between run time and column efficiency, 4 ml/min was chosen as a suitable flow rate to use in further investigations.

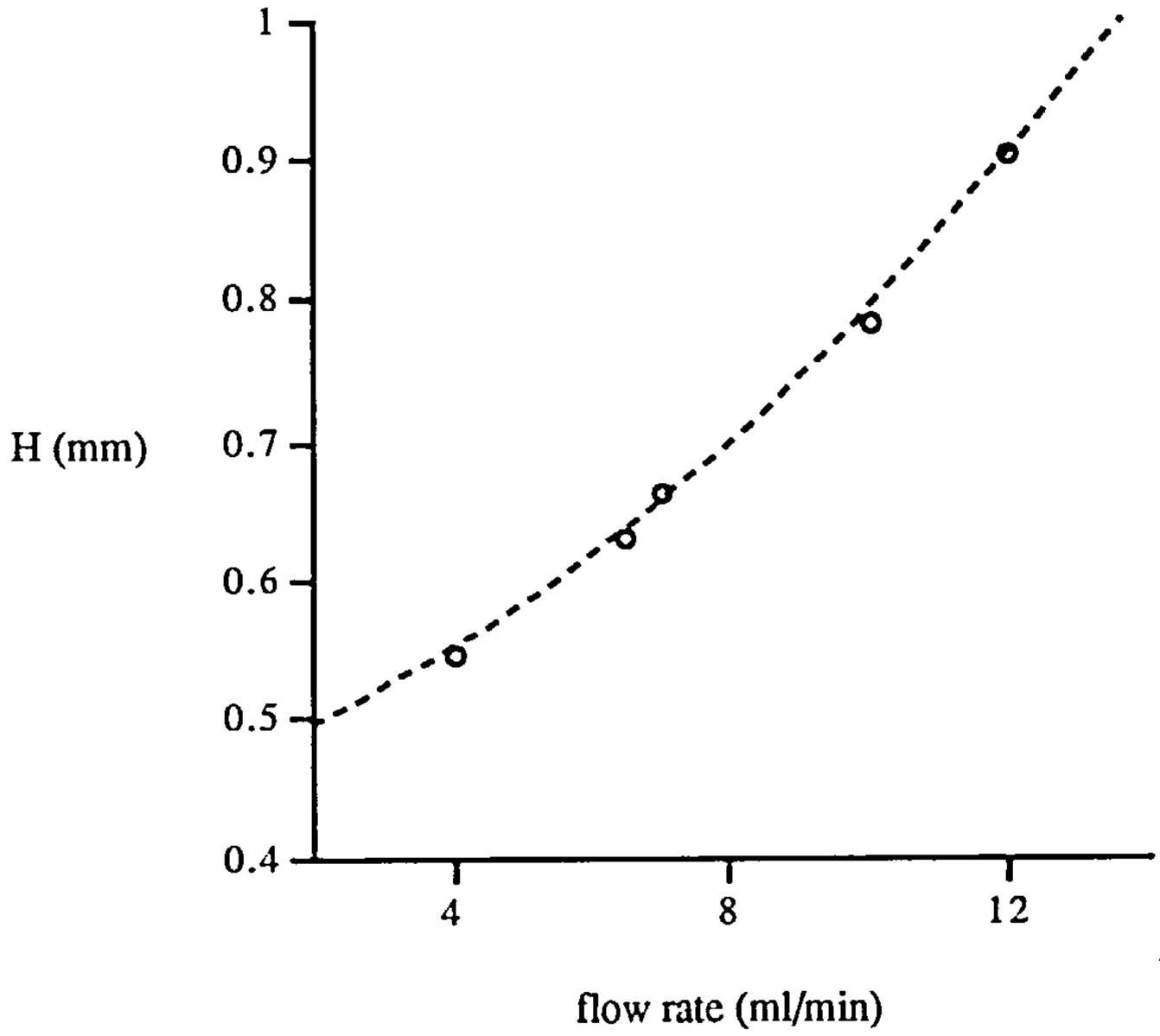

Figure 5-3 Plate height (H) versus flow rate for flash column (24 mm i.d.) packed with 20% w/w CDMPC-coated 40-63 µm Davisil SI (40g). Sample (-) BME (20 mg). Eluent: hexane/2-propanol (90:10 v/v).

5.3.3 Further Examples of Chiral Separations on Flash Chiral Column

Eight chiral analytes (5 neutral: ATFE, 4-PB, BME, FLAV and 1-PB; 1 basic: OXP and 2 acidic: 2-PXPA and 2-MPAA) which had a range of separations on column **26** (Table 5-1) were chosen to further investigate the utility of the flash chiral column.

Table 5-1 Chromatographic Parameters for chiral analytes on column **26**

Analyte	k'_1	k'_2	α	Rs
ATFE	1.60	4.68	2.93	8.55
4-PB	1.32	2.32	1.76	4.37
BME	0.90	1.44	1.60	3.19
FLAV	1.24	1.77	1.43	2.89
1-PB	1.10	1.42	1.29	1.94
OXP	2.44	4.68	2.75	6.69
2-PXPA	0.64	1.63	2.55	5.58
2-MPAA	2.28	2.69	1.18	1.49

Mobile phases: ATFE, BME and FLAV: hexane/2-propanol (90:10 v/v); 4-PB and 1-PB: hexane/n-butanol (90:10 and 95:5 v/v respectively); OXP: hexane/2-propanol (80:20 v/v + 0.1% diethylamine); 2-PXPA: hexane/2-propanol (90:10 v/v + 0.5% trifluoroacetic acid) and 2-MPAA: hexane/ethanol (95:5 v/v + 0.5% trifluoroacetic acid). Flow rate: 0.5 ml/min.

A 20 mg sample of each chiral analyte was loaded onto the flash column and the HPLC mobile phase compositions listed at the bottom of Table 5-1 were used. The fractions collected were analysed using column **26** and the peak areas of the components were plotted against volume of elution solvent. The flash chiral separations observed are shown in Figure 5-4.

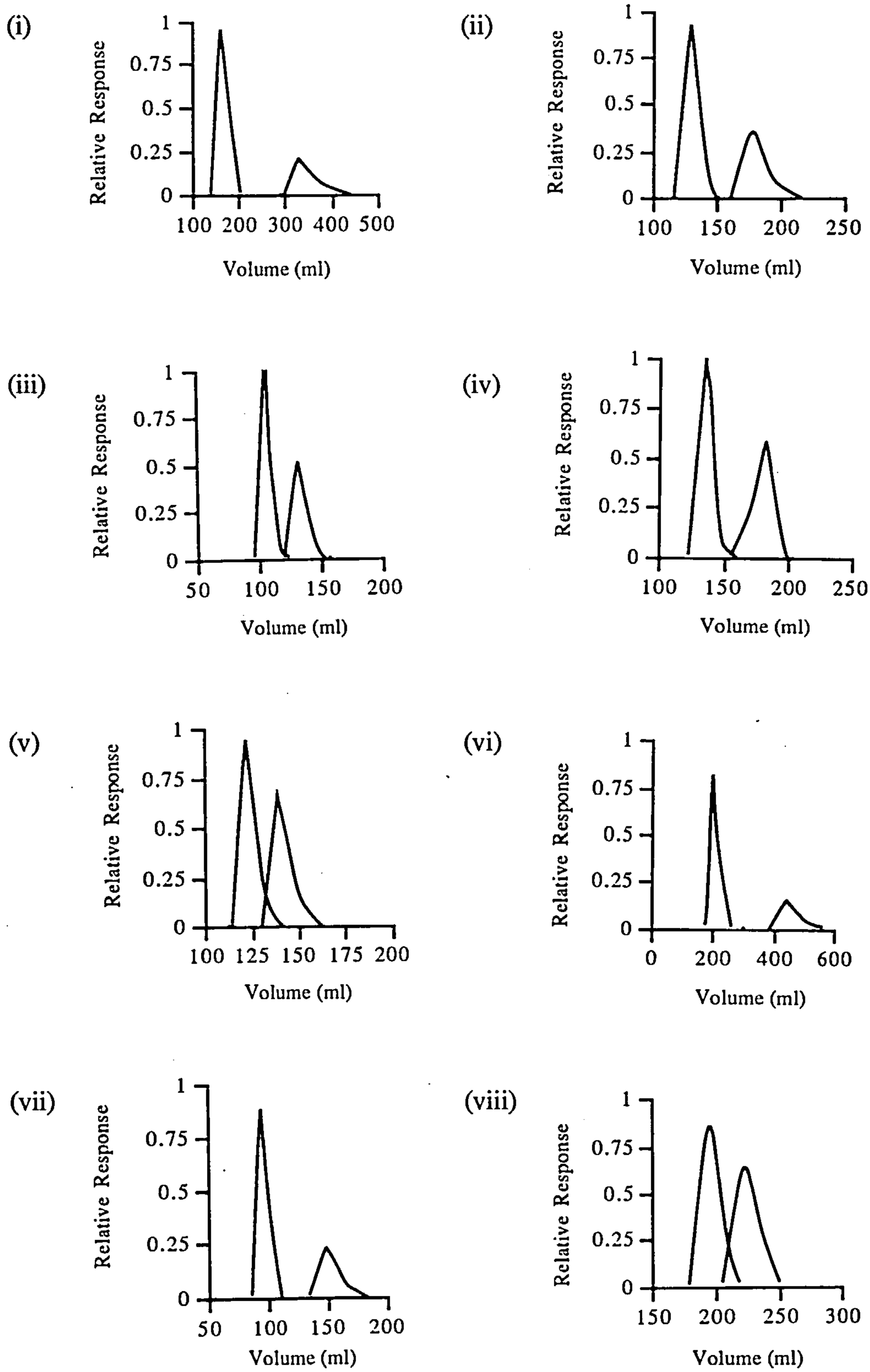

Figure 5-4 Separations of chiral analytes (20 mg) on flash chiral column (24 mm i.d.) packed with 20% w/w CDMPC-coated 40-63 µm Davisil SI (40 g) (i) ATFE; (ii) 4-PB; (iii) BME; (iv) FLAV; (v) 1-PB; (vi) OXP (vii) 2-PXPA and (viii) 2-MPAA. Mobile phases listed at the bottom of Table 5-1. Flow rate ca. 4 ml/min.

The separation and resolution of each of chiral analyte on the flash column were measured and compared to the separation and resolution on column **26** (Table 5-2).

Table 5-2 Chromatographic parameters for analytical HPLC and preparative (20 mg) flash chromatographic separation of several chiral analytes

Analyte	HPLC column **26**		Flash preparative column			
					Recovery	
	α	Rs	α	Rs	Peak 1	Peak 2
ATFE	2.93	8.55	2.93	2.45	100	100
4-PB	1.76	4.37	1.66	1.70	100	100
BME	1.60	3.19	1.58	1.44	100	97
FLAV	1.43	2.89	1.62	1.91	100	100
1-PB	1.29	1.94	1.29	0.93	72	50
OXP	2.75	6.69	2.79	2.56	100	100
2-PXPA	2.55	5.58	2.63	2.32	100	100
2-MPAA	1.18	1.49	1.21	0.82	87	65

The α values observed on the flash column were very similar to those obtained on column **26**. Therefore, the HPLC column can be used not only to analyse the eluted fractions, but also to establish optimum preparative conditions. However, as expected, Rs values on the coarser irregular silica flash column are much lower than on the 5 μm spherical HPLC column.

For the chiral analytes ATFE, 4-PB, OXP and 2-PXPA with analytical HPLC Rs values of 8.55 - 4.37 ($\alpha = 2.93$ to 1.76), better than baseline resolution was achieved for a 20 mg loading on the flash column. Therefore, there is the potential for further increase in preparative loading for these compounds.

For the neutral chiral analytes BME and FLAV, with HPLC Rs values of 3.19 and 2.89 (α = 1.60 and 1.43), baseline resolution was just achieved on the flash column. Therefore, whilst almost 100% recovery of optically pure enantiomers could be achieved from a 20 mg injection, larger sample amounts would result in enantiomer overlap.

For the alcohol 1-PB and the acid 2-MPAA, the lower Rs values on the analytical column resulted in overlapping peaks on the flash column for a 20 mg sample load. For these two analytes, preparative scale-up using these chromatographic conditions is unlikely to yield larger quantities of pure enantiomers. However, the column bed height could be increased in order to improve Rs and adjustments may be made in the mobile phase to increase α.

The peak shapes of the enantiomers are extremely important and can be dramatically influenced by the quality of the column packing. Peak tailing, particularly by the first eluting enantiomer, can substantially reduce the recovery of the second eluting enantiomer. The separation of BME on a flash column which was packed by allowing the particles to settle slowly is shown in Figure 5-5.

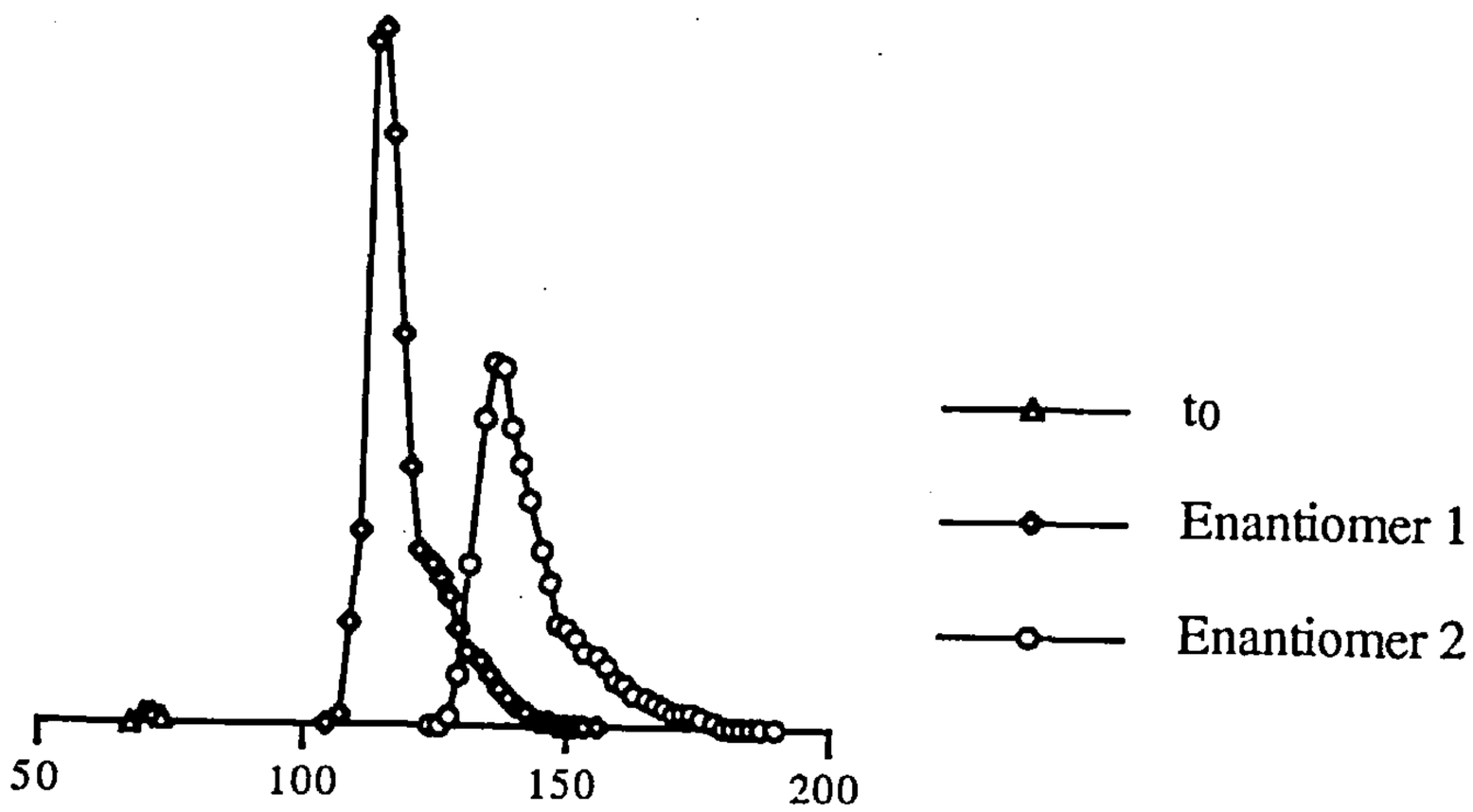

Figure 5-5 Separation of BME on a poorly packed flash column. Eluent: hexane/2-propanol (90:10 v/v). Flow rate: 4 ml/min.

5.3.4 Sample Loading Capacity

The sample loading capacity of the flash column obviously depends on the extent of separation. The recovery of the enantiomers of 4-PB, a chiral analyte which resolves well on column **26** (α = 1.76; Rs = 4.37) was investigated over the sample range 20 - 250 mg. See Figure 5-6 (note: the points were connected by a curve fitting polynomial routine using the Cricket-Graph software package).

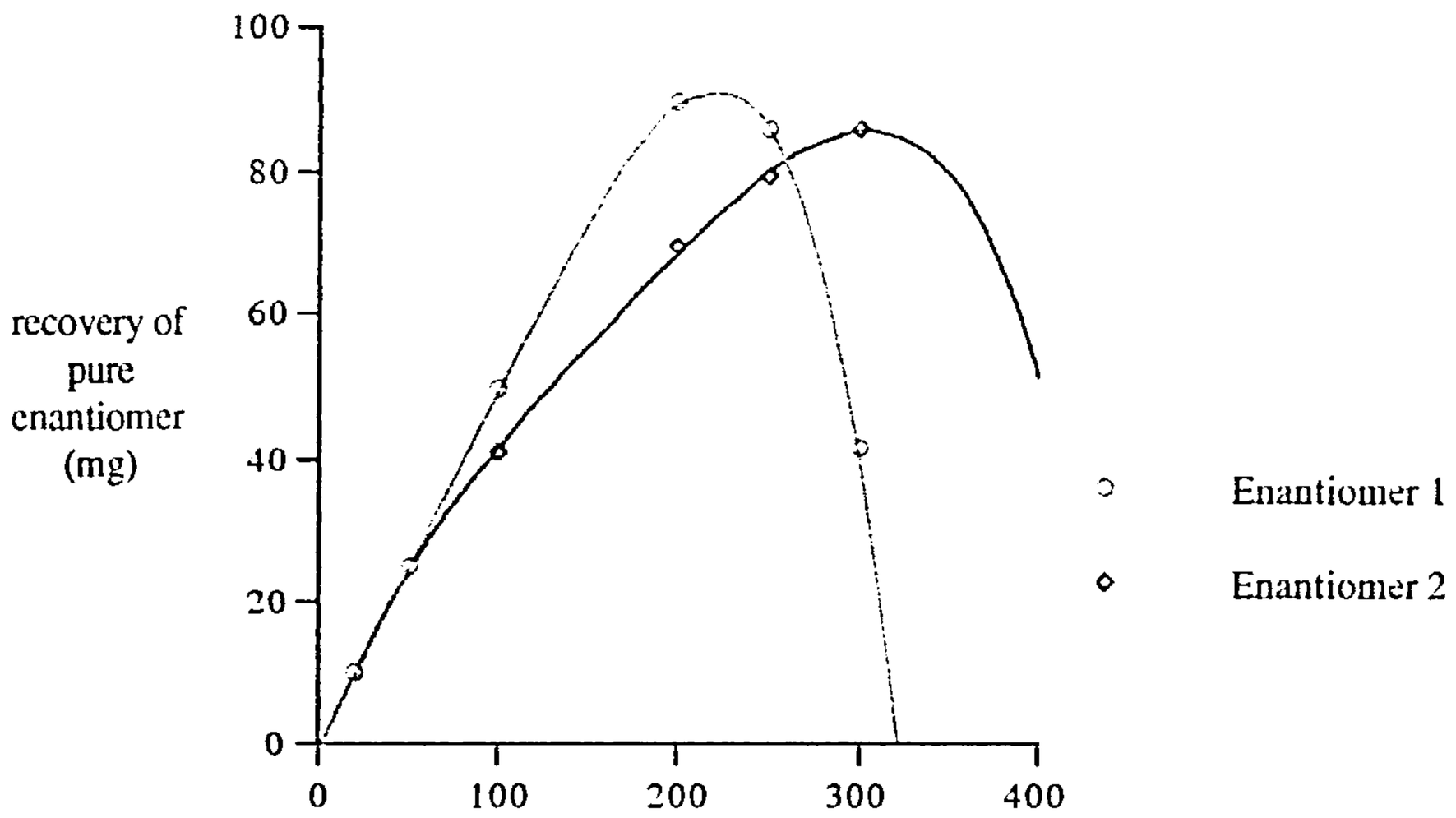

Figure 5-6 Effect on recovery of pure enantiomer of 4-PB on flash column as sample size is increased.

The approximate sample load at which the maximum throughput per unit time (at 4 ml/min) would be achieved was found to be 220 mg (5.5 mg per gram of CSP). Subsequent recycling of the overlapped portions would allow quantitative recovery of the pure enantiomers.

In a more difficult separation, a 100 mg sample of BME (HPLC: $\alpha = 1.43$; $R_S = 2.89$) gave 94% and 29% recovery of the first and second enantiomers respectively after one pass. The overlapped fractions were pooled and after concentrating, were loaded back onto the column. Significantly more of the second enantiomer was recovered and a net yield of 98% and 93% of the first and second enantiomers respectively were achieved for the two combined passes.

5.4 MODIFICATION OF THE FLASH COLUMN TO ALLOW ON-LINE DETECTION

The method for the flash separation of chiral enantiomers described so far works satisfactorily. However, analysis of the fractions to check for the presence of the enantiomers is very tedious and time consuming. Therefore, the bottom of the glass column was modified so that a connection could be made to a UV detector.

The main priority, was the need to keep the dead volume of the system to a minimum to prevent the separated enantiomers from post column mixing. This was accomplished by having a piece of 1/4 inch od. narrow bore glass tubing fused to the base of the column body in place of the tap. This allowed a 1/4 inch analytical column end fitting with a teflon ferrule to be attached and the tubing from a UV detector with a preparative flow cell was then connected. A sketch of the apparatus is shown in Figure 5-7.

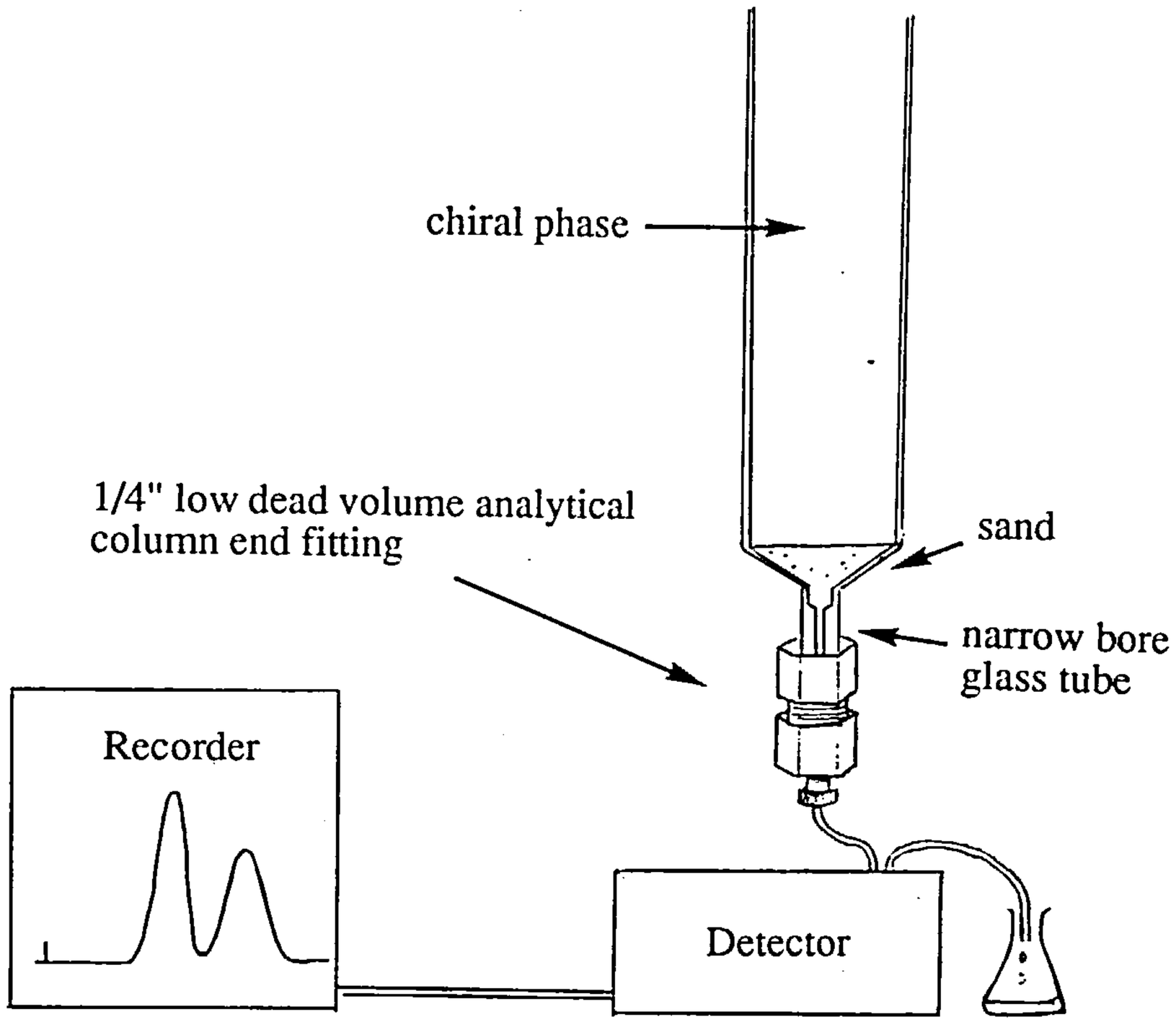

Figure 5-7 Apparatus for flash chiral chromatography with on-line detection.

The equipment allows the chromatographic resolution of the chiral analytes to be monitored continuously and thus only the eluate containing the enantiomers need be collected.

The flash separations of two chiral analytes (20 mg), which had been used to test the previous flash column model: BME and 1-PB and two chiral analytes not yet tested: 1-PE and 2-phenoxybutyric acid (2-PXBA; V) were examined using a column with on-line detection. The chromatograms are shown in Figure 5-8.

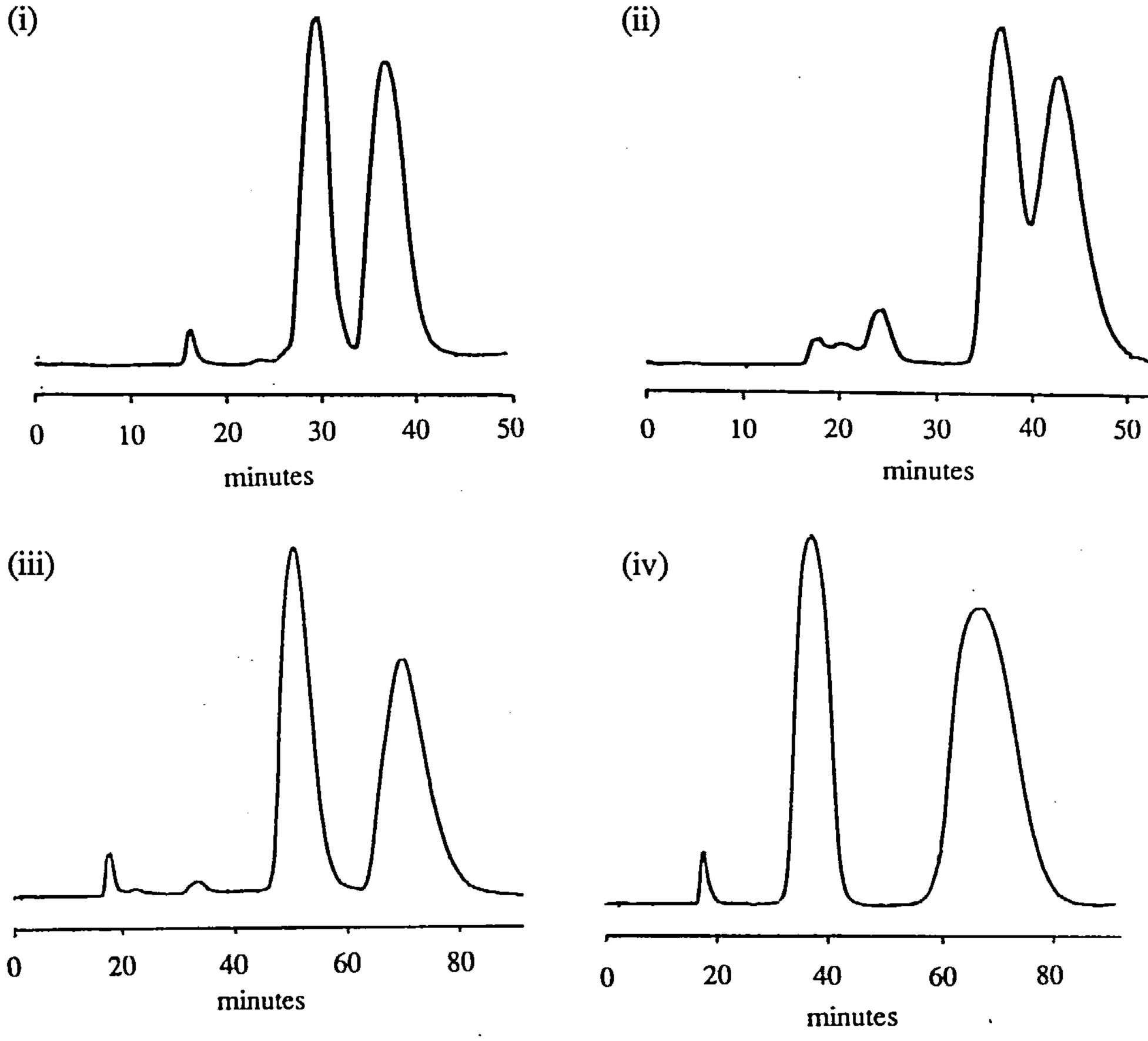

Figure 5-8 Separation of (i) BME, (ii) 1-PB, (iii) 1-PE and (iv) 2-PXBA (20 mg) on a flash chiral column (24 mm id.) packed with 20% w/w CDMPC-coated 40-63 μm Davisil SI (40 g). Eluents: BME: hexane/2-propanol (90:10 v/v); 1-PB and 1-PE: hexane/n-butanol (95:5 v/v) and 2-PXBA: hexane/2-propanol (95:5 v/v + 0.5% v/v trifluoroacetic acid). Flow rate: 4 ml/min.

The calculated chromatographic parameters were compared with separations achieved on column **26** and for BME and 1-PB, also with the separations achieved on the previous flash column equipment (Table 5-3).

Table 5-3 Chromatographic parameters for chiral analytes on column **26** and on the flash column using on-line detection

	HPLC column **26**		Flash preparative column	
Analyte	α	Rs	α	Rs
BME	1.60	3.19	1.60 (1.58)	1.23 (1.44)
1-PB	1.29	1.94	1.29 (1.29)	0.84 (0.93)
1-PE	1.50	3.77	1.58	1.57
2-PXBA	2.85	6.77	2.63	2.11

For BME and 1-PB the results obtained on the flash column using off-line analysis of fractions are shown in parentheses.

As seen previously (Table 5-2), α values for the HPLC and flash columns are very similar whereas Rs values on the flash column are significantly lower than on the HPLC column. The agreement between α values for the off-line and on-line detection methods for analytes BME and 1-PB is very good. However, Rs values on the flash column with on-line detection are slightly lower than calculated for the off-line detection method. This was probably due to the dead volume provided by the detection apparatus.

5.5 THE USE OF CDMPC-COATED FLASH GRADE ODS FOR THE SEPARATION OF BASIC CHIRAL ANALYTES[154]

As shown in Chapter 3 (section 3.2.2) the separation of basic chiral analytes can be significantly affected by the surface chemistry of the underlying support. In this study, it was shown that basic analytes with non sterically hindered amine groups gave very broad peak shapes when SI was used as a support for the cellulose carbamates. This was though to be due to strong non-stereoselective interactions between the basic moiety on the analyte and acidic silanol groups on the surface of the support. However, although some peak

tailing was still observed, the peak widths were significantly reduced by the addition of a larger quantity (1% compared with 0.1 % v/v) of diethylamine, a silanol suppressor, to the mobile phases.

The flash chiral separation of OXP has already been illustrated, (Figure 5-4). For this basic analyte, α and Rs values on column **26** were extremely high (2.75 and 6.69 respectively) and thus baseline separation of a 20 mg sample on the flash chiral column was achieved. However, when we examined the flash chiral separation of ALP and propranolol (PROP; **Q**) (20 mg), two other β-blockers which had lower α values on column **26** (α = 1.44 and 1.39 respectively) the resolution was far worse than expected (Figure 5-9). The peak tailing for these two analytes would significantly limit the amounts of pure enantiomers that could be collected.

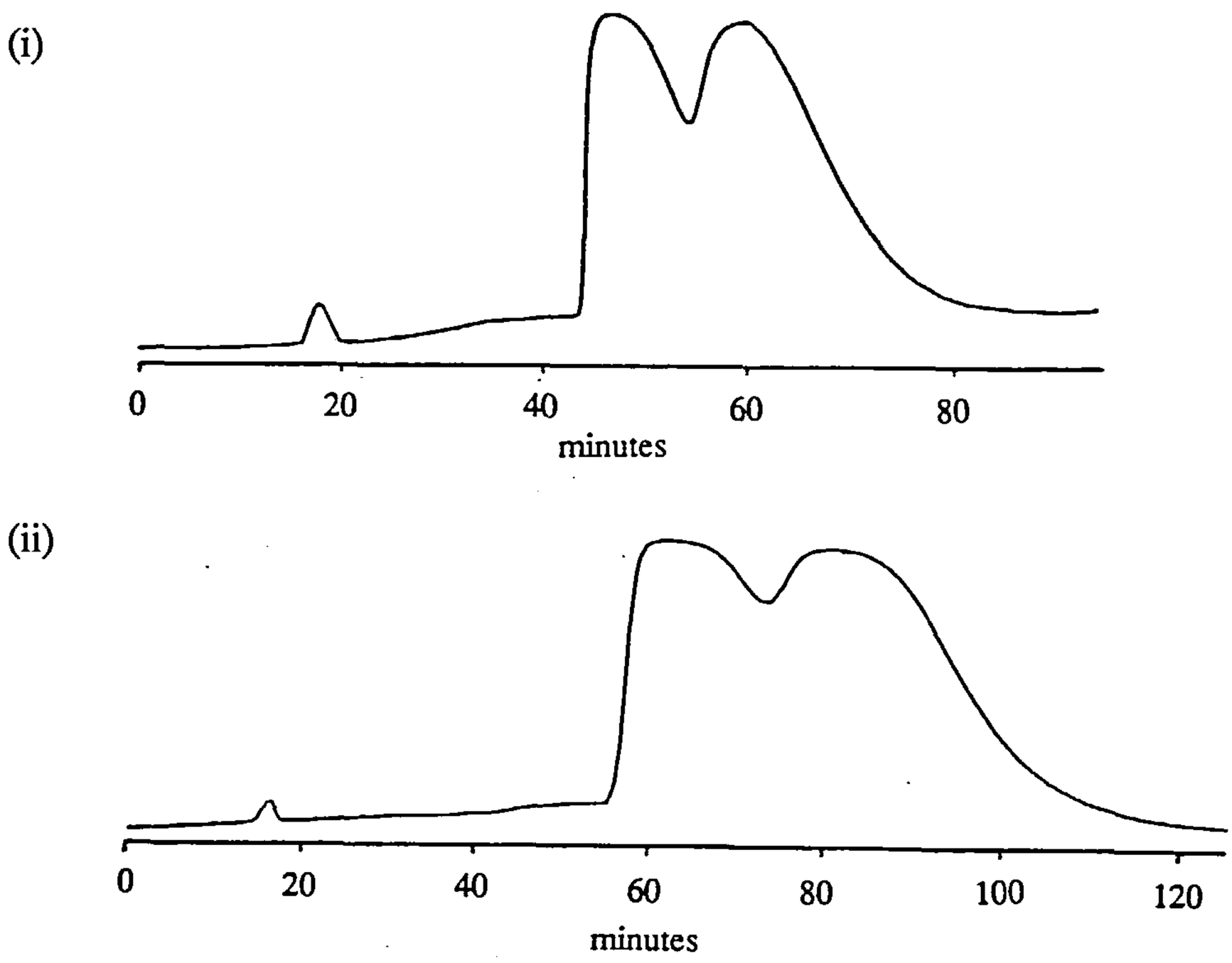

Figure 5-9 Separation of (i) ALP and (b) PROP (20 mg) on flash chiral column (24 mm id.) packed with 20% w/w CDMPC-coated 40-63 µm Davisil SI (40g). Eluent: hexane/2-propanol (80:20 v/v + 1% v/v diethylamine). Flow rate: 4 ml/min.

During the study reported in section 3.2.2, it was also noted that, in contrast to SI, ODS was potentially a much more suitable cellulose carbamate support for the separation of basic analytes. The retention times, especially for basic analytes with non-hindered amine moieties, were found to be much shorter and α values were higher on the CDMPC-coated ODS phase than on the CDMPC-coated SI or APS phases. Therefore, we decided to investigate the use of flash grade ODS silica for the flash chiral separation of ALP and PROP.

Another observation from the work described in section 3.2.2 was that the 120Å, Hypersil ODS support appeared to significantly exclude CDMPC from its pore volume. This resulted in Rs values that were slightly lower than might have been expected. Therefore, a Bondapak irregular ODS flash grade material (37-55 µm) which had a pore size of 300Å was chosen as a potentially suitable flash chromatography support. It was anticipated that the larger pore would more easily accommodate the CDMPC coating.

The 300Å, Bondapak ODS readily accepted a 20% w/w CDMPC loading (**CDMPC-6**) and the phase (**37/55µ-1**; 40 g) was packed into the flash chromatography column which had been adapted for on-line detection. The separation of ALP and PROP (20 mg) on this column are shown in Figure 5-10.

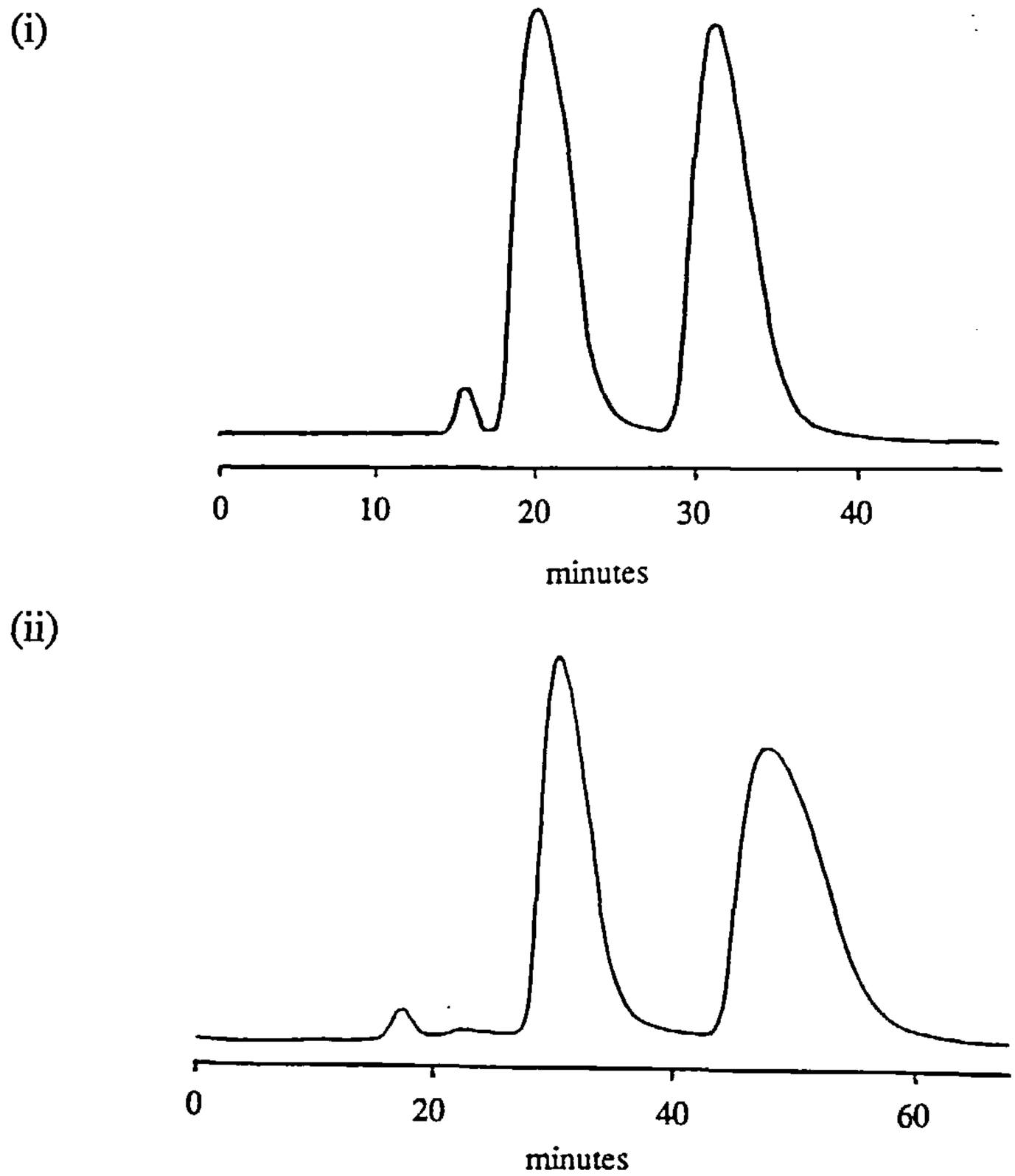

Figure 5-10 Separation of (i) ALP and (ii) PROP (20 mg) on flash chiral column (24 mm id.) packed with 20% w/w CDMPC-coated 37-55 μm Bondapak ODS (40 g). Eluent: hexane/2-propanol (80:20 v/v + 0.1% v/v diethylamine). Flow rate: 4 ml/min.

The efficiency of the CDMPC-coated ODS flash column was calculated using the first eluting enantiomer of BME and was compared to the efficiency of the CDMPC-coated Davisil SI column. For the same flash column height (250 mm), the number of plates for the coated-Davisil SI phase was approximately 550, whereas the coated Bondapak ODS phase had approximately 1450 plates, nearly three times greater than the Davisil phase.

As an illustration of the advantage of the extra efficiency observed with the 20% w/w CDMPC-coated ODS phase, the separation of 100 mg of BME is shown in Figure 5-11.

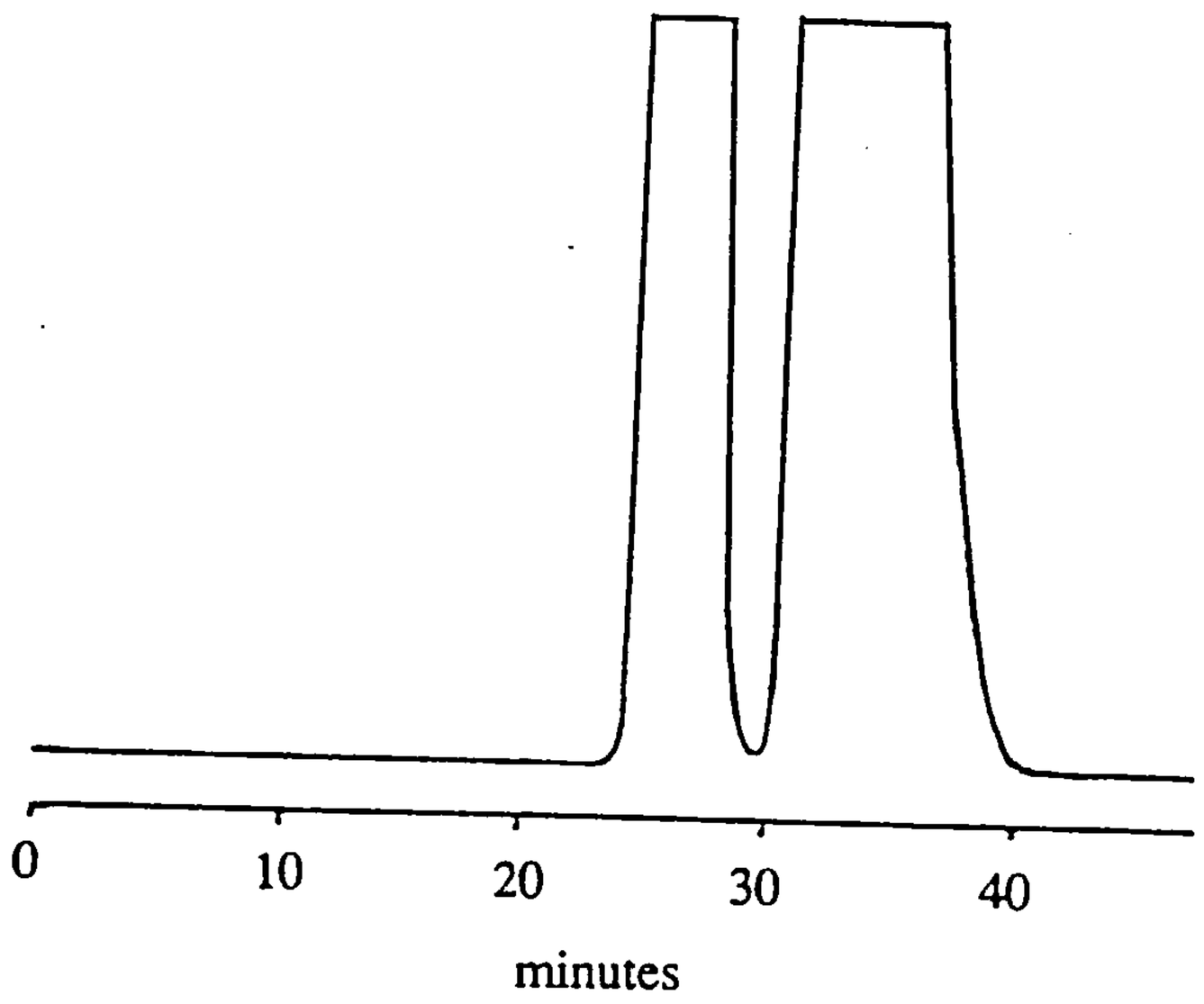

Figure 5-11 Separation of BME (100 mg) on flash chiral column (24 mm id.) packed with 20% w/w CDMPC-coated 37-55 µm Bondapak ODS (40 g). Eluent: hexane/2-propanol (90:10 v/v). Flow rate: 4 ml/min.

Previously, using CDMPC-coated Davisil SI, a 100 mg sample of BME required recycling in order to obtain almost quantitative recovery (section 5.3.4). Whereas, on the CDMPC-coated Bondapak ODS flash column, almost quantitative recovery was obtained in one pass.

The mean particle size distributions are similar for the CDMPC-coated Davisil SI and Bondapak ODS phases and would thus be expected to pack similarly. Therefore, the high efficiency of the 20% w/w CDMPC-coated Bondapak ODS phase appears to be due to the nature of the CDMPC coating on this wider pore ODS support.

5.6 LONG TERM USE OF THE FLASH CHIRAL COLUMN

Due to the difficulties in ensuring that exactly the same flow rate and sample loading procedure are used for each separation, no formal stability assessment has been carried out. However, the same 20% w/w CDMPC-coated

Davisil SI flash column has been retained and reused many times for the separation of different compounds (over 30 separate analyses). Different mobile phases with up to 20% v/v 2-propanol in hexane and additives such as diethylamine (1% v/v) and trifluoroacetic acid (0.5% v/v) were used. During this intensive testing period, the separation and resolution of BME was measured intermittently. The results are shown in Table 5-4.

Table 5-4 Chromatographic parameters for 4 intermittent tests of BME (20 mg) on a flash column (2.4 mm id.) packed with 20% w/w CDMPC-coated Davisil SI (40 g) during an intensive testing period.

Test Number	α	Rs
1 (day 1)	1.58	1.44
2 (day 4)	1.60	1.37
3 (day 10)	1.59	1.46
4 (day 20)	1.57	1.43

Eluent: hexane/2-propanol (90:10 v/v). Flow rate: 4 ml/min.

The α and Rs values for BME did fluctuate slightly. However, these variations may be within experimental error. Therefore, it appears that in agreement with the CDMPC-coated HPLC phases, the CDMPC-coated Davisil SI phase is stable to the typical normal phase eluents used for the separation of neutral, basic and acidic chiral analytes.

The flash chiral phase can be stored in hexane/2-propanol in the column and left for several weeks without any detectable deterioration in performance. For example, α and Rs values for BME after leaving the column (20% w/w CDMPC-coated Davisil SI) for 6 weeks in hexane/2-propanol (90:10 v/v) were $\alpha = 1.59$ and Rs = 1.42, compared with the previously result of $\alpha = 1.56$ and Rs = 1.46.

The flash chiral phase can also be unpacked, stored and then repacked into the flash column at a later date. The separations were found to be comparable to the previous column. For example, α and Rs values for BME after leaving the flash chiral phase (20% w/w CDMPC-coated Davisil SI) slurried in hexane/2-propanol (90:10 v/v) for 4 weeks was $\alpha = 1.62$ and $Rs = 1.47$, compared with the previously result of $\alpha = 1.59$ and $Rs = 1.42$.

It was considered to be preferable not to let the unpacked phase dry out, but to store the coated material in hexane/2-propanol (90:10 v/v). Although we have no firm evidence, we believe that this may help to prolong the life of the phase since the drying process may desolvate the cellulose carbamate coating and may potentially lead to changes in α and Rs. Before repacking, the sand needs to be removed and this can easily be carried out by slurrying the column contents in a hexane/2-propanol mixture and pouring into another vessel. The much heavier sand particles will not slurry well and can be left behind during decanting. If this is carried out several times, there is minimal loss of the CDMPC-coated phase.

The most expensive component of the CDMPC-coated SI flash phase, is the CDMPC coating. If the efficiency of the column deteriorates, for instance due to constantly repacking the phase, the majority of the CDMPC can be reclaimed by extraction with THF and used to coat a new batch of silica . The chromatographic parameters for 4-PB and BME (20 mg) on a flash column packed with reclaimed CDMPC coated onto Davisil SI are shown in Table 5-5.

Table 5-5 Chromatographic parameters for 4-PB and BME (20 mg) on flash column (2.4 mm id.) packed with reclaimed CDMPC (20% w/w) coated on Davisil SI (40 g).

Analyte	Initial flash column (off-line detection)		Flash column with reclaimed CDMPC (on-line detection)	
	α	Rs	α	Rs
4-PB	1.76	1.70	1.89	1.79
BME	1.58	1.44	1.63	1.48

Eluent: 4-PB: hexane/butanol (90:10 v/v); BME: hexane/2-propanol (90:10 v/v). Flow rate: 4 ml/min.

Efficiency at least as good as to that of the previous flash column was regained for both analytes.

5.7 SUMMARY AND CONCLUSIONS

An extremely easy, rapid and inexpensive method for the separation of a wide range of chiral analytes has been demonstrated. Separations have been monitored both indirectly, by fraction collection with subsequent HPLC analysis, and directly, using an on-line UV detector.

Sample loading capacities on our CDMPC-coated flash columns were significantly better than those quoted by Pirkle et al[153] on their covalently bonded flash column. For example, for a sample with an HPLC separation of $\alpha = 1.43$, we were able to completely separate 2.5 mg per gram of CSP in one pass (Pirkle et al were only able to separate 0.67 mg per gram of CSP of a sample with an HPLC separation of $\alpha = 2$).

A similarly coated HPLC phase has been shown to be useful not only for analysing the fractions collected if an off-line method of detection is used, but can also be used to optimise the separation conditions.

Loadings of tens to hundreds of milligrams of racemic analytes have been achieved using 40 g of flash chiral packing. The method therefore has the potential for gram scale separations on somewhat larger columns.

A CDMPC-coated Bondapak ODS flash chiral column has been shown to give extremely efficient resolution of basic analytes with non-sterically hindered amine moieties. This column was also found to be significantly more efficient than the CDMPC-coated Davisil SI phase. However, the cost of the Bondapak ODS was over 10 times more than the Davisil SI (£160 for 100 g compared to £12 for 100 g of Davisil SI).

The same column can be retained and reused many times for the separation of the same or different compounds, without appreciable loss of efficiency. If the column performance deteriorates, the CDMPC may be reclaimed by solvent extraction and recoated onto a new batch of flash silica.

The methods described above could easily be modified to suit the user's need. The on-line method was shown to be particularly easy and it should be possible to automate the sample collection by using a programmable fraction collector. A medium pressure chromatography system could be purchased to allow a continuous solvent flow and more reproducible injections. Other sources of irregular flash silica could be tested. Large particle spherical silicas may give better efficiencies than the irregular silicas. The potential improvements that can be made are only limited by the user's budget.

CHAPTER 6

EXPERIMENTAL

6.1 CHEMICALS AND SOLVENTS

All Hypersil spherical silicas (particle size, pore size, pore volume, surface area and surface chemistry are listed with each experiment) were purchased or received as a gift from Shandon HPLC (UK). Davisil irregular silica (40-63 μm; 150Å) was purchased from Aldrich (UK). Bondapak irregular ODS (37-55 μm) was purchased from Waters (USA).

Sigmacel cellulose was purchased from Sigma (UK) and Avicel cellulose was purchased from Merck (Germany). Pyridine was obtained from Fluka. Isocyanates were purchased from Lancaster (UK). Chiral analytes were purchased from either Sigma or Aldrich (UK). N,N-DMA, diethylamine and trifluoroacetic acid was purchased from Aldrich (UK). All other solvents (HPLC grade) were obtained from Rathburn (UK).

6.2 PREPARATION OF CPC AND CDMPC

Amounts of starting materials used for the preparation of CPC and CDMPC are shown in Table 6-1. Cellulose, which had been dried for 24 hours over phosphorous pentoxide in a vacuum desiccator, was refluxed for 24 hours in dry pyridine (dried over potasium hydroxide). After cooling, 3.5 equivalents of either phenyl isocyanate or 3,5-dimethylphenyl isocyanate were added and the mixture refluxed for a further 72 hours. The cooled orange/brown solution was poured into 1.5 litres of methanol and stirred for 1 hour. The white solid was filtered, washed well with methanol and dried under vacuum at 50°C to constant mass. Yields are shown in Table 6-1.

Table 6-1 Amounts of starting materials and yields for cellulose carbamate batches

Sample	Cellulose Type	Amount of Cellulose (g)	Amount of isocyanate (g)	Yield (g)	% Yield
CPC-1	Sigmacel	10	25.7	27.5	85.9
CPC-2	Sigmacel	5	12.9	14.2	88.7
CDMPC-1	Sigmacel	6.3	20	19.7	84.0
CDMPC-2	Sigmacel	3.1	10	10.5	91.0
CDMPC-3	Sigmacel	6.3	20	20.3	86.6
CDMPC-4	Avicel	6.3	20	19.3	82.3
CDMPC-5	Avicel	6.3	20	19.9	84.9
CDMPC-6	Avicel	6.3	20	20.5	87.4

6.2.1 Elemental Analysis

Duplicate C, H and N analysis for each cellulose carbamate batch was carried out at either MEDAC or Warwick University (Leeman Labs. Inc. CE440 elemental analyser) . Results (mean C, H and N data) are shown in Table 6-2.

Table 6-2 C, H and N analyses for cellulose carbamate batches

Sample	%C	%H	%N	% -OH groups derivatised*
CPC Theoretical	62.42	4.85	8.09	-
CPC-1	61.17	4.77	7.84	81.3
CPC-2	61.30	4.82	7.94	83.0
CDMPC Theoretical	65.66	6.18	6.96	-
CDMPC-1	64.88	6.18	6.83	87.7
CDMPC-2	64.65	6.09	6.79	85.0
CDMPC-3	64.94	6.07	6.82	88.7
CDMPC-4	64.44	6.17	6.82	82.3
CDMPC-5	64.55	6.09	6.80	83.7
CDMPC-6	64.78	6.09	6.81	86.7

* = calculated by fitting a curve (using Cricket Graph, Apple Macintosh) through %C results calculated for mono-, di- and tri- substituted glucose units and substituting in for %C observed. Curve of best fit for CPC: $y = 14.526\log z + 55.549$; for CDMPC: $y = 15.633\log z + 58.305$; where y = %C and z = number of substituted groups. % -OH derivatised = z/3 x 100

6.2.2 Gel Permeation Chromatography

GPC was carried out on a Polymer Laboratories (PL) Modular System with Caliber GPC/SEC software using refractive index detection. Two PL Plgel 5 µm Mixed-C columns (300 x 7.5 mm) in series and a Plgel 5 µm guard column (50 x 7.5 mm) were used, with THF as eluent and toluene (0.2% v/v) as an internal standard and flow marker. Columns were calibrated with polymethylmethacrylate standards with molecular weight range 1100 - 333000.

6.3 PREPARATION OF CPC AND CDMPC-COATED PHASES

6.3.1 Preparation of CPC-coated APS Phases for HPLC

Amounts of starting materials used for the preparation of the CPC-coated phases are shown in Table 6-3. APS was placed in a 250 ml round bottom flask, with four indents, and was refluxed in THF for 30 minutes. After cooling, an appropriate amount of CPC which had been dissolved in THF (by stirring) was added to the refluxed APS. The solvent was removed under vacuum at room temperature using a rotary evaporator set at a low rotation speed. Once dry, the contents of the flask were removed and dried in a vacuum oven at 50°C for 1 hour. The coated material was gently brushed through a sieve (38 μm) to ensure a free flowing powder suitable for packing.

Table 6-3 Amounts of starting materials used for the CPC coated phases for HPLC

Sample	Amount of Silica (g)	Reflux Volume (ml)	% w/w CPC Loading	Amount of CPC (g)	Dissolution Volume (ml)
5μ-1	3.0	40	5.0	0.16	20
5μ-2	3.0	40	10.0	0.33	20
5μ-3	3.0	40	15.0	0.53	20
5μ-4	3.0	40	20.0	0.75	20

6.3.2 Preparation of CDMPC-coated SI, APS and ODS Phases for HPLC

Amounts of starting materials used for the preparation of the CDMPC chiral stationary phases are shown in Table 6-4. An identical method to that described in 6.3.1 was used except CDMPC was used in place of CPC, THF/N,N-DMA (9:1 v/v) was used as the dissolution solvent for CDMPC and the material was dried in the oven at 50°C for 3 hours.

Table 6-4 Amounts of starting materials used for the CDMPC-coated phases for HPLC

Sample	Amount of Silica (g)	Reflux Volume (ml)	% w/w CDMPC Loading	Amount of CDMPC (g)	Dissolution Volume (ml)
2.5μ-1	0.5	10	15.0	0.088	5
2.5μ-2	2.5	40	15.0	0.44	15
2.5μ-3	7.0	80	15.0	1.24	40
3μ-1 - 3μ-3	2.5	40	15.0	0.44	15
3μ-4	2.5	40	20.0	0.625	15
5μ-5	7.0	80	15.0	1.24	40
5μ-6	0.5	10	15.0	0.088	5
5μ-7	0.5	10	12.5	0.071	5
5μ-8	0.5	10	15.0	0.088	5
5μ-9	0.5	10	20.0	0.125	5
5μ-10	0.5	10	17.5	0.11	5
5μ-11	3.0	40	12.5	0.43	20
5μ-12	3.0	40	15.0	0.53	20
5μ-13	3.0	40	17.5	0.64	20
5μ-14	3.0	40	15.0	0.53	20
5μ-15	3.0	40	20.0	0.75	20
5μ-16	3.0	40	25.0	1	20
5μ-17	3.0	40	20.0	0.75	20
10μ-1	7.0	80	15.0	1.24	40

6.3.3 Preparation of 25% w/w CDMPC-coated PGC

PGC (1.5 g) was placed in a 250 ml round bottom flask which contained four indents and was refluxed in THF for 30 minutes. The suspension was allowed to cool. CDMPC (0.5 g; 25% w/w) was split into five 0.1 g amounts. Each 0.1 g portion was dissolved in THF (20 ml). The first portion was added to the refluxed PGC and the solvent was removed under vacuum at room temperature using a rotary evaporator set at a low rotation speed. This coating process was repeated until all the CDMPC solutions had been added. Once dry, the contents of the flask were removed and dried in a vacuum oven at 50°C for 1 hour. The coated material was gently brushed through a sieve (38 μm) to ensure a free flowing powder suitable for packing.

6.3.4 Preparation of CDMPC-coated SI and ODS Phases for Flash Chromatography

The flash silica support (Davisil SI or Bondapak ODS; 37 g) was placed in a 1 litre buchner flask which contained four indents and was refluxed in THF (300 ml) for 30 minutes. After cooling, CDMPC (9.25 g) which had been dissolved in THF/N,N-DMA (95:5 v/v; 100 ml) was added to the refluxed silica. The solvent was removed under vacuum at room temperature using a rotary evaporator set at a low rotation speed. Once dry the contents of the flask were removed and dried in a vacuum oven at 50°C for 3 hours. The coated material was gently brushed through a sieve (250 μm) to ensure a free flowing powder suitable for packing.

6.3.5 Determination of Particle Size Distribution

Particle size distributions were measured using a Malvern MasterSizer X. The test cell was filled with HPLC grade methanol and a blank reading was taken. Approximately 20 mg of sample was sonicated in HPLC grade methanol (5 ml) for 5 minutes. The slurry was pipetted (ca. 5 drops) into the test cell until

the obscuration measurement was in the 'normal' range and a reading was taken. The mean particles sizes and comments about the distribution for the coated and uncoated samples are shown in Tables 6-5 to 6-10.

Table 6-5 Comparison of particle size distributions for uncoated and coated 2.5 μm Hypersil APS

Sample	Carbamate Loading (% w/w)	Mean Particle Size (μm)	Comment on particle size distribution
Uncoated APS	0	2.51	narrow, gaussian
2.5μ-1	15	3.32	v. broad, fines and agg. particles
2.5μ-2	15	2.68	sl. broader than u/c
2.5μ-3	15	2.64	sl. broader than u/c

v. = very; sl. = slightly; agg. = aggregated
u/c = uncoated material

Table 6-6 Comparison of particle size distributions for uncoated and coated 3 μm Hypersil supports

Sample	Carbamate Loading (% w/w)	Mean Particle Size (μm)	Comment on particle size distribution
Uncoated SI	0	3.04	narrow, gaussian
3μ-1	15	3.17	sl. broader than u/c
3μ-4	20	3.22	sl. broader than u/c, more fines
Uncoated APS	0	3.04	narrow, gaussian
3μ-2	15	3.14	sl. broader than u/c
Uncoated ODS	0	3.30	sl. broader than u/c SI or APS
3μ-3	15	3.24	sl. broader than u/c, more fines

sl. = slightly; u/c = uncoated material

Table 6-7 Comparison of particle size distributions for uncoated and coated 5 μm Hypersil supports

Sample	Carbamate Loading (% w/w)	Mean Particle Size (μm)	Comment on particle size distribution
Uncoated APS	0	5.23	narrow, gaussian
5μ-1	5	5.18	narrow, gaussian
5μ-2	10	6.08	broader than u/c
5μ-3	15	6.13	broader than 5μ-2
5μ-4	20	6.29	v. broad, fines and agg. particles
5μ-5	15	5.65	sl. broader than u/c
5μ-6	15	6.03	v. broad, fines and agg. particles
5μ-7	12.5	5.51	sl. broader than u/c, more fines
5μ-8	15	5.31	sl. broader than u/c
5μ-9	20	6.08	v. broad, fines and agg. particles
5μ-10	17.5	5.43	sl. broader than u/c, more fines
5μ-11	12.5	5.81	sl. broader than u/c, more fines
5μ-12	15	5.63	sl. broader than u/c, more fines
5μ-13	17.5	5.33	sl. broader than u/c, more fines
5μ-14	15	5.51	sl. broader than u/c, more fines
5μ-15	20	6.08	sl. broader than u/c, more fines
5μ-16	25	6.64	v. broad, fines and agg. particles
Uncoated SI	0	5.13	narrow, gaussian
5μ-17	20	5.18	sl. broader than u/c, more fines

v. = very; sl. = slightly; agg. = aggregated

u/c = uncoated material

Table 6-8 Comparison of particle size distributions for uncoated and coated 10 μm Hypersil APS

Sample	Carbamate Loading (% w/w)	Mean Particle Size (μm)	Comment on particle size distribution
Uncoated APS	0	10.11	narrow, gaussian
10μ-1	15	10.33	sl. broader than u/c, more fines

sl = slightly; u/c = uncoated material

Table 6-9 Comparison of particle size distributions for uncoated and coated 40-63 μm Davisil SI

Sample	Carbamate Loading (% w/w)	Mean Particle Size (μm)	Comment on particle size distribution
Uncoated SI	0	55.92	gaussian, some fines
40/63μ-1	20	56.00	similar to u/c
40/63μ-2	20	54.80	similar to u/c

u/c = uncoated

Table 6-10 Comparison of particle size distributions for uncoated and coated 37-55 μm Bondapak ODS

Sample	Carbamate Loading (% w/w)	Mean Particle Size (μm)	Comment on particle size distribution
Uncoated ODS	0	61.32	gaussian, some fines
37/55μ-1	20	58.99	similar to u/c

u/c = uncoated

6.3.6 Pore Diameter, Pore Volume and Surface Area Measurements

All measurements were made at Shandon HPLC. Pore diameter and pore volume measurements were made by an automated mercury intrusion method and surface area was calculated from the adsorption of nitrogen onto the surface (BET method).

6.3.7 Scanning Electron Microscopy

All SEM was carried out at SmithKline Beecham Pharmaceuticals, Brockham Park using a Hitachi 2500C with a LaB6 electron gun. Samples were prepared by dusting onto adhesive discs attached to aluminium specimen stubs and sputter coated with platinum prior to examination at x kV (where x = kV value displayed at the bottom of the photograph).

6.4 COLUMN PACKING PROCEDURE

Stainless steel HPLC columns, 150, 100 and 30 mm in length, 2.4 mm id. with female end fittings and 2 μm frit were purchased from Hichrom (UK). Glass flash columns (24 mm id.) were made in house by the glass blowing workshop. Either a tap or narrow bore glass tubing was attached to the base of the column (see Figures 5-1 and 5-7).

6.4.1 HPLC Packing Procedure for 150 mm and 100 mm Columns

The coated phase (ca. 2.8 g for 150 mm column; ca. 2.2 g for 100 mm column) was suspended in hexane/2-propanol (1:1 v/v; 80 ml) and was sonicated for 3 minutes. The Haskel 780-3 column packer was purged with the packing solvent (hexane/2-propanol 80:20 v/v). The slurry was quickly transferred to the column packing reservoir (80 ml), which was already connected to the column packer and the HPLC column was connected to the top of the reservoir. The

column was upward slurry packed at 4000 psi. for 1 minute, then pressure was increased to 6000 psi. After approximately 5 minutes or after 100 ml solvent was passed, the column was turned over and the column was downward packed until approximately 200 ml of packing solvent had been passed. The pressure was released slowly down to atmospheric and the column was removed from the reservoir. Normally a 1-2 cm slug of packing material was left in the neck of the reservoir. The column was equilibriated on an HPLC pump using hexane/2-propanol (90:10 v/v) at 0.5 ml/min for 24 hours before using.

6.4.2 HPLC Packing Procedure for 30 mm Columns

The same packing procedure was used except 1.0 g of coated material was used and a 12 ml packing reservoir replaced the 80 ml reservoir.

6.4.3 Flash Column Packing Procedure

This procedure is relevant to both the unmodified and modified glass flash chromatography columns. The glass column (500 x 24 mm) was prepared for use by inserting a plug of glass wool in the neck above the outlet, followed by a layer of fine sand (analytical grade). The coated material (40 g) was slurried in hexane/2-propanol (80:20 v/v) which had been previously sonicated (5 minutes) to remove any dissolved air. The slurry was poured into the glass column and packed immediately using full air pressure (30 psi.). This was accompanied by gentle tapping with a piece of thick rubber tubing to ensure a well packed column bed. The column bed height (250 ±10 mm) was topped with a further layer of sand to facilitate easier sample loading with minimal bed disturbance. After packing, the column was equilibrated in hexane/2-propanol (90:10 v/v).

6.5 EVALUATION OF CELLULOSE CARBAMATE-COATED PHASES FOR HPLC

6.5.1 Apparatus

HPLC in Section 2.2

Separations were carried out on a Beckman Gold system containing a 126 binary pump, 166 UV detector and 506 autosampler fitted with a 10 µl injection loop. Data were acquired using a Waters 860 Expertease package.

HPLC in Sections 2.3, 3.2 and 4.3

Separations were carried out on a system comprising a Beckman 114M pump, a Beckman System Gold 166 UV detector and a Promise autosampler and 10 µl injection loop unless otherwise stated. Data were acquired using a Waters 860 Expertease package.

HPLC in Sections 3.3 and 5.3

Separations were carried out on a system comprising a Waters 510 pump, a Cecil CE-2012 UV detector, Rheodyne 7125 injector with a 10 µl loop and a J J Instruments CR650 chart recorder.

6.5.2 Chromatographic Conditions

All chromatography was performed at ambient temperatures using the chromatographic conditions listed with each experiment. A suitable wavelength was used to detect each analyte (see appendix II). Mobile phases were degassed by sonicating for 5 minutes prior to use. The dead time (t_0) of the columns was determined by an injection of 1,3,5-tri-*tert*-butylbenzene.

6.5.3 Chromatographic Calculations

The separation factor (α) was calculated as $\alpha = k'_2/k'_1$ and capacity factor (k') as $k'_1 = (t_1 - t_0)/t_0$ and $k'_2 = (t_2 - t_0)/t_0$, where t_1 and t_2 refer to the retention times for the first and second eluting enantiomers, respectively. The resolution factor (Rs) was calculated by the formula: $Rs = 2(t_2 - t_1)/(w_1 + w_2)$ where w_1 and w_2 are the peak base widths for the first and second eluting enantiomer peak respectively. See Figure 1-3.

Column dead volume was calculated using t_0 x flow rate.

6.6 EVALUATION OF CDMPC-COATED PHASES FOR FLASH CHROMATOGRAPHY

6.6.1 Apparatus

The nature of the glass flash column is described with each experiment. HPLC analysis of the fractions collected from the flash column were carried on a system comprising a Waters 510 pump, a Cecil CE-2012 UV detector, Rheodyne 7125 injector with a 10 µl loop and a J J Instruments CR650 chart recorder. Separations which were monitored by on-line detection used a Cecil CE-212 variable wavelength UV detector and a Kipp and Zonen chart recorder.

6.6.2 Chromatographic Conditions

All chromatography was performed at ambient temperatures using the chromatographic conditions listed with each experiment. A suitable wavelength was used to detect each analyte (see appendix II). Mobile phases were degassed by sonicating for 5 minutes prior to use. The dead time (t_0) of the columns was determined by an injection of 1,3,5-tri-*tert*-butylbenzene.

6.6.3 Chromatographic Calculations

For the separations in which fractions were collected and then analysed off-lineby HPLC, the chromatogram was constructed by plotting the peak area against the eluent volume using the computer program, Cricket Graph (Apple Macintosh).

The same chromatographic calculations described in section 6.5.3 were applied to both the constructed chromatograms and the separations in which on-line detection was used.

6.7 RECOVERY OF CDMPC FROM FLASH PHASES

The CDMPC-coated silica (ca. 40 g) was suspended in THF(100 ml) and sonicated for 15 minutes. After allowing the silica to settle, the solution was decanted and retained. The silica was again suspended in THF (100 ml) and the process was repeated 5 times. The combined THF extracts were reduced to approximately 100 ml using a rotary evaporator at 30°C and then poured into methanol (1 litre). After stirring for 1 hour, the white solid was filtered, washed well with methanol and dried under vacuum at 50°C to constant mass. The yield obtained was 7.12 g, 89.0%.

REFERENCES

1 L. Pasteur, *Comptes Rendus de l'Academie des Sciences*, 1848, **26**, 535.

2 J. H. Van't Hoff, *Arch. Netherland Sci. Extracts et Naturelles*, 1874, **9**, 445.

3 J. A. Le Bel, *Bull. Sci. Chimique de France*, 1874, **22**(2), 337.

4 G. Blaske, H. P. Kraft, H. Markgraf, *Chem. Ber.*, 1980, **113**, 2318.

5 E. J. Ariens, *Eur. J. Clin. Pharmacol.*, 1984, **26**, 663.

6 E. J. Ariens, *Eur. J. Drug Metab. Pharmacol.*, 1988, **13**, 307.

7 T. G. Burlingame and W. H. Pirkle, *J. Am. Chem. Soc.*, 1966, **88**, 4294.

8 G. M. Whitesides and D. W. Lewis, *J. Am. Chem. Soc.*, 1970, **92**, 6979.

9 M. Verzele and C. Dewaele, Preparative Liquid Chromatography: A Practical Guide, TEC, 1986.

10 V. R. Meyer, Practical High-Performance Liquid Chromatography, Wiley and Sons, Chichester, England, 1988.

11 R. P. W. Scott, *Chem. Rev.*, 1992, **10**, 137.

12 K. K. Unger, Porous Silica, *J. Chromatogr. Library*, 16, Elsevier, Amsterdam, Holland, 1979.

13 J. van Deemter, J. Zuiderweg and A. Klinkenberg, *Chem. Eng. Sci.*, 1958, **5**, 271.

14 J. LePage, W. Lindner, G. Davies and B. Karger, *Anal. Chem.*, 1979, **51**, 443.

15 P. E. Hare and E. Gil-Av, *Science*, 1979, **204**, 1226.

16 W. H. Pirkle and T. C Pochapsky, *Chem. Rev.*, 1989, **89**, 347.

17 S. Allenmark, Ed., Chromatographic Separation. Methods and Applications, Ellis Horwood, Chichester, England, 1991.

18 A. M. Krstulovic, Ed., Chiral Separations by HPLC: Applications to Pharmaceutical Compounds, Ellis Horwood, Chichester, England, 1989.

19 W. J. Lough, Ed., Chiral Liquid Chromatography, Blackie and Sons, Glasgow, Scotland, 1989.

20 G. Subramanian, Ed., A Practical Approach to Chiral Separations by Liquid Chromatography, VCH, New York, USA, 1994.

21 D. R. Taylor and K. Maher, *J. Chromatogr. Sci.*, 1992, **30**, 67.

22 I. W. Wainer, A Practical Guide to the Selection and Use of HPLC Chiral Stationary Phases, J. T. Baker, Phillipsburg, USA, 1988.

23 C. Vandenbosch, D. Massart and W. Lindner, *J. Pharm. & Biomed. Anal.*, 1992, **10**, 895.

24 E. Francotte, *J. Chromatogr.*, 1994, **666**, 565.

25 I. W. Wainer, oral communication.

26 W. H. Pirkle, D. W. House and J. M. Finn, *J. Chromatogr.*, 1980, **192**, 143.

27 C. J. Welch, *J. Chromatogr.*, 1994, **666**, 3.

28 L. R Sousa, D. H. Hoffman, L. Kaplan and D. J. Cram, *J. Am. Chem. Soc.*, 1974, **96**, 7100.

29 G. Dotsevi, Y. Sogah and D. J. Cram, *J. Am. Chem. Soc.*, 1975, **97**, 1259.

30 S. C. Peacock, L. A. Domeier, F. C. Gaeta, R. C. Helgeson, J. M. Timko and D. J. Cram, *J. Am. Chem. Soc.*, 1978, **100**, 8190.

31 D. W. Armstrong, T. J. Ward, R. D. Armstrong and T. E. Beesley, *Science*, 1986, **232**, 1132.

32 A. M. Stalcup, J. R. Faulkner Jr, Y. Tang, D. W. Armstrong, L. W. Levy and E. Regalado, *Biomed. Chromatogr.*, 1991, **5**, 3.

33 A. M. Stalcup, S. -C. Chang, D. W. Armstrong and J. Pitha, *J. Chromatogr.*, 1990, **513**, 181.

34 T. Hargitai, Y. Kaida and Y. Okamoto, *J. Chromatogr.*, 1993, **628**, 11.

35 H. Yuki, Y. Okamoto and I. Okamoto, *J. Am. Chem. Soc.*, 1980, **102**, 6356.

36 Y. Okamoto, S. Honda, K. Hatada and H. Yuki, *J. Chromatogr.*, 1985, **350**, 127.

37 S. Allenmark, B. Bomgren and H. Boren, *J. Chromatogr.*, 1982, **237**, 473.

38 S. Allenmark and Bomgren, *J. Chromatogr.*, 1982, **25**, 297.

39 J. Hermansson and M. Eriksson, *J. Liq. Chromatogr.*, 1986, **9**, 621.

40 J. Hermansson, *Trends Anal. Chem.*, 1989, **8**, 251.

41 K. M. Kirkland, K. L. Neilson and D. A. McCombs, *J. Chromatogr.* 1991, **504**, 445.

42 D. W. Armstrong, Y. Tang, S. Chen, Y. Zhou, C. Bagwill and J. -R Chen, *Anal. Chem.*, 1994, **66**, 1473.

43 D. W. Armstrong, Y. Liu and K. Helen Ekborgott, presented at the *6th ISCD*, St. Louis, 1995.

44 C. Roussel and P. Picas, presented at the *3rd ISCD*, Tubingen, 1992.

45 B. Koppenhoefer, R. Graf, H. Holzschuh, A. Nothdurft, U. Trettin, P. Picas and C. Roussel, *J. Chromatogr.*, 1994, **666**, 557.

46 D. M. Johns, Binding to cellulose, in Chiral Liquid Chromatography, Blackie and Sons, Glasgow, Scotland, 1989.

47 C. E. Dent, *J. Biochem.*, 1948, **43**, 169.

48 M. Kotake, T. Sakan, N. Nakamura and S. Senoh, *J. Am. Chem. Soc.*, 1951, **73**, 2973.

49 C. E. Dalgleish, *J. Biochem.*, 1952, **52**, 3.

50 C. E. Dalgleish, *J. Chem. Soc.*, 1952, 3940.

51 S. Yuasa, A. Shimada, K. Kameyama, M. Yasui and K Adzuma, *J. Chromatogr. Sci.*, 1980, **18**, 311.

52 G. Gubitz, W. Jellenz, D. Schomleber, *J. High. Resolut. Chromatogr., Chromatogr. Commun.*, 1980, **3**, 31.

53 T. Fukuhara, M. Isoyama, A. Shimada, M. Hoki and S. Yuasa, *J. Chromatogr.*, 1987, **387**, 562.

54 G. Hesse and R. Hagel, *Chromatographia*, 1973, **6**, 277.

55 G. Hesse and R. Hagel, *Liebigs Ann. Chem.*, 1976, 966.

56 G. Hesse and R. Hagel, *Chromatographia*, 1976, **9**, 62.

57 K. R. Lindner and A. Mannschreck, *J. Chromatogr.*, 1980, **193**, 308.

58 A. Hussenius, R. Isaksson and O. Matsson, *J. Chromatogr.*, 1987, **405**, 155.

59 M. Mintas, Z. Orhanovic, K. Jakopcic, H. Koller, G. Stuhler and A. Mannschreck, *Tetrahedron*, 1985, **41**, 229.

60 H. Koller, K, -H, Rimbock and A Mannschreck, *J. Chromatogr.*, 1983, **282**, 89.

61 G. Blaschke, *Angew. Chem. Int. Ed. Engl.*, 1980, **19**, 13.

62 G. Blaschke, *J. Liq. Chromatogr.*, 1986, **9**, 341.

63 T. Shibata, I. Okamoto and K. Ishii, *J. Liq. Chromatogr.*, 1986, **9**, 313.

64 A. Ichida, T. Shibata, I. Okamoto, Y. Yuki, H. Namikoshi and Y. Toga, *Chromatographia*, 1984, **19**, 280.

65 Y. Okamoto, M. Kawashima, K. Yamamoto and K. Hatada, *Chem. Lett.*, 1984, 739.

66 Y. Okamoto, M. Kawshima and K. Hatada, *Polymer Preprints, Jpn.* 1984, **33**, 1607.

67 Y. Okamoto, M. Kawshima and K. Hatada, *J. Am. Chem. Soc.*, 1984, **106**, 5357.

68 T. Shibata, H. Namikoshi, H. Nakamura, I. Okamoto, A. Ichia, Y. Yuki, K. Shimizu and Y. Toga, *Polymer Preprints, Japan*, 1984, **33**, 1599.

69 Y. Okamoto, M. Kawashima and K. Hatada, *J. Chromatogr.*, 1986, **363**, 173.

70 Y. Okamoto, R. Aburatani and K. Hatada, *J. Chromatogr.*, 1987, **389**, 95.

71 E. Francotte and R. M. Wolf, *Chirality*, 1990, **2**, 16.

72 T. Shibata, T. Sei, H. Nishimura and K. Deguchi, *Chromatographia*, 1987, **24**, 552.

73 I. Wainer and M. C. Alembik, *J. Chromatogr.*, 1986, **358**, 85.

74 I. W. Wainer, M. C. Alembik and E. Smith, *J. Chromatogr.*, 1987, **388**, 65.

75 I. W. Wainer, R. M. Stiffin and T. Shibata, *J. Chromatogr.*, 1987, **411**, 139.

76 E. Francotte and R. M. Wolf, *Chirality*, 1991, **3**, 43.

77 E. Francotte, R. M. Wolf, *J. Chromatogr.*, 1992, **595**, 63.

78 Y. Okamoto, R. Aburatani, T. Fukumoto and K. Hatada, *Chem. Lett.*, 1987, 1857.

79 Y. Okamoto and Y. Kaida, *J. Chromatogr.*, 1994, **666**, 403.

80 Y. Okamoto, Y. Kaida, H. Hayashida and K. Hatada, *Chem. Lett.*, 1990, 909.

81 Y. Kaida and Y. Okamoto, *Chirality*, 1992, **4**, 122.

82 B. Chankbetadze, E. Yashima and Y. Okamoto, *Chem. Lett.*, 1992, 617

83 B. Chankvetadze, E. Yashima, Y. Okamoto, *J. Chromatogr.*, 1994, **670**, 39.

84 Y. Kaida and Y. Okamoto, *Bull. Chem. Soc. Jpn.*, 1992, **65**, 2286.

85 J. Whatley, *J. Chromatogr.*, 1995, **697**, 251.

86 Z. Juvancz, K. Grolimund and E. Francotte, *Chirality*, 1992, **4**, 459.

87 E. Yashima, J. Noguchi and Y. Okamoto, *Chem. Lett.*, 1992, 1959.

88 Y. Okamoto, R. Aburatani, K. Hatano and K. Hatada, *J. Liq. Chromatogr.*, 1988, **11**, 2147.

89 Y. Okamoto, R. Aburatani, Y. Kaida, K. Hatada, N. Inotsume and M. Nakano, *Chirality*, 1989, **1**, 239.

90 M. E. Tiritan, S. A. Matlin, Q. B. Cass and D. R. Boyd, presented at *6th ISCD*, St Louis, 1995.

91 B. Chankvetadze, E. Yashima and Y. Okamoto, *J. Chromatogr.*, 1995, **694**, 101.

92 Y. Okamoto, R. Aburatani, K. Hatada, M. Honda, N. Inotsume and M. Nakano, *J. Chromatogr.*, 1990, **513**, 375.

93 Q. B. Cass, A. L. Bassi and S. A. Matlin, presented at *6th ISCD*, St Louis, 1995.

94 G. Felix and T. Zhang, *J. Chromatogr.*, 1993, **639**, 141.

95 G. Felix and T. Zhang, *J. High Res. Chromatogr.*, 1993, **16**, 364.

96 R. Aburatani, Y. Okamoto and K. Hatada, *Bull. Chem. Soc. Jpn.*, 1990, **63**, 3606.

97 Y. Okamoto, oral communication, *6th ISCD*, St Louis, 1995.

98 Y. Okamoto, R. Aburatani, S. Miura and K. Hatada, *J. Liq. Chromatogr.*, 1987, **10**, 1613.

99 E. Yashima, H. Fukaya and Y. Okamoto, *J. Chromatogr.*, 1994, **677**, 11.

100 L. Oliveros, P. Lopez, C. Minguillon and P. Franco, *J. Liq. Chromatogr.*, 1995, **18**, 1521.

101 L. Oliveros, P. Lopez, C. Minguillon and P. Franco, presented at *HPLC 95*, Innsbruck, 1995.

102 A. M. Stalcup and K. Williams, *J. Chromatogr.*, 1995, **695**, 185.

103 G. Blaschke, *Angew. Chem.*, 1980, **92**, 14.

104 E. Francotte, R. M. Wolf, D. Lohmann and R. Mueller, *J. Chromatogr.*, 1985, **347**, 25.

105 E. Francotte and A. Junker-Buchheit, *J. Chromatogr.*, 1992, **576**, 1.

106 M. H. Gaffney, R. M. Stiffin and I. Wainer, *Chromatographia*, 1989, **27**, 15.

107 U. Vogt and P. Zugenmaier, *Makromol. Chem. Rapid. Commun.*, 1983, **4**, 759.

108 E. Yashima, M. Yamada, Y. Kaida, Y. Okamoto, *J. Chromatogr.*, 1995, **694**, 347.

109 W. H. Pirkle and T. C. Pochapsky, *J. Am. Chem. Soc.*, 1987, **109**, 5975.

110 K. B. Lipkowitz, S. Raghothama and J. Yang, *J. Am. Chem. Soc.*, 1992, **114**, 1554.

111 E. Yashima, M. Yamada and Y. Okamoto, *Chem. Lett.*, 1994, 579.

112 K. Oguni, H. Oda and A. Ichida, *J. Chromatogr.*, 1995, **694**, 91.

113 H. Y. Aboul-Enein and M. Rafiqul Islam, *J. Liq. Chromatogr.*, 1990, **13**, 485.

114 R. J. Bopp, T. M. Anderson, J. Lee and K. Tachibana, presented at *6th ISCD*, St Louis, 1995.

115 Y. Okamoto, M. Kawashima, R. Aburatani, K. Hatada, T. Nishiyama and M. Masuda, *Chem. Lett.*, 1986, 1237.

116 Y. Okamto, T. Aburatani, Y. Kaida and K. Hatada, *Chem. Lett.*, 1988, 1125.

117 J. Dingenen, Polysaccharide Phases in Enantioseparations, in A Practical Approach to Chiral Separations by Liquid Chromatography, VCH, New York, USA, 1994..

118 K. Ichida, T. Hamasaki, H. Kohno, T. Ogawa, T. Matsumoto and J. Sakai, *Chem. Lett.*, 1989, 1089.

119 A. Ishikawa and T. Shibata, *J. Liq. Chromatogr.*, 1993, **16**, 859.

120 L. Miller, R. Bergeron, *J. Chromatogr.*, 1993, **648**, 381.

121 D. T. Witte, J-P. Franke, F. J. Bruggeman, D. Dijkstra and R. A. de Zeeuw, *Chirality*, 1992, **4**, 389.

122 L. Miller and C. Weyker, *J. Chromatogr.*, 1993, **653**, 219.

123 K. -H. Rimbock, F. Kastner and A. Mannschreck, *J. Chromatogr.*, 1985, **329**, 307.

124 A. M. Rizzi, *J. Chromatogr.*, 1989, **478**, 101.

125 R. Isaksson, P. Erlandsson, L. Hansson, A. Holmberg and S. Berner, *J. Chromatogr.*, 1990, **498**, 257.

126 L. Miller, D. Honda, R. Fronek and K. Howe, *J. Chromatogr.*, 1994, **658**, 429.

127 P. E. C. Goissedet, U.S. Patent 1,357,450, 1920, Nov 2.

128 J. W. Baker and J. B. Holdsworth, *J. Chem. Soc.*, 1947, 713.

129 Y. Okamoto, K. Hatada, T. Shibata, I Okamoto, H. Nakamura, H. Namikoshi and Y. Yuki, European Patent 0, 147, 804, 1984, Dec 20.

130 A. Crawford, A Study of carbohydrate stationary phases for the separation of enantiomers by high performance liquid chromatography, PhD Thesis, Dec. 1993.

131 S. J. Grieb, S. A. Matlin, A. M. Belenguer, J. G. Phillips and H. J. Ritchie, *Chirality*, 1994, **6**, 129.

132 H. Wannman, A. Walhagen and P. Erlandsson, *J. Chromatogr.*, 1992, **603**,121.

133 L. Snyder, *Anal. Chem.*, 1967, 39, 698.

134 A. Wehrli, W. Hermann and J. Huber, *J. Chromatogr.*, 1976, **125**, 59.

135 J. Kirkland, W. Yau, H. Stoklosa and C. Dilks, *J. Chromatogr. Sci.*, 1977, **15**, 103.

136 M. Krause and R. Galensa, *J. Chromatogr.*, 1990, **502**, 287.

137 S. J. Grieb, S. A. Matlin, A. M. Belenguer and H. J. Ritchie, *J. Chromatogr.*, 1995, **697**, 271

138 H. Y. Aboul-Enien and V. Serignese, *J. Liq. Chromatogr.*, 1993, **16**, 197.

139 S. J. Grieb, S. A. Matlin, A. M. Belenguer, H. J. Ritchie and P. Ross, *J. High Res. Chromatogr. Commun.*, in press

140 J. H. Knox and B. Kaur, *J. Chromatogr.*, 1986, **352**, 3.

141 A. Karlsson and C. Petterson, *J. Chromatogr.*, 1991, **543**, 287.

142 E. Heldin, N. Hang Huynh and C. Petterson, *J. Chromatogr.*, 1992, **592**, 339.

143 J. E. Mama, A. F. Fell and B. J. Clark, *Anal. Proc.*, 1989, 26.

144 S. M. Wilkins, D. R. Taylor and R. J. Smith, *J. Chromatogr.*, 1995, **697**, 587.

145 Hypercarb Guide, Shandon HPLC, 1994.

146 B. J. Bassler, E. Garfunkel, R. A. Hartwick and R. Kaliszan, *J. Chromatogr.*, 1989, **461**, 139.

147 G. Gu and C. K. Lim, *J. Chromatogr.*, 1989, **515**, 183.

148 M. F. Emery and C. K. Lim, *J. Chromatogr.*, 1989, **479**, 212.

149 M. Josefsson, B. Carlsson and B. Norlander, *J. Chromatogr.*, 1994, **684**, 23.

150 Chiralcel and Chiralpak CSP Brochures, Daicel.

151 W. C. Still, M. Kahn and A, Mitra, *J. Org. Chem.*, 1978, **43**, 2923.

152 W. H. Pirkle, A. Tsipouras and T. J. Sowin, *J. Chromatogr.*, 1985, **319**, 392.

153 S. A. Matlin, S. J. Grieb and A. M. Belenguer, *J. Chem. Soc., Chem. Commun.*, 1995, 301.

154 S. J. Grieb, S. A. Matlin and A. M. Belenguer, *J. Chromatogr.*, in press.

APPENDIX I

Column Nº	Contents (all coatings w/w; all silicas Hypersil)	Column Length (mm) (4.6 mm i.d.)
1	5% CPC (s), 5 µm APS (120Å)	150
2	10% CPC (s), 5 µm APS (120Å)	150
3	15% CPC (s), 5 µm APS (120Å)	150
4	20% CPC (s), 5 µm APS (120Å)	150
5	15% CDMPC (s) on 2.5 µm APS (120Å)	100
6	15% CDMPC (s) on 2.5 µm APS (120Å)	30
7	15% CDMPC (s) on 2.5 µm APS (120Å)	100
8	15% CDMPC (s) on 2.5 µm APS (120Å)	150
9	15% CDMPC (s) on 5 µm APS (120Å)	30
10	15% CDMPC (s) on 5 µm APS (120Å)	100
11	15% CDMPC (s) on 5 µm APS (120Å)	150
12	15% CDMPC (s) on 10 µm APS (120Å)	30
13	15% CDMPC (s) on 10 µm APS (120Å)	100
14	15% CDMPC (s) on 10 µm APS (120Å)	150
15	12.5% CDMPC (s) on 5 µm APS (90Å)	150

APPENDIX I continued

Column Nº	Contents (all coatings w/w; all silicas Hypersil)	Column Length (mm) (4.6 mm i.d.)
16	15% CDMPC (s) on 5 µm APS (120Å)	150
17	17.5% CDMPC (s) on 5 µm APS (500Å)	150
18	15% CDMPC (s) on 3 µm SI (120Å)	100
19	15% CDMPC (s) on 3 µm APS (120Å)	100
20	15% CDMPC (s) on 3 µm ODS (120Å)	100
21	20% CDMPC (s) on 3 µm SI (120Å)	100
22	25% CDMPC (s) on 7 µm PGC (250Å)	100
23	15% CDMPC (a) on 5 µm APS (120Å)	150
24	20% CDMPC (a) on 5 µm APS (120Å)	150
25	25% CDMPC (a) on 5 µm APS (120Å)	150
26	20% CDMPC (a) on 5 µm SI (120Å)	150

s = prepared from Sigmacel cellulose

a = prepared from Avicel cellulose

APPENDIX II

Letter	Compound name and abbreviation	Structure	Detection wavelength (nm)
A	trans stilbene oxide TSO	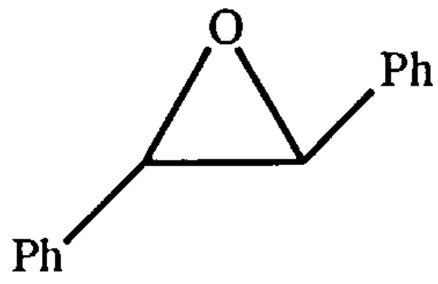	240
B	1-(9-anthryl)-2,2,2-trifluroethanol ATFE	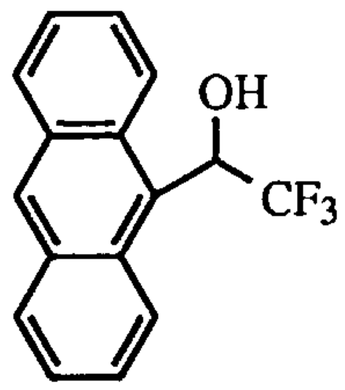	254
C	1-phenylethanol 1-PE	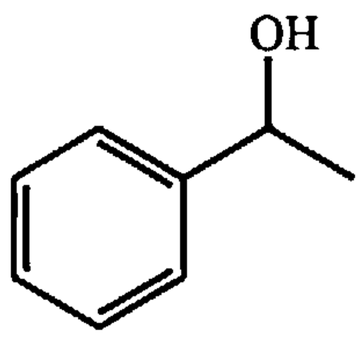	254
D	1-phenyl-2-butanol 1-PB	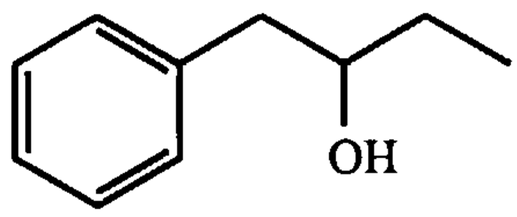	254
E	4-phenyl-2-butanol 4-PB	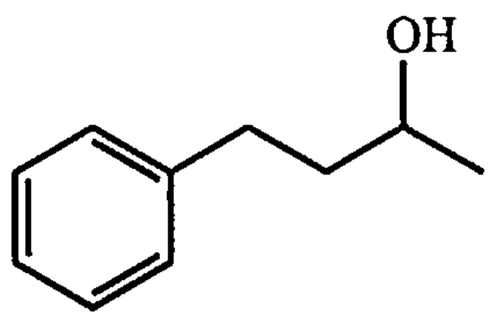	254
F	benzoin BZ	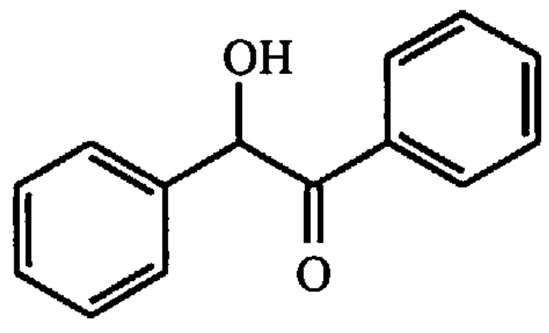	254

APPENDIX II (continued)

Letter	Compound name and abbreviation	Structure	Detection Wavelength (nm)
G	benzoin methyl ether BME	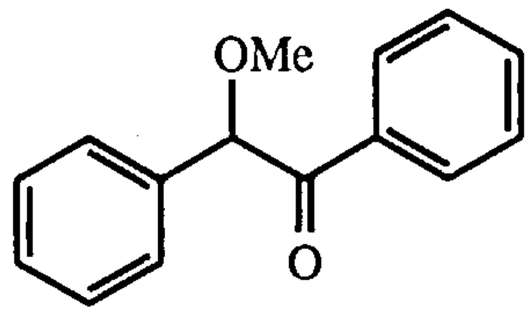	254
H	flavanone FLAV	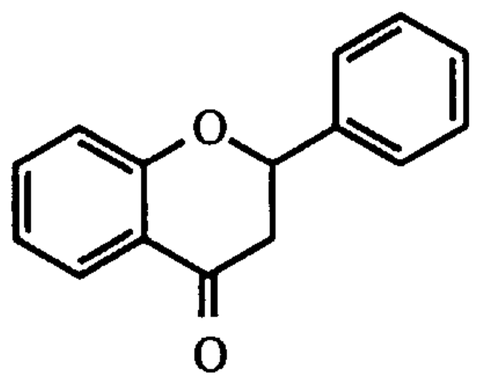	254
J	benzyl mesityl sulfoxide BMS	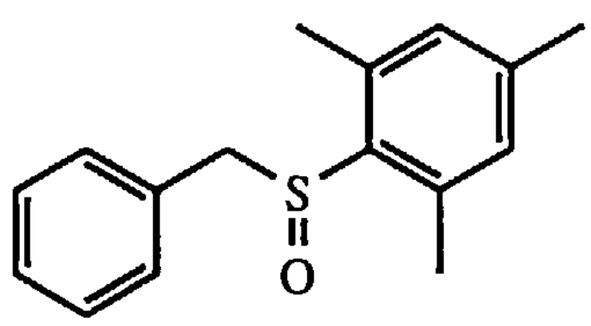	254
K	Trogers base TB	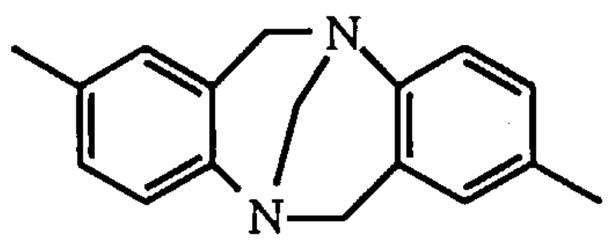	240
L	homatropine HOMA	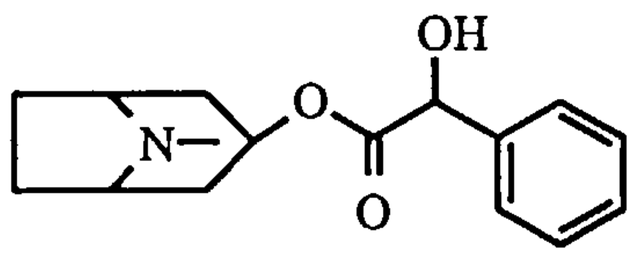	220
M	orphenadrine ORP	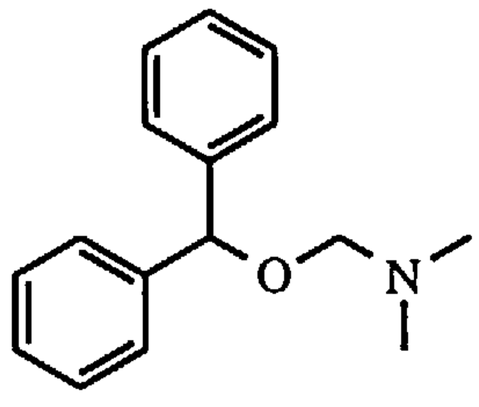	254

APPENDIX II (continued)

Letter	Compound name and abbreviation	Structure	Detection wavelength (nm)
N	alprenolol ALP	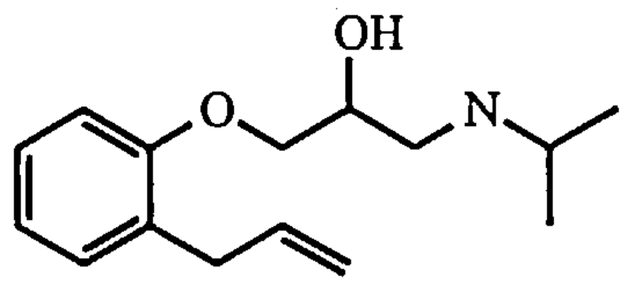	273
P	oxprenolol OXP	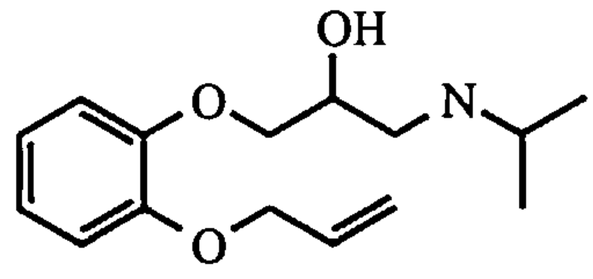	273
Q	propranolol PROP	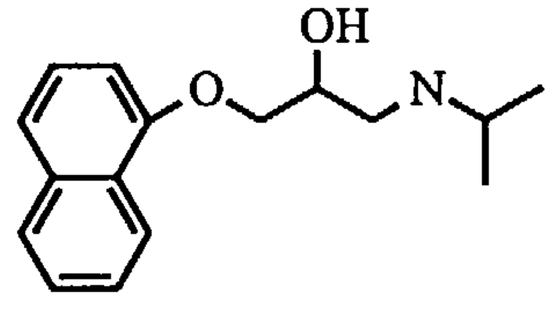	254
R	2-phenylpropionic acid 2-PPA	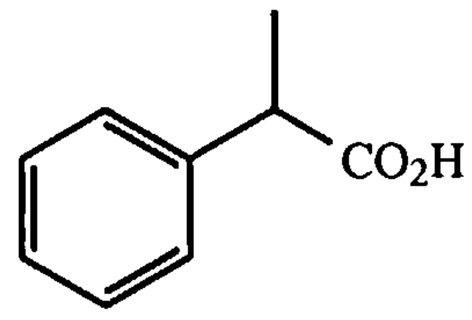	254
S	mandelic acid MA	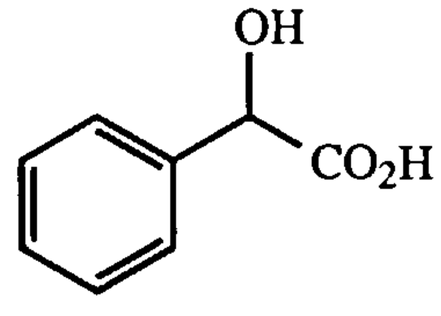	254
T	2-methoxyphenyl acetic acid 2-MPAA	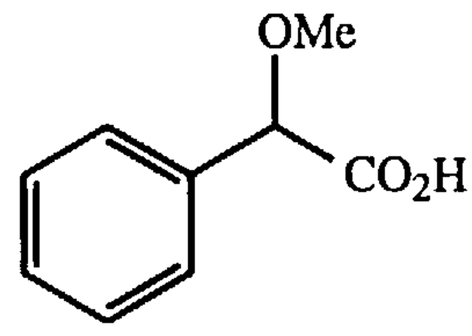	254

APPENDIX II (continued)

Letter	Compound name and abbreviation	Structure	Detection wavelength (nm)
U	2-phenoxypropionic acid 2-PXPA	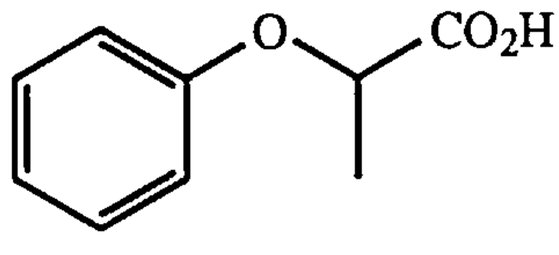	254
V	2-phenoxybutyric acid 2-PXBA	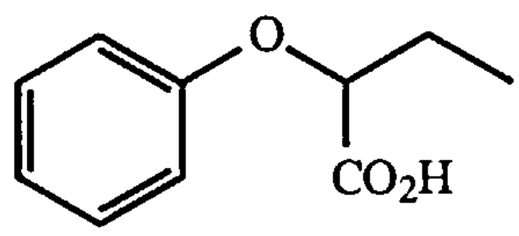	254
W	trans 2-phenylcyclopropane carboxylic acid 2-PCCA	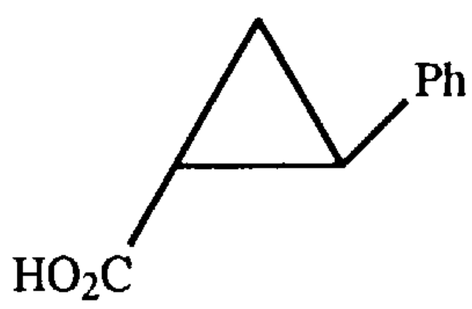	254
X	suprofen SUP	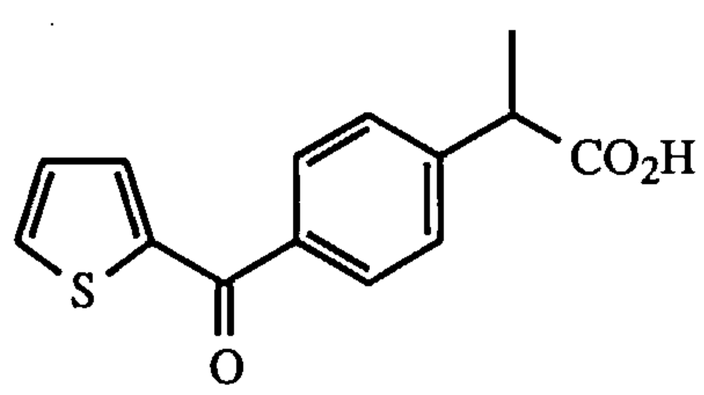	254